



Provided by the author(s) and University of Galway in accordance with publisher policies. Please cite the published version when available.

Title	Preclinical assessment of the novel compound EL102 in prostate cancer
Author(s)	Toner, Aidan
Publication Date	2015-03-31
Item record	http://hdl.handle.net/10379/5019

Downloaded 2024-05-20T22:44:02Z

Some rights reserved. For more information, please see the item record link above.





**O'É Gaillimh
NUI Galway**

Preclinical Assessment of the Novel Compound EL102 in Prostate Cancer

Aidan Toner M.Sc. B.Sc.

Thesis submitted to the
National University of Ireland, Galway
for the award of Ph.D. in the
School of Medicine



Supervisors:

Dr. Sharon Glynn Ph.D. M.P.H.

Prof. Frank Sullivan MB MRCPI FFR RCSI

March 2015

Contents	Page
Contents	i
Declaration	vii
Research Outputs	viii
List of Figures	x
List of Tables	xii
List of Abbreviations	xiii
Abstract	xxi
Acknowledgements	xxii
Dedication	xxiv
Chapter 1: General Introduction	1
1.1 Prostatic Disease	2
1.1.1 The Human Prostate	2
1.1.2 Prostatitis	3
1.1.3 Benign Prostatic Hyperplasia	4
1.1.4 Prostate Cancer Diagnosis and Incidence	5
1.2 Prostate Cancer Treatment	11
1.2.1 Prostatectomy	11
1.2.2 Radiotherapy	12
1.2.2.1 Brachytherapy	12
1.2.2.2 External Beam Radiation Therapy	13
1.2.3 Hormone Therapy	13
1.2.3.1 Androgen Receptor	14
1.2.3.2 Gonadotropin-Releasing Hormone Agonists and Antagonists	16
1.2.3.3 Hormone-Responsive Anti-Androgen Therapy	17
1.2.3.4 Castrate-Resistant Anti-Androgen Therapy	18
1.2.3.5 Surgical Anti-Androgen Therapy	20
1.2.4 Prostate Cancer Chemotherapy	20
1.2.4.1 Paclitaxel	20
1.2.4.2 Docetaxel	22

1.2.4.3 Cabazitaxel	23
1.2.4.4 Mitoxantrone	24
1.2.4.5 Anthracyclines	24
1.2.4.6 Estramustine	25
1.2.5 Chemoresistance in Prostate Cancer	25
1.2.5.1 Multi-Drug Resistance Efflux Protein Pumps	26
1.2.5.2 AR-Mediated Chemoresistance	27
1.2.5.3 Chemoresistance Through Proliferation and Survival Pathways	28
1.2.5.4 Chemoresistance Conferred by Cancer Stem Cells	28
1.3 Recent Advances in Prostate Cancer Treatment	29
1.3.1 Sipuleucil-T	29
1.3.2 Radium-223	29
1.3.3 HIF1α Inhibitors	30
1.3.3.1 Heteroaryl and Aromatic HIF1 α Inhibitory Agents	31
1.3.3.2 Steroidal HIF1 Inhibitors	32
1.3.3.3 RNA Antagonists	33
1.3.3.4 mTor Inhibitors	33
1.3.3.5 HSP90 Inhibitors	33
1.3.3.6 Non-Steroidal Anti-Inflammatory Drugs	34
1.3.3.7 Chetomin	34
1.4 Toluidine Sulphonamides	34
1.4.1 ELR510444	30
1.4.2 ELR510552 (EL102)	35
Chapter 2: Materials and Methods	38
2.1 Cell Culture	39
2.1.1 Cell Lines	39
2.1.2 Culture Conditions	40
2.2 Cell Viability and Apoptosis Assays	41

2.2.1 Resazurin-Based Assays	42
2.2.2 Sulforhodamine B-Based Assays	42
2.2.3 Toxicity in Multi-Drug Resistant Cell Lines	43
2.2.4 DEVD Caspase 3/7 Activation Assays	44
2.2.5 Sub-G₁ and Cell Cycle Analysis	45
2.2.6 Analysis of PARP Cleavage	46
2.3 Protein Analysis	46
2.3.1 Antibodies	46
2.3.2 Protein Isolation and Quantification	47
2.3.3 Western Blot Analysis	49
2.3.3.1 In-House Gel/Wet Transfer Methodology	49
2.3.3.2 Precast Gel/Dry Transfer Methodology	52
2.3.3.3 Detection of Proteins	52
2.3.4 Cellular Fractionation of Proteins	53
2.3.5 Immunocytochemistry	54
2.3.5.1 Cell Fixation	54
2.3.5.2 Immunostaining	54
2.3.6 HIF1 TransAM ELISA	55
2.4 Genetic Analysis	56
2.4.1 Plasmid Preparation	56
2.4.1.1 Bacterial Transformation	56
2.4.1.2 Miniprep	57
2.4.1.3 Restriction Digest	58
2.4.1.4 Making Glycerol DH5 α Stocks	59
2.4.1.5 Maxiprep	59
2.4.2 Transient Transfections	61
2.4.3 Reporter Gene Assays	62
2.4.3.1 Cell Lysis	62
2.4.3.2 CPRG Assay	62
2.4.3.3 Luciferase Assay	63
2.4.4 Total RNA Isolation	63

2.4.5 cDNA Synthesis	64
2.4.6 qPCR	65
2.4.7 Primers	66
2.5 Cell Migration Assays	67
2.6 Tumour Xenograft Models	67
2.7 Preliminary Methodology: Elara Pharmaceuticals Findings	68
2.7.1 Proteomic Analysis of HIF1 α Activity	68
2.7.2. Binding Assays	69
2.7.2.1 Kinase Binding Screen	69
2.7.2.2 <i>In Vitro</i> Pharmacology: Diversity Profile	70
2.8 Statistical Analysis	71
2.9 Suppliers and Distributors	72
Chapter 3: Analysis of the Cytotoxic Profile of EL102 in A Panel of Prostate Cancer Cell Lines	74
3.1 Introduction	75
3.2 Results	77
3.2.1 Cell Viability Assays and Determination of the IC ₅₀ Values of EL102	77
3.2.2 Tumour Volume Analysis of an <i>In Vivo</i> CWR22 Murine Xenograft Model	79
3.2.3 <i>In Vitro</i> Analysis of the Combined Effect of EL102 and Docetaxel	83
3.2.4 Cell Death and Induction of Apoptosis in EL102-Dosed Prostate Cancer Cell Lines	84
3.3 Discussion	90
3.3.1 EL102 Treatment Reduces Prostate Cancer Cell Viability <i>In Vitro</i>	90
3.3.2 Combined Therapeutic Effect of EL102 and Docetaxel <i>In Vivo</i> Differs <i>In Vitro</i>	90
3.3.3 EL102-Induced Apoptosis Induction	91

3.3.4 Clinical Potential For EL102 as a Chemotherapeutic Agent	92
Chapter 4: Exploring the <i>In Vitro</i> Mechanisms of EL102 in Drug-Resistance, Microtubule Dynamics and HIF1α Signalling	94
4.1 Introduction	95
4.2 Results	97
4.2.1 EL102 and Microtubule Dynamics <i>In Vitro</i>	97
4.2.2 The Impact of EL102 Treatment on the Growth of Two Multi-Drug Resistant Cell Models	100
4.2.3 Examining the Inhibitory Effects of EL102 on a Panel of Kinases	103
4.2.4 EL102 Reduces Cellular HIF1 α Protein <i>In Vitro</i>	104
4.2.5 Examining the Effects of EL102-Mediated HIF1 α Deactivation	106
4.3 Discussion	110
4.3.1 EL102 Destabilises Microtubule Structures	110
4.3.2 EL102 Circumvents Two Classic Models of Drug Resistance <i>In Vitro</i>	112
4.3.3 The Ability of EL102 to Inhibit HIF1 α and Certain Kinases May Have Significant Clinical Implications	113
Chapter 5: Investigating the Potential Role of EL102 as a Disruptor of Androgen Signalling in Prostate Cancer	115
5.1 Introduction	116
5.2 Results	117
5.2.1 Ligand–Nuclear Receptor Interaction In the Presence of EL102	117
5.2.2 Determination of the Cytotoxic Profile of EL102 in AR-Positive Cell Line, LNCaP	119
5.2.3 EL102 Decreases AR Protein and AR Gene Expression <i>In Vitro</i>	120

5.2.4 Analysis of the Expression Patterns of AR Protein Following EL102 Treatment	122
5.2.5 EL102 Disrupts the Binding of AR to Androgen Response Elements in a Dose-Dependent Manner	124
5.2.6 Investigating the <i>In Vitro</i> Effects of EL102 on AR-Induced CXCR4 Expression and CXCR4-Mediated Migration	126
5.3 Discussion	128
5.3.1 EL102 Inhibits the Binding of Androgen and Progesterone to AR and PR, Respectively, in a Cell-Free Assay	128
5.3.2 EL102 Inhibits Expression and Activation of AR <i>In Vitro</i>	129
Chapter 6: Final Discussion	131
6.1 Overview	132
6.2 HIF1 α Inhibition and Microtubule Disruption in Prostate Cancer Treatment	133
6.3 Castration-Resistance and Chemotherapy Resistance in Prostate Cancer	134
6.4 Experimental Critique	136
6.5 Conclusions	138
Chapter 7: Bibliography	139
Appendices	170
Appendix I – Cell Line Specifications	171
Appendix II – The novel toluidine sulphonamide EL102 shows pre-clinical <i>in vitro</i> and <i>in vivo</i> activity against prostate cancer and circumvents MDR1 resistance Toner et al. Br J Cancer (2013)	181
Appendix III – Ambit KinomeScan Results	194
Appendix IV – Cerep Diversity Profile	201

Declaration:

I, Aidan Toner, certify that this thesis is my own work, with the exception of instances wherein I have presented collaborative data and have clearly identified and credited the collaborating party by name and/or appropriate citation. I also, certify that I have not previously obtained a degree in this University or elsewhere else on the basis of any of this work.

Signed: _____ Date: _____

Research Outputs:

Peer-Reviewed Research Publication:

The novel toluidine sulphonamide EL102 shows pre-clinical *in vitro* and *in vivo* activity against prostate cancer and circumvents MDR1 resistance. *Toner et al. Br J Cancer. 2013 Oct 15; 109 (8):2131-41.*

Oral Presentations:

EL102, A Novel Chemotherapeutic Candidate for the Treatment of Prostate Cancer, Inhibits HIF1 α Activity, AR Expression and Microtubule Stability. NUIG College of Medicine, Nursing and Health Science Postgraduate Research Day, May 28, 2014.

Introducing novel toluidine sulfonamide EL102: A potential chemotherapeutic agent in prostate cancer. (Abstract published Journal of Clinical Urology. September 2013 vol. 6 no. 5 p338). Irish Society of Urology Annual Meeting 2013 Sept. 20-21.

Introducing novel toluidine sulphonamide EL102, a potential chemotherapeutic in prostate cancer. (Abstract published 2013 BJU International, Vol.111, Supplement 3, p61.) British Association of Urological Surgeons (BAUS), Manchester, U.K., June 17th – 20th 2013.

Abstracts and Poster Presentations:

Further preclinical assessment of compound EL102 in the treatment of prostate cancer. Journal of Clinical Oncology, 2014 ASCO Annual Meeting Abstracts. Vol 32, No 15_suppl (May 20 Supplement), 2014.

Characterisation of a New Class of Prostate Cancer Chemotherapeutics. Irish Association for Cancer Research (IACR) Annual Meeting, Galway Bay Hotel, Galway. Feb 27 & 28, 2014.

Preclinical analysis of EL102, a novel compound proposed for the treatment of prostate cancer. 3rd Annual Academic Screening Workshop Sheraton Baltimore North Hotel, MD. Sept 17 & 18, 2013.

Introducing Novel Toluidine Sulfonamide EL102, A Potential Chemotherapeutic In Prostate Cancer.' Irish Association for Cancer Research (IACR) Annual Meeting, Crowne Plaza, Dublin. Feb 28 - Mar 1, 2013.

Treatment of Prostate Cancer Using Novel Compound EL102 In Combination With Taxane Chemotherapy. Royal Academy of Medicine in Ireland (RAMI) Biomedical Sciences Section Conference, Bailey Allen Hall, NUIG. Jun 14, 2012.

Prostate cancer inhibitory activity of a novel dual inhibitor, EL102, in combination with docetaxel and its effects on MDR1-mediated drug resistance *in vitro*. J Clin Oncol 30, 2012 (suppl; abstr e15126).

EL102: A Novel Dual Inhibitor which Demonstrates Additive Prostate Cancer Inhibitory Activity in Combination with Docetaxel *in vitro* and in Mouse Models. Irish Association for Cancer Research (IACR), Belfast, Northern Ireland. Feb 29 - Mar 2, 2012.

EL102: A novel dual inhibitor which demonstrates additive prostate cancer inhibitory activity in combination with docetaxel *in vitro* and in mouse models. (Abstract published Cancer Research February 6, 2012 72; B18). American Association for Cancer Research (AACR) Advances in Prostate Cancer Research, Orlando, FL, USA. Feb 6 - 9, 2012.

Pre-clinical development of the novel, broad spectrum, anti-cancer agent EL102. (Abstract published *Cancer Res April 15, 2011; 71(8 Supplement): LB-385*). American Association for Cancer Research (AACR) 102nd Annual Meeting, Orlando, FL, USA. 2011- Apr 2 - 6, 2011.

Travel Bursary:

Irish Cancer Society Travel Bursary: The First Annual Prostate Cancer Charity (UK) Meeting, Whitehall, Westminster, London. Oct 13 & 14, 2011.

List of Figures

- 1.1 – Sagittal view of the male genitourinary system.
- 1.2 – Determining risk of prostate cancer progression.
- 1.3 – Gleason scoring of prostate cancer.
- 1.4 – Androgen receptor activation and structure.
- 1.5 – The activities of (A) GnRH agonists and (B) GnRH antagonists.
- 1.6 – Basic schematic of HIF1 α activities.
- 1.7 – Chemical structure of ELR510444.
- 1.8 – Preliminary EL102 data.
- 2.1 – Typical protein standard curve in BCA protein quantification.
- 3.1 – Comparative dose response curves of a panel of prostate cancer cell lines to EL102 and docetaxel.
- 3.2 – Impact of EL102 and docetaxel alone and in combination in CWR22 xenograft models.
- 3.3 – *In vitro* cytotoxic profiles of combined exposure to EL102 and docetaxel in a panel of prostate cancer cell models.
- 3.4 – EL102-induced caspase3-like activity in prostate cancer cell lines.
- 3.5 – Flow cytometric analysis of sub-G₁ populations resulting from EL102 and docetaxel treatment over 72 h.
- 3.6 – Cell cycle analysis of DU145 cell accumulations in G₁, S, G₂/M, and sub-G₁ phase after EL102, docetaxel or combination treatment.
- 4.1 – Tubulin polymerisation assay.
- 4.2 – Immunofluorescent staining of β -tubulin and acetylated tubulin in DU145 following 24 h EL102 and docetaxel treatment.
- 4.3 – EL102 dose-response curves of a panel of drug-resistant cell lines.
- 4.4 – Kinase inhibitory potential of EL102 treatment.
- 4.5 – Analysis of HIF1 α protein expression levels *in vitro* following EL102 treatment.

- 4.6 – HIF1 α is deactivated through the activities of EL102 *in vitro*.**
- 4.7 – Analysis of HIF1 α transcriptional targets in PC-3 cells following EL102 treatment.**
- 5.1 – Radiolabelled nuclear receptor ligand binding assay.**
- 5.2 – EL102 dose response curve of LNCaP cells.**
- 5.3 – LNCaP protein and gene expression of AR following simultaneous treatment with EL102 and 1nM R1881/vehicle.**
- 5.4 – Immunocytofluorescence of AR and acetylated-tubulin (Ac-Tub) in the presence or absence of 1 nM R1881 and microtubule disruptors.**
- 5.5 – Reporter gene assay of endogenous AR activation in response to EL102 antagonism.**
- 5.6 – Analysis of CXCR4 expression and function in response to EL102 treatment *in vitro*.**

List of Tables

- 1.1 – The D’Amico system of patient risk stratification.**
- 2.1 – Cell lines.**
- 2.2 – List of antibodies.**
- 2.3 – List of qPCR primers.**
- 2.4 – Supplier and distributor information.**
- 3.1 – Table 3.1 – Prostate cancer cell lines: 50 % cell survival (IC_{50}) following 72 h docetaxel or EL102 treatment.**
- 3.2 – One way analysis of variance with Tukey’s multiple comparison test of murine xenograft experiment: analysis of difference in tumour volumes between treatment groups.**
- 3.3 – One way analysis of variance with Tukey’s multiple comparison test of murine xenograft experiment: analysis of difference in body weight between treatment groups.**
- 4.1 – Cross-resistance profile of DLKP, DLKPA, DLKPA-SQ and DLKP-SQ-Mitox**

List of Abbreviations

°C – Degrees Celcius

2/3D-QSAR – Two/three-dimensional quantitative structure-activity relationship

2ME2 – 2-methoxyestradiol

5-ARI – 5-*alpha* reductase inhibitor

aa – Amino acid

ABC – Adenosine triphosphate binding cassette

Ac-Tub – Acetylated tubulin

AD – Androgen deprivation

ADT – Androgen deprivation therapy

AFU – Arbitrary fluorescent units

AIF – Apoptosis-inducing factor

ANOVA – Analysis of variance

APS – Ammonium per sulphate

AR – Androgen receptor

ARE – Androgen response element(s)

ARNT – Aryl hydrocarbon receptor nuclear translocator protein

ATCC – American Type Culture Collection

ATP – Adenosine triphosphate

AZ – Anterior zone

BCA – Bicinchoninic acid

BCRP – Breast cancer resistance protein

bHLH – Basic helix-loop-helix

BMS – Bristol-Myers Squibb

BOO – Bladder outlet obstruction

BPH – Benign prostatic hyperplasia

BSA – Bovine serum albumin

CAR – Constitutive androstane receptor

cdNA – Complementary deoxyribonucleic acid

CDX – Casodex (Bicalutamide)

CHAPS – 3-[(3-Cholamidopropyl)dimethylammonio]-1-propanesulfonate

CHAARTED – Chemohormonal Therapy versus Androgen Ablation
Randomized Trial for Extensive Disease in Prostate Cancer

cm – Centimetre

CMV – Cytomegalovirus

CNS – Central nervous system

CO₂ – Carbon dioxide

CoCl₂ – Cobalt chloride

CPRG – Chlorophenol red-β-D-galactopyranoside

CRADA – Cooperative research development agreement

CRPC – Castrate-resistant prostate cancer

CRT – Conformal radiotherapy

CSCs – Cancer stem cells

CS-FBS – Charcoal-stripped foetal bovine serum

CT – Computed tomography

Ct – Threshold cycle

CTE – Carboxyl terminal extension

CV – Coefficient variance

CXCL12 – C-X-C motif chemokine twelve (SDF1α)

CXCR4 – Chemokine (C-X-C motif) receptor 4

CYP2C9 – Cytochrome P450 2C9

CZ – Central zone

DAPI – 4',6-diamidino-2-phenylindole

DBD – Deoxyribonucleic acid-binding domain

D-box – Distal box

DEPC – Diethylpyrocarbonate

DEVD – Tetra-peptide aspartic acid-glutamic acid-valine-aspartic acid

dH₂O – Distilled water

DHT – Dihydrotestosterone

DMSO – Dimethyl sulfoxide

DNA – Deoxyribonucleic acid

dNTP – Deoxyribonucleotide triphosphate(s)

dPBS – Dulbecco's modified phosphate buffered saline

DRE – Digital rectal exam

DTT – DL-dithiothreitol

EBRT – External beam radiation therapy

ECL – Electrogenerated chemiluminescence

ED – Erectile dysfunction

EDTA – Ethylenediaminetetraacetic acid

EGF – Epithelial growth factor

EGFR – Epithelial growth factor receptor

EGTA – Ethylene glycol-bis(2-aminoethylether)-*N,N,N',N'*-tetraacetic acid

ELISA – Enzyme-linked immunosorbent assay

EPO – Experimental Pharmacology and Oncology

ER – Oestrogen receptor

ERE – Oestrogen response element(s)

ERR α – Oestrogen-related receptor

FBS – Foetal bovine serum

FDA – Food and Drug Administration

FFbF – Freedom from biochemical failure

FIH – Factor inhibiting hypoxia inducible factor

GA – Geldanamycin

GAPDH – Glyceraldehyde 3-phosphate dehydrogenase

GLUT1 – Glucose transporter one

GMBH – Gesellschaft mit beschränkter Haftung (Company with limited liability)

GM-CSF – Granulocyte-macrophage colony stimulating factor

GnRH – Gonadotropin-releasing hormone (LH-RH)

GR – Glucocorticoid receptor

Gy – Gray

h – Hour(s)

HBSS – Hanks' Balanced Salt Solution

HDR – High dose rate

HEPES – 4-(2-Hydroxyethyl)piperazine-1-ethanesulfonic acid, N-(2-Hydroxyethyl)piperazine-N'-(2-ethanesulfonic acid)

HIF1 α – Hypoxia-inducible factor one *alpha*

HNPCC – Hereditary non-polyposis colorectal cancer

HRE – HIF1 α response element(s)

HRP – Horseradish peroxidase

HSP – Heat shock protein(s)

IC₅₀ – Concentration of an inhibitor where the response (or binding) is reduced by half

ICC – Immunocytochemistry

IGF – Insulin-like growth factor

IGFR – Insulin-like growth factor receptor

IgG – Immunoglobulin G

IL-6 – Interleukin six

IMRT – Intensity-modulated radiotherapy

iv – Intravenous

Kb – Kilobase(s)

KCl – Potassium chloride

L – Litre

LB – Lysogeny broth

LDHA – Lactate dehydrogenase A

LDR – Low dose rate

LH – Luteinising hormone

LH-RH – Luteinising hormone-releasing hormone (GnRH)

LSD1 – Lysine-specific demethylase one

LUTS – Lower urinary tract symptoms

M – Mole(s)

mA – Milliampere(s)

mAb – Monoclonal antibody

mCRPC – Metastatic castrate resistant prostate cancer

MDR1 – Multi-drug resistance one

MEM – Minimum essential medium

mg – Milligram(s)

MgCl₂ – Magnesium chloride

min – Minute(s)

ml – Millilitre(s)

mm – Millimetre(s)

mM – Millimole(s)

MMTV – Mouse mammary tumour virus

MR – Mineralocorticoid receptor

MRI – Magnetic resonance imaging

mRNA – Messenger ribonucleic acid

MRP1 – Multi-drug resistance associated protein one

MT – Microtubule

NAB – Nanoparticle albumin bound

NaCl – Sodium chloride

NaOH – Sodium hydroxide

NDA – New drug application(s)

NFκB – Nuclear factor *kappa* B

NGF – Nerve growth factor

NLS – Nuclear localisation signal

nm – Nanometre(s)

nM – Nanomole(s)

NSAIDs – Non-steroidal anti-inflammatory drugs

NSCLC – Non-small cell lung carcinoma

O₂ – Oxygen

OD – Optical density

pAb – Polyclonal antibody

PAGE – Polyacrylamide gel electrophoresis

PAP – Prostatic acid phosphatase

PARP – Poly (adenosine diphosphate-ribose) polymerase

P-box – Proximal box

PCD – Programmed cell death

PCNA – Proliferating cell nuclear antigen

PCR – Polymerase chain reaction

PFA – Paraformaldehyde

P-gp – P-glycoprotein (MDR1)

PI – Propidium iodide

PIA – Proliferative inflammatory atrophy

PIN – Prostatic intraepithelial neoplasia

po – *Per os* (orally)

PPARγ – Peroxisome proliferator activator receptor *gamma*

PR – Progesterone receptor

PRF – Phenol red-free

PSA – Prostate-specific antigen

PTEN – Phosphatase and tensin homolog

PVDF – Polyvinylidene fluoride or polyvinylidene difluoride

PXR – Pregnane X receptor

PZ – Peripheral zone

qPCR – Quantitative polymerase chain reaction

R1881 – Methyltrienolone

RLU – Relative light unit(s)

RNA – Ribonucleic acid

rpm – Revolutions per minute

RPMI – Roswell Park Memorial Institute

RT – Room temperature

RTCA – Real-time cell analyser

RT-PCR – Reverse transcription polymerase chain reaction

SBRT – Stereotactic body radiation therapy

SC – Subcutaneous

SD – Standard deviation

SDF1 α – Stromal cell-derived factor one *alpha* (CXCL12)

SDS – Sodium dodecyl sulphate

sec – Second(s)

SEM – Standard error of the mean

SFM – Serum-free medium

SOC – Super Optimal broth with Catabolite repression

SRB – Sulforhodamine B

TAE – Tris acetate ethylenediaminetetraacetic acid

TBS – Tris-buffered saline

TBST – Tris-buffered saline with tween-20

TCA – Trichloroacetic acid

TEMED – Tetramethylethylenediamine

TF – Transcription factor

TKI – Tyrosine kinase inhibitor

TR – Thyroid hormone receptor

TRAIL – Tumour necrosis factor-related apoptosis-inducing ligand

TUMT – Transurethral microwave therapy

TUNA – Transurethral needle ablation

TZ – Transition zone

UK – United Kingdom

USA – United States of America

V – Volt(s)

VCR – Vincristine

VDR – Vitamin D receptor

VEGF – Vascular endothelial growth factor

VEGFR – Vascular endothelial growth factor receptor

VHL – Von Hippel-Lindau

WB – Western blot

WR – Working reagent

β-gal – *Beta*-galactosidase

μg – Microgram(s)

μl – Microliter(s)

μM – Micromole(s)

Abstract

Prostate cancer remains a growing problem for the male population, globally. Though there have been clinical advances in recent years, there still remains a need to develop drugs that can slow or stop progression beyond the organ-confined phase to distal aggressive metastases. Using the NCI-60 drug screen panel, the novel compound, EL102, was identified as a potent cytotoxin from a large screen of small molecule inhibitors. Classified as a toluidine sulphonamide, EL102 had displayed strong anti-cancer potential in the range of cell types assayed. Among these cell lines were prostate cancer models, PC-3 and DU145. These cell lines, along with fellow prostate cancer *in vitro* models CWR22, 22Rv1 and LNCaP were investigated further for their response to EL102 treatment. A 50 % reduction in cell viability was observed upon EL102 treatment of the *in vitro* panel, at a dose range of 20–50 nM. When EL102 was administered to CWR22 murine xenograft models, in combination with clinically-used docetaxel, a significant reduction in the rate of tumour growth was observed when compared to mice treated with either drug alone. Importantly, body weights remained consistent between the treatment arms, suggesting doses were well-tolerated, within this cohort. These data suggest the suitability of EL102 as a companion treatment. Separately, this study has determined that EL102 is a microtubule destabiliser that induces apoptosis.

A previous 3D-quantitative structure-activity relationship (QSAR) study of toluidine sulphonamides, predicted these compounds directly inhibit hypoxia inducible factor 1 *alpha* (HIF1 α). The findings of this document support that prediction. Moreover, the current study has detailed a role for EL102 as an androgen receptor (AR) antagonist which gives credence to the rationale for use as an anti-prostate cancer therapy. *In vitro* investigations, detailed within this study, have also asserted that EL102 has the capacity to overcome acquired drug-resistance mechanisms associated with MDR1 and BCRP up-regulation. Overall, EL102 is a multimodal compound which serves to impede prostate cancer cell survival through direct inhibition of important cell survival cues.

Acknowledgements

I would first like to thank my supervisors, Dr. Sharon Glynn and Prof. Frank Sullivan, for taking a chance on me and offering me four rewarding years of research.

I am immensely grateful to Prof. Frank Giles, Dr. Joe Lewis and all at Elara Pharmaceuticals for providing me with the opportunity to work on such an interesting compound.

Of course this research would not have been possible without solid financial backing. I would like to thank the University Foundation for their generous support over the course of my studies.

I have been very fortunate to have met some truly remarkable people in my time in the NCBES, ARC and PCI. I would like to say thanks to all who offered advice, experience, support and friendship during my studies. You made the life of this miserable Ph.D. student so much easier in the face of impossible tasks: Thanks Gemma (of course you are top of my list!), Siobhán, Alex, Mike, Ger, Robert, Aideen, Liam, Hanno, Shirley and Triona.

I would like to thank my fellow labmates in the PCI for all the good times over the years: Carol, Amy, Sarah, Rónán, Ali, Pablo and Karen.

RANDOM ANIMALS! : Thanks a million for these Michelle, Sinead and Jill and for so many days of laughs, antibodies, pseudonyms, puns, slides, chocolate, nail varnish.... You guys almost kept me sane!

Mary soon to be **Ní** no longer! Go maire tú! I wish you and Brian, both, full health and all the happiness life can offer! My undisputed oldest friend in the lab! I was so lucky to have joined you in 202. Thanks for putting up with me, my pizza, my HEPES and 2 tickets!!

I owe a huge debt of thanks to Prof. Corrado Santocanale and his exemplary lab (over the years): Gemma, Edel McG, Edel Mullrz, Aisling, Kevin, Mike, Alex, Guan-Nan, Aga, Breege, Jennifer and David. (All keeping the world populated since 2008!)

Thanks to my brother and sisters for putting up with all of my complaining and for your eternally unmatched friendship and support: **Siblings:** Elaine, John, Breege (Congratulations Breege!!) and Maeve. **In-laws:** Gerry, Karyn and soon... Barry. And of course who could forget my niece Freya and nephews Stephen, Conall and Ethan...keep 'em comin'! I love you all!

Last, but not least, I am forever indebted to three people, without whom, there would be no thesis: Dr. Jill McMahon and, my parents, Annie and Pat Toner. Thank you so much for all of your help, support and laughs through tough times and, in particular, these past few months.

Jill you are an amazing scientist and friend. I just don't know how I can ever repay your kindness and generosity. Can I start with a Bay Ale!? There really are no words good enough. Thank you!

Thanks Mum and Dad, you have given so much to me without ever asking in return. The opportunities that I have gotten in life have only been the result of your commitment to providing a future for your children. You have, both, instilled in me the true value of hard work, persistence, friendship, fairness, compassion and decency. You have always taken an interest in our learning and given us the best chance to succeed in life. It frustrates me, to know that I can never repay such a debt. I love you both and thanks!

I wish to dedicate this thesis to my parents, Annie and Pat Toner for their unfailing love and support through all my endeavours.

Chapter 1:

General

Introduction

1.1 Prostatic Disease

1.1.1 The Human Prostate

The male accessory exocrine gland known as the prostate is a compound gland, comprised of a collective of 30–50 tubuloacinar glands bound by a fibrous muscular vascularised capsule and is located immediately inferior to the bladder, where it surrounds the urethra and urinary duct. The average fully developed prostate weighs 20 grams and is often compared to a walnut in appearance and size, measuring 2x3x4 cm. Its primary function is the production of an alkaline liquid which contributes to 20 % of the total volume of semen (Aumüller, 1979; Moore & Dalley, 2006; Steive, 1930). Secondary to this, the prostate aids at the point of ejaculation through the contraction of its encapsulating fibrous muscular layer which transects the prostatic tissue into 4 zones: the peripheral zone (PZ), the anterior zone (AZ), the central zone (CZ) and the transition zone (TZ). Each zone maintains a distinct ductal system (Kumar & Majumder, 1995; McNeal, 1980). The human prostate is unusual in that, outside of the central nervous system, it is the most abundant producer of nerve growth factor (NGF) (Murphy *et al.*, 1984).

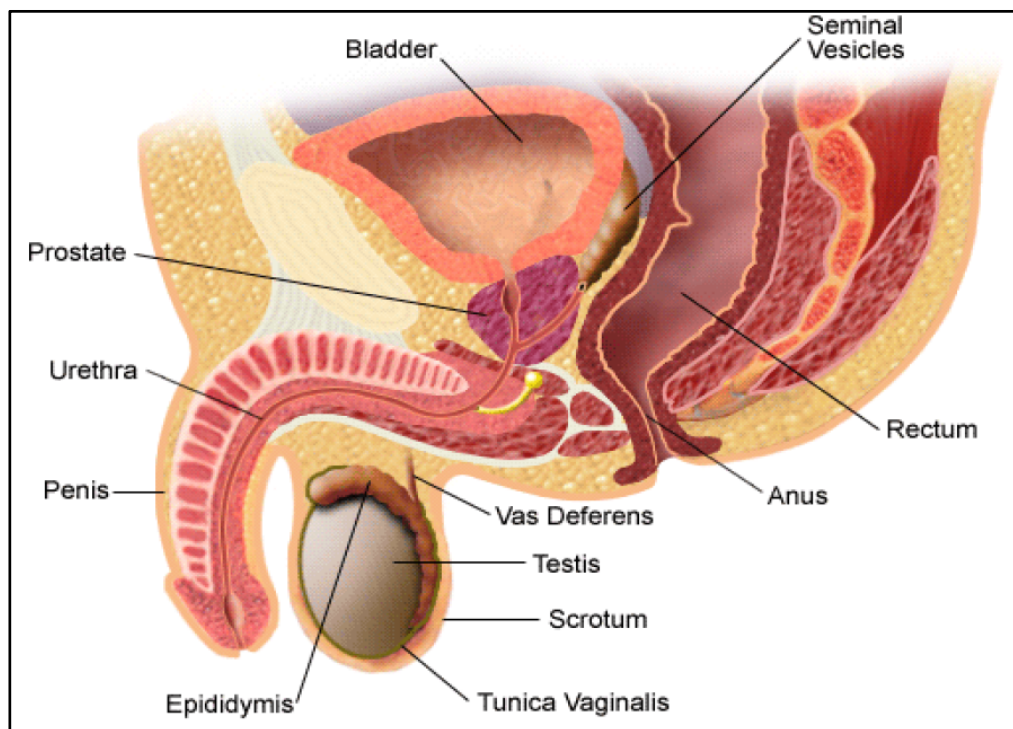


Figure 1.1 – Sagittal view of the male reproductive system (Lepor, 1999).

1.1.2 Prostatitis

Infection of the prostate can sometimes cause a temporary localised inflammation and occurs in men of all ages. This is known as prostatitis (Ritz, 1983). There are three types of prostatitis: acute bacterial prostatitis, chronic bacterial prostatitis and chronic non-bacterial prostatitis (Hua & Schaeffer, 2004; Persson & Ronquist, 1996). Acute bacterial prostatitis, though rare, is considered the most severe, in terms of symptoms, with patients usually presenting with acute urinary tract infection and increased urinary frequency with urgency. Also, patients often exhibit pyrexia, nausea, vomiting and burning sensation when urinating. Acute bacterial prostatitis requires immediate intervention, as the condition can lead to bladder infections, prostatic abscesses or, in extreme cases, complete urinary obstruction. If untreated, the condition can result in low blood pressure, and may be fatal. This form of prostatitis is usually treated with intravenous (iv) antibiotics, iv analgesics and iv fluids (Lockie, 1981). Often the product of repeated urinary tract infections that have spread to the prostate gland, chronic bacterial prostatitis is widely thought to be asymptomatic for several years in men before manifesting. Though symptoms are similar to acute bacterial prostatitis, they are less severe and can fluctuate in intensity. Diagnosis can be difficult as bacteria are not readily identified in urine. A 1–3 month course of oral antibiotics is the preferred method of treatment. Chronic non-bacterial prostatitis or chronic pelvic pain syndrome, as it is also known, is the most commonly diagnosed form of prostatitis, accounting for 90 % of incidence (Lockie, 1981). Symptoms include urinary and genital pain which can be confused with interstitial cystitis. Though bacteria are absent from urine, alternate markers of inflammation are detected. *Alpha*-adrenergic blockers and non-steroidal anti-inflammatories (NSAIDs) are given to patients with this form of prostatitis as treatment (Dunzendorfer & Feller, 1981; Rivero *et al.*, 2007). While inflammation of tissues has been implicated in the occurrence of many cancer types, it is still presently debated whether prostatitis increases the risk of prostate cancer. It is however postulated that exposure to environmental factors such as microbes and dietary carcinogens, as well as hormonal imbalances could result in prostatic injury and development of

chronic inflammation and regenerative signalling lesions. This has been termed proliferative inflammatory atrophy (PIA) and may escalate to the onset of prostatic intraepithelial neoplasia (PIN) and eventually prostatic adenocarcinoma development (De Marzo *et al.*, 2007; Sfanos *et al.*, 2014).

1.1.3 Benign Prostatic Hyperplasia

Originating in the transition zone, benign prostatic hyperplasia (BPH) is the enlargement of the prostate and is diagnosed through digital rectal exam (DRE) owing to the proximity of the gland to the rectal wall, and detection of elevated prostate specific antigen (PSA) in blood tests (McNeal, 1978). It comes about through the proliferation of epithelial and smooth muscle cells in the transition zone and is diagnosed histologically following biopsy (Bostwick *et al.*, 1992). The reason for this growth is thought to be orchestrated by an adulthood reawakening of embryonic processes owing to similarities observed in prostate morphogenesis during embryonic stages and prostatic hyperplasia (Lowsley, 1912; McNeal, 1978; Price, 1963). The increased mass of the prostate may occur in two ways: the direct obstruction of bladder outlet (BOO) and the obstruction of the dynamic phase of the prostate through increased smooth musculature (Roehrborn, 2008). Though not considered life threatening, the lower urinary tract symptoms (LUTS) mentioned can impact considerably on quality of life. LUTS increases with age. This, when combined with the fact that population life expectancies are on the rise, makes probable that the incidence of these problems is set to augment in the coming decades (Verhamme *et al.*, 2002). BPH is normally treated with an array of pharmacological options. *Alpha* blockers such as alfuzosin and doxazosin, used singularly or in combination with the 5-*alpha*-reductase inhibitors, dutasteride or finasteride are the current options open to BPH patients. Anticholinergic agents, also known as muscarinic receptor antagonists, such as tolterodine may serve to alleviate the overactive bladder symptoms that may coexist in cases of BPH (Bautista *et al.*, 2003; Kaplan *et al.*, 2006; MacDonald & Wilt, 2005). A number of surgical measures are available in complement of or as alternatives to chemical intervention. These include the minimally invasive procedures of transurethral needle ablation (TUNA) and transurethral microwave thermotherapy (TUMT) or the more

aggressive techniques of open prostatectomy or transurethral resection of the prostate (TURP). TUNA is widely regarded as a relatively safe process reporting low perioperative complications (such as bleeding) with a low to non-existent rate of associated erectile dysfunction (ED). If given the choice over a more invasive therapy like open prostatectomy, which is typically performed on patients with prostate volumes greater than 80 to 100 ml, TUNA may be preferred in terms of post-procedure quality of life (Malaeb *et al.*, 2012). It has not been overlooked that there is a strong link between BPH and prostate cancer occurrence. In fact, in recent years it has become clear that those hospitalised as a result of BPH were twice as likely, to develop prostate cancer than age matched individuals, in the general population while those who underwent BPH-related surgery were three times more at risk of prostate cancer (Orsted & Bojesen, 2013).

1.1.4 Prostate Cancer Diagnosis and Incidence

As the second leading cause of cancer-related death in men of the Western World, prostate cancer between individuals can be quite diverse in terms of symptoms and quality of life (Jemal *et al.*, 2011; WHO, 2014). In Ireland, approximately 3000 cases are diagnosed annually with higher incidence reported on the west coast (NCRI, 2011). Recent statistical data indicate that over 500 deaths occur each year in Ireland as a direct consequence of prostate cancer progression (NCRI, 2014). Prostate cancer initially manifests itself through discovery of a lump or enlargement upon DRE and/or detection of elevated serum levels of PSA following blood tests (Aus *et al.*, 2005). In Ireland there is currently no national screening programme for the disease. A number of risk factors have been identified with regard to prostate cancer however these remain poorly understood. What is known is that age certainly plays a significant role in risk with diagnosed cases in those less than 40 years of age being rare, while 60 % of prostate cancer cases are found in those over 65 years of age (Greenlee *et al.*, 2001; Nelson *et al.*, 2003). Studies in the United States of America (USA) have found that those of African descent were found to be not only more at risk of developing prostate cancer but were two times more likely to die from the disease than age matched non-Hispanic white counterparts. Also, men of Asian descent or

Hispanic/Latino extraction were less inclined to be diagnosed than non-Hispanic white counterparts. When taken together, these data suggest that ethnicity could play a substantial role in terms of risk of prostate cancer (Mettlin & Murphy, 1994; Mettlin *et al.*, 1995). A genetic predisposition has been put forward as the cause of a subset of prostate cancer incidence as men reported to possess inherited mutations in BRCA1 and BRCA2 as well as those diagnosed with Lynch syndrome (hereditary non-polyposis colorectal cancer (HNPCC)) are deemed higher risk candidates. To fully understand these risk factors several studies have been commissioned and research is ongoing (Castro *et al.*, 2013; Chang *et al.*, 2014; Tryggvadottir *et al.*, 2007).

Clinicians have endeavoured to anticipate the correct clinical course of action with regard to treatment so as to minimise the risk of recurrence, progression or threat to patient survival. To that end, methods of risk assessment have been developed and are used worldwide to determine optimal individual treatment based on risk. One such risk assessment is the D'Amico method which utilises tumour size (T-stage) determined upon rectal examination (more often, in combination with ultrasound examination), PSA level and Gleason score to categorise risk as low, intermediate and high. Table 1.1 summarises the criteria for these three levels of risk. Though considered an effective tool in prostate cancer treatment, D'Amico classification does not account for a multitude of other risk factors (D'Amico *et al.*, 1998). To tackle these shortcomings, the mathematical models of nomograms and CAPRA scoring have been implemented to add to the list of variables when assessing risk in prostate cancer therapy. Frequently, clinicians will use a series of prognostic nomograms as a way to predict the likelihood of prostate cancer metastases. This parallel co-ordinate system was developed by the French engineer Philbert Maurice d'Ocagne as a way to replace standard Cartesian co-ordinates. As is shown in the example in Figure 1.2 (A), a nomogram consists of a series of parallel scales, each representing a particular variable. In prostate cancer treatment, nomograms are used in prediction of outcome only after the method of intervention has been decided upon (Kattan *et al.*, 1998; Kattan *et al.*, 2001; Kattan *et al.*, 2000). CAPRA

scoring is a method developed at the University of California, San Francisco, by which variables are assigned points which when totalled amount to a score on a scale of 1 to 10 (Cooperberg *et al.*, 2006; Cooperberg *et al.*, 2005). An example of this method can be seen in Figure 1.2 (B).

Table 1.1 – The D’Amico system of patient risk stratification.			
	Low	Intermediate	High
PSA	≤ 10	10–20	> 20
Gleason score	≤ 6	7	> 8
T-stage	T 1–2a	T 2b	T 2c–3a

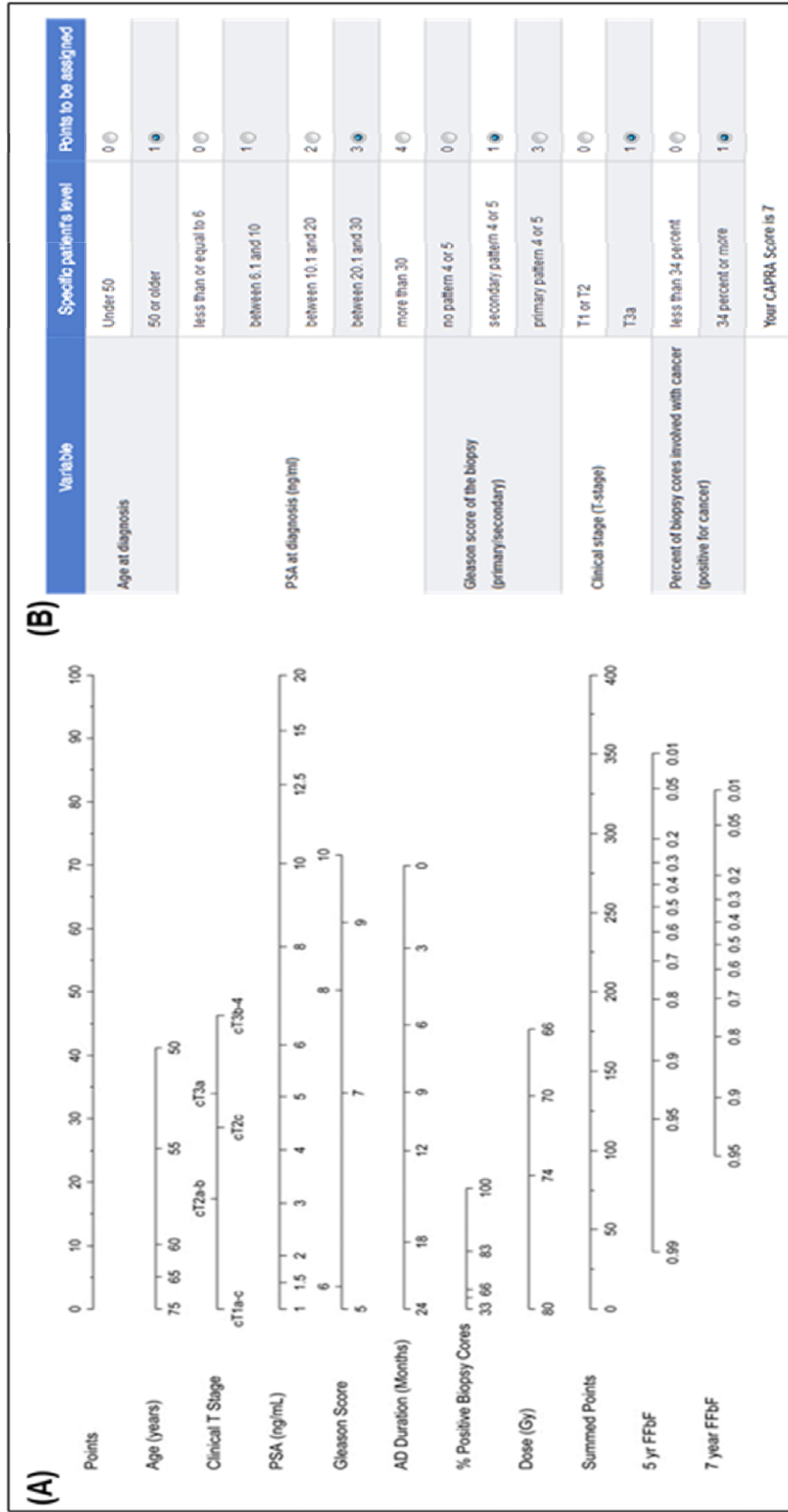


Figure 1.2 – Determining risk of prostate cancer progression. (A) Use of prognostic nomograms to determine risk (Williams et al., 2008). **(B)** Calculating a patient's UCSF-CAPRA score.

The most common form of prostate cancer is prostatic adenocarcinoma with 70 % developing in the PZ and 20 % occurring in the TZ (Chodak *et al.*, 2015; McNeal, 1969; McNeal, 1978). Early stages of the disease are asymptomatic which is why, often, only a more progressed stage is detected. Initial symptoms prompting medical intervention include, but are not limited to, nocturia, increased frequency of urination, pain upon urination, bone pain (in ribs, pelvis and/or spine) and ED (Huggins, 1947). Owing to the large number of false positives and false negatives for prostate cancer associated with detection through PSA testing, it, alone, is not advised as a diagnostic measure and for this reason, biopsies are required (Catalona *et al.*, 1994). Biopsy of the prostate can be achieved through transurethral, transrectal or transperineal routes with insertion of core biopsy needles (Veenema, 1953). The most common method of prostatic tissue collection is transrectal biopsy (Grabstald & Elliott, 1953). Tissue is then fixed and stained for microscopic examination.

Gleason scoring is a standard method of histologically-determining the aggressiveness of prostate tumours and anticipating the likelihood of progression this cancer and patient prognosis. It was devised the 1960's by Dr. Donald Gleason and colleagues at the University of Minnesota (Bailar *et al.*, 1966). The scoring system works on a scale of 1–5, with each number corresponding to a particular glandular histological pattern and cytological appearance. Within the specimens, the two most prominent scores are added together, giving the final Gleason score. According to the classic method, final scores range from 2–10, where a score of 2 offers the best prognosis and 10 represents the worst. Figure 1.3 (A) outlines, pictographically, the original criteria of Gleason scoring (Gleason, 1977). Clinically, however, more recent advances in histological assessment have led to the establishment of global consensus guidelines and practices amongst histopathologists as to what determines a Gleason score. Figure 1.3 (B) shows the most up-to-date schematic of Gleason scores. Cancer diagnosis is given at detection of Gleason score ≥ 6 (3 + 3) and patterns 1 and 2, depicted in Figure 1.3 (A) are never reported owing to a

reclassification of such tissues as atypical adenomatous hyperplasia (adenosis).

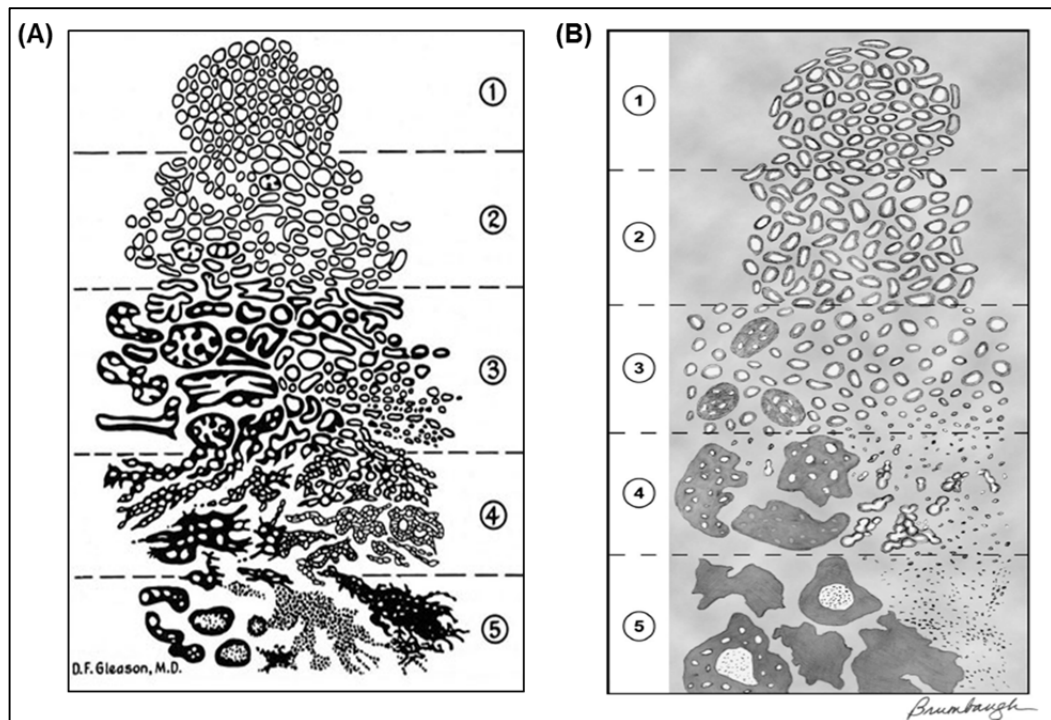


Figure 1.3 – Gleason scoring of prostate adenocarcinomas. (A) Original schematic of Gleason scoring (Gleason, 1977). **(B)** Modern, or modified schematic of Gleason scoring (Epstein *et al.*, 2005).

Like the process of PSA testing, prostatic biopsy also has its limitations. The variability of the number of cores collected and the locations within the prostate from which cores are obtained have the most profound impact on cancer detection rates. Recommendations over the past number of years suggest collection of 10–12 core biopsies, incorporating tissues from each of the prostatic zones. The use of ultrasound technology has assisted in the more precise guiding of biopsy needles by the operator (Bjurlin *et al.*, 2013; Sfakianos *et al.*, 2011). Although rates of cancer detection have increased through biopsy, entire sections of the prostate remain histologically unexplored, following the procedure, giving rise to potential oversight of particularly aggressive tumours. Also, transrectal biopsies carry considerable risk of causing serious infection, when used. It is for these reasons that much research has been carried out to determine less invasive methods of diagnosis and to identify more accurate novel diagnostic biomarkers of the

disease as well as to develop techniques of genetic typing to distinguish those most at risk of developing prostate carcinomas (Haiman *et al.*, 2013; Kim & Kislinger, 2013).

Prostate cancer can be categorised into three main disease states, namely organ-confined, locally-advanced and advanced (or metastatic) prostate cancer. In its organ-confined state, prostate cancer is found solely within the tissues of the four zones of the gland while locally advanced prostate cancer sees tumour progression in tissues that are prostate-adjacent, such as the seminal vesicles or the bladder, in addition to those of the prostate (Fellows *et al.*, 1992). Advanced prostate cancer is defined as the spread, or metastasis, of cancer arising in the prostate to distant sites within the body. The most common routes of metastasis are to osseous and lymphatic tissues (Coffey & Pienta, 1987). A major conduit for the relocation to bone is widely believed to be the prostatic venous plexus which connects with the internal iliac vein which in turn connects to the vertebral venous plexus (Batson, 1940). Distal lymph node metastases result through migration of cancer to the pelvic lymph node (Datta *et al.*, 2010).

1.2 Prostate Cancer Treatment

1.2.1 Prostatectomy

Prostatectomy is the process of surgical removal of the prostate gland. Partial removal of the prostate in a surgical process known as subtotal prostatectomy may only be required in benign circumstances, for example, urinary obstruction. Malignant occurrences such as that of prostate cancer require the more invasive approach of radical prostatectomy, where the whole prostate along with the seminal vesicles and vas deferens are removed, together with a small portion of the surrounding normal tissue. Treatment of low to intermediate risk level prostate cancers may be offered clinically in the form of radical prostatectomy alone or in combination with another treatment such as radiation. Advanced prostate cancer incidence, where metastasis is known to have occurred will not present this option of treatment. Metastasis is determined by bone scans, magnetic resonance imaging (MRI), computed tomography (CT) or more modern imaging

techniques such as positron emission tomography (PET). Failure of radiotherapy is sometimes cause for removal of the prostate (Bill-Axelsson *et al.*, 2005). Alterations to prostatic tissues, brought about through radiotherapy may present as a complication in the removal of the prostate (Walsh *et al.*, 1983). Prostatectomies may be 'open' such as suprapubic (through incision of the lower abdomen and through the bladder), retropubic (through the lower abdomen and through the pubic bone) and transperineal (through the perineum) or may be laparoscopic which may be either free-hand or robot-assisted (Moslemi & Abedin Zadeh, 2010; Walsh, 1988). Robot-assisted laparoscopic prostatectomy is a minimally invasive advancement which has been carried out with great success in the past number of years. It requires a series of small incisions (usually three) to be made along the abdomen through which the robotic arms and high resolution camera are placed. The operator, a specially trained surgeon, sits a short distance from the surgical table and controls the robotic assembly using two joysticks, guided by three-dimensional (3D) images projected by the high-resolution camera. The system is designed to give greater dexterity to the surgeon, minimising perioperative complication risk. This procedure shortens patient recovery time, reduces postoperative discomfort and pain as well as the risk of infection due to surgery (Guillonneau & Vallancien, 2000).

1.2.2 Radiotherapy

1.2.2.1 Brachytherapy

Brachytherapy is a radioactivity-based therapeutic technique that involves the surgical introduction of strategically-placed radioactive isotopes within the tumours of an array of cancers. It is frequently used in the treatment of prostate cancer to much success as evidenced by the reduction in size of tumours combined with low impact on a patient's quality of life. The procedure of implantation is minimally invasive and often offered on an outpatient basis. It presents reduced side effects compared to those posed by either external beam radiation therapy (EBRT) or prostatectomy (DeMuelenaere & Sandison, 1976; Lawton *et al.*, 1991). The isotopes or 'seeds', as they are more commonly known, are composed of Iodine-125

(¹²⁵I), palladium-103 (¹⁰³Pd) and caesium-131 (¹³¹Cs) which emit low yield X-rays to the surrounding tissue. The resulting DNA damage induced by these emissions incurs apoptosis in the tumours of the prostate. Seeds are implanted using a needle inserted through the perineum and may deliver low dose rate (LDR) of 2–12 gray per hour (Gy h⁻¹) or high dose rate (HDR) of >12 Gy h⁻¹ (Ash *et al.*, 2000; Salembier *et al.*, 2007; Wojcieszek & Bialas, 2012). Brachytherapy may be carried out in combination with chemotherapy and/or EBRT.

1.2.2.2 External Beam Radiation Therapy

Conventional EBRT is on the decline as modern advancements become more widely available. A method of shaping a radiation beam to match the 3D-conformation of the prostate, and affected surrounding tissues, is used frequently in early-stage prostate cancer treatment. This technique is known as 3D-conformal radiotherapy (CRT) (Zietman *et al.*, 2005). Intensity-modulated radiation therapy (IMRT) is another method of EBRT, designed to deliver highly conformal dynamic fields to prostate cancer patients. With the utility of sophisticated algorithmic software, a highly focused delivery of radiation to the intended tumour tissue targets, and not the adjoining normal tissues, is achieved (Jaffray *et al.*, 1999). Increasingly, the hypofractionation EBRT method of stereotactic body radiation therapy (SBRT) for prostate cancer is being offered clinically (Buyyounouski *et al.*, 2010)

1.2.3 Hormone Therapy

Androgens are central to prostate morphogenesis during human embryonic development and continue to have importance in the maintenance of healthy adult prostate function. When adenocarcinoma arises within prostatic tissue, androgen receptor signalling is utilised by the affected cells to sustain progression of the disease (Huggins & Hodges, 1941). The realisation of this fact has prompted the establishment of methods to disrupt this opportunistic mechanism of survival. Although an effective method of slowing prostate cancer progression, this androgen deprivation therapy (ADT) should be done in combination with another treatment such as radiotherapy (Milecki *et al.*, 2010).

1.2.3.1 Androgen Receptor

The androgen receptor (AR) belongs to the nuclear receptor superfamily and more specifically to the subfamily of steroid receptors, NR3 (Consortium, 1999; Laudet & Gronemeyer, 2002; Robinson-Rechavi *et al.*, 2003). With a 10 kb mRNA sequence coding for 900–920 amino acids (aa), AR is a large protein expressed in most tissues but especially male reproductive tissues, female ovarian and uterine tissues as well as the skeletal muscle, adrenal and hepatic tissues of both sexes (Bookout *et al.*, 2006). AR can be expressed as one of 2 isoforms A or B (Wilson & McPhaul, 1994). AR and the other members of the NR3 subfamily (such as mineralocorticoid receptor (MR) and progesterone receptor (PR)) share highly-conserved functional domains. Two zinc fingers, chelated by 8 out of 9 cysteine residues present, comprise the DNA-binding domain (DBD) (Gronemeyer, 1992).

Secreted androgens enter target cells by passive diffusion. The cytosolic AR is held inactive by a heat shock protein (HSP) complex until binding of the androgen occurs. This institutes a conformational change in AR causing the dissociation of the HSP complex and homodimerisation of the receptor before translocation to the nucleus. Within the nucleus, AR carries out its transcription factor (TF) role by coactivator-assisted interaction with genomic DNA segments termed androgen response elements (AREs). These are palindromic repeat sequences, each spaced by one codon (Roy *et al.*, 2001). Interaction with these sequences is regulated by the glycine-serine-cysteine-lysine-valine (GSCKV, aa 577–581) sequence also known as the proximal-box (P-box) located on the first zinc finger of the DBD. The stability of this interaction is believed to be determined by the distal-box (D-box), located on the second zinc finger of the DBD. The D-box consists of an alanine-serine-lysine-asparagine-aspartic acid residue sequence (aa 596–600) (Claessens *et al.*, 2008). The D-box, it is widely believed, influences AR homodimerisation (Claessens *et al.*, 1996; Umesono & Evans, 1989). Determinants of AR nuclear localisation are held within the hinge region which houses the carboxyl terminal extension (CTE). The CTE is thought to orchestrate the transactivation of the sequence that immediately succeeds the second zinc finger. The 4 aa sequence preceding the CTE and within the

hinge sequence is known as the T-box. The T-box is essential for DNA interaction as deletion studies have shown that this function is abrogated (Wilson *et al.*, 1992). Figure 1.4 summarises the activation of AR and shows the structure of the functional domains of AR.

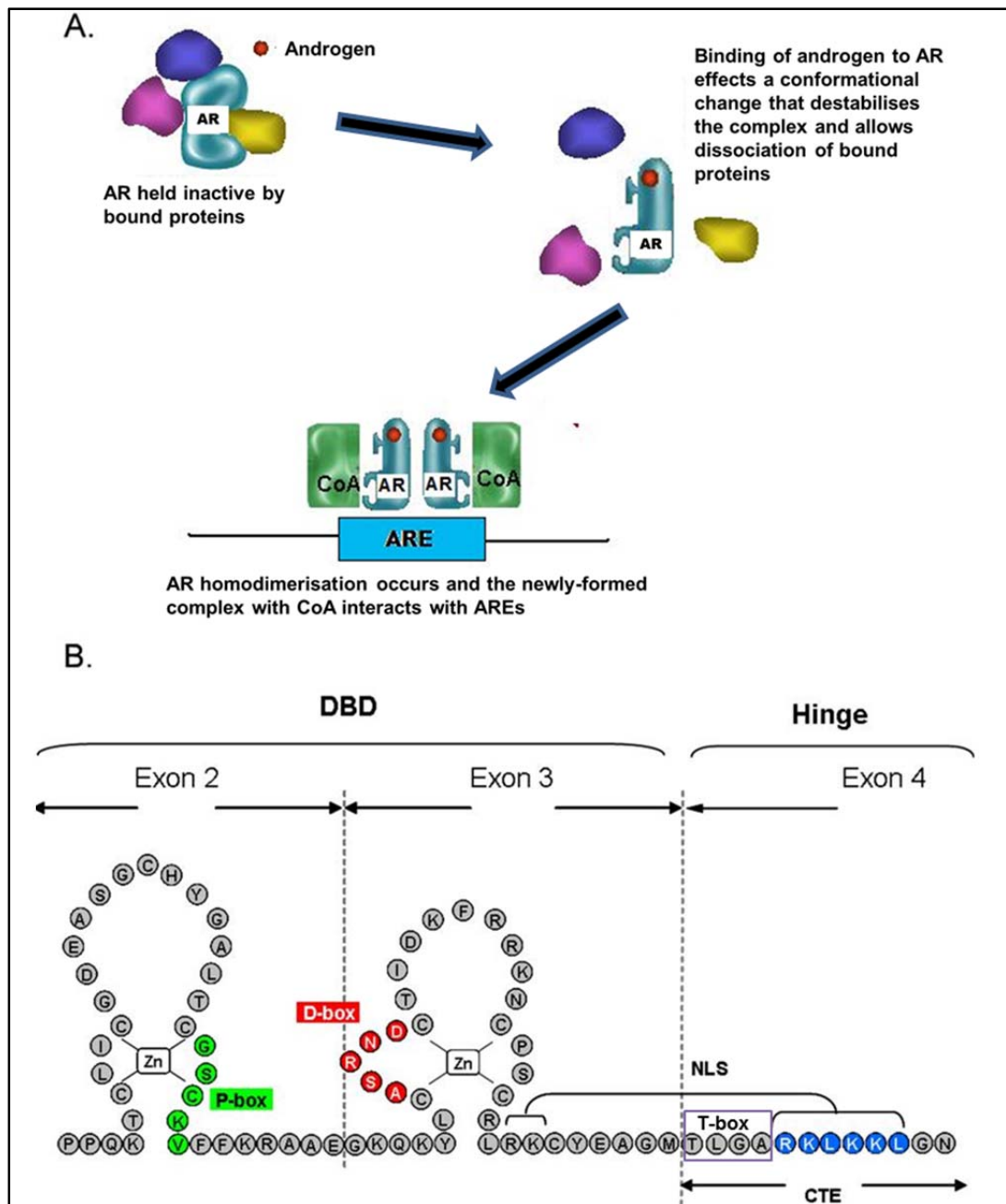


Figure 1.4 – Androgen receptor activation and structure. (A) Schematic of AR activation, translocation and dimerization (modified, (Toner, 2008)). (B) Schematic of the functional domains of AR with P-box in green, D-box in red and the nuclear localisation signal (NLS) in blue (modified, (Claessens *et al.*, 2008)).

1.2.3.2 Gonadotropin-Releasing Hormone Agonists and Antagonists

Testosterone is an androgen produced in the Leydig cells of the testes of males and in small amounts in the adrenal glands of males and females (Davison & Bell, 2006; Nussey & Whitehead, 2001). Ovarian production of minute testosterone quantities has been reported in females (Adashi, 1994). Testosterone is a precursor to the three times more potent dihydrotestosterone (DHT). The testes, adrenal glands and prostate all orchestrate the conversion of testosterone to DHT through the secretion of 5 α -reductase. A reduction of DHT triggers the release of a hormone from the hypothalamus, known as the gonadotropin releasing hormone (GnRH) which, in turn, effectuates pituitary gland production of luteinising hormone (LH). LH stimulates testosterone production by the Leydig cells allowing testosterone conversion to DHT (Blackburn & Albert, 1959; Saartok *et al.*, 1984). GnRH agonists are given to prostate cancer patients at an advanced hormone-responsive stage of the disease to disrupt this process of DHT synthesis. The agonists, goserelin and buserelin are frequently used in the setting of prostate cancer (Nicholson *et al.*, 1980). Administration of these agents initially causes a temporary surge in the amount of systemic testosterone production which may have deleterious effects. Side effects of LH agonists include hypogonadism. An alternate method considered clinically for the disruption of this signalling cascade is treatment with GnRH antagonists such as degarelix (Doehn *et al.*, 2006). These bind to pituitary GnRH receptors instituting a blockade of LH release without the initial testosterone surge witnessed with GnRH agonist exposure. The fall in testosterone levels is dramatic if the patient is responsive. It is for this reason that these antagonists are given to patients requiring immediate intervention. A decrease in prostate size is common side effect of treatment with this antagonist and responsiveness can be charted through the lowering of PSA blood levels (Nicholson *et al.*, 1980). Both GnRH agonists and GnRH antagonists though having opposing cellular effects, ultimately have the same systemic effect. Together, the effects elicited by GnRH agonist and GnRH antagonist regimens, is termed chemical castration.

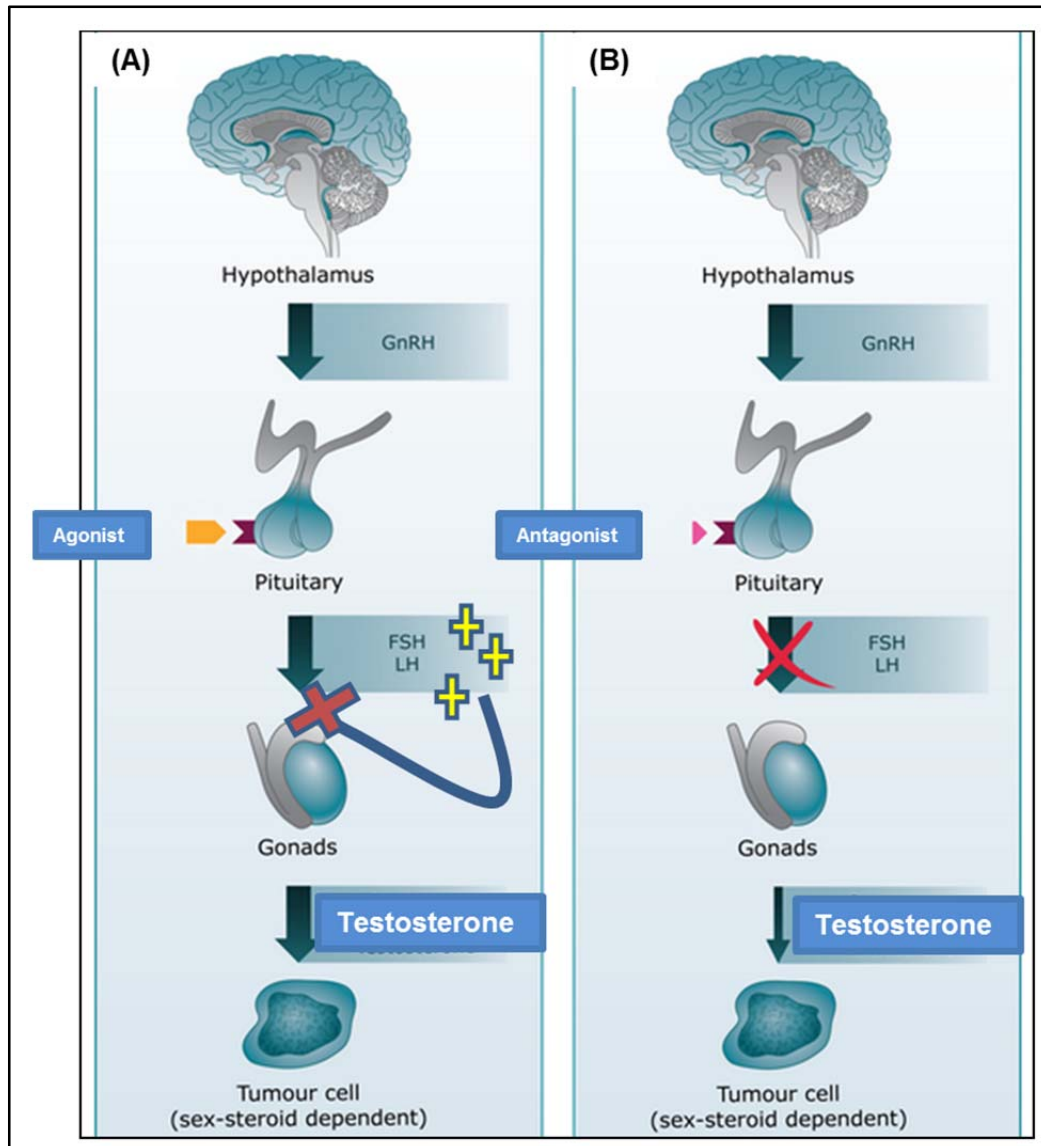


Figure 1.5 – The activities of (A) GnRH agonists and (B) GnRH antagonists (modified (Engel & Schally, 2007)).

1.2.3.3 Hormone-Responsive Anti-Androgen Therapy

Rather than affecting the release of testosterone, anti-androgens function either through the inhibition of androgen synthesis or by blocking the binding of androgens to AR which is expressed in abundance in prostate cancer cells. Since the discovery of anti-androgens, early last century, much research has been conducted into synthesising potent compounds to halt the signalling of AR. One class of anti-androgens serve to block the conversion of testosterone to DHT through inhibition of 5 α -reductase. Finasteride and the more potent dutasteride are two clinically-used 5 α -reductase inhibitors (5-ARIs) in the treatment of prostate cancer that are capable of binding each

of the three known 5 α -reductase isoenzymes (I, II and III) (Vermeulen *et al.*, 1989; Yamana *et al.*, 2010).

Another class of anti-androgens administered during advanced androgen-responsive prostate cancer treatment are known as AR antagonists. Bicalutamide (Casodex or CDX) is one such antagonist that is often given to patients undergoing chemical castration and is the next generation treatment replacing widely defunct flutamide and nultamide, two anti-androgens that exhibit higher adverse side effects and a shorter extension of life (Kolvenbag *et al.*, 1998) .

Although each of the above methods have proved to be widely effective in the control of prostate cancer, it has been shown that following hormone deprivation, testosterone mediated production of DHT can be circumvented when DHT is synthesised by the catalysis of androstenedione by SRD5A1 to 5 α -androstenedione. 5 α -androstenedione can be readily converted to DHT (Chang *et al.*, 2011). Furthermore, there progresses a more aggressive form of the disease where the effectiveness of each of the above therapies is nullified. In response to this problem, medical research has directed its focus to developing a means to slow the progression of this castrate-resistant prostate cancer (CRPC). In essence, CRPC is prostate cancer which is unaffected by or has adapted to ADT.

1.2.3.4 Castrate-Resistant Anti-Androgen Therapy

Even more effective than bicalutamide is anti-androgen enzalutamide which has only been approved for clinical use in those with CRPC since 2012. Enzalutamide is a multifunctional anti-androgen which works to inhibit the nuclear translocation of the AR to which it binds (unlike its predecessor) as well as disrupting the binding of AR co-activators and AR to DNA binding. It has been shown to effectively extend the survival times of those diagnosed with castrate-resistant disease (Aragon-Ching, 2014).

Abiraterone acetate is an anti-androgen approved for use in CRPC patients since 2011. Abiraterone is capable of inactivating the conversion potential of steroid intermediates to testosterone through the inhibition of key cytochrome

P450 enzyme 17-*alpha*-monooxygenase and results in reduced levels of circulating androgen and slower progression of prostate cancer. Abiraterone is an analogue of ketoconazole and was developed by a division of the Cancer Research Institute, London, UK. This biosynthesis inhibitor has been shown to extend the median survival times of patients by several months (de Bono *et al.*, 2011).

Orteronel, also known as TAK-700, is an alternate form of anti-androgen which functions to inhibit CYP17A1, an enzyme capable of the catalysis of pregnenolone and progesterone to form androgens that are testosterone precursors (Jarman *et al.*, 1998). With the aim of approval for the treatment of CRPC patients, clinical development for this androgen biosynthesis inhibitor ceased in June 2014 following publication of the findings of a phase III clinical trial that showed its administration had no positive outcome as regards the extension to life of the patient (Saad *et al.*, 2015).

A novel anti-androgen currently in phase III clinical trials for the treatment of CRPC is Galeterone. Initial data indicate this treatment carries out multiple anti-androgenic roles as a CYP17A inhibitor, an androgen receptor antagonist and initiator of AR degradation (Purushottamachar *et al.*, 2013).

ARN-509 is another AR-inhibiting compound which is currently undergoing phase III clinical trials in patients presenting with CRPC that is non-metastatic. To date, this drug has proven to be more efficacious than many of the other currently-used AR antagonists as evidenced by its superior anti-tumour effects in murine xenograft models of human CRPC when compared to those treated with enzalutamide (Tran *et al.*, 2009). ARN-509 offers a high therapeutic index, indicating potential as a combination therapy and upon treatment, delivers a lower basal rate of AR activation, nuclear localisation and resultant transcriptional activity following ADT failure than bicalutamide, over which ARN509 has a 7–10 fold greater AR-binding affinity (Clegg *et al.*, 2012).

1.2.3.5 Surgical Anti-Androgen Therapy

Orchiectomy, also known as orchidectomy, is the surgical removal of the testes. This option, though effective in causing instant withdrawal of androgens from the body, has been offered less and less over the decades owing to breakthroughs in the above-mentioned anti-androgen therapies (Huggins & Hodges, 1941).

1.2.4 Prostate Cancer Chemotherapy

1.2.4.1 Paclitaxel

In the USA, in the 1960's, the National Cancer Institute (NCI) commissioned numerous screening programmes of naturally-derived compounds, as potential treatments for cancers. This was a mammoth undertaking and one such screen had concluded that crude tree bark extract of the Pacific yew, or *Taxus brevifolia* was shown to have notable activity in tumours of the murine variety. It was not until 1971 that a compound, designated *alpha*-numerically as NSC 125973, was definitively identified as the active ingredient of this bark extract, by researchers at the Research Triangle Institute, North Carolina. Here, it was given the name 'taxol' owing to the fact that it had been discovered in the plant genus and that the compound possessed an abundance of hydroxyl groups, a characteristic of alcohol (Wani *et al.*, 1971). There followed a decade of suspension from the development of taxol due, in large part, to the lack in ease of obtaining and extracting the compound through the method of fractionation used. In this period, taxol's mechanism of action was noted by one group to enable an incessant stabilisation of microtubules and thus preventing cell division (Manfredi & Horwitz, 1984; Schiff *et al.*, 1979). A fungal endosymbiont of the Pacific yew bark, *Taxomyces andreanae*, was later found culpable for the drug's production. This made possible the commercialisation of taxol which was eventually given the generic designation 'paclitaxel' (Stierle *et al.*, 1993). Renewed interest in the drug was observed in the succeeding years, following a review of the nature-derived compound programmes and the dawn of new models such as xenografts and newly developed cell lines (Goodman & Walsh, 2001). It was not until almost two decades after it was first discovered that

paclitaxel was entered by the NCI into phase I clinical trials. Some of these trials faced closure due to adverse hypersensitivity reactions. Major contributions to managing these side effects were to introduce premedication and to switch from periodic administration (infusion) to continuous 24 hour (h) regimen infusion (N.C.I., 1991; Weiss *et al.*, 1990). Such refinement of protocol as well as the advancements in technology and biological models has greatly assisted in the outcomes of subsequent clinical trials for next generation taxanes as well as drugs of other classes.

Evidence for the anti-cancer potential of paclitaxel was further strengthened when, in 1989, use of the drug in clinical trials of ovarian patients showed a marked (30 %) response in patients, the bulk of whom had become apparently resistant to the conventional treatment regimens of platinum containing cisplatin and carboplatin. This opened up an entirely new avenue of regard for paclitaxel as a circumventor of emerging drug resistance in many cancer forms (Holmes *et al.*, 1991; McGuire *et al.*, 1989; Murphy *et al.*, 1993). The same year of publication of this clinical assessment in ovarian cancer patients, the NCI canvassed for applications of interested industrial parties to form a partnership in developing mass production of the drug. Bristol-Myers Squibb (BMS) was the successful candidate and Cooperative Research Development Agreement (CRADA) was drawn up, giving exclusivity of data to BMS, allowing them to detect alternate sources and rights to New Drug Application (NDA). Some two years later, BMS delivered on their agreement, in excess of the amount that had been agreed in the CRADA and submitted for NDA. Clinical trials were such a success that paclitaxel received Food and Drug Administration (FDA) approval for use in patients deemed resistant to conventional clinical treatment (Goodman & Walsh, 2001). In 2005, the FDA authorised the first in a new class of drugs called nanoparticle albumin bound (NAB) compounds. This drug, called Abraxane, was authorised for use in breast cancer patients that are unresponsive to conventional therapy. This is paclitaxel bound to albumin. In recent years, steps have been taken to evaluate Abraxane treatment for patients with metastatic CRPC (mCRPC) (Shepard *et al.*, 2009).

1.2.4.2 Docetaxel

In the mid-1980's, while the founding member of the clinically significant taxane family was enjoying the limelight of clinical investigation, a second generation taxane was identified and was slowly gathering attention. Discovered and developed by French-based company Rhône-Poulenc Rorer (which through a series of mergers is now part of Sanofi), this compound known as Taxotere, or its generic name, docetaxel was patented as (i) a new compound and (ii) the first semisynthetic paclitaxel derived from a non-cytotoxic precursor compound 10-deacetyl baccatin III which is found in extract of the needles of *Taxus baccata* (English or European yew) (Collin *et al.*, 1989a; Collin *et al.*, 1989b). The relative brevity of docetaxel's preclinical testing phase was due mainly to the abundance of the renewable source of the drug and showed great promise in murine models of colon adenocarcinomas. Also, docetaxel seemed to be more potent than its predecessor paclitaxel, when equivalent toxic doses were compared between the two agents in the B16 melanoma model (Bissery *et al.*, 1991). The extent of docetaxel's preclinical testing meant that there need only be a 4 year wait between submission of the patents and entering into phase I clinical trials. Neutropenia, the dose-limiting toxicity of paclitaxel, was also observed upon docetaxel administration.

In 1992, an array of phase II clinical trials was undertaken with a selection of US phase II clinical trials facilitated by the signing of a CRADA between the NCI and Rhône-Poulenc Rorer (Burriss *et al.*, 1993; Extra *et al.*, 1993; Pazdur *et al.*, 1992). In the 5 year period of 2000–2005, docetaxel had been approved by the FDA for therapeutic use in advanced-stage cancers of the lung, breast and prostate. Over the next 5 years, docetaxel was also proven to lengthen survival times of patients diagnosed with certain types of stomach and head and neck cancers, when used in combination with the mainstay chemotherapeutics. In more recent years, the use of docetaxel in combination with prednisone treatment has been proven to be modestly more advantageous than the previously used DNA-intercalating compound mitoxantrone-prednisone combinational chemotherapy in late stage prostate cancer (Petrylak *et al.*, 2004; Tannock *et al.*, 2004). Docetaxel-prednisone

has since become the first line chemotherapy choice for advanced stage CRPC. Phase III clinical trial, Chemohormonal Therapy versus Androgen Ablation Randomized Trial for Extensive Disease in Prostate Cancer (CHAARTED), shows early indications of significantly increased overall survival of patients treated with docetaxel during ADT when compared with those who are not. There are also emerging data suggesting there is a pronounced elongation of the time to diagnosis of castrate resistant cancers in those offered this novel sequence of treatment versus classical androgen ablation (Sweeney & Chamberlain, 2015).

1.2.4.3 Cabazitaxel

Despite the success of the above-mentioned taxanes, there is still a mechanism in cancer cells that can make drug resistance possible. The efflux protein pumps (described further in 1.2.5.1) often bind, with high affinity, to both drugs. It is for this reason that investigators at Sanofi began looking for alternate taxanes that do not succumb so readily to these modulators of resistance. From a panel of semi-synthetic compounds derived from the European yew, one which demonstrated the most reduced efflux resistance potential was XRP6258 (RPR 116258A), more commonly known by its generic name cabazitaxel. Initial phase I clinical trials, looking at the effects of this drug in advanced cancers, were brought to completion in mid to late 2000's, with the treatment appearing to show high grade activity in patients with advanced prostate cancer. From here, the drug progressed with relative ease through phase II and phase III trials, when compared with the progress of its predecessor taxanes. Cabazitaxel was seen to be effective in the treatment of advanced-stage patients who were unresponsive to docetaxel treatment. FDA approval for the use of cabazitaxel in patients who experienced resurgence following failure of hormone deprivation therapy came in 2010. Clinically, this new combination is becoming more prevalent. It should be noted, however, despite its effectiveness at circumventing classic taxane resistance, the toxicity of this next generation drug, in the form of neutropenia is still a common side effect. Also, eventual resistance to cabazitaxel is almost certain to occur (Sanofi-Aventis, 2010). It is a common consideration, therefore, that there exists a need for the establishment of

companion compounds to mute these side effects whilst improving desired efficacy.

Cabazitaxel is currently undergoing phase I clinical trials in combination of next generation drugs such as abiraterone acetate. FDA approval for abiraterone in combination with prednisone, for use in those with mCRPC and who had not received prior docetaxel constituent chemotherapy was issued in 2011. This approval was expanded in 2012 to include all patients who had previously received chemotherapy. Significant improvements in quality of life for the patient were noted upon administration of this drug. One of the aims of current clinical trials, which are being co-ordinated by Sanofi, is to determine the efficacy of combining these two agents in anti-tumour activity with regard to PSA levels. Another purpose of these trials is to establish a guide as to the maximum tolerated doses and also dose limiting toxicities associated with treatment with both drugs.

1.2.4.4 Mitoxantrone

Up until the approval of docetaxel as the first line chemotherapeutic treatment for advanced prostate cancer, mitoxantrone, in combination with prednisone treatment, was the only approved option (Tannock *et al.*, 1996). Mitoxantrone belongs to the anthracenedione class of drugs and has antineoplastic properties. Although it does not elongate patient survival times, it has been shown to improve quality of life through a reduction in pain levels. Mitoxantrone is structurally similar to the anthracycline class of drugs which have also been used in the treatment of prostate cancer (Moore *et al.*, 1994).

1.2.4.5 Anthracyclines

Anthracyclines function by their intercalation of RNA and DNA which stalls replication within the rapidly multiplying cancerous cells and brings about apoptosis. Anthracyclines have also been shown to inhibit topoisomerase II and are responsible for DNA damage through their generation of free oxygen radicals. As mentioned previously, the anthracyclines share structural similarities with that of the anthracenediones which have been shown to be less toxic (Minotti *et al.*, 2004). Doxorubicin is one anthracycline which alone

may exhibit a significant palliative effect, but has minimal overall activity in the reduction of CRPC progression (Gewirtz, 1999). In one study, weekly iv dose of 20 mg m² doxorubicin generated objective radiological responses in 15 % of CRPC patients. Moreover, during a phase II clinical trial of a cohort of 35 prostate cancer patients, doxorubicin was examined in combination with an elevating dose regimen of cyclophosphamide. From the cohort, 15 patients presented with considerable disease advance. Of these 15, 5 patients evidenced a significant response to treatment while 16 individuals out of the whole sample group, representing 46 %, exhibited a more than 50 % reduction in their levels of PSA. While the combined regimens were well-tolerated, grade 4 neutropenia occurred in a third of participants and some reported pyretic neutropenia (Small *et al.*, 1996). An analogue of doxorubicin, known as epirubicin, has been shown to have equal effectiveness as a second line therapy when compared to its predecessor but with a reduction in the adverse systemic toxicity (Hernes *et al.*, 1997). Patients with metastatic CRPC exhibited improvements to quality of life as well as survival upon weekly treatments of epirubicin (Culine *et al.*, 1998).

1.2.4.6 Estramustine

Although previously widely used, this compound has been withdrawn from the national standard treatment plans for prostate cancer in Ireland, Norway and Australia (Bissinger *et al.*, 2013). It is, however, still used palliatively in the management of metastatic CRPC sufferers in the USA and in the UK, as a final effort of treatment of those who are unresponsive to alternative chemotherapeutic approaches (deKernion & Lindner, 1984). This compound is classed as a nitrogen-mustard which was derived from the oestrogen estradiol, meaning that it binds cells expressing oestrogen receptor (ER) and indiscriminately alkylates DNA (Tew, 1983; Tew *et al.*, 1983). Estramustine has shown some success in combined treatment with doxorubicin in reducing PSA levels significantly (Culine *et al.*, 1998).

1.2.5 Chemoresistance in Prostate Cancer

In spite of the successes of the chemotherapeutics mentioned here, none of these agents has proven to be curative. Instead, the disease is kept more

indolent until cancer cells develop mechanisms to overcome the toxic potential of treatment regimens.

1.2.5.1 Multidrug Efflux Protein Pumps

In the 1970's research began to focus on understanding the mechanisms by which cancer cells become endowed with resistances to a variety of differently acting compounds following serial treatment of cultures with just one. To start with, actinomycin D was noted to induce cellular resistance to a range of compounds including anthracyclines, antibiotics and vinca alkaloids (Biedler & Riehm, 1970). The ATP-dependent drug efflux pump, P-glycoprotein (P-gp), also referred to as MDR1, was discovered to be the causative protein for this resistance. This transmembrane protein binds to and transports over 300 known agents out of the cell (Chen *et al.*, 2012; Wang *et al.*, 2011). Upon cellular resistance to the taxanes, as noted in 1.2.4.2, MDR1 is upregulated (Bellamy, 1996). Pregnane X receptor (PXR) (Breier *et al.*, 2013), thyroid hormone receptor (TR) (Nishio *et al.*, 2005; Saeki *et al.*, 2011), peroxisome proliferator activator receptors (PPARs) (Apostoli & Nicol, 2012), vitamin D receptor (VDR) (Durk *et al.*, 2012) and constitutive androstane receptor (CAR) (Wang *et al.*, 2010) are all known MDR1 gene transcriptional regulators.

Another efflux protein identified as a mediator of drug resistance is the breast cancer resistance protein (BCRP). This is structurally related to MDR1 and, like MDR1, is a member of the ATP-binding cassette (ABC) protein family. BCRP is upregulated upon chemotherapeutic treatment and is responsible for ridding cancer cells of a diversity of cytotoxins, promoting progression of the disease (Doyle *et al.*, 1998; Janvilisri *et al.*, 2003). The promoter regions of BCRP contain hypoxia response elements (HRE) as well as oestrogen response elements (ERE) suggesting heavy transcriptional regulation by interaction with activated ER and HIF1 α (Benderra *et al.*, 2004; Krishnamurthy *et al.*, 2004).

A third subset of ABC proteins exist in the form of the multidrug resistance-associated protein (MRP) subfamily. The best characterised of these is MRP1 although other members include MRP-2, -3, -4, -5, -6, -7 and -8. Both

MDR1 and MRP1 have shared substrates, with MRP1 displaying a higher range of diverse binding, making its overexpression a common attribute of chemoresistant cancers (Lee *et al.*, 1998; Munoz *et al.*, 2007; Sullivan *et al.*, 1998).

1.2.5.2 AR-Mediated Chemoresistance

The normal function of activated AR is to recruit transcriptional coactivators to help carry out its role in cell dynamics. This process is hijacked in the onset of prostate cancer, as abnormal expression of these coactivators leads to deregulated transcriptional activation and institutes a bypass of anti-androgen techniques. Lysine specific demethylase-1 (LSD1) is one such signalling molecule whose aberrant activities have been well-documented, particularly in its role in potentiating hormone responsive prostate cancer and CRPC. It serves to demethylate histone marks that would otherwise repress AR transcriptional activities (Kahl *et al.*, 2006; Metzger *et al.*, 2005). During ADT, prostate cancer cells develop mechanisms to overcome the reduction in available androgen. Overexpression of AR, mutations with constitutively activate AR and intracrine biosynthesis of androgens through increased local enzymatic activity and substrate supply are methods employed by many of these tissue types in navigating ADT (Eisermann *et al.*, 2013; Koivisto *et al.*, 1997; Montgomery *et al.*, 2008). Such challenges of researchers have encouraged the development of more potent anti-androgens, as described previously (1.2.3), which have greatly improved the treatment of CRPC. Mutations in β -tubulin expressed by cancer cells, incur a resistance to taxanes as well as other tubulin disrupting chemotherapies. As emerging evidence suggest that the actions of these drugs may serve to disrupt microtubule routed AR translocation, overcoming such activities may be doubly adverse to cancer progression (Darshan *et al.*, 2011; Zhu *et al.*, 2010). Also of interest is the apparent induction of multidrug resistance-associated proteins (MRPs) by AR which may be beneficial to generation of CRPC (Ho *et al.*, 2008).

1.2.5.3 Chemoresistance through Proliferation and Survival Pathways

Differences in the regulated activation of multiple receptor tyrosine kinase pathways have been extensively researched for the roles they play in the development of chemoresistance in CRPC (Seruga *et al.*, 2011). Androgen-mediated regulation of the activities of epidermal growth factor (EGF) and vascular endothelial growth factor (VEGF), the signalling of their receptors, EGFR and VEGFR, the mTOR pathway and MAPK/ERK signalling is contingent on hypoxia inducible factor 1 *alpha* (HIF1 α) activation (Boddy *et al.*, 2005). In fact HIF1 α activation has been shown to favour the progression of metastasis in CRPC. Following a withdrawal of androgens during ADT, increased secretion of VEGF-C directly upregulates BAG-1L, a known enhancer of AR translocation and thus cell survival (Rinaldo *et al.*, 2007). Insulin-like growth factor 1 (IGF1) and transforming growth factor *beta* (TGF β) show evidence of contributions to chemoresistant states of prostate cancer during ADT, through modified expression patterns (Nickerson *et al.*, 2001; Pollak, 2001; Pollak *et al.*, 1998; Zhu & Kyprianou, 2005). This contrasts with the activities of nuclear factor *kappa* B (NF κ B), interleukin-6 (IL-6) and Hedgehog signalling pathways which have been shown to reinstate sensitivities to taxane treatment (Domingo-Domenech *et al.*, 2006; Mimeault *et al.*, 2007).

1.2.5.4 Chemoresistance Conferred by Cancer Stem Cells

It has been widely reported that populations of interstitial adult stem cells that normally facilitate the function and repair of prostatic tissue may be co-opted to influence the progression and spread of prostate cancer (Marcinkiewicz *et al.*, 2012). These are known as cancer stem cells (CSCs). Two classically held theories as to the origins of such stem cells suggest either that stem cells arising in normal tissues transform following manipulation by mutation or epigenetic factors, or that these stem cells are produced by cancer cells themselves (Goldstein *et al.*, 2008; Leong *et al.*, 2008; Mani *et al.*, 2008; Richardson *et al.*, 2004). In any case, the ability of CSCs to repair chemotherapeutic damage to tumours, make this cell type an obstacle in the treatment of CRPC. Moreover, as CSCs are AR negative their population

remain unaffected by ADT (Oldridge *et al.*, 2012). CSCs also have been found to express elevated levels of an array of drug efflux proteins such as MDR1 and BCRP (Frame & Maitland, 2011). Analysis of taxane-resistant sub-populations of CSCs, using microarrays, has determined a more pronounced expression of the pro-tumorigenic Oct4 gene (Frame & Maitland, 2011; Linn *et al.*, 2010).

1.3 Recent Clinical Advances in Prostate Cancer

1.3.1 Sipuleucel-T

This method of prostate cancer-specific immunotherapy has been heralded as a major breakthrough in the personalized treatment of prostate cancer patients. According to IMPACT phase III clinical trials, this immunostimulant has the potential to lengthen median survival time by 4.1 months (Schellhammer *et al.*, 2013). Approved in 2010 by the FDA for use in metastatic CRPC patients that are asymptomatic, sipuleucel-T works by, following leukapheresis, incubating a sample of a patient's dendritic cells with, a two part complex containing the antigen specific to the majority (95 %) of prostate cancer cells known as prostatic acid phosphatase (PAP). This PAP is fused to an immunogenic cytokine known as granulocyte-macrophage colony stimulating factor (GM-CSF) which, altogether, forms an activated blood product APC8015. It is this product which is re-administered to the patient's body as the sipuleucel-T treatment. As a result of this, an immune response is generated against PAP-presenting cancer cells. Typically sipuleucel-T is administered three times over 6 weeks (Kantoff *et al.*, 2010). As this immunotherapeutic strategy is the first to be approved in prostate cancer, the ongoing research into identification of alternate prostate cancer biomarkers makes possible the development of similar acting treatments. Current phase III trials are examining the use of sipuleucel-T in combination with other methods of tackling prostate cancer clinically (Chang, 2007; Graff & Chamberlain, 2015).

1.3.2 Radium-223

Although the use of radium is not a novel technique in treating cancer, radium-223 (^{223}Ra) is the generic designation of what was formerly known as

Alpharadin and which is now marketed under the name Xofigo, offers an alternate treatment option to CRPC patients with osseous metastases, in place of strontium-89 (^{89}Sr). ^{89}Sr is a *beta*-ray (β -ray) emitter with a half-life ($t_{1/2}$) of over 40 days. ^{223}Ra , on the other hand, emits ~95 % *alpha*-rays (α -rays) with a $t_{1/2}$ of 11.4 days meaning that it emits at a shorter distance and for a shorter time, reducing negative impact on surrounding non-targeted tissues (Pinto & Cruz, 2012). Owing to its structural similarity to calcium, ^{223}Ra is readily absorbed by osseous tissue (Bruland *et al.*, 2006; Henriksen *et al.*, 2002; Nilsson *et al.*, 2005). An increase in the survival times of patients undergoing this treatment in phase II and phase III clinical trials paved the way for an expedited FDA approval in 2013 (Sartor *et al.*, 2014).

1.3.3 HIF1 Inhibitors

HIF1 belongs to the aryl hydrocarbon receptor nuclear PER-translocator (ARNT)-SIM (PAS) protein subfamily and is a basic helix loop helix (bHLH) heterodimeric TF composed of both α - and β - subunits. HIF1 is crucial to mammalian life as demonstrated by the murine perinatal lethality upon HIF1 deletion. It is a TF of variable function *in vivo* but its most obvious function is that it is a cell's first respondent to a fall in environmental oxygen (hypoxia) (Semenza & Wang, 1992; Shweiki *et al.*, 1992; Wang *et al.*, 1995). HIF1 α in normoxic conditions is hydroxylated post-translationally at the proline residues 402 and 564 by prolyl hydroxylase which leaves the subunit in its inert phase and bound by the von Hippel Lindau (VHL) component of ubiquitin ligase E3, an interaction which brings on rapid proteolysis (Iwai *et al.*, 1999; Maxwell *et al.*, 1999; Yu *et al.*, 2001). Secondary to this proline hydrolysis is that of asparagine residue 803 by factor inhibiting HIF (FIH) (Hewitson *et al.*, 2002; Kallio *et al.*, 1999). Stabilisation and nuclear translocation of HIF1 α is brought about by a reduction in both hydroxylases in response to hypoxic conditions. It is within the nucleus that HIF1 α heterodimerises with HIF1 β (Ivan *et al.*, 2001; Jaakkola *et al.*, 2001). When this occurs the dimer can interact with the promoter regions of a large number of genes at specific points called hypoxia response elements (HREs). Such interactions have widespread and profound effects on a great many cellular functions such as metabolic cues, angiogenesis and

proliferation, to name a few (Wenger, 2002) . Given the prowess of this TF in effectuating cellular survival at low oxygen levels and its utility on a broad range of cell dynamics, it is not surprising that HIF1 α has a clear role to play in the progression of numerous cancer types (Semenza, 2003; Zhong *et al.*, 1999). It is for this reason that the protein has been the focus of many researchers, globally as a therapeutic target in the progression of cancer (Folkman, 2007; Pouyssegur *et al.*, 2006).

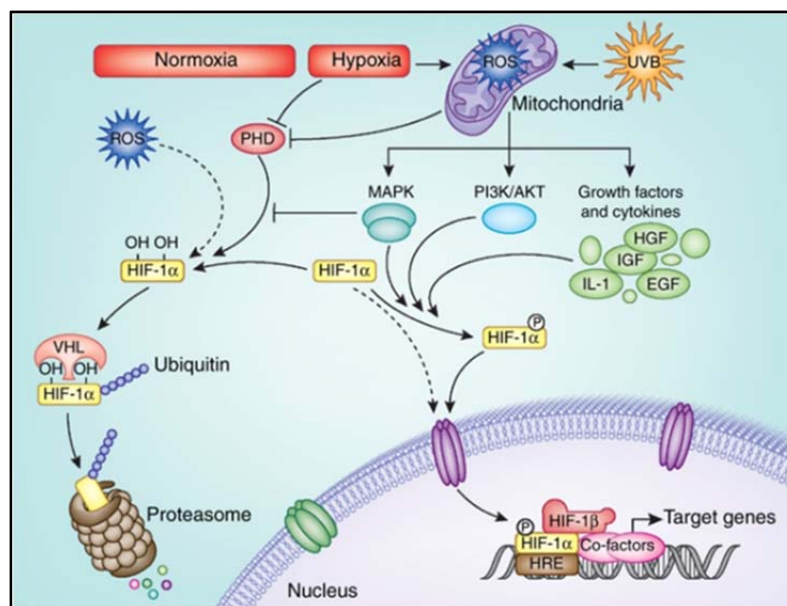


Figure 1.6 – Basic schematic of HIF1 α activities (Rezvani *et al.*, 2011).

1.3.3.1 Heteroaryl and Aromatic HIF1-Inhibitory Agents

A test panel of small molecules containing 1-chloro-N-pyridin-3-ylacetamide analysed in HRE-transfected glioma cell line U251 demonstrated a specificity index of more than 20 when assayed (Kumar *et al.*, 2009). Drawing on this result a related analogue, P2630, was synthesised. Considerable HIF1 α inhibition (IC_{50} 500 nM) was associated with exposure of this next generation compound in hypoxia (1 % O_2) which was investigated for its anti-proliferative potential in a panel of cancer cell lines including prostate cancer cell lines DU145 and PC-3, ovarian cancer model Ovar-3, colorectal cancer cell line, HCT116 and the pancreatic cancer model Panc-1, using the 3H thymidine incorporation assay. In addition, the same assay was carried out on noncancerous *in vitro* models of MRC-5 and WI-38. Of the panel and with an IC_{50} of 1 μM , PC-3 exhibited the most pronounced loss of proliferation

while the least was noted in the noncancerous MRC-5 and WI-38 with respective IC_{50} s of over 10 μ M and 6.5 μ M. Further *in vivo* analysis with a PC-3 xenograft over 19 days with a twice daily regimen 50 mg kg^{-1} determined a substantial reduction in tumour growth when compared to the control arm. Importantly, the dosages were well tolerated as evidenced by the lack of significant weight loss compared to the control (Yewalkar *et al.*, 2010).

Thalidomide is an aromatic compound with proven efficacy in the treatment of cancer and has been approved for the treatment of multiple myeloma. Following HUVEC assays, thalidomide analogues, like their predecessor, exhibited inhibition of angiogenesis. Furthermore, at a concentration of 10 μ M, PC-3 cells showed ~80–90 % reduction in HIF1 α expression. This result suggests a potential role for such compounds in treating prostate cancer (Noguchi *et al.*, 2005).

Lonidamide an example of an indazole-3-carboxylic acid derivative capable of the inhibition of nuclear and whole cell HIF1 α expression in AR-positive and AR-negative cell lines LNCaP and PC-3 at a dose range of 100–600 μ M, with 400 μ M abolishing expression entirely (Jian-Xin *et al.*, 2006). Other studies have suggested that analogues of this compound could be more efficacious in this respect (Grugni *et al.*, 2006).

1.3.3.2 Steroidal HIF1 Inhibitors

A panel of 1, 3, 5 (10)-estratrienes demonstrate considerably potent inhibition of angiogenesis and HIF1 α protein expression, amongst other features (Laderoute *et al.*, 2006). The strongest effect of these compounds was witnessed by treatment of *in vitro* analysis of metastatic prostate cancer cell line PC-3 and MDA-MB-231 cell with candidate SR-16388. Notably, the compound did not affect the viability of RAW264.7, a macrophage cell line controlling for a 'normal' or noncancerous phenotype. Additionally, a 50 % reduction in tumour growth of PC-3 murine xenograft models, when treated with a 30 mg kg^{-1} SR-16388 concentration, was witnessed upon comparison with untreated controls. Testing the estratriene in combination with 7.5 mg kg^{-1} clinically used chemotherapeutic paclitaxel within this model revealed

that 10 mg kg⁻¹ SR-16388 had a much greater impact on the growth of tumour growth. Further *in vitro* investigations revealed that apart from its role as an inhibitor of HIF1 α , SR-16388 binds to oestrogen related receptor *alpha* (ERR α), disrupting its action at transcriptional levels while having no effect on the activities of ERR β or ERR γ . This suggests a dual role for the compound (Duellman *et al.*, 2010).

1.3.3.3 RNA Antagonists

The messenger RNA (mRNA) of HIF1 α can be directly bound by the novel RNA antagonist EZN-2968 thus preventing the translation of HIF1 α protein. *In vitro* examinations of the effects on prostate cancer and glioblastoma HIF1 α levels following EZN-2968 treatment have determined the IC₅₀ range of between 1 and 5 nM resulting in considerable cell viability reduction. Significant reductions in tumour volumes were also observed in DU145 xenograft models upon this antagonist's administration. Moreover, in a phase I clinical trial of patients with advanced malignancies that had previously undergone chemotherapy, EZN-2968 doses were well tolerated. One of the drawbacks of this antagonist, however, is that it cannot be administered orally (Greenberger *et al.*, 2008).

1.3.3.4 mTOR Inhibitors

Rapamycin is an extensively reported inhibitor of the mTOR pathway and has proven efficacious in the treatment of Kaposi's sarcoma, attributed to renal transplantation, as well as the treatment of a subset of lymphomas (Roy *et al.*, 2013). The mTOR pathway is known to facilitate the upregulation of HIF1 α protein levels in normoxic conditions in response to growth factor signalling. mTOR-directed HIF1 α translation is a well-documented response to the loss of PTEN in numerous cancer cell types including those of the prostate (Majumder *et al.*, 2004). It stands to reason, therefore, that inhibition of the mTOR pathway presents a therapeutic benefit (Jiang *et al.*, 2001).

1.3.3.5 Hsp90 Inhibitors

The antibiotic geldanamycin (GA) is a benzoquinone ansamycin which, through competition of binding to the adenosine triphosphate (ATP)-binding

sites of the target proteins of the chaperone heat shock protein 90 (Hsp90), marks them for proteasome degradation. *In vitro* examination has determined that GA has the ability to institute the described protein clearance of HIF1 α in prostate cancer cell lines LNCaP and PC-3 under both normoxia and hypoxia in a VHL-free manner (Mabjeesh *et al.*, 2002).

1.3.3.6 Non-Steroidal Anti-Inflammatory Drugs

The non-selective non-steroidal anti-inflammatory drug ibuprofen has demonstrated HIF1 α and HIF2 α inhibition in the prostate cell lines DU145 and PC-3 as well as a decrease in the angiogenic potential as demonstrated by a loss of VEGF expression (Palayoor *et al.*, 2003).

1.3.3.7 Chetomin

Anti-microbial agent chetomin is a metabolic product of fungus *Chaetomium* and is responsible for the disruption of p300-HIF1 α interaction which disallows hypoxia-mediated transcription. Its potency in tumour reduction has been shown in PC-3 and HCT116 xenograft models (Kung *et al.*, 2004).

1.4 Toluidine Sulphonamides

Owing chiefly to the existing literature which suggests that aryl-sulphonamide molecules have a pre-disposition towards inhibiting the activities of key cytochrome P450 enzyme CYP2C9, it was first believed that toluidine sulphonamides made for poor therapeutic agents. Not until initiation of extensive 3-dimensional quantitative structural activity relationship (3D-QSAR) analysis, having exhausted 2D-QSAR methods, were compounds of this class discovered to have influence over HIF1 activity. Suggested structural modifications in a subset of this series, specifically, through a methoxy substitution in the sulfonylphenyl fragment at the 4-position combined with a further substitution of toluidine ring members with a methoxy moiety, resulted in elevated HIF1 interaction while CYP2C9 inhibition was abolished. The importance in maintaining systemic CYP2C9 activity lies in its role in the clearance of endogenous materials such as arachidonic acid as well as exogenous compounds such as warfarin (Miners & Birkett, 1998; Rettie & Jones, 2005; Williams *et al.*, 2003). This paved the

way for the synthesis of a wide range of similar candidates for testing. In spite of this, very little is known about the biological effects of toluidine sulphonamides which have been patented and researched exclusively by Elara Pharmaceuticals and associate research collaborators (Alonso *et al.*, 2012).

1.4.1 ELR510444

A member of a subset of toluidine sulphonamides classed as thiophenes, ELR510444 was investigated for its potential as an inhibitor of HIF1 α . During *in vitro* investigation, the drug showed strong microtubule disrupting capability. This, upon further examination, led to the assertion that the drug is also an anti-angiogenic compound. Sulforhodamine B (SRB) cell viability assays conducted in melanoma cell line MDA-MB-435 and 2H-11 which is a tumour endothelial cell line, determined IC₅₀s of 9.0 nM (\pm 0.5) and 11.7 (\pm 0.4) nM, while breast cancer cell line MDA-MB-231 generated a higher IC₅₀ value of 30.9 \pm 2.3 nM. In a cell free assay, ELR510444 was not shown to be a substrate for MDR1-mediated drug resistance. Furthermore, the anti-vascular activities of this compound were seen to mimic the effects of microtubule-disrupting combretastatin A4, suggesting a similar mode of activity (Risinger *et al.*, 2011). In a follow up study using renal cell carcinoma cell lines RCC4, 786-O, A498, Caki-1, Caki-2, and Achn, ELR510444 inhibited HIF1 α and HIF2 α which, in turn, resulted in a downregulation of VEGF. This drop in VEGF expression levels was observed in tumour tissues of A498 and 786-O xenografts which may explain the significant reduction in tumour volume observed upon ELR510444 dosing (Carew *et al.*, 2012).

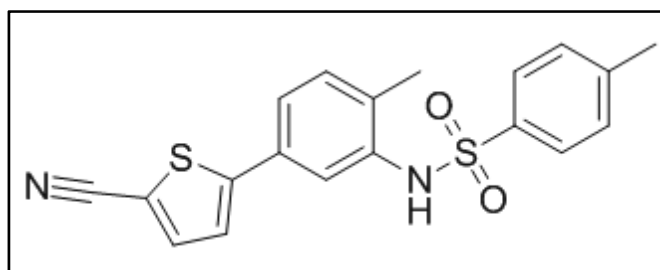
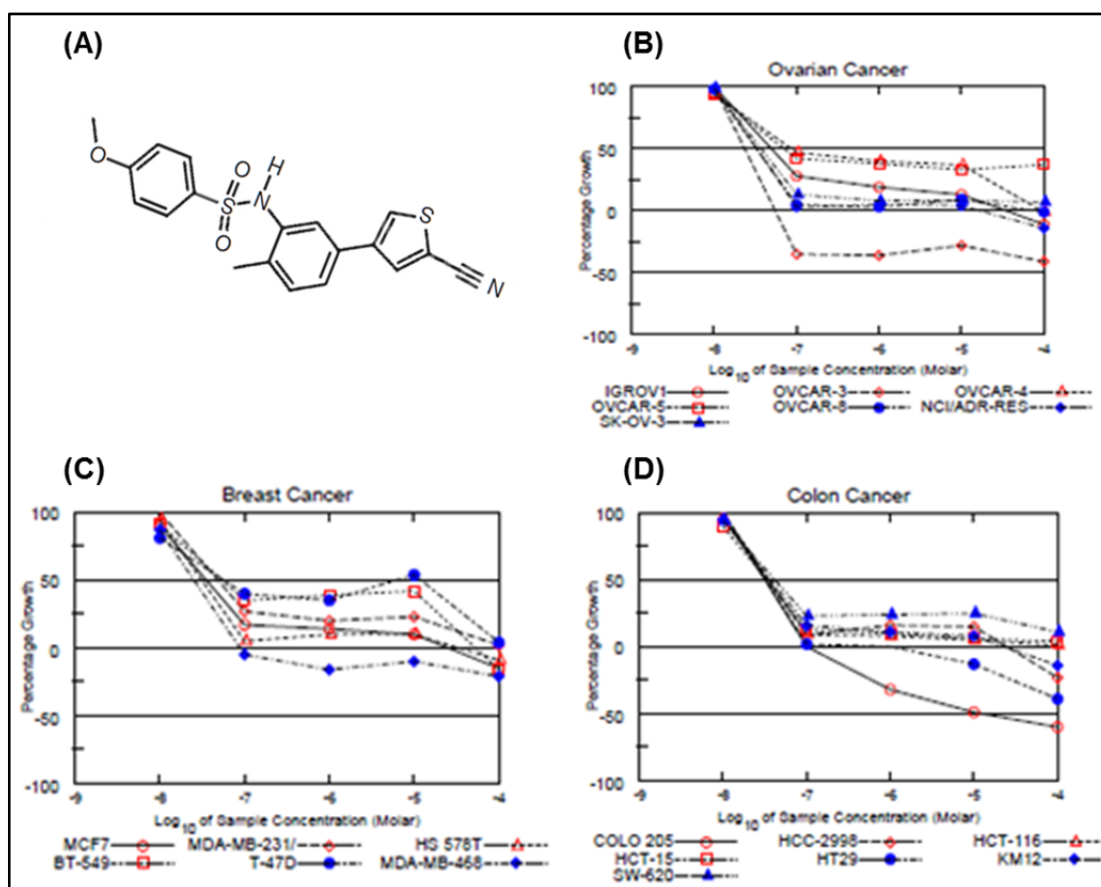


Figure 1.7 – Chemical structure of ELR510444 (Carew *et al.*, 2012).

1.4.2 ELR510552 (EL102)

Identified from the NCI-60 human cancer cell line screen, ELR510552 or EL102, as it is abbreviated, showed efficacy in significantly reducing the proliferative potential of an array of cancer cell types (Monks *et al.*, 1991; Shoemaker, 2006). Figure 1.8 (A) shows the chemical structure of EL102 which is similar to ELR510444. Amongst the cell lines assayed, and that displayed a high response to EL102 doses, were cancer cell lines of the prostate, breast, lung, ovary, skin, colon, kidney, blood and CNS. The results of the follow-up dose response curves (5 concentrations of EL102) can be seen in Figure 1.8 (B) (Unpublished data). Further analysis of the effects of EL102 was carried out at Elara Pharmaceuticals GMBH, Heidelberg, Germany in collaboration with the Prostate Cancer Institute, Galway. This thesis outlines the data obtained from these investigations.



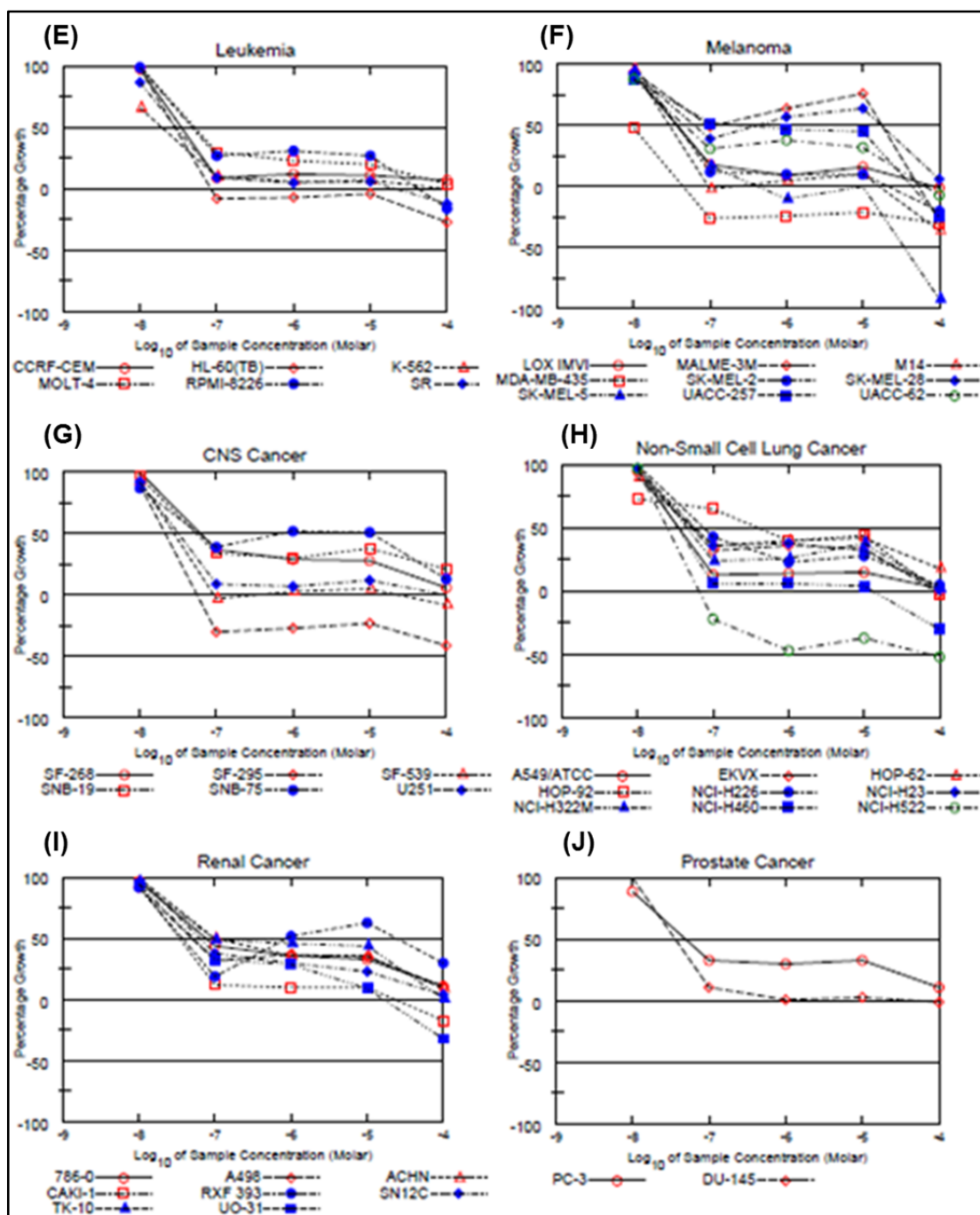


Figure 1.8 – Preliminary EL102 data. (A) Chemical structure of EL510552 (EL102) (Toner *et al.*, 2013). Dose response curves in logarithmic scale of the top NCI-60 selected respondents to a screen of 10 μM EL102 (B) ovarian, (C) breast, (D) colon, (E) leukaemia, (F) melanoma, (G) CNS cancer, (H) non-small cell lung cancer, (I) renal cancer and (J) prostate cancer (Unpublished, (Schultes & Lewis, 2009)).

Chapter 2:

Materials and Methods

Immediately following the first mention of a laboratory item, both, the manufacturer and the catalogue code (denoted by a preceding hash symbol (#)), are provided in parentheses. A list of the contact details for the local Irish national distributors or suppliers of these manufacturers can be found at the end of this chapter (Table 2.4).

2.1 Cell Culture

2.1.1 Cell Lines

The cell lines of CWR22, 22Rv1, PC-3, DU145 and LNCaP were obtained from the American Type Culture Collection (ATCC). Access to work with DLKP, DLKPA, DLKP-Mitox and DLKP-Mitox-BCRP was kindly granted by Prof. Martin Clynes (National Institute of Cellular Biotechnology, Dublin City University). Table 2.1 summarises general cell line information.

Cell Line	Organ/Disease	Source	Doubling Time (h)	Comments	Reference
CWR22	Prostate Carcinoma	Prostate	35–40	AR Positive, Androgen Sensitive	(Pretlow <i>et al.</i> , 1993)
22Rv1 (ATCC #CRL-2505)	Prostate Carcinoma	Prostate (Progeny of CWR22)	35–40	AR Positive, Weak Androgen Sensitivity	(Sramkoski <i>et al.</i> , 1999)
PC-3 (ATCC #CRL-1435)	Prostatic Adenocarcinoma	Bone Metastasis	24–30	AR Negative, Androgen Insensitive	(Kaighn <i>et al.</i> , 1978)
DU145 (ATCC #HTB-81)	Prostate Carcinoma	Brain Metastasis	20–30	AR Negative, Androgen Insensitive	(Stone <i>et al.</i> , 1978)
LNCaP (ATCC #CRL-1740)	Prostate Carcinoma	Lymph Node Metastasis	30–40	AR Positive, Androgen Sensitive	(Horoszewicz <i>et al.</i> , 1980)

DLKP	Lung Squamous Carcinoma	Lung	30–40	Poorly Differentiated	(Clynes <i>et al.</i> , 1992)
DLKP-A	Lung Squamous Carcinoma	Lung (Progeny of DLKP)	30–40	Doxorubicin-Selected, MDR1 up-regulated	(Clynes <i>et al.</i> , 1992)
DLKP-Mitox	Lung Squamous Carcinoma	Lung (Progeny of DLKP)	30–40	Anoikis-resistant, Mitoxantrone-Selected	(Murphy <i>et al.</i> , 2007)
DLKP-Mitox-BCRP	Lung Squamous Carcinoma	Lung (Progeny of DLKP-Mitox)	30–40	Anoikis-resistant, Mitoxantrone-Selected, BCRP Up-regulated	(Murphy <i>et al.</i> , 2007).

Note: All cell lines were authenticated by LGC Logistics and were mycoplasma-free.

2.1.2 Culture Conditions

CWR22, 22Rv1 and LNCaP were maintained in RPMI 1640 (Sigma-Aldrich, #R8758). The DU145 cell line was maintained in minimum essential medium *alpha* (MEM α) (Gibco, Life Technologies #22561-021) and the PC-3 cell line was cultured in F12 HAMS medium (Gibco, Life Technologies #21765-029). In each instance, culture medium was supplemented with 10 % Fetal Bovine Serum (FBS) (Sigma-Aldrich, #F7524) which had, before use, been heat inactivated at 56 degrees Celsius ($^{\circ}$ C) for 30 minutes (min), and 1 X Anti-mycotic/Anti-biotic (Gibco, Life Technologies #15240062). For androgen deprivation studies, cells were maintained in phenol red-free (PRF) RPMI (Gibco, Life Technologies #32404014), supplemented with 10 % charcoal-stripped foetal bovine serum (CS-FBS) (Gibco, Life Technologies #12676029), 10 mM HEPES buffer (Gibco, Life Technologies #15630056), 1 X Anti-mycotic/Anti-biotic, 1 X Glutamax (Gibco, Life Technologies #35050038), 1 X sodium pyruvate (NaPyr) (Gibco, Life Technologies #11360039). Each of these adherent cell lines were cultured in T-75 cm³ (Sarstedt #83.1813.302) or T-175 cm³ (Sarstedt #83.1812.302) cell culture flasks until 60–80 % confluent at which point, the medium was withdrawn

and the monolayer was rinsed with Dulbecco's modified phosphate buffered saline (dPBS) (Sigma-Aldrich #D8537). The monolayer was then trypsinised in 0.05 % EDTA trypsin (Gibco, Life Technologies #25300054) for 5–10 min at 37 °C. To stop trypsinisation, an equal volume of 10 % FBS-containing medium was added to the trypsinised cell suspension. The suspension was centrifuged at 200 x g in sterile a 15 ml tube (Sarstedt #62.554.001) or 50 ml tube (Sarstedt #62.559.001). The resulting cell pellet was re-suspended in the appropriate medium and cell counting was performed using a haemocytometer (Fisher Scientific #12342168), if necessary. Otherwise, cells were returned to culture in optimum conditions and medium, in accordance with cell data sheet instructions (Appendix I). Each of the cell lines cultured were authenticated and confirmed mycoplasma-free by LGC Logistics. In experiments requiring the culture of cells (DU145 and PC-3) in hypoxia, culture dishes were seeded as described above and placed in a humidified Hypoxic Glove Box (Coy Lab Products # 8375065) set to 37 °C, 5 % CO₂ and 1 % O₂.

2.2 Cell Viability and Apoptosis Analysis

Cytotoxicity assays were carried out to determine the dose range of the various compounds for use in experimentation. Resazurin (Sigma-Aldrich #199303)(also sold commercially as Alamar Blue) based assays were first utilised to determine the IC₅₀ values for EL102, docetaxel (Sigma-Aldrich #01885), paclitaxel (Sigma-Aldrich #T7191) and doxorubicin (Sigma-Aldrich #D1515) in 4 cell lines 22Rv1, CWR22, PC-3 and DU145. These results were later confirmed by sulforhodamine B (SRB) solution (Sigma-Aldrich #S1402) based assays. It should be noted that although routinely referred to as “cell viability assays”, resazurin based assays are more accurately a measure of cellular reductase activity meaning it is difficult to discriminate between whether the cells are senescent, arrested or dead. Similarly, SRB assays measure cellular protein content and cannot differentiate between the different cell states at time of elution of fixed culture. Protocols were followed, as outlined below.

2.2.1 Resazurin-Based Assays

Cells were trypsinised and re-suspended in fresh medium at a density of 2×10^4 cells/ml. 100 μ l of cell suspension was seeded to each well of a Cell+ 96-well plate (Sarstedt #83.1835.300) and cultured overnight in 5 % CO₂ at 37 °C. Varying concentrations of dimethyl sulfoxide (DMSO) (Sigma-Aldrich #D2650) diluted docetaxel, paclitaxel, EL102 (Elara Pharmaceuticals), water soluble doxorubicin hydrochloride and controls of water only and DMSO only, were added to replicate wells (n=8) and incubated at 37 °C in 5 % CO₂ for a further 72 h. After the 72 h incubation, 40 μ l of 560 μ M resazurin (Sigma-Aldrich #199303) reconstituted in Hanks' Balanced Salt solution (HBSS) (Sigma-Aldrich #H6648) was added to each well and incubated for 3 h at 37 °C. Plates were read using the dual-beam Cytofluor 4000 fluorimeter (filters used were for excitation, 530/25 and for emission 620/40). A percentage (%) survival curve was calculated based on these values and the IC₅₀ was determined using the untreated control cultures as reference comparison for uninhibited (100 %) growth. Error was presented at \pm the percentage coefficient variance (% CV). All cytotoxicity assays were performed at least 3 times with representative results shown.

2.2.2 Sulforhodamine B-Based Assays

The relevant amounts of compound (EL102, docetaxel, etc.) were preloaded into a v-bottomed well Sterilin 96-well plate (Fisher Scientific 11309163) using the Janus Automated Workstation (Perkin-Elmer). Cells were trypsinised, counted and dispensed into 96-well Cell+ plates, containing compounds at varying concentrations, at a cell density of 1.9×10^4 cells per well. Cells were cultured for 72 h at 37 °C in a 5 % CO₂ incubator. Separately, 3 rows of a non-drug treated 96-well plate were seeded with the same cell density. After a 2–4 h incubation at 37 °C, 5 % CO₂, to allow for attachment of cells, 100 μ l of fixative, cold 10 % trichloroacetic acid (TCA) (Sigma-Aldrich #T0699) was added to the wells and left to incubate at 4 °C for 30 min. Wells were then submerged in distilled water and tapped dry 4 times, to ensure complete removal of TCA. The plate was left to air dry. This plate served as “day zero” plate. The 72 h incubated drug-treated plates

were fixed in the same way. All plates were subsequently stained with 0.057 % SRB w/v in 1 % acetic acid for 30 min and washed four times with 1 % acetic acid, to remove excess stain. Plates were allowed to air dry. Stain was eluted by addition of 10 mM Tris base (Sigma-Aldrich #T6066) solution to the wells followed by a 30 min room temperature (RT) incubation. Plates were read at 531 nm using a Victor X5 Multilabel plate reader (Perkin-Elmer). Mean optical density (OD) values of Day 0 plates were subtracted from those of sample plates. A percentage viability curve was calculated based on these values and the IC₅₀ was determined. Error was presented at ± % CV. Each cytotoxicity assay was repeated at least thrice with representative results shown.

2.2.3 Toxicity in Multi-Drug-Resistant Cell Lines

Cells were trypsinised and resuspended in fresh, complete medium at a density of 2×10^4 cells/ml. 100 µl of cell suspension was seeded into each well of a 96-well plate and cultured overnight in 5 % CO₂ at 37 °C. Varying concentrations of EL102 were added in replicate (n=8) and incubated at 37 °C for a further 72 h. Following incubation, medium was removed from each well which was then washed twice with 100 µl dPBS. Having aspirated the last of the dPBS, 100 µl of freshly prepared phosphatase substrate (10 mM p-nitrophenol phosphate in 0.1 M sodium acetate (Sigma-Aldrich #N7653-100ML), 0.1 % Triton X-100, pH 5.5) was added to each well. Plates were incubated in the dark at 37 °C for 2 h. The enzymatic reaction was stopped by the addition of 50 µl of 1 M NaOH (Sigma-Aldrich #S5881) to each well. The plates were read on a dual beam plate reader at 405 nm with a reference wavelength of 620 nm. A percentage viability curve was calculated based on these values and the IC₅₀ was determined. Error was presented at ± % CV. All cytotoxicity assays were conducted in triplicate with representative data shown.

2.2.4 DEVD Caspase 3/7 Activation Assay

Each cell line was seeded at a density of 1×10^6 cells into individual T-25 flasks (Sarstedt #83.1810.302). Cells were incubated overnight to allow cell attachment to the flask. Cells were then treated with 1, 10 and 100 nM EL102 or vehicle (DMSO). 24 h following treatment, the entire contents of each flask was harvested. Cell scrapers (Sarstedt #83.183) were used to mechanically detach cells from the base of the flask. The contents of each flask were transferred to individual 15 ml tubes and centrifuged at $350 \times g$ at 4°C for 5 min. The supernatant was removed and the pellet was re-suspended in 1 ml dPBS. The contents were centrifuged again at $350 \times g$ for 5 min at 4°C . The supernatant was discarded and the pellet was re-suspended in 110 μl of lysis buffer (50 mM HEPES pH 7.2; 5 mM EGTA (Sigma-Aldrich #E3889); 10 mM KCl (Sigma-Aldrich #60128); 2 mM MgCl_2 (Sigma-Aldrich #M8266); 2 mM DTT (Sigma-Aldrich #D0632); 1.6 mM CHAPS (Sigma-Aldrich #C9426). Lysates were then stored at -80°C if not used immediately. 90 μl of each supernatant was transferred to a 96-well microtest plate (Sarstedt #82.1581.501) for apoptosis measurement, while the remaining 20 μl of sample was retained for protein quantification using the Pierce BCA (bicinchoninic acid) Protein Assay Kit (Fisher Scientific #23227) in accordance with manufacturer's instructions. To each of the sample containing wells, an equal volume (90 μl) of caspase3 substrate (N-acetyl-Asp-Glu-Val-Asp-7 amino trifluoromethyl coumarin or 'Ac-DEVD-AFC' (BD Pharminogen #556574)) containing buffer (50 mM HEPES pH 7.2; 5 mM EGTA; 10 mM KCl; 2 mM MgCl_2 ; 2 mM DTT; 40 μM Ac-DEVD-AFC) was added. The release of AFC over 120 min was measured using Cytofluor 4400 at 37°C (excitation 400 nm, emission 508 nm), after which, the caspase3-like levels were normalised to total protein concentration. Activity was expressed as arbitrary fluorescent units (AFU) per minute per mg of protein.

2.2.5 Sub-G₁ and Cell Cycle Analysis

Cells were seeded at a density of 1.3×10^5 cells per well in a final volume of 2 ml per well in a 6-well Cell+ culture plate (Sarstedt #83.1839.300) and left to attach overnight at 37 °C in a 5 % CO₂ incubator. Cells were treated with 1 ml of medium spiked with appropriate concentrations of EL102, docetaxel or both. Following treatments, plates were returned to the incubator for 24, 48 and 72 h. The medium from each well's liquid fraction was transferred to labelled 15 ml tubes. Remaining attached cells were gently washed with 300 ml HBSS at RT. These washings were retained and added to the medium in the appropriate labelled 15 ml tubes. Cells were trypsinised with 750 ml trypsin-EDTA for 5 min at 37 °C. Trypsinisation was stopped by re-addition of 1 ml of medium from the appropriate well of origin. Cell suspensions were combined with the medium in the appropriate 15 ml tubes, and cell pellets were collected by centrifugation at 1000 x g at 4 °C for 5 min using soft acceleration. The supernatant was removed and the cell pellets were placed on ice. Pellets were re-suspended in 500 µl ice-cold dPBS and transferred to labelled 1.5 ml tubes (Sarstedt #72.706.200). Cell pellets were again recovered following centrifugation at 4 °C for 5 min at 1000 x g and supernatant was discarded. Cells were re-suspended in 150 µl dPBS. A volume of 350 µl ice-cold 100 % ethanol (Sigma-Aldrich #E7023) was added drop-wise to the cell suspension while vortexing, to avoid clumping. Cells were incubated on ice for 30 min. Following overnight storage at 20°C, cells were then centrifuged at 1000 x g for 5 min using soft acceleration. Each pellet was washed in 500 µl dPBS and suspension was centrifuged at 1000 x g for 5 min using soft acceleration, after which supernatant was removed. Each cell pellet was resuspended in propidium iodide, PI/RNase staining buffer (BD Pharmingen, #550825). Sample suspensions were incubated in the dark for 15–20 min and measured by flow cytometry on BD FACSCanto II (BD Biosciences), channel PE. Logarithmic and linear regression was performed as needed for sub-G₁ and cell cycle analyses. Flow cytometric analyses were conducted using Cyflogic software (CyFlo Ltd, Turku, Finland).

2.2.6 Analysis of PARP-Cleavage

PARP-cleavage is an indicator of apoptosis. Cells were seeded in 10 cm³ Cell+ dishes (Sarstedt #83.1802.003) at a cell density of 1 x 10⁶ per dish, and treated with the relevant doses of DMSO, EL102 and docetaxel for 24 and 48 h. After incubation, total cell protein was harvested, quantified and analysed by Western blot, as described in sections 2.3.2 and 2.3.3.

2.3 Protein Analysis

2.3.1 Antibodies

Antibody	Host/ Isotype	Company	Product #	Applications	Dilution
Anti-PARP	Rabbit pAb	Cell Signaling	9542	WB (in 5 % Milk-TBS-Tween 0.1 %)	1:1000
Anti-AR (PG-21)	Rabbit pAb	Millipore	06-680	WB (in 3 % Milk-TBS)	1:500
				ICC (in 5 % FBS-PBS-0.1 % Tx-100)	1:200
Anti-HIF1 α (Discontinued)	Rabbit pAb	Cell Signaling	07-628	WB (in 5 % Milk-TBS)	1:1000
Anti-HIF1 α	Rabbit pAb	Novus Biologicals	NB100-479	WB (in 5 % Milk-TBS)	1:2000
				ICC (in 5 % FBS-PBS-0.1 % Tx-100)	1:200
Anti- β -Actin	Mouse mAb	Pierce	MA1-91399	WB (in 5 % Milk-TBS-Tween 0.1 %)	1:200000
Anti-PSA	Mouse mAb	R&D Systems	MAB1344	WB (in 5 % Milk-TBS-Tween 0.1 %)	1:2000
Anti-CXCR4	Mouse mAb	R&D Systems	MAB171-100	WB (in 5 % Milk-TBS-Tween 0.1 %)	1:1000

Anti- β -tubulin	Rabbit pAb	Abcam	AB6046	ICC (in 5 % FBS-PBS-0.1 % Tx-100)	1:200
Anti-PCNA	Mouse mAb	Santa-Cruz	SC-56	WB (in 5 % Milk-TBS-Tween 0.1 %)	1:1000
Anti-Acetylated Tubulin	Mouse mAb	Sigma-Aldrich	T6793	ICC (in 5 % FBS-PBS-0.1 % Tx-100)	1:200
IRDye 680LT Anti-Mouse IgG	Goat pAb	LI-COR	926-68020	WB (in 5 % Milk-TBS)	1:20000
IRDye 800CW Anti-Rabbit IgG	Goat pAb	LI-COR	926-32211	WB (in 5 % Milk-TBS)	1:20000
Rhodamine Red-X-AffiniPure Fab Fragment	Goat pAb	Jackson Immuno-research Laboratories	115-297-020	ICC (in 5 % FBS-PBS-0.1 % Tx-100)	1:50
Alexa Fluor 647	Donkey pAb	Invitrogen	A-31573	ICC (in 5 % FBS-PBS-0.1 % Tx-100)	1:200
Alexa Fluor 488	Goat pAb	Invitrogen	A-11001	ICC (in 5 % FBS-PBS-0.1 % Tx-100)	1:200

2.3.2 Protein Isolation and Quantification

Cells were seeded at a density of $1-2 \times 10^6$ cells per 10 cm^3 dish or $1-2 \times 10^5$ cells per well of a 6-well Cell+ tissue culture plate and cultured in optimum conditions, to allow for attachment before necessary treatments were carried out. As was the case for most of those harvested for protein analysis, cells were rinsed twice with cold dPBS and lysed directly on the dish/place with (10 cm^3 dish, 300 μl ; 50 μl per well, 6-well plate) cold RIPA buffer (Thermo Scientific Pierce #89900) supplemented with protease inhibitor cocktail (Thermo Scientific Pierce, #78410 or #12841640) and scraped, using a cell lifter (Corning #3008) or a cell scraper (Sarstedt #83.1830), to the bottom of the well/plate and transferred to a 1.5 ml tube. Tubes were then centrifuged at 12000 x g for 15 min at 4 °C. The resulting

supernatant was collected and stored at $-20\text{ }^{\circ}\text{C}$, short-term, or $-80\text{ }^{\circ}\text{C}$, long-term. When required for further analysis by Western blot, extracted protein was quantified using a BCA kit. To do this, a standard curve, such as the example in Figure 2.1, was generated through the serial dilution of 2 mg ml^{-1} bovine serum albumin (BSA) (Sigma-Aldrich #A3059) as follows:

Vial	Volume of Water (μl)	Standard Stock Volume (μl)	Final BSA Concentration ($\mu\text{g ml}^{-1}$)
A	0	300 from 2 mg ml^{-1}	2000
B	125	375 from 2 mg ml^{-1}	1500
C	325	325 from 2 mg ml^{-1}	1000
D	175	175 from vial B	750
E	325	325 from vial C	500
F	325	325 from vial E	250
G	325	325 from vial F	125
H	400	100 from vial G	25
I	400	0	(BLANK)

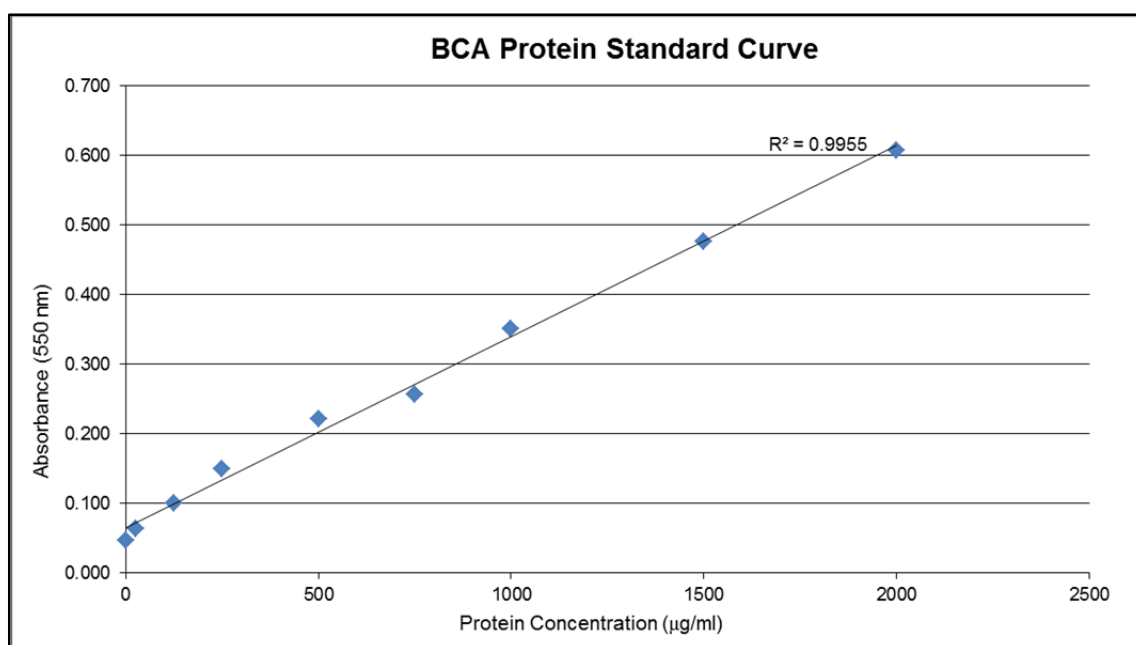


Figure 2.1 – Typical protein standard curve in BCA protein quantification.

The amount of working reagent (WR) required for the BCA was determined as follows:

(no. of standards + no. of samples)*(2 replicates)*(200 µl WR) = Total required WR

A 50:1 ratio of BCA Reagent A:Reagent B was used to make up the WR. 25 µl of each of the standards as well as 25 µl of a 1 in 5 dilution of the each of the samples was added to duplicate wells of a 96-well microplate. 200 µl of the WR was added to each well. The plate was then covered and incubated in a 37 °C oven for 30 min. The plate was brought to RT and read in a plate reader at 550 nm. Using the standard curve as a reference, sample protein concentrations could be determined.

2.3.3 Western Blot Analysis

A combination of pre-cast 10 % Bis-Tris Protein Gels, 1.5 mm, 10-well (Novex®, Life Technologies #NP0315) and 15-well (Novex, Life Technologies #NP0316), and in-house cast 15-well 10 % or 12 % Tris-glycine gels were used for the separation of proteins through sodium dodecyl sulphate (SDS) polyacrylamide gel electrophoresis (PAGE). Following loading, precast gels were run at 200 Volts (V) in the XCell SureLock™ Mini-Cell Electrophoresis System (Novex®, Life Technologies #EI0001).

2.3.3.1 In-House Gel/Wet Transfer Methodology

Gels were cast in-house and run through use of materials of the Mini-PROTEAN® Tetra Handcast System (Bio-Rad #165-8000FC) combining Tris (0.5 M pH 6.8, 1.5 M pH8.8) dH₂O, acrylamide/Bis-acrylamide 30 % solution (Sigma-Aldrich #A3699), freshly hydrated 10 % ammonium persulfate (APS) (Sigma-Aldrich #A3678), 10 % SDS (Sigma-Aldrich #L3771) and N,N,N',N'-Tetramethylethylenediamine (TEMED) (Sigma-Aldrich #T9281) at the following volumes:

10 % Resolving (Lower) Gel	1 Gel
dH ₂ O (ml)	4.2
Acrylamide/Bis-acrylamide, 30 % solution (ml)	3.3
Lower/1.5 M Tris pH 8.8 (ml)	2.5
10 % SDS (μl)	100
10 % APS (μl)	50
TEMED (μl)	5

OR

12 % Resolving (Lower) Gel	1 Gel
dH ₂ O (ml)	3.5
Acrylamide/Bis-acrylamide, 30 % solution (ml)	4
Lower/1.5 M Tris pH 8.8 (ml)	2.5
10 % SDS (μl)	100
10 % APS (μl)	50
TEMED (μl)	5

A glass gel casting cell was set up, consisting of a clean, dry glass plate (Bio-Rad #165-3308), 1.5 mm glass spacer (Bio-Rad #165-3312) that were held together in a casting frame (Bio-Rad #165-3304) and a casting stand (Bio-Rad #165-3303). Approximately 7 ml of the above mentioned solution (resolving gel) was transferred to this apparatus, immediately after the addition of the TEMED. A volume of 500 μl dH₂O was added to the surface of the solution to prevent drying. Following the setting or polymerisation of the lower gels (~1 h), the surface liquid was decanted and the following stacking or loading gel was cast by mixing the following volumes:

4 % Loading (Upper) Gel	2 Gel
dH ₂ O (ml)	6.1
Acrylamide/Bis-acrylamide, 30 % solution (ml)	1.4
Upper/0.5 M Tris pH 6.8 (ml)	2.5
10 % SDS (μl)	100
10 % APS (μl)	75
TEMED (μl)	20

Immediately after the addition of TEMED, the 4 % solution was transferred to the remainder of the glass chamber. A 10 or 15 tooth PAGE comb was inserted into this still-liquid solution and allowed to set for approximately 1 h. The displaced gel overflow after comb insertion was mopped up with a piece of tissue paper. Running buffer was made up as follows:

1 X Running Buffer (1L)	Volume (ml)
*10 X Tris-glycine	200
10 % SDS (μ l)	20
dH ₂ O	1780

(* A 1 L stock of 10 X Tris-glycine : 30 g Tris, 144 g glycine and up to 1 L of dH₂O)

These in-house gels, along with holders were removed from the casting cell and placed on the electrode assembly which was placed into the gel tank. The inner- and outer- chambers of the electrode assembly were filled with the running buffer. Gel combs were withdrawn from the loading gel. 3 μ l pre-stained SeeBlue Plus2 protein standard (Invitrogen, Life Technologies #LC5925) was loaded to the first well of the gel. This served as a molecular weight standard comparison for samples detected following western blot. Subsequent wells were filled with up to 50 μ g of protein samples. The electrode assembly was connected to a power supply via the repositioned tank lid. A current of 100–200 V for 1–2 h was sufficient for migration of the lower molecular weight proteins to the end of the gel. For each of the in-house gels, a wet transfer was performed. This was done by means of a Mini Trans-Blot Module (Bio-Rad #170-3935). In brief, following electrophoresis, the gel, was removed from the glass spacer and placed in a dish containing cold transfer buffer (For 2 L: 200 ml 10 X Tris-glycine, 1.4 L dH₂O and 400 ml methanol (Sigma-Aldrich #10675112). The black coloured side of the opened gel holder cassette was submerged and laid flat against the bottom of the transfer buffer container. In the following order, a stack was made upwards, atop the black-coloured side of the cassette: a pre-soaked fibre pad, wet filter card (Whatman, GE Healthcare #3030-861), the pre-equilibrated gel, a wet nitrocellulose membrane (Amersham Protran, GE Healthcare #10600004), a wet filter card and a pre-soaked fibre pad. Keeping this stack submerged in

the transfer buffer, air bubbles were rolled out of the stack as these disrupt the transfer of protein from the gel to the membrane. The cassette was closed and placed in the 2 cassette transfer module. The transfer module was placed in the buffer tanked which was filled with pre-chilled transfer buffer and moved to 4 °C. A magnetic stirring bar was placed at the bottom of the tank and the module's electrodes were connected to a power supply via the tank lid. The tank was placed atop an active magnetic stirring unit. A constant current of 40-50 mA was maintained overnight for protein transfer to occur.

2.3.3.2 Precast Gel/Dry Transfer Methodology

The iBlot® 7 min, gel dry transfer system was used for the transfer of protein from the precast gels via iBlot gel transfer stacks (Life Technologies #IB3010-02 or #IB3010-01) to an integrated PVDF membrane.

2.3.3.3 Detection of Proteins

The relative expression of specific proteins transferred to either membrane was detected through use of the appropriate primary and secondary antibodies listed in Table 2.2. Antibodies were diluted (Table 2.2) in 3 % or 5 % skimmed milk (Sigma-Aldrich #70166) reconstituted in 1 X Tris-buffered saline (TBS) (25 mM Tris; 3 mM potassium chloride (KCl); 68.5 mM sodium chloride (NaCl) (Sigma-Aldrich #S3014) (pH8) with preservative 0.05 % sodium azide (Sigma-Aldrich #S2002) and with or without 0.1 % Tween (Sigma-Aldrich #P1379). Following either 1 h of RT blocking or overnight at 4 °C blocking of the membrane in 3 % or 5 % skimmed milk in TBS, the antibody dilution was added to the transfer membrane (Nitrocellulose/PVDF) and rocked overnight at 4 °C. Primary antibodies against endogenously expressed controls were used to confirm uniform protein loading. Following incubation with primary antibody, the antibody solution was decanted to a pre-labelled tube and stored at 4°C, short-term or -20 °C, long-term. Diluted antibodies were re-used no more than twice. Blots were then washed three times for 3–5 min in TBST. The appropriate secondary antibodies used against each of the primary antibodies used, were detected using the LI-

COR ODYSSEY CLx imaging system. A complete list of primary and secondary antibody information is shown in Table 2.2.

2.3.4 Cellular Fractionation of Proteins

Cells were seeded at a density of 1×10^6 per 10 cm^3 tissue culture dish and cultured in optimum conditions, to allow for attachment before necessary treatments were carried out. After the required incubation time, cells were carefully washed twice in 1 ml pre-chilled dPBS. Cold dPBS/1 mM EDTA was added to the culture dish. Cells were scraped in this buffer and pelleted by a 5 min centrifugation at 3,000 rpm at 4°C . Supernatant was discarded and the pellet was re-suspended in 200 μl Harvest Buffer (10 mM HEPES pH 7.9, 50 mM NaCl, 0.5 M sucrose, 0.1 mM EDTA, 0.5 % Triton X-100, with the following freshly-added on the day of fractionation: 1 mM DTT, 10 mM sodium pyrophosphate, 100 mM sodium fluoride, 17.5 mM β -glycerophosphate and 1 X protease inhibitor cocktail III (Fisher Scientific #12841640)) and left to incubate on ice for 5 min. The cell suspension was spun at $220 \times g$ for 10 min. The resulting supernatant and pellet were both retained and the supernatant was placed in a fresh tube and centrifuged at $17000 \times g$ for a further 20 min before transferring to another 1.5 ml tube for storage at -80°C . This supernatant contained the membranous and cytosolic fraction of the cellular protein. The pellet retained from the previous centrifugation step, contained the crude extract of nuclear proteins and required a re-suspension and washing in 500 μl of Buffer A (10 mM HEPES pH7.9, 10 mM KCl, 0.1 mM EDTA, 0.1 mM EGTA and with 1 mM DTT and 1 X protease inhibitor cocktail III freshly-added on the day of fractionation). After another 10 min 4°C centrifugation at $220 \times g$, the supernatant was discarded, while the pellet was dislodged with 200 μl of Buffer C (10 mM HEPES pH7.9, 10 mM KCl, 0.1 mM EDTA, 0.1 mM EGTA 0.1 % IGEPAL CA-630 (Sigma-Aldrich #I8896) and 1 mM DTT and 1 X protease inhibitor cocktail III freshly added on the day of fractionation). At 4°C , the contents were initially vortexed for 5 min at high speed to ensure complete dislodgement of the pellet. There followed a 10 min vortex at medium speed, also at 4°C . The suspension was then centrifuged at 4°C , for 20 min at $17,000 \times g$. The resulting supernatant was retained and frozen at -80°C .

Both cytosolic and nuclear fractions were quantified by BCA and analysed by Western blot, as previously described.

2.3.5 Immunocytochemistry

2.3.5.1 Cell Fixation

Coverslips were sterilised in 100 % ethanol, and rinsed twice with sterile dPBS. If necessary for the individual cell type, to assist attachment, coverslips were coated in sterile poly-L-lysine (Sigma-Aldrich #P4707), and allowed to air-dry in a sterile biosafety cabinet. The coverslips were then inserted to the base of each well of a 6-well plate. Cells were trypsinised as previously mentioned and seeded at a density of 1×10^5 per well and allowed overnight attachment at 37 °C, in a 5 % CO₂ incubator. Cell treatments were carried out and at the relevant time-points, cell fixation was achieved by (A) 10 min incubation in ice-cold methanol at -20 °C or (B) 2 % paraformaldehyde (PFA) (Agar Scientific #AGR1026) at RT for 15 min. In the instance of androgen deprivation and using the LNCaP cell line, cells had to first be seeded in complete optimum RPMI 1640 for 24 h, followed by a 72 h incubation in replacement complete PRF RPMI. For hypoxia experiments, DU145 cells were allowed overnight attachment in normoxic (20 % O₂) conditions before plates were moved to hypoxic (1 % O₂) conditions for the allotted time periods.

2.3.5.2 Immunostaining

For immunostaining of intracellular proteins it was at first necessary to permeabilise cells. While cell fixation had initiated this, incubation of the coverslip-mounted fixed cells were twice incubated in dPBS/Triton X-100 (0.1 %) for 3 min. Cells were blocked for 30 min with 5 % FBS/dPBS/Triton X-100 (0.1 %). Fresh blocking solution was used for the appropriate dilution of primary antibodies (Table 2.2). This solution was added to the coverslips which were incubated at RT for 1 h in a water-filled staining tray (Slideshow, Jilks Plastics # 6844-30BL). Following incubation, coverslips underwent 3 washes in dPBS. In blocking solution appropriate dilutions of secondary fluorescent conjugated antibodies specific for the primary antibodies were made. These were added to the coverslips and incubated at RT for 1 h in the

water-filled staining tray which was protected from light. Coverslips underwent 3 further washes in dPBS. Coverslips were counterstained with mounting medium Slow Fade Gold anti-fade reagent (Life Technologies S36936) supplemented with 0.5 mg ml^{-1} 4,6-diamidino-2-phenylindole dihydrochloride (DAPI) (Sigma-Aldrich #D8417) diluted 1 : 100 and coverslips were fixed to slides using nail varnish. Staining was imaged using Delta Vision Core Imaging System C0607 with SoftWoRx software (Applied Precision, Issaquah, WA, USA) or the Olympus BX51 Upright Fluorescent Microscope with Improvision Optgrid System and Improvision Volocity Software. Final image analysis was conducted using FIJI software (General Public Licence v2).

2.3.6 HIF1 TransAM ELISA

HIF1 TransAM ELISA was carried out as per manufacturer's instructions. Briefly, nuclear protein extraction of EL102-treated hypoxic and normoxic PC-3 cells was performed as described in 2.3.3. Protein concentration was determined by BCA (2.3.2). Each nuclear extract was diluted to 25 μg per well and added to individual wells of the 8-well strips which were pre-coated in complete binding buffer. 10 μg of positive control (HELA + CoCl_2) was added to separate wells. Wells were covered and incubated with mild agitation, on a rocking platform, for 1 h. After the incubation, wells were each washed 3 times with 200 μl wash buffer. A 1:500 dilution of the provided HIF1 antibody was made in antibody binding buffer and 100 μl of the antibody dilution was added to each well. The wells were covered and incubated, undisturbed at RT for 1 h. Each well underwent 3 washes with 200 μl wash buffer. 100 μl of provided HRP-conjugated (pre-diluted 1:1000 in antibody binding buffer) was added each well. Wells were again covered and incubated undisturbed at RT for 1 h. Developing solution was brought to RT. Wells were washed 4 times with 200 μl wash buffer. 100 μl RT developing solution was added to each of the wells and protected from light for 8–12 min RT incubation. 100 μl stop solution was added to each well and the absorbance values of contents was read within 5 min at 450 nm with reference wavelength 655 nm using a spectrophotometer.

2.4 Genetic Analysis

2.4.1 Plasmid Preparation

Reporter gene assays to test the androgen receptor response were carried out using the constructs MMTV-luc (de Ruiter *et al.*, 1995) and PSA-407E-luc (Zhang *et al.*, 1997). These plasmids were generously gifted by Prof. Daniel E. Frigo, Center for Nuclear Receptors and Cell Signaling, University of Houston, Texas. The pCMV- β -gal plasmid (Clontech) was generously donated by Dr. Jill McMahon, National Centre for Biomedical Engineering Science, NUI Galway.

2.4.1.1 Bacterial Transformation

Each plasmid was delivered to the lab in a 1.5 ml tube suspended in a few ml of RT water. Before opening, tubes were spun to save any droplets that may have formed around the tube cap from being lost. Sub-cloning Efficiency™ DH5 α ™ Competent Cells (Invitrogen, Life Technologies #18265-017) were transformed as per supplier's instructions. Briefly, one vial of competent cells was thawed on ice and an aliquot of 50 μ l of cells was added to individual tubes for each transformation. Any unused cells were frozen in a dry ice ethanol bath for 5 min before being returned to the -80 °C freezer for storage. 1 μ l of each of the plasmid suspensions was added to the cells which were gently mixed by swirling or tapping. One of the tubes had no DNA added, as a control. Tubes were left to incubate on ice for 30 min. During this incubation a heating block (Fisher Scientific #11751637) was set to 42 °C and tubes were then placed in this for a heat shock of 20 sec before returning to ice for a further 2 min. 950 μ l of pre-warmed SOC medium (Invitrogen, Life Technologies #15544-034) was added to each of the tubes which were shaken at 225 rpm at 37 °C for 1 h. For each of the transformations, both a 50 μ l and a 150 μ l volume of transformed culture suspension was spread across the surface of individual pre-warmed 100 μ g ml⁻¹ ampicillin (LB agar (Fisher Scientific #10081163) nutrient petri-dishes (Sarstedt #82.1472) using an L-shaped spreader (Fisher Scientific #11836191). (Note: In this instance, each of the plasmids, used, conferred ampicillin resistance). Plates were placed in a 37 °C oven for 30 min with the

lid-side-up, and were then inverted for overnight culture. Control cultures introduced to selective plates did not produce visible colonies whereas the opposite was true for those that were transformed. Although positive for ampicillin resistance, confirmation of successful transformation was only achieved through subsequent purification of the plasmids and through visualisation by electrophoresis of linearized DNA, the product of restriction digest. An isolated colony was picked from each of the plates and a sample was taken using a 10 µl pipette tip which was ejected into a 15 ml tube to inoculate a 4 ml volume of 100 µg ml⁻¹ ampicillin (Sigma-Aldrich #A9518) containing (pre-autoclave sterilised) LB Broth Miller (Fisher Scientific #10113293). These cultures were shaken at 225 rpm overnight at 37 °C after which the medium became murky due to the increase in optical density of proliferating bacterial cells. The inoculating tip was removed and each the culture was pelleted by centrifugation at 200 x g for 5 min at 4 °C. At this point the pellet could have been stored at -20 °C until need for plasmid purification.

2.4.1.2 Miniprep

The Qiagen QIAprep Spin Miniprep Kit (Qiagen #27104) was used for this initial purification of the plasmid. Before starting, RNase A was added to Buffer P1 and if the pellets were frozen, they were left to thaw at RT for 20 min. 250 µl Buffer P1 was added to the tubes to re-suspend the pellets. This suspension was transferred to 1.5 ml tubes which were vortexed until cell clumps had been dissolved. 250 µl Buffer P2 was added to each suspension and inverted six times to allow for adequate mixing. 350 µl of Buffer N3 was added and immediately mixed by six further inversions of tubes. This action turned the liquid cloudy. The samples were spun for 10 min at 17900 x g. The supernatant was retained and applied to QIAprep spin columns by decanting or pipetting while the pellet was discarded. The supernatants were passed through the spin columns by centrifugation at 1000 x g for 60 sec. The flow-through was discarded. The columns were washed through addition of 750 µl Buffer PE to the spin column and centrifugation at 1000 x g for 60 sec. The flow-through was again discarded and the column was centrifuged for an extra 60 sec. The spin column was then placed in a fresh 1.5 ml tube.

50 µl of Buffer EB (10 mM Tris-Cl, pH 8.5) was added to the centre of the spin column and allowed to sit at RT for 1 min. After this brief incubation, the spin column in the 1.5 ml tube was spun at 1000 x g for 1 min. The concentration of the plasmid DNA eluted was determined by nanodrop measurement.

2.4.1.3 Restriction Digest

In order to linearize the circular plasmids, a restriction digest was carried out. In this instance the endonuclease enzyme selected for all four plasmids was BamHI-HF™ (New England BioLabs #R3136S). The following was added to each 30 µl digestion reaction:

Reagent	Volume (µl)
1 µg Circular DNA plasmid	X
10 X Buffer	3
Restriction Enzyme (BamHI-HF)	1
Molecular Grade dH ₂ O	Up to 10 µl

The above was added to a 1.5 ml tube and contents were mixed through pipetting up and down a couple of times. The tube was paced in a 37 °C heating block for 1 h. A 0.8 % agarose (Sigma-Aldrich #A9539) gel was made by adding 0.4 g of agarose to a flat bottomed flask of 50 µl 1 X TAE (diluted from 10 X TAE: 48.4g Tris, 11.4 ml glacial acetic acid, 3.7 g EDTA and the remainder of the 1 L stock was comprised of dH₂O) and heated in a microwave until the agarose has gone fully into solution. The contents were allowed to cool slightly before adding 5 µl of 10000 X Gel Red Nucleic Acid Gel Stain (VWR #730-2958). This was then poured into the gel casting portion of the comb-containing Mini-Sub Cell GT Cell (Bio-Rad #164-0300) and left at RT for 30 min to solidify. The gel was immersed in 1 X TAE the gel tank with the gel oriented with the wells closest to the negative end. 5 µl of 6 X gel loading dye (New England BioLabs #B7024S) was added to the product of the restriction digest. 5 µl of 1 kilobase (kb) pre-stained DNA ladder (New England BioLabs #N0468S) was added to the first lane's well, while the subsequent wells were loaded with 18 µl of the samples. With the gel loaded, the lid was returned to the electrophoresis tank and electrodes

were connected to the power supply set to 110 V for 1–1.5 h, until the pinkish red band had migrated 80–90 % the length of the gel (Figure 2.1). The power supply was terminated and electrodes were disconnected. The gel was removed from the tank and placed in a gel imager (Bio-Rad #170-9460), where lanes were imaged in red channel. Referring to the plasmid maps, anticipated excision and band size confirm the identities of the purified plasmids.

2.4.1.4 Making Glycerol DH5 α Stocks

Before proceeding to Maxiprep purification of plasmids for transfection, glycerol stocks of plasmid-positive colonies were made. Sample cells were taken from the same colonies selected for Miniprep purification in the same way. This time 5 ml of selective medium was inoculated prior to 37 °C incubated 225 rpm shaking for 5 h. At 5 h, six 800 μ l volumes of the growing cultures were pipetted in sterile 1.8 ml cryovials (Sarstedt #72.380.004). 200 μ l of pre-autoclaved 80 % glycerol was added to each of these vials which were briefly mixed by vortexing. The vials were stored at -80 °C. When needed, the vial was taken out of the freezer, but not thawed, and a sterile tip was touched to the surface of the contents then ejected into 5 ml of selective (100 μ g ml⁻¹ ampicillin) medium.

2.4.1.5 Maxiprep

High purity, high yield plasmids were purified using the EndoFree Plasmid Maxi Kit (Qiagen #12362). A colony was selected from a glycerol stock, as mentioned, previously. A starter culture of 5 ml was shaken for 5 h at 37 °C before 300 μ l of the culture was diluted into the larger volume 120 ml of fresh and sterile, similarly selective, LB broth medium in a pre-autoclaved 500 ml flat bottomed flask and shaken overnight in the same conditions. 100 ml of the culture was spun at 6000 x g for 15 min at 4 °C and the resulting cell pellet could be stored at -20 °C until a later time, if necessary. Proceeding, 10 ml Buffer P1 (with RNase added) was used to re-suspend the pellet. An equal volume of Buffer P2 was added and mixed by vigorous inversion 6 times and incubated at RT for 5 min. During this incubation a screw cap is placed onto the outlet nozzle of a QIAfilter Maxi Cartridge and placed in a

standing 50 ml tube. 10 ml of pre-chilled Buffer P3 was added to the lysate and mixed through vigorous inversion 6 times. Immediately after mixing, the suspension was poured into the barrel of the QIAfilter Cartridge and left undisturbed at RT for 10 min. Following the incubation, the cap was removed from the Cartridge outlet and returned to the receiving 50 ml, as a plunger is gently fitted to the top of the Cartridge barrel. The plunger is gently but persistently lowered into the column until all 25 ml of the lysate had passed into the 50 ml tube. A 120 µl aliquot was taken from this and labelled 'sample 1' for quality control purposes. 2.5 ml of Buffer ER was added to the flow-through of the column and mixed through 10 tube inversions before 30 min incubation on ice. During this incubation, a QIAGEN-tip 500 was equilibrated through application of 10 ml Buffer QBT to the column which was allowed to flow through by gravity to the receiving 50 ml tube. When flow-through ceased, the 50 ml tube was emptied. Fresh from its 30 min on-ice incubation, the lysate was decanted into the QIAGEN-tip. 120 µl of the flow-through was retained and labelled 'sample 2' for quality control purposes. The QIAGEN-tip was washed twice with Buffer QC and each time, 120 µl of the flow-through was retained only to be combined and labelled 'sample 3' for quality control purposes. DNA was eluted by 15 ml Buffer QN. A 50 µl aliquot of this eluate was retained and labelled 'sample 4' for quality control purposes. DNA precipitation was carried out through addition of 10.5 ml RT isopropanol to the elution. This was immediately mixed and centrifuged at 5000 x g for 1 h at 4 °C. The supernatant was discarded by careful decanting so as not disturb the pellet which was washed with 5 ml endotoxin-free 70 % ethanol and spun again for 1 h at 5000 x g. The supernatant was again carefully discarded and the pellet was allowed to air-dry for about 8 min before it was re-suspended in Buffer TE. Note: over-drying can make re-suspension difficult. The concentration of DNA was determined through use of a nanodrop (Thermo Scientific #ND-2000).

2.4.2 Transient Transfections

LNCaP and PC-3 cells were seeded at densities of 5×10^4 cells per well and 1×10^4 cells per well, respectively of individual Cellbind 24-well plates (Corning #3337). The cells were cultured for 24 h in a 37 °C, 5 % CO₂ incubator in respective optimum media (RPMI 1640 and F12 Hams) to allow attachment. These media were withdrawn and replaced with phenol red free (PRF) RPMI medium (supplemented with 10 mM HEPES buffer; 1 X Glutamax; 1 X sodium pyruvate (NaPyr); 1 X Anti-mycotic Antibiotic ; 10 % charcoal stripped FBS) and left to culture for a further 24 h in a 37 °C 5 % CO₂ incubator. On day 3, transient transfection was carried out. To do this, a 1:20 Lipofectin reagent (Invitrogen, Life Technologies #18292011) : OPTI-MEM (Gibco, Life Technologies #11058021) mixture was made and incubated at 37 °C for 45 min. A 2-3 µg stock of plasmid DNA, containing the reporter genes, was made up in OPTI-MEM with 81 ng per 100 ng transfection to be used. Exhausted PRF medium was carefully aspirated from each of the wells of the 24-well plates. Cells were briefly and carefully rinsed with 200 µl OPTI-MEM which was then withdrawn and carefully replaced with 400 µl fresh OPTI-MEM per well. The DNA dilutions in OPTI-MEM were combined with 325 µl of pre-incubated Lipofectin : OPTI-MEM mix and vortexed briefly. This solution was incubated at RT for 15 min. 50 µl of Lipofectin : OPTI-MEM : DNA was carefully added to each well of the 24-well plate already containing 400 µl OPTI-MEM per well. These plates were incubated for 3–5 h, after which the transfection mix was withdrawn and cells were carefully rinsed with 200 µl dPBS. 900 µl of fresh complete PRF RPMI was added to each well and incubated in a 37 °C, 5 % CO₂ incubator for 24 h. Incubation with or without hormones, and in the presence or absence of EL102 or bicalutamide (Sigma-Aldrich #B9061) was carried out over 24 h in a 37 °C 5 % CO₂ incubator with each condition conducted in triplicate. At this time-point, cells were lysed and analysed through reporter gene assays.

2.4.3 Reporter Gene Assays

2.4.3.1 Cell lysis

Cells were transiently transfected, as described previously (2.4.2), and treated with drug concentrations simultaneous with vehicle ethanol or 1nM methyltrienolone (R1881)(Sigma-Aldrich #R0908) for 24 h. 5 X Luciferase Cell Culture Lysis Buffer (Promega #E1500) was diluted to 1 X concentration in water and brought to RT. To each well of the 24-well plate, 65 μ l of 1 X lysis buffer was added and complete coverage of the monolayer was ensured by rocking the plates back and forth. (At this point, plates may be stored at -80 degrees C.) This lysate was used to directly measure the luciferase and -galactosidase levels of the cells following the treatment conditions. This was done by way of luciferase (Promega) and CPRG assays (G-Biosciences), respectively.

2.4.3.2 CPRG Assay

Reagents from the *Beta*-galactosidase Assay kit (G-Biosciences #786-651) were used to carry out this assay. Firstly, anhydrous substrate chlorophenol red- β -D-galactopyranoside (CPRG) was reconstituted to 25 X by the addition of 550 μ l CPRG Assay Reaction Buffer which was then briefly vortexed to ensure adequate mixing. Next, the 25 X CPRG was diluted to 1 X in water. To obtain the amount of 1 X needed to conduct 100 reactions, all 550 μ l of the 25 X substrate was added to 13.5 ml water. Individual 25 μ l samples of the 65 μ l cell lysate, prepared as described previously, were added to each well of black-walled, clear-bottomed 96-well plate (Corning #3603). (Note: Sufficient time was allowed for lysates to thaw if stored at -20 °C). A note was made of the time of addition when 125 μ l 1 X CPRG reagent were added to each sample-containing well of the 96-well plate. The plate was wrapped in aluminium foil and incubated at 37 °C with readings being taken from 30 min or up to 72 h (until a colour change occurs). A plate reader capable of readings at wavelengths 570–595 nm, was used to detect the colour changes over time. This data serves as a normalizing factor for transfection.

2.4.3.3 Luciferase Assay

Reagents, specifically 5 X Lysis Buffer, Luciferase Assay Substrate (Luciferin) and Luciferase Assay Buffer were obtained from the Luciferase Reporter Assay system (Promega #E1500). The 5 X Lysis Buffer was used in the lysis of cells for both CPRG and luciferase assays. Luciferin was reconstituted by addition of 10 ml Luciferase Assay Buffer. Note: Exposure of reconstituted luciferin to both light and multiple freeze-thaw cycles was avoided. Another 25 µl of each cell lysate was added to individual wells of a black-walled, clear-bottomed 96-well plate. 95 µl of luciferin was added to each of the wells. Plates must be read instantly in a plate reader capable of 2 sec measures of luminescence. The results were normalised through dividing by the corresponding CPRG sample reads. With each condition these data, known as relative light units (RLU), were averaged and represented graphically (with error being expressed as ± standard error of the mean (SEM)).

2.4.4 Total RNA Isolation

Cells were seeded at a density of $1-2 \times 10^6$ and cultured in 10 cm³ tissue culture dishes and treated as necessary for the relevant time period in a 37 °C, 5 % CO₂ incubator. Next, cells were taken from the incubator, medium was removed and cells were washed twice in 1 ml of cold dPBS. After the dPBS had been removed, 1 ml of cold Tri-Reagent (Sigma-Aldrich # T9424) was added to each of the plates. This was done in a fume hood. Complete coverage of the monolayer was achieved by rocking the plates back and forth. The contents of the dish were homogenised through repeated pipetting up and down before moving to pre-labelled 1.5 ml tubes on ice. These can be stored for up to 1 month at -80 °C. Harvests were left at RT for 5 min to ensure complete dissociation of nucleoprotein complexes. 200 µl of chloroform was added to the harvest solution and shaken vigorously for 15 sec. Tubes were allowed to stand undisturbed for 15 min at RT. Tubes were moved to a refrigerated centrifuge and spun at 4 °C for 15 min at 12000 x g. The resulting upper aqueous phase of each tube was transferred to fresh, pre-labelled 1.5 ml tubes along with 500 µl RT isopropanol (Sigma-Aldrich #I9516). This was mixed through several inversions of the tube and

incubated at RT for 10 min before moving to -20 °C overnight. Tubes were again removed to the 4 °C centrifuge and spun at 12000 x g for 10 min. The resulting supernatant was carefully removed so as not to disturb the pellet which was washed in 1 ml 70 % ethanol. After a brief vortex, tubes were centrifuged at 7500 x g for 5 min at 4 °C. The supernatant was again removed carefully and the RNA pellet was allowed to air-dry for 5–10 min at RT. Note: Over-drying the pellet makes its re-suspension difficult. The RNA pellet was re-suspended in 50 µl DEPC water and mixed by repeat pipetting. The RNA was quantified by nanodrop. Samples with an A260/A280 ratio of RNA >1.7 were stored at -80 °C.

2.4.5 cDNA Synthesis

To synthesise complementary DNA (cDNA) from each of the samples of total RNA containing messenger RNA (mRNA), a reverse transcription polymerase chain reaction (RT-PCR) was carried out. The Tetro cDNA Synthesis Kit (Bioline, Meridian Life Science #BIO-65043) was used. Each 20 µl reaction contained the following:

Reagent	Volume (µl)
1 µg Total RNA	X
5 X RT Buffer	4
Primer: Oligo (dT) ₁₈	1
10 m dNTP Mix	1
Tetro Reverse Transcriptase (200 u µl ⁻¹)	1
DEPC Treated water	up to 20 µl

The above contents were gently mixed in a 0.2 ml PCR tube (Eppendorf #0030124359) by repeated pipetting and then placed in a thermal cycler, which was programmed, for 1 cycle, to heat the tubes to 45 °C for 30 min followed by 85 °C for 5 min, to inactivate the enzyme. The reaction tube was held at 4 °C. The reaction was stored at -20 °C until ready to proceed with quantitative PCR (qPCR). Note: A common control for this reaction is to take a sample of pooled RNA and carry out the reaction above replacing the transcriptase with RNase-free water.

2.4.6 qPCR

With the cDNA synthesised, as described previously, qPCR was used to determine the relative expression of specific genes between samples normalised by the expression of an endogenously expressed gene, in this case, 36B4. qPCR was carried out using a 96-Microwell ThermoFast qPCR plate (Abgene, Thermo Scientific #AB-1900) and a SensiFAST™ SYBR Hi-ROX Kit (Bioline, Meridian Life Science #BIO-92005). Each well contained a 13 µl reaction with the following constituents:

Reagent	Volume (µl)
Sample cDNA Template	0.2
Forward Primer (10 µM)	0.5
Reverse Primer (10 µM)	0.5
2 X SensiFAST SYBR Hi-Rox Mix	6.5
Molecular-Grade dH ₂ O	5.3
	<hr/>
	13

Following addition of the above constituents to each of the wells, the PCR plate was sealed with an adhesive optically clear seal (Abgene, Thermo Scientific #AB1170) and pulse-spun at 300 x g for 30 sec. The plate was then placed in a StepOnePlus™ Real-Time PCR System (Applied Biosystems #4376600). The following cycling protocol was used for all PCR Reactions unless otherwise indicated: STEP1: One cycle at 95 °C for 5 min. STEP2: This was followed by 40 cycles of 95 °C for 30 sec, 60 °C for 30 sec and 72 °C for 30 sec. STEP3: A final cycle of 72 °C for 7 min followed. Step4: A melt curve was generated from 70–90 °C to detect the presence of primer dimers or other transcripts. Each cDNA sample was run in triplicate and normalized to levels of 36B4 with error represented as ± SD. The average Ct was calculated for the gene of interest and for the normalizing gene. The ΔCt (Ct gene of interest – Ct normaliser) was calculated. From this the $2^{-\Delta Ct}$ could be determined and the levels of gene expression calculated compared to control cells. Each qPCR was performed at least 3 times with representative data shown.

2.4.7 Primers

Primers were purchased from Sigma-Aldrich and were delivered lyophilised. These were reconstituted in molecular grade dH₂O to a master concentration of 100 µM and stored at -20 °C. 10 µM working stocks were made by making a 1 in 10 dilution. The sequences for each of the primers used can be found in Table 2.3. Where possible, primers were designed to span exon-intron boundaries so as to reduce genomic DNA amplification. Each instance a primer set was used for the first time, a standard curve was generated with a 1 in 5 serial dilution of pooled cDNA (dilution series: 1.0, 0.2, 0.04, and 0.008). This was done to determine the percentage amplification efficiencies (% amplification Efficiency = $(10^{-1/\text{slope}}) \times -1 \times 100$) of the individual primer sets. Each primer set's sequences and % efficiency is shown in Table 2.3.

Primer	Sequence	% Efficiency
AR	Forward: 5'-GAATTCCTGTGCATGAAAGCA-3'	99
	Reverse: 5'-CGAAGTTCATCAAAGAATTTTTGATT-3'	
CXCR4	Forward: 5'-TGGCCTTATCCTGCCTGGTAT-3'	93
	Reverse: 5'-AGGAGTCGATGCTGATCCCAA-3'	
36B4	Forward: 5'-GGACATGTTGCTGGCCAATAA-3'	98
	Reverse: 5'-GGGCCCAGACCAGTGTT-3'	
LDHA	Forward: 5'-CACCATGATTAAGGGTCTTTAC-3'	108
	Reverse: 5'-AGGTCTGAGATTCCATTCTG-3'	
GLUT1	Forward: 5'-GACGGGTCGCCTCATGCTGG-3'	92
	Reverse: 5'-GCGGTGGACCCATGTCTGGT-3'	

2.5 Cell Migration Assays

Migration assays were performed using the Real Time Cell Analyser or RTCA (ACEA). In brief, 1×10^6 LNCaP cells were seeded to 10 cm^3 tissue culture dishes and allowed to attach by culturing undisturbed in optimum conditions for 24 h. Cells were then deprived of androgens for 72 h by withdrawal of RPMI 1640 and replacement with complete PRF RPMI (outlined in section 2.1.2). After the 72 h period, cells were trypsinised as described previously, with the 10 % serum-containing PRF RPMI stopping the reaction. The cell pellet was washed by re-suspension in 10 ml serum-free PRF RPMI (SFM), re-pelleted by centrifugation at $200 \times g$ and seeded in SFM to the top chamber of a CIM-16 plate. SFM was added to each of the lower chambers with one of the following conditions: no chemoattractant, 10 % normal FBS or $100 \text{ ng } \mu\text{l}^{-1}$ of CXCL12 (SDF1 α). Any additional treatments with chemotherapeutic agents to be performed in the top chamber were initially added to the bottom chamber so as not to introduce an unwanted gradient between both chambers. After a 30 min equilibration period to allow the cells to settle to the bottom of the upper chamber, the CIM-Plate 16 was inserted into the RTCA docks and cell migration was measured in real-time with the level of impedance to an electrical current, the measure of the rate at which cells migrated from top chamber to bottom over a period of 48 h.

2.6 Murine Xenograft Models

CWR22 tumours were taken from an *in vivo* passage, cut into small fragments and transplanted subcutaneously (SC) into the flank of 48 nude mice. At day 13, when the tumours were palpable, mice were randomised into 10 groups with 8 mice each and treatment initiated. The groups included: (A) vehicle (10 % DMSO, 10 % cremophor, aqua *per os* (po), (B) intravenous (iv) docetaxel 12 mg kg^{-1} , (C) EL102 12 mg kg^{-1} po (0700 hours and 1700 hours daily), (D) EL102 15 mg kg^{-1} po (E) docetaxel 12 mg kg^{-1} iv and EL102 12 mg kg^{-1} po and (F) docetaxel 12 mg kg^{-1} iv and EL102 15 mg kg^{-1} po. The injection volume was 5 ml kg^{-1} . The different tumour groups were sacrificed on separate days for ethical reasons (large tumours). Tumour

diameter of the SC tumour, and mouse body weights were measured twice a week with a calliper. Tumour volumes were calculated according to:

$$V = (\text{length} \times (\text{width})^2)/2.$$

Tumour xenograft models were performed at EPO Experimental Pharmacology and Oncology, Berlin-Buch GMBH, Germany. These studies were performed under the approval A0452/08 (Landesamt für Gesundheit und Soziales, Berlin). The study was performed according to the German Animal Protection Law and the UICCR, 2010.

2.7 Preliminary Methodology: Elara Pharmaceuticals Findings

2.7.1 Proteomic Analysis of HIF1 α Activity

For the preliminary analysis of cellular HIF1 α protein expression following EL102 treatments, Elara Pharmaceuticals commissioned a basic proteomic investigation at Hypoxium Ltd (Cambridge, UK). Here, HCT116 cells were seeded at a density of 5×10^6 cells per well to 6-well plates and allowed to adhere overnight under normoxia. The 3 mM stock of DMSO diluted EL102 was further diluted to give final concentrations of 100 and 500 nM, while control wells were treated with vehicle DMSO. The DMSO content was constant across the wells. EL102 and vehicle treatments were incubated with the cells for 4 h at 37 °C and 5 % CO₂ in a humidified atmosphere under normoxia (21 % O₂) or hypoxia (1 % O₂). Cells were harvested and lysed on ice. Protein concentrations were calculated by BCA assay and equal amounts of protein (20 μ g) were resolved by SDS-PAGE electrophoresis. Following Western transfer, membranes were blocked and then probed for HIF1 α (BD Transduction Laboratories #610958), 1:1000, and β -actin (Sigma-Aldrich #A5441), 1:750000, overnight at 4 °C. (Antibodies were both diluted in 5 % x/v non-fat dry milk, 1 X TBS, 0.1 % Tween-20.) Detection was carried out using HRP-conjugated secondary antibodies, incubation with ECL-Plus and exposure to film. Film exposures were scanned to provide an electronic copy.

2.7.2 Binding Assays

2.7.2.1 Kinase-Binding Screen

A kinase inhibitor screen known as KINOMEscan™ (DiscoverX Corporation, San Diego, California, USA.) was carried out on 442 DNA-labelled kinases (some of which were common mutant variants) to assay EL102 and as a control, the EL102 diluent, DMSO. KINOMEscan™, which is based on a competition binding assay, quantitatively measured the ability of EL102 to compete with an immobilized, active-site directed ligand. The assay was performed by combining three components: DNA-tagged kinase; immobilized ligand; and EL102. The ability of EL102 to compete with the immobilized ligand was measured by qPCR of the DNA tag. For most assays, kinase-tagged T7 phage strains were grown in parallel in 24-well blocks in an *Escherichia coli* (*E.coli*) host derived from the BL21 strain. *E.coli* were grown to log-phase and infected with T7 phage from a frozen stock (multiplicity of infection = 0.4) and incubated with shaking at 32 °C until lysis (90–150 min). The lysates were centrifuged (6000 x g) and filtered (0.2 µm) to remove cell debris. The remaining kinases were produced in HEK-293 cells and subsequently tagged with DNA for qPCR detection. Streptavidin-coated magnetic beads were treated with biotinylated small molecule ligands for 30 min at RT to generate affinity resins for kinase assays. The ligand-affixed beads were blocked with excess biotin and washed with blocking buffer (SEA BLOCK (Thermo Scientific, Pierce # 37527), 1 % BSA, 0.05 % Tween 20, 1 mM DTT) to remove unbound ligand and to reduce non-specific phage binding. Binding reactions were assembled by combining kinases, ligand-affixed affinity beads, and test compounds (EL102 and DMSO) in 1 X binding buffer (20 % SeaBlock, 0.17 X dPBS, 0.05 % Tween 20, 6 mM DTT). 1 µM EL102 (and equal volume DMSO) were prepared as 40 X stocks in 100 % DMSO and directly diluted into the assay. All reactions were performed in polypropylene 384-well plates in a final volume of 0.04 ml. The assay plates were incubated at RT with shaking for 1 h and the affinity beads were washed with wash buffer (1 X dPBS, 0.05 % Tween 20). The beads were then re-suspended in elution buffer (1 X dPBS, 0.05 % Tween 20, 0.5 µM non-biotinylated affinity ligand) and incubated at RT with shaking for 30 min.

The kinase concentration in the eluates was measured by qPCR. Results for primary screen binding interactions were reported as percentage control, where lower numbers indicate stronger hits. In the current study, a percentage control ≤ 65 was deemed significant.

$$\% \text{ Control} = \frac{\text{Test Compound Signal} - \text{Positive Control Signal}}{\text{Negative Control Signal} - \text{Positive Control Signal}} \times 100$$

2.7.2.2 *In Vitro* Pharmacology: Diversity Profile

Elara Pharmaceuticals commissioned an investigation of the effects of EL102 by various *in vitro* receptor binding assays which were carried out at Cerep (Celle l'Evescault, France). The binding of 71 specific radio-labelled ligands to cognate receptors was measured by scintillation counting. In each experiment, the respective reference compound was tested concurrently with 1 μM EL102 and data were compared with historical values determined by Cerep. Results that had shown an inhibition, of higher than 50 %, were deemed to represent significant effects of the test compound (EL102). 50 % was considered the most common cut-off value for further investigation (determination of IC_{50} or EC_{50} values from concentration response curves). Here, EL102 concentrations used were 0 nM (DMSO), 10 nM, 100 nM, 300 nM, 1 μM and 3 μM . The specific ligand binding to the receptors was defined as the difference between total binding and the non-specific binding determined in the presence of an excess of unlabelled ligand. The results were expressed as a percentage of control specific binding ((measured specific binding/control specific binding) \times 100) obtained in the presence of EL102. The IC_{50} values (concentration of half the maximal inhibition of control specific binding) and Hill coefficients (nH) were determined by non-linear regression analysis of the competition curves generated by the mean replicate values using Hill equation curve fitting ($Y = D + [(A - D)/(1 + (C/C_{50})^{nH})]$), where Y = specific values binding, D = minimum specific binding, A = maximum specific binding, C = compound concentration, C_{50} =

IC₅₀ and nH = slope factor). This analysis was performed using a software package developed at Cerep (Hill Software) and validated by comparison with data generated by the commercially available software SigmaPlot® 4.0 for Windows® (© 1997 by SPSS Inc.). The inhibition constants (K_i) were calculated using the Cheng Prusoff equation ($K_i = IC_{50}/(1+(L/KD))$), where L = concentration of radioligand in the assay, and KD = affinity of the radioligand for the receptor). A scatchard plot is used to determine the K_d.

2.8 Statistical Analysis

All values are presented as the mean with error presented at either ± standard deviation (SD) of the mean of n or ± SEM, where n ≥ 3. Data sets were tested for significance using the One-Way ANOVA (non-parametric) and Tukey post-hoc test between-group comparison. A power (p) level of p ≤ 0.01 or 0.05 was considered statistically significant. These statistical analyses were used unless otherwise stated. Graphical data was generated, using software packages GraphPad Prism5.04 and Microsoft Excel 2010.

2.9 Suppliers and Distributors

Table 2.4: Supplier and distributor information.	
Distributor:	Supplier:
Sigma-Aldrich Ireland, Vale Road, Arklow, Co. Wicklow, Ireland.	Sigma-Aldrich, Corning
Bio-Sciences Ireland, 3, Charlemont Terrace, Crofton Rd, Dun Laoghaire, Co. Dublin, Ireland.	Gibco, Invitrogen, Novex
VWR Ireland, Orion Business Park, North West Business Park, Ballycoolin, Dublin, Ireland.	G-Biosciences, Sterilin, GE Helathcare-Biosciences
Sarstedt Ltd, Sinnottstown Lane, Drinagh, Co. Wexford, Ireland.	Sarstedt
Merck Millipore Ireland Tullagreen, Carrigtwohill, Co. Cork, Ireland.	Merck-Millipore
Fisher Scientific Ireland Ltd, Suite 3, Plaza 212, Blanchardstown Corporate Park 2, Ballycoolin, Dublin, Ireland.	Thermo Scientific, Pierce, Abgene
Medical Supply Company Ireland, Damastown Green, Fingal, Dublin, Ireland.	BioLine, Meridian Life Science
Peprtech	Peprtech
Qiagen, Skelton House, Lloyd Street North, Manchester M15 6SH, UK.	Qiagen
Abcam, 330 Cambridge Science Park Cambridge, CB4 0FL, UK.	Abcam
MyBio Ltd., Annfield House, Dunbell, Kilkenny, Ireland.	Promega
Tebu-Bio Ltd, Unit 7, Flag Business Exchange, Vicarage Farm Road, Peterborough, Cambridgeshire, PE1 5TX, UK.	Cytoskeleton
Brennan & Co., Unit 61, Birch Avenue, Stillorgan Industrial Park, Stillorgan, Co. Dublin, Ireland.	New England BioLabs
Roche Diagnostics, Charles Avenue, Burgess Hill, West Sussex, RH15 9RY, UK.	ACEA
BD Biosciences, Edmund Halley Road - Oxford Science Park, OX4 4DQ, Oxford, UK.	BD PharMingen

R&D Systems Europe Ltd, 19 Barton Lane, Abingdon OX14 3NB, Oxford, UK.	R&D systems, Novus Biologicals
Cambridge Bioscience Ltd., Munro House, Trafalgar Way, Bar Hill, Cambridge CB23 8SQ, UK.	ACEA
Fannin House, South County Business Park, Leopardstown, Dublin 18, Ireland.	Bio-Rad
Elektron Technology UK Ltd, Unit 7, M11 Business Link, Parsonage Lane, Stansted, Essex, CM24 8GF, UK.	Agar Scientific
Laboratory Instruments and Supplies, Pamaron House, Ballybin Road, Co. Meath, Ireland.	Laboratory Instruments and Supplies
Jackson ImmunoResearch Europe Ltd, Unit 7, Acorn Business Centre, Newmarket, Suffolk, CB8 7SY, UK.	Jackson ImmunoResearch Laboratories
Cell Signaling Technology Europe, B.V., Schuttersveld 2, 2316 ZA, Leiden, The Netherlands.	Cell Signaling
Wolf Laboratories Ltd., Colenso House, 1 Deans Lane, Pocklington, YORK, YO42 2PX, UK.	Coy Lab Products.
Jilks Plastics 31 Trowers Way, Redhill RH1 2LH, UK.	

Chapter 3:

Analysis of the Cytotoxic Profile of EL102 in a Panel of Prostate Cancer Cell Lines

**With the exception of Figure 3.4 (A) and (B) and associated
commentary, all data in Chapter 3 was published in the
British Journal of Cancer.**

(Toner *et al.*, 2013) (See Appendix II)

3.1 Introduction

Prostate cancer is the second most common cancer diagnosed in men globally, accounting for 13.6 % of all cancer cases in men worldwide in 2008 (<http://globocan.iarc.fr>). In the United States, the National Cancer Institute (NCI) estimates that 241,740 men were diagnosed with, and 28,170 men died of, cancer of the prostate in 2012 (<http://seer.cancer.gov>). Several choices exist for the treatment of early prostate cancer, including radical prostatectomy, external beam radiation and prostate brachytherapy, and all have similar outcomes (Peinemann *et al.*, 2011). Despite advances in primary treatment of prostate cancer, in a subset of patients, the disease progresses and distant metastases develop. While these patients can initially be treated with androgen ablation therapies, eventually their cancer will become hormone refractory and they will succumb to their illness. In the mid-2000s, introduction of taxane-based therapies improved the outcomes of mCRPC patients, extending survival by several months. The taxane family, which includes paclitaxel, docetaxel and the newly approved cabazitaxel, are natural or semi-synthetic plant derivatives that are widely used in the treatment of mCRPC (see section 1.2.4). Their mechanisms of action have been widely reported (Jackson *et al.*, 2007; Rowinsky *et al.*, 1990) and have been shown to act as mitosis arresting agents (Douros & Suffness, 1981; Wani *et al.*, 1971). The dynamic ability of a cell to assemble and disassemble the architecture of the microtubules from and to tubulin components, respectively, is curtailed greatly by the introduction of taxanes (Manfredi & Horwitz, 1984). Phase III trials have demonstrated that docetaxel–estrामustine combinations can confer median survival advantage of ~3 months compared with the standard mitoxantrone–prednisone combination (Berthold *et al.*, 2008; Petrylak *et al.*, 2004). Since 2010, an additional six drugs have been approved for use in patients with mCRPC. These include drugs targeting androgen receptor activity (abiraterone acetate and enzalutamide), drugs targeting bone metastasis and the microenvironment (denosumab and ^{223}Ra), immunotherapeutics (Sipuleucel-T) and new taxanes (cabazitaxel) (Heidegger *et al.*, 2013).

It is postulated that combination treatments of docetaxel with alternative cytotoxics could prevent this late-stage resistance, with such other compounds acting in an additive or synergistic fashion. While phase II trials with various combinations of new drugs have suggested promise for emerging docetaxel combination therapies (Ferrero *et al.*, 2006; Garcia *et al.*, 2011; Kikuno *et al.*, 2007; Oh *et al.*, 2003; Tester *et al.*, 2006), of note is the fact that no drug has yet been shown to provide survival benefit when combined with docetaxel in phase III trials (Antonarakis & Eisenberger, 2013). This suggests that there is a need to identify novel compounds for efficacy as single agents or for use in combination with taxane-based therapies.

EL102 is a later generation derivative of the family of toluidine sulphonamides (Alonso *et al.*, 2012). The first indication of EL102's capacity as an effective chemotherapeutic agent was determined by the compound's potential in the reduction in viability of a number of cancer cell types of the NCI-60 panel including the prostate cancer cell lines PC-3 and DU145. Both appeared particularly susceptible to the effects of the compound in this respect as can be seen in Figure 1.5 (B). This preliminary work was conducted by Elara Pharmaceuticals. The data generated here, charts the ability of EL102 to induce cell death and its efficacy *in vitro* against prostate cancer cell lines and in an *in vivo* prostate cancer xenograft mouse model. This work also highlights the potential of EL102 to work in combination with clinically-used docetaxel. This is the first report on the biological actions of EL102 on cancer cells, focusing on its use as an anti-prostate cancer chemotherapeutic.

In order to determine whether EL102 could truly have utility as a treatment in prostate cancer, the effects to cell viability of increasing doses of EL102 on a panel of prostate cancer cell lines in comparison to the clinically used docetaxel, was performed. The methods of cell viability detection, in this instance, measured the inter-well fluorescent reductase activity differential of drug-treated cultures and the colorimetric differential of fixed cell stained protein content by means of the resazurin- (alamar blue-) and sulforhodamine B- (SRB-) based assays, respectively. The resazurin-based

assays were first optimised by selection of a uniform cell count per well across the cell lines used. An initial dose range of 0–1 μM was also used to narrow the working nanomolar range of EL102 (0–150 nM). The SRB assay was pre-optimised (Vichai & Kirtikara, 2006) and the general protocol was adopted for each cell line and served as confirmation of the results of the resazurin-base assays. The panel of cell lines included CWR22 (an androgen receptor (AR)-positive, androgen dependent, non-metastatic cell line, sourced from a primary prostate tumour); a daughter variant of CWR22 known as 22Rv1 (an AR-positive, androgen-independent, non-metastatic cell line which was derived from the resulting tumour of a serially propagated CWR22 murine xenograft following initial regression and relapse upon castration); PC-3 (an AR-negative, androgen independent cell line derived from a metastatic bone lesion); and DU145 (AR-negative, androgen insensitive cell line derived from metastatic brain lesion).

3.2 Results

3.2.1 Cell Viability Assays and Determination of the IC_{50} Values of EL102

Figures 3.1 (A) and (B) demonstrate the effects of increasing doses of EL102 and docetaxel as single agents, respectively, on the viability of the 4 prostate cancer cell lines following a 72 h exposure. This demonstrates that, while docetaxel is a more potent agent than EL102, both compounds decrease prostate cancer cell viability in a dose-dependent manner. Table 3.1 summarises the IC_{50} values and shows that CWR22 and 22Rv1 are equally sensitive to docetaxel with an IC_{50} of 0.4–0.6 nM. With an IC_{50} of 3.8 nM, bone metastatic cell line, PC-3, is 2.5–10 fold more resistant to docetaxel than any of the other cell lines. EL102 inhibited cell proliferation with an IC_{50} of 21–40 nM across the cell lines assayed. By comparison, bone metastatic PC-3 cells were 2-fold more resistant than CWR22 and 22Rv1 to EL102, and were equally as sensitive as brain metastatic cell line DU145.

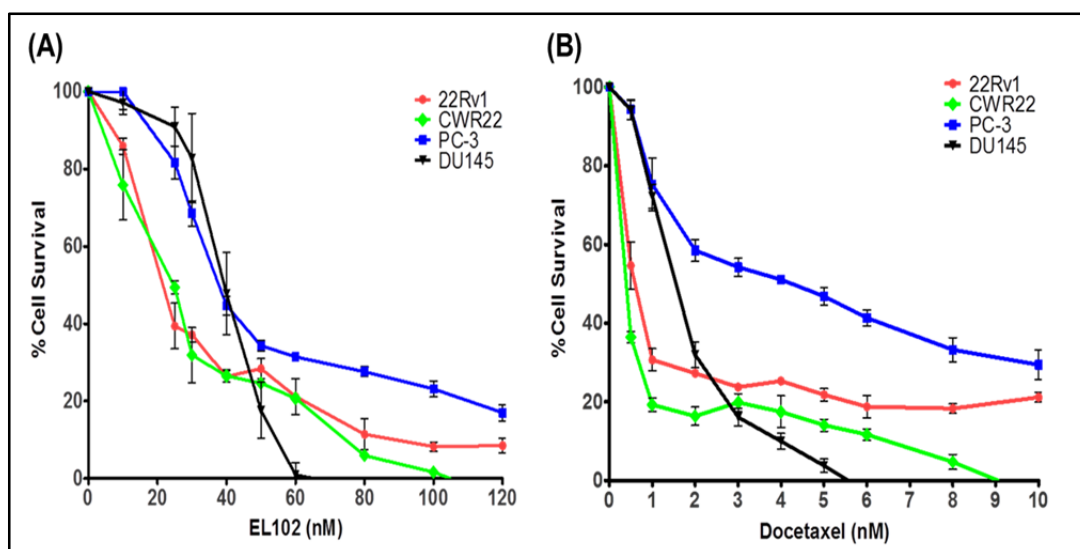


Figure 3.1 – Comparative dose response curves of a panel of prostate cancer cell lines to EL102 and docetaxel. (A) Dose-response curves of prostate cancer cell lines following 72 h EL102 exposure. **(B)** Dose-response curves of prostate cancer cell lines following 72 h docetaxel exposure.

Table 3.1 – Prostate cancer cell lines: 50 % cell survival (IC ₅₀) following 72 h docetaxel or EL102 treatment.		
Cell Line	Docetaxel (nM) IC ₅₀ ± SD	EL102 (nM) IC ₅₀ ± SD
CWR22	0.4 ± 0.01	24 ± 1.41
22Rv1	0.6 ± 0.15	21.7 ± 2.31
DU145	1.5 ± 0.18	40.3 ± 7.71
PC-3	3.8 ± 0.76	37 ± 2.00

3.2.2 Tumour Volume Analysis of *In Vivo* CWR22 Murine Model

To determine the effectiveness of EL102 as a combination treatment with docetaxel *in vivo*, a CWR22 xenograft mouse model was conducted. The aim of this study was to examine the ability of the combination of docetaxel with EL102 to inhibit tumour growth which is shown in Figure 3.2 (A). While administration of 12 mg kg⁻¹ EL102 using a 5-day on/2-day off regimen had not significantly inhibited the rate of tumour growth compared with vehicle, increasing the dosage to 15 mg kg⁻¹ EL102 had inhibited the rate of growth when compared with vehicle treatment. Dosing of 12 mg kg⁻¹ docetaxel decreased the rate of tumour growth more efficiently than EL102, while the combination of both drugs had the largest effect on the inhibition of tumour growth, suggesting that these drugs work well together in combination *in vivo*. Comparison of the docetaxel arm vs the combination arms showed a significant difference in the rate of tumour growth, indicating that the addition of EL102 to docetaxel improves anti-tumour activity (*F*-test, *P*<0.0001). Table 3.2 describes the results of a one-way ANOVA test on this model, using a Tukey's *post-hoc* test to assess statistical differences in tumour volume between the treatment arms at different time points. Additionally, to determine if combining EL102 and docetaxel was well tolerated by the mice with minimal adverse effects, the changes in mean body weight between the treatment arms were compared. As can be seen in Figure 3.2 (B), no significant differences in body weight were found between the groups compared with vehicle or between different treatment arms. Table 3.3 describes the results of a one-way ANOVA test on this model, using a Tukey's *post-hoc* test to assess statistical difference in body weights between the treatment arms at different time points.

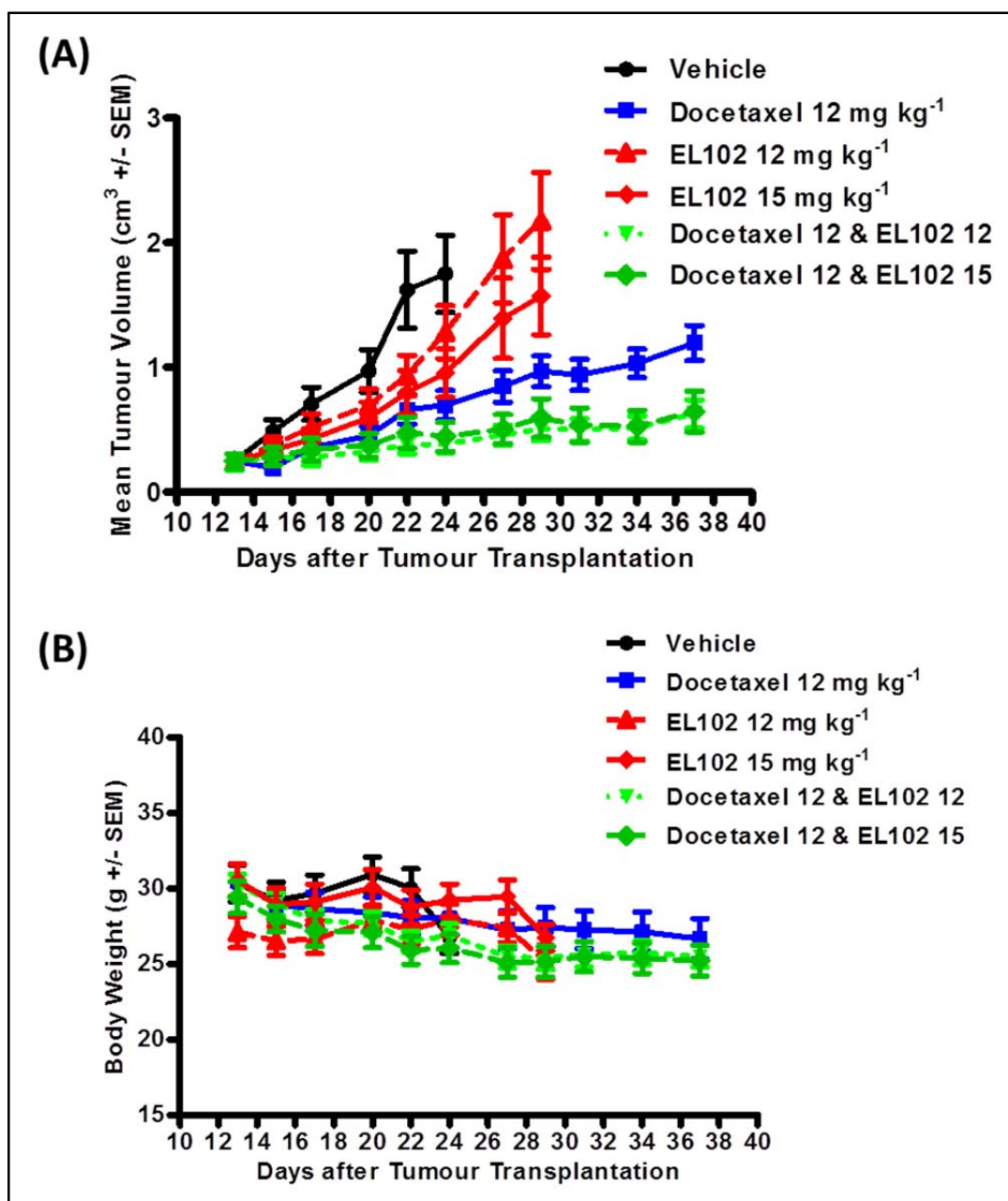


Figure 3.2 – Impact of EL102 and docetaxel alone and in combination in CWR22 xenograft models. (A) Effect of vehicle versus 12 mg kg⁻¹ docetaxel ,versus 12 mg kg⁻¹ EL102, versus 15 mg kg⁻¹ EL102, versus 12 mg kg⁻¹ docetaxel plus 12 mg kg⁻¹ EL102, versus 12 mg kg⁻¹ docetaxel plus 15 mg kg⁻¹ EL102, on CWR22 tumour volume using a 5 day on/2 day off schedule (tumour volume (cm³) ± SEM). **(B)** Difference in mean body weights between vehicle and treatment groups.

	Day 13	Day 15	Day 17	Day 20	Day 22	Day 24	Day 27	Day 29	Day 31	Day 34	Day 37
One-way analysis of variance, p-value	1.000	0.088	0.0298	0.0033	0.0002	<0.0001	0.0003	< .0001	0.0295	0.005	0.0137
Bonferroni's Multiple Comparison Test	P <0.05	P <0.05	P <0.05	P <0.05	P <0.05	P <0.05	P <0.05	P <0.05	P <0.05	P <0.05	P <0.05
Vehicle vs Docetaxel	ns	ns	ns	*	**	**					
Vehicle vs EL102 12 mg kg ⁻¹	ns	ns	ns	ns	ns	ns					
Vehicle vs Combo 12 mg kg ⁻¹	ns	ns	*	**	***	***					
Vehicle vs EL102 15 mg kg ⁻¹	ns	ns	ns	ns	*	*					
Vehicle vs Combo 15 mg kg ⁻¹	ns	ns	ns	**	***	***					
Docetaxel vs EL102 12 mg kg ⁻¹	ns	ns	ns	ns	ns	ns	*	*			
Docetaxel vs Combo 12 mg kg ⁻¹	ns	ns	ns	ns	ns	ns	ns	ns	*	*	*
Docetaxel vs EL102 15 mg kg ⁻¹	ns	ns	ns	ns	ns	ns	ns	ns	ns	ns	ns
Docetaxel vs Combo 15 mg kg ⁻¹	ns	ns	ns	ns	ns	ns	ns	ns	ns	*	*
EL102 12 mg kg ⁻¹ vs Combo 12 mg kg ⁻¹	ns	ns	ns	ns	ns	*	**	***			
EL102 12 mg kg ⁻¹ vs EL102 15 mg kg ⁻¹	ns	ns	ns	ns	ns	ns	ns	ns	ns	ns	ns
EL102 12 mg kg ⁻¹ vs Combo 15 mg kg ⁻¹	ns	ns	ns	ns	ns	*	**	***			
Combo 12 mg kg ⁻¹ vs EL102 15 mg kg ⁻¹	ns	ns	ns	ns	ns	ns	*	*			
Combo 12 mg kg ⁻¹ vs Combo 15 mg kg ⁻¹	ns	ns	ns	ns	ns	ns	ns	ns	ns	ns	ns
EL102 15 mg kg ⁻¹ vs Combo 15 mg kg ⁻¹	ns	ns	ns	ns	ns	ns	ns	ns	ns	ns	ns

(Note: (Combo 12 mg kg⁻¹ = Docetaxel 12 mg kg⁻¹ combined with EL102 12 mg kg⁻¹) (Combo 15 mg kg⁻¹ = Docetaxel 12 mg kg⁻¹ combined with EL102 15 mg kg⁻¹). (ns = p>0.05 (not significant)) (* = p<0.05) (** = p<0.01) (***) = p<0.001))

Table 3.3: One way analysis of variance with Tukey's multiple comparison test of mouse xenograft experiment: analysis of difference in body weight between treatment groups.													
	Day 13	Day 15	Day 17	Day 20	Day 22	Day 24	Day 27	Day 29	Day 31	Day 34	Day 37		
One-way analysis of variance, p-value	0.1698	0.3944	0.3229	0.0885	0.0724	0.281	0.0355	0.3931	0.426	0.4664	0.5959		
Bonferroni's Multiple Comparison Test	P <0.05	P <0.05	P <0.05	P <0.05	P <0.05	P <0.05	P <0.05	P <0.05	P <0.05	P <0.05	P <0.05	P <0.05	P <0.05
Vehicle vs Docetaxel	ns	ns	ns	ns	ns	ns	ns	ns	ns	ns	ns	ns	ns
Vehicle vs EL102 12 mg kg ⁻¹	ns	ns	ns	ns	ns	ns	ns	ns	ns	ns	ns	ns	ns
Vehicle vs Combo 12 mg kg ⁻¹	ns	ns	ns	ns	ns	ns	ns	ns	ns	ns	ns	ns	ns
Vehicle vs EL102 15 mg kg ⁻¹	ns	ns	ns	ns	ns	ns	ns	ns	ns	ns	ns	ns	ns
Vehicle vs Combo 15 mg kg ⁻¹	ns	ns	ns	ns	ns	ns	ns	ns	ns	ns	ns	ns	ns
Docetaxel vs EL102 12 mg kg ⁻¹	ns	ns	ns	ns	ns	ns	ns	ns	ns	ns	ns	ns	ns
Docetaxel vs Combo 12 mg kg ⁻¹	ns	ns	ns	ns	ns	ns	ns	ns	ns	ns	ns	ns	ns
Docetaxel vs EL102 15 mg kg ⁻¹	ns	ns	ns	ns	ns	ns	ns	ns	ns	ns	ns	ns	ns
Docetaxel vs Combo 15 mg kg ⁻¹	ns	ns	ns	ns	ns	ns	ns	ns	ns	ns	ns	ns	ns
EL102 12 mg kg ⁻¹ vs Combo mg kg ⁻¹	ns	ns	ns	ns	ns	ns	ns	ns	ns	ns	ns	ns	ns
EL102 12 mg kg ⁻¹ vs EL102 15 mg kg ⁻¹	ns	ns	ns	ns	ns	ns	ns	ns	ns	ns	ns	ns	ns
EL102 12 mg kg ⁻¹ vs Combo 15 mg kg ⁻¹	ns	ns	ns	ns	ns	ns	ns	ns	ns	ns	ns	ns	ns
Combo 12 mg kg ⁻¹ vs EL102 15 mg kg ⁻¹	ns	ns	ns	ns	ns	ns	ns	ns	ns	ns	ns	ns	ns
Combo 12 mg kg ⁻¹ vs Combo 15 mg kg ⁻¹	ns	ns	ns	ns	ns	ns	ns	ns	ns	ns	ns	ns	ns
EL102 15 mg kg ⁻¹ vs Combo mg kg ⁻¹	ns	ns	ns	ns	ns	ns	ns	ns	ns	ns	*	ns	ns

(Note: (Combo 12 mg kg⁻¹ = Docetaxel 12 mg kg⁻¹ combined with EL102 12 mg kg⁻¹) (Combo 15 mg kg⁻¹ = Docetaxel 12 mg kg⁻¹ combined with EL102 15 mg kg⁻¹). (ns = p>0.05 (not significant)) (* = p<0.05)

3.2.3 *In Vitro* Analysis of the Combined Effect of EL102 with Docetaxel

As seen previously, EL102 treatment appears to have a greater effect with respect to the reduction of tumour volume *in vivo* when simultaneously administered with docetaxel. To explore this additive effect further, a 72 h *in vitro* analysis of the cytotoxic profiles of a combined dose versus individual drug treatment on the panel of previously mentioned cell lines was carried out. Once again SRB and resazurin assays were utilised at least three times, in triplicate 96-well plates. As is shown in Figure 3.3, none of the cell lines assayed exhibited the synergistic effects witnessed in the CWR22 murine xenograft model. It was noted that the compounds appeared to be acting antagonistically as evidenced by the apparent increase in cell viability upon simultaneous EL102 and docetaxel addition to cultures when compared to those treated singularly by either drug.

These seemingly opposing effects of both drugs prompted an examination of whether the dose dependent reduction in cell viability by EL102 was due to the occurrence of its mediated induction of apoptosis or cytostasis.

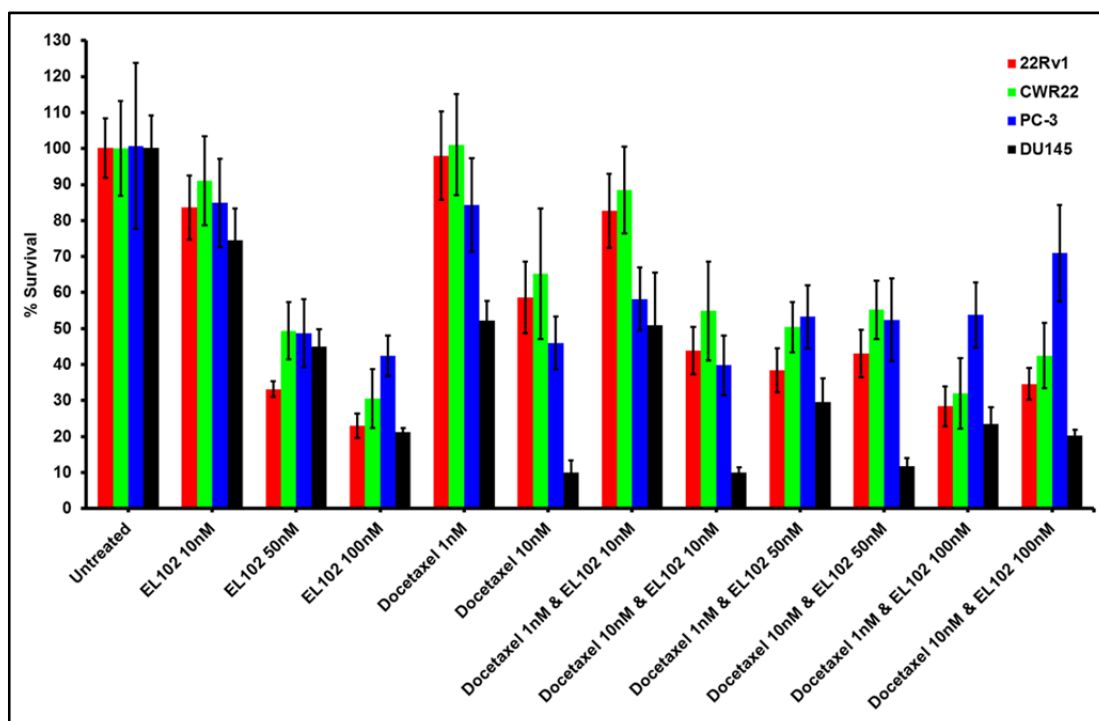


Figure 3.3 – *In vitro* cytotoxic profiles of combined exposure to EL102 and docetaxel in a panel of prostate cancer cell models.

3.2.4 Cell Death and Induction of Apoptosis in EL102-Dosed Prostate Cancer Cell Lines

To first determine whether the EL102-induced decrease in cell viability witnessed was the product of apoptosis, the levels of caspase3-like activity were analysed by way of the DEVD fluorogenic substrate assay. Lysate protein from the previously mentioned panel of prostate cancer cell lines was assayed following a 24 h exposure to vehicle, DMSO, or 10, 50 and 100 nM EL102. The results in Figure 3.4 (A) show that while the rate of caspase3 activity doubled in CWR22 and trebled in 22Rv1 following 100 nM EL102 treatment, the rates in PC-3 deviate very little from that of the basal rate. Interestingly, DU145 which has a relatively short doubling time when compared to the other cell lines and which previously had exhibited (Figure 3.3) low cell viability when treated with 100 nM EL102, showed the least evidence of potential apoptosis induction. Moreover, Figure 3.4 (B) shows, at 48 h, post-addition of 10 nM docetaxel, either singularly or in combination with 30 nM EL102 had seemingly, no effect on caspase3 activation in DU145. In the 22Rv1 cohort assayed, however, docetaxel-induced caspase3-like activity is halved by the presence of 30 nM EL102. This evidence further supports the notion that both drugs are acting antagonistically, *in vitro*. Contrary to the findings of the DEVD assays, when lysates were harvested from DU145 following 24 and 48 h treatments, with either drug singularly or in combination, PARP-cleavage was seen to increase. The highest expression of PARP cleavage was observed in Figure 4.4 (C) following combined treatment for 48 h.

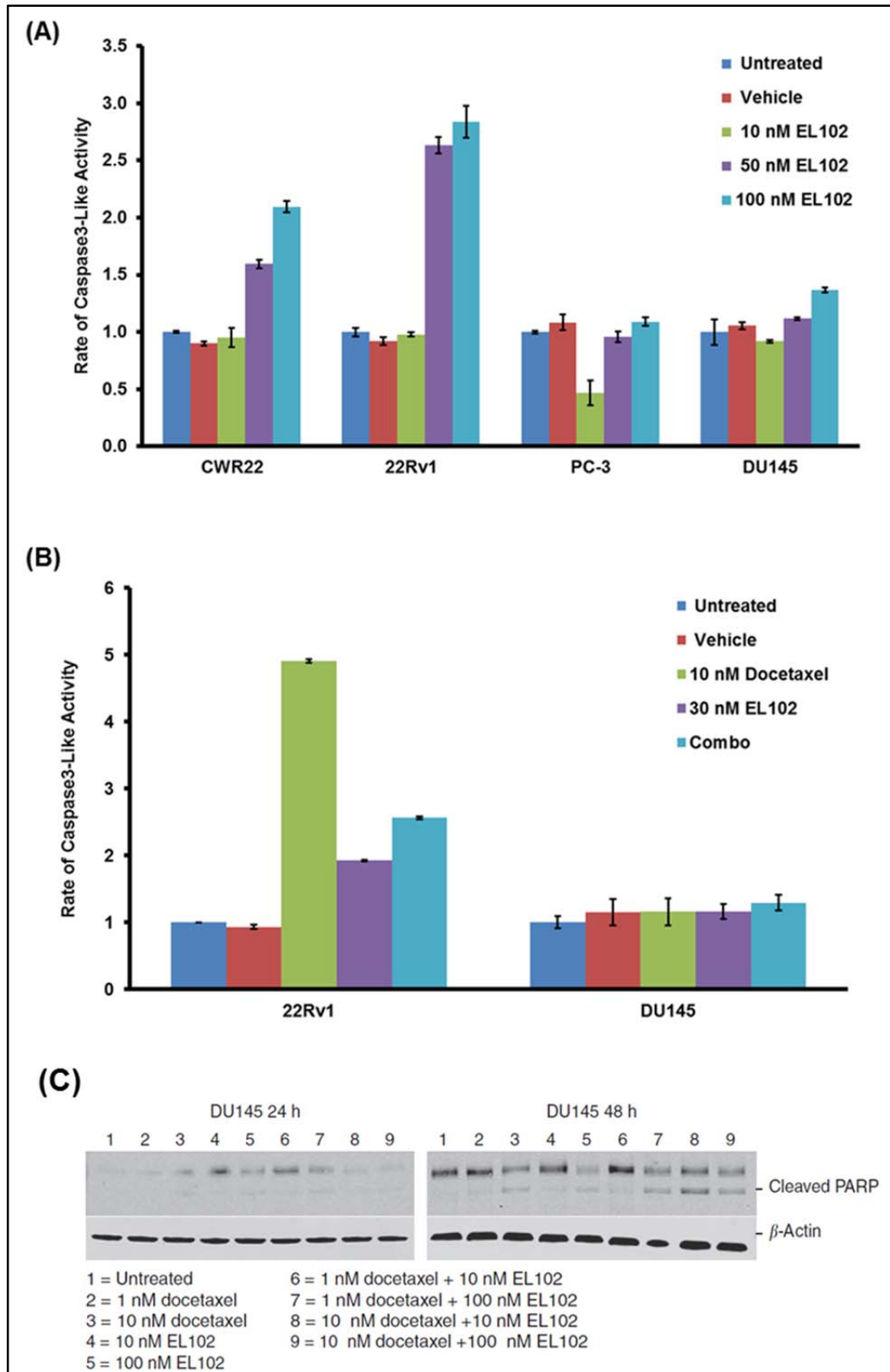


Figure 3.4 – EL102-induced caspase3-like activity in prostate cancer cell lines. (A) Caspase3-like activity in CWR22, 22Rv1, PC-3 and DU145, 24 h post-treatment. (B) Caspase3-like activity in 22Rv1 and DU145, 48 h post-treatment. (C) Western blot of PARP-cleavage in DU145, 24 and 48 h post-treatments 1-9.

While the fluorogenic assay for quantification of caspase3-like activity is a strong indicator of apoptosis induction, it is not the sole measure of apoptosis. To investigate this further, the same panel of cell lines were treated with increasing concentrations of EL102 and docetaxel, singularly and in combination, and the number of cells in the sub-G₁ phase was measured. An increasing number of cells in sub-G₁ was quantified at three time-points (24, 48 and 72 h) post-treatment, indicating a loss of cellular DNA and an entry of cells into late apoptosis as determined by logarithmic scale propidium iodide flow cytometry (Figure 3.5 (A)–(D)). EL102 was an equally strong inducer of cell death at 100 nM in all 4 prostate cancer cell lines, while the compound failed to induce death at a concentration of 10 nM (Figure 3.5 (A)–(D)), despite inhibiting cell viability by approximately 25–30 % at 10 nM (Figure 3.3). Apoptosis was detectable using this method at 24 h and steadily increased by the 72 h mark. This finding indicates that EL102-dependent inhibition of cell viability is, at least in part, due to cytotoxic effects, namely, the induction of apoptosis. Similarly, docetaxel induced apoptosis in all four cell lines, in a dose-dependent and temporal manner. When EL102 and docetaxel were administered in combination *in vitro*, no additive effects to the levels of apoptosis were seen in the cell lines assayed (Figure 3.4 (B)) as was consistent with the cell viability assays (Figure 3.3). Of note, though, is that while 10 nM of EL102 failed to induce increased apoptosis (Figure 3.4), treatment with this concentration did lead to a significantly decreased percentage of cell viability when compared to control (Figure 3.3) in each cell line. This indicates that EL102 maintains non-apoptotic effects at low concentrations.

Figures 3.6 (A) and (B) show representative histograms from these experiments in the DU145 prostate cancer cell line. In addition to demonstrating an increase in sub-G₁ accumulation, the histograms indicate that combining the agents altered the cell cycle dynamics. The effects in DU145 were quantified at 24, 48 and 72 h and shown in Figure 3.6 (C) and (D). These demonstrate that combining EL102 and docetaxel causes a greater loss of cells from G₁ and an accumulation in G₂/M than either alone by 24 h at low doses. Also of interest, in the combination cell cycle profile

images, is a peak beyond that of G₂/M which represents a subset of cells with increased DNA content (8X).

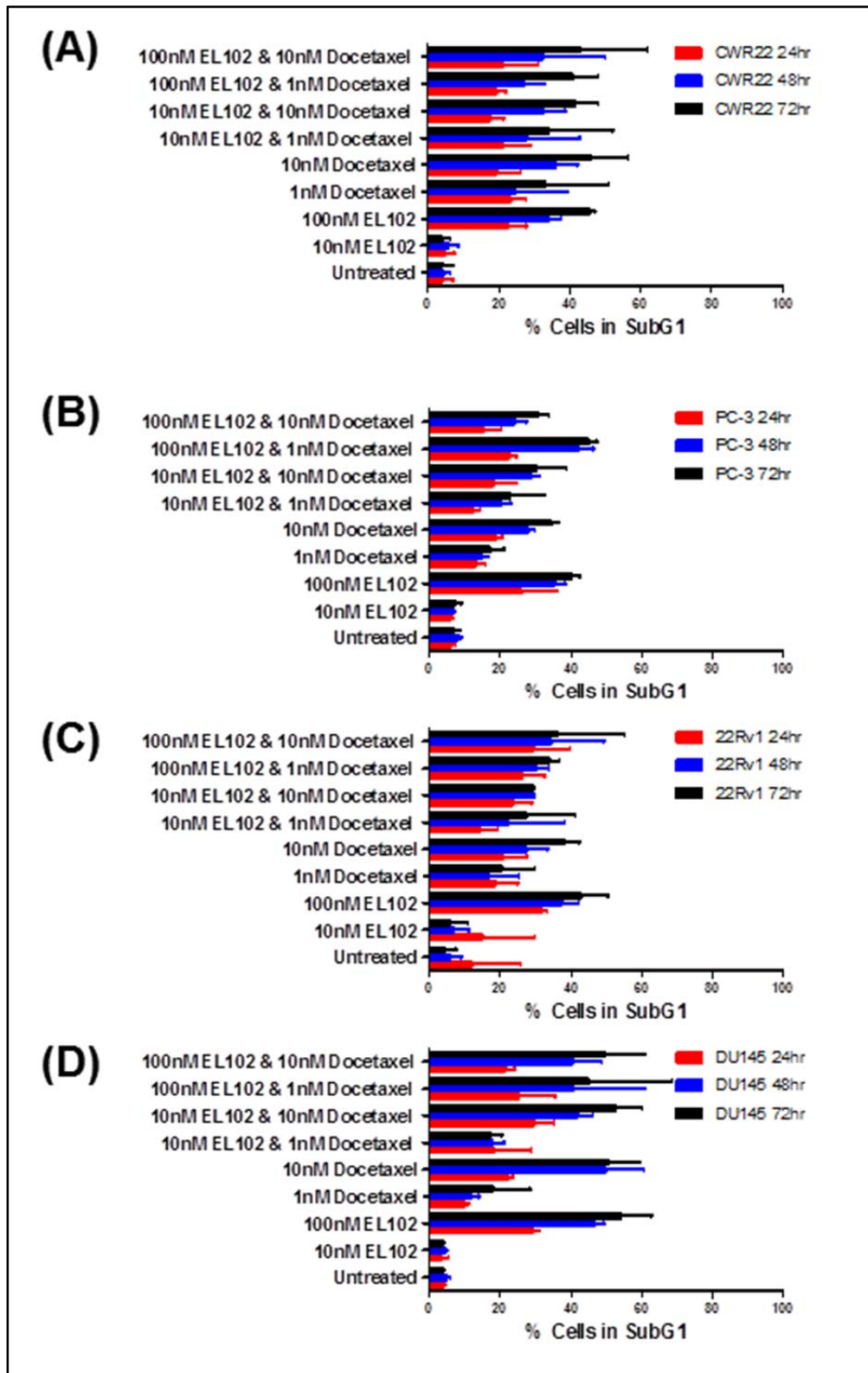
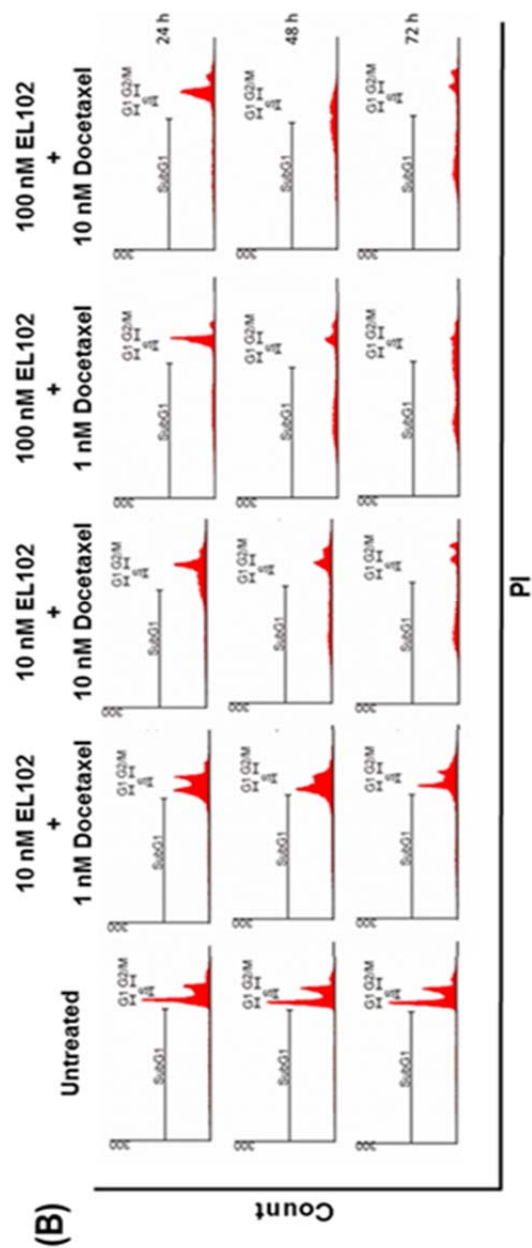
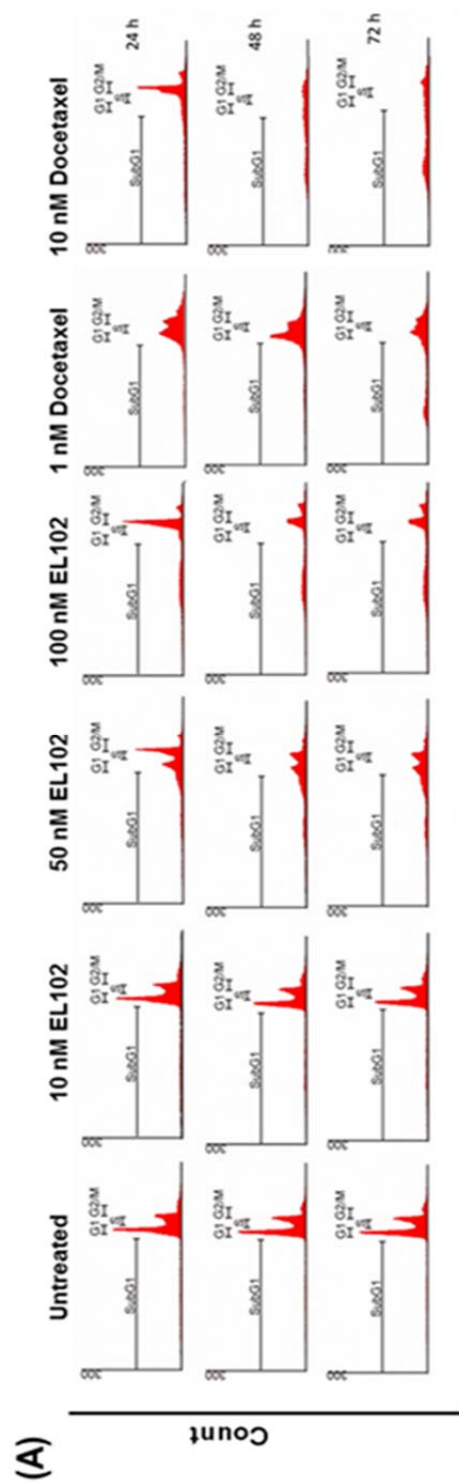


Figure 3.5 – Flow cytometric analysis of sub-G₁ populations resulting from EL102 and docetaxel treatment over 72 h. Percentage of (A) CWR22, (B) PC-3, (C) 22Rv1 and (D) DU145 cells in sub-G₁.



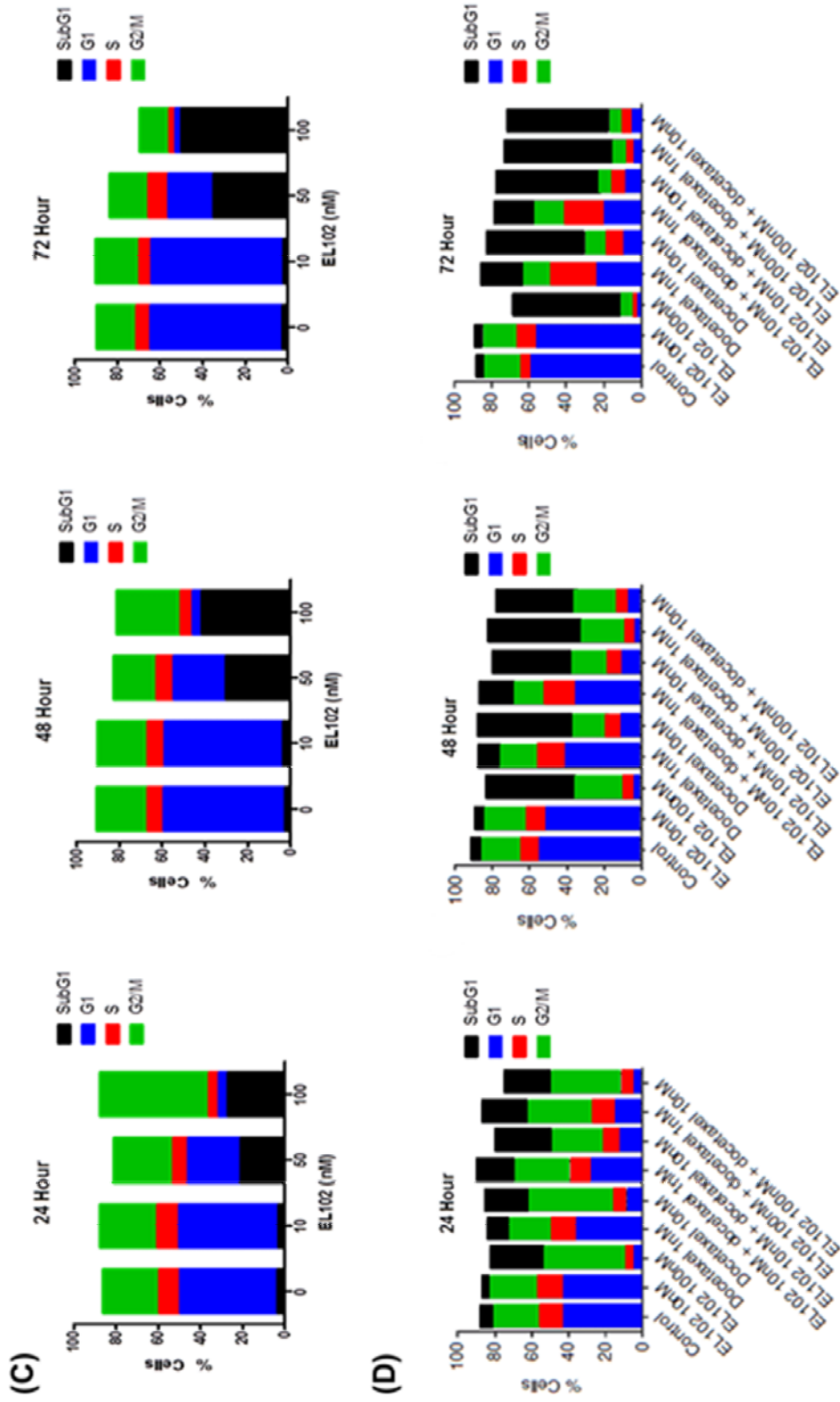


Figure 3.6 – Cell cycle analysis of DU145 cell accumulation in G₁, S, G₂/M and sub-G₁ after EL102, docetaxel or combination treatment. (A) Cell cycle profiles of DU145 in the G₁, S, G₂/M and sub-G₁ phase in response to 0, 10, 50 and 100 nM EL102, 1 and 10 nM docetaxel at 24, 48 and 72 h. **(B)** Cell cycle profiles of DU145 in response to combination of EL102 and docetaxel treatment at 24, 48 and 72 h. **(C)** and **(D)** histograms summarising the findings of **(A)** and **(B)**, respectively.

3.3 Discussion

3.3.1 EL102 Treatment Reduces Prostate Cancer Cell Viability *In Vitro*

Having further established the potential of the novel toluidine sulphonamide EL102 as a candidate drug for prostate cancer through *in vitro* optimisation of both the resazurin and SRB-assays and subsequent elucidation of its dose range, investigation of the cytotoxic and cytostatic effects could begin. Prostate cancer cell lines were sensitive to EL102 at an IC₅₀ range of 20–40 nM. The metastatic prostate cancer cell lines PC-3 and DU145, which are both AR negative and represent castrate-resistant metastatic disease, are equally responsive to EL102. The AR-positive cell lines CWR22 and 22Rv1 are two-fold more sensitive to EL102 than the metastatic DU145 and PC-3 cell lines and serve to model an earlier stage of the disease.

3.3.2 The Combined Therapeutic Effect of EL102—Docetaxel *In Vivo* Differs *In Vitro*

EL102 is a next-generation derivative of a prototype toluidine sulphonamide HIF1 inhibitor (Wendt *et al.*, 2011a) and was identified as a potential chemotherapeutic agent during a screen of similar novel derivatives of this class, using the NCI-60 cell line panel assessing for growth inhibition potential, as shown previously (Figure 1.8 (B)). Therefore, we assessed its efficacy for use in the treatment of prostate cancer as a single agent and in combination with the clinically available docetaxel. Docetaxel is a member of the taxane family and is approved for use in prostate cancer patients with castrate-resistant metastatic disease. This was as a result of having been found to provide a modest increase in median survival time when used in combination with prednisone, when compared with mitoxantrone and prednisone (19.2 months vs 16.3 months median survival) in the TAX327 trial (Berthold *et al.*, 2008). Also, a landmark study found that a more favourable patient outcome is observed when docetaxel is administered in combination with estramustine compared with mitoxantrone and prednisone (17.5 months vs 15.6 months median survival) as detailed in the SWOG9912 trial (Petrylak *et al.*, 2004). Until the approval of six new agents in the past 5 years, docetaxel had been the standard of care in the castrate-resistant

metastatic setting. Attempts to combine docetaxel with other agents have been largely unsuccessful in terms of efficacy and side-effects (Antonarakis & Eisenberger, 2013).

In our *in vivo* study, an apparent synergistic effect was observed when EL102 was administered in combination with docetaxel. This was evidenced by the greater reduction in tumour volumes of mice treated with a combined dose when compared to the tumours of mice dosed with either EL102 or docetaxel alone. Such synergism did not appear to occur in the combination treatments *in vitro*. If anything, the cell viability assays showed that the drugs seemed to be working antagonistically when combined. This was particularly true for PC-3 cells that when exposed to 10 nM docetaxel and 100 nM EL102, for 72 h, exhibited increased viability than singularly treated controls. From this it is hypothesised that the effect seen *in vivo* could have been coordinated either through some residual inflammatory response in the mice or through alternate signalling from resident stromal cells. It is also possible that cellular uptake of one of the drugs may have been more gradual or sustained-longer than the other *in vivo* due to environmental variables not mimicked *in vitro*. A histological analysis of the excised tumours could have shed some light on these findings, had they been retained. Whatever the reason for this disparity, it is certain that further *in vitro* investigation of EL102 is needed, to determine its precise molecular targets.

3.3.3 EL102-Induced Apoptosis Induction

The current study has shown that EL102 is an effective cytotoxic agent and also displays cytostatic properties, through flow cytometric analysis of PI-stained cells, cultured for 24, 48 and 72 h, following treatment. This was evidenced by the increased number of cells seen in sub-G₁ and G₂/M phase of cell cycle. This demonstrates that EL102 induces apoptosis and causes G₂/M arrest, which prevents the cell from entering into mitosis. Induction of apoptosis, following 24 and 48 h EL102 treatment was confirmed through western blot analysis of PARP cleavage in the lysates of treated cells. This contradicts an earlier finding which showed that at similar concentrations, EL102 had failed to initiate caspase3 activation in either of the metastatic cell

lines, PC-3 or DU145. This could suggest that the mechanism of EL102-induced caspase activation is cell line specific although the singular treatment of docetaxel does not produce the expected activity. Previously, studies have shown that the induction of apoptosis can be achieved by AIF in a process that is caspase independent (Cande *et al.*, 2004). Furthermore, PARP-cleavage is not a characteristic unique to apoptosis as it is also observed at necrotic and autophagic cellular events (Artal-Sanz *et al.*, 2006; Saelens *et al.*, 2005). The findings of the DEVD assays shown are the product of three separate attempts to investigate caspase3-like activity.

3.3.4 Clinical Potential for EL102 as a Chemotherapeutic

Several clinical trials have been conducted in recent years, exploring the potential of neoadjuvant chemotherapy in patients with high-risk localised prostate cancer (Narita *et al.*, 2012; Ross *et al.*, 2012; Womble *et al.*, 2011). The results of these trials suggest a benefit to patients in terms of reductions in tumour volume and PSA levels (Narita *et al.*, 2012; Ross *et al.*, 2012). Given the equal sensitivity of AR-positive CWR22 and 22Rv1 to EL102, despite their different sensitivity to androgen, there is a suggestion that EL102 could potentially be used in a castrate sensitive setting before the development of hormone resistance. To further investigate this, we postulated that CWR22 cells would respond to EL102 as single agent. This was confirmed in the CWR22 prostate xenograft model. As mentioned previously, attempts to combine docetaxel with other agents have been largely unsuccessful (Antonarakis & Eisenberger, 2013). In this study, our *in vivo* investigations found that the combination of EL102 and docetaxel decreased proliferation of CWR22 xenograft tumours to a greater extent than either drug alone. The combination of docetaxel and EL102 significantly decreased tumour growth to a greater extent than either alone in a xenograft model of CWR22. While combining the drugs *in vitro* does not have an additive effect on induction of apoptosis, it appears to increase the loss of cells from G₁ and accumulation in G₂/M than either drug alone suggesting the combination may increase cytostatic effects. Although taken together, these findings show promise for the compound as a chemotherapeutic, a

considerable amount of investigation must be done to ascertain the mode of action of this small molecule inhibitor before clinical trials can be reached.

There is no current cure for castrate-resistant metastatic prostate cancer. Novel adjuvant chemotherapies are continually being developed to address this, with the approval of six new agents since 2010. In summary, here, data is presented on the efficacy of EL102 as a novel chemotherapeutic agent with potential for the treatment of prostate cancer. We show that EL102 is active in both androgen-sensitive and castration-resistant prostate cancer cell lines. EL102 enhances the potency of docetaxel in a CWR22 prostate cancer xenograft model.

Chapter 4:

**Exploring the Effects of
EL102 on Microtubule
Dynamics, Chemoresistance
and HIF1 α Signalling
*In Vitro***

**Part of the data, and associated commentary, in this chapter
also contributes to a publication in the
British Journal of Cancer.**

(Toner *et al.*, 2013)

(See Appendix II)

4.1 Introduction

As noted previously (Chapter 3), EL102 induces cell death in the form of apoptosis. Evidence for this is the accumulation of sub-G₁ cells and induction of cleaved PARP following exposure to the compound 24, 48 and 72 h either singularly or in combination with docetaxel. The mechanism by which microtubule (MT) disruptors, such as docetaxel, induce prostate cancer cell death has been the subject of much investigation. It is widely held that MT disruptor induction of programmed cell death (PCD) is presided over by the activities of caspase3 and or caspase2 as well as the seemingly caspase-independent mode of mitotic catastrophe (Fabbri *et al.*, 2008; Kramer *et al.*, 2006; Roninson *et al.*, 2001). Mitotic catastrophe is brought on through an untimely entry of cells into mitosis by stresses such as those exerted by chemotherapeutics (for example taxanes) or ionising radiation. In this form of cell death, mitosis is first delayed through impaired MT dynamics or defects in cell cycle checkpoints. Studies have revealed that by inhibiting caspases or overexpressing Bcl-2, mitotic catastrophe still occurs. So too does apoptosis induction by the tumour necrosis factor related apoptosis inducing ligand (TRAIL) however caspase-free PCD induction remains largely unexplained (Broker *et al.*, 2005; Fabbri *et al.*, 2008; Mediavilla-Varela *et al.*, 2009). In any case, the primary mechanism of the compound docetaxel is the disruption of MT dynamics. Like the other members of this taxane family, docetaxel potentiates tubulin polymerisation which disallows the disassembly of MTs leading to mitotic arrest. The method by which EL102 exerts its effects needs to be addressed. To that end, here, EL102 is investigated, *in vitro*, for its mode of activity with regard to MT dynamics. This is to determine any commonality or discord afforded to the mechanism of docetaxel for use as a companion drug *in vivo*.

Patients in the latter stages of prostate cancer undergo treatment with docetaxel or the DNA intercalator mitoxantrone in combination with prednisone (Tannock *et al.*, 2004). While both mitoxantrone and docetaxel offer different ways of targeting prostate cancer, a patient with metastatic form of the disease will inevitably develop a more aggressive drug-resistant tumour phenotype (Linn *et al.*, 2010). The mechanisms of resistance that

arise make it possible for the cancer cells to easily develop cross-resistance to other chemotherapeutics such as paclitaxel and doxorubicin. This emphasises the need for the discovery of more effective therapies that have the ability to circumvent these modes of resistance or to perhaps potentiate the effects of existing treatments and delay the onset of such a disease state. The current study utilises established *in vitro* models of drug resistance, efflux pumps MDR1 and BCRP, and demonstrates the potential therapeutic role EL102 could have in this area.

Additionally, this section explores the mechanism by which EL102 brings about cell cycle arrest. As mentioned previously (1.4), precursor molecules of EL102 which are also members of the toluidine sulphonamide family of small molecule inhibitors, were formulated but presumed to function in the same way as known aryl sulphonamides, namely the binding and inhibition of cytochrome p450 2C9 (CYP2C9) (Wendt *et al.*, 2011a). CYP2C9 is a key contributor to the clearance of many exogenous materials like warfarin as well as endogenous biomolecules such as arachidonic acid. An inhibition of this key enzyme could have potentially dangerous consequences for the administration of agents with normally low therapeutic indices, causing unwanted drug-drug interactions (Miners & Birkett, 1998; Rettie & Jones, 2005; Williams *et al.*, 2003). The three-dimensional quantitative structure-activity relationship (3D-QSAR) model constructed by Wendt *et al.*, determined a method of predicting synthesis of molecules with high binding affinity for HIF1 α while reducing the likelihood of CYP2C9 interaction. One of the next generation compounds resulting from this method is EL102 (Alonso *et al.*, 2012). In this chapter, analysis of the HIF1 α -inhibiting quotient of EL102 is elucidated in a biological setting. HIF1 α is an important transcription factor (TF) employed in a multitude of cellular functions such as metabolism, chemotaxis and cell survival (Papandreou *et al.*, 2006; Schioppa *et al.*, 2003). It is expressed at high levels in an array of cell lines. Among these are the *in vitro* prostate cancer models DU145 and PC-3 (Zhong *et al.*, 1999). Induction and activation of HIF1 α results from different cell stresses, the most obvious of these being hypoxia. HIF1 α is also upregulated in response to androgens and certain chemotherapeutics (Cao *et al.*, 2013; Mabjeesh *et*

al., 2003b). Although HIF1 α is regarded as a key player in the life of a cancerous cell, the synthesis of a direct therapeutic inhibitor of HIF1 α remains elusive. Many of the inhibitors formulated for this purpose, thus far, are regulators of downstream targets or act as inhibitors of potentiators of the TF.

To summarise, the aim of this chapter is to determine the mechanisms of EL102 with regard to MT dynamics and the cell survival processes of drug resistance and HIF1 α signalling.

4.2 Results

4.2.1 EL102 and Microtubule Dynamics *In Vitro*

Investigating the potential of EL102 as a disruptor of MT dynamics, a cell-free assay was undertaken to analyse whether or not the compound served to prevent the polymerisation or depolymerisation of tubulin. As mentioned previously, the taxane docetaxel has been approved as a treatment for the advanced stage of prostate cancer. This MT disruptor super-stabilises the tubulin structures, preventing MT disassembly leading to mitotic arrest. In the current study, the rate of polymerisation of purified tubulin was measured, over the period of 1 h, in the presence of EL102, docetaxel, a combination of the two compounds or tubulin destabiliser, nocodazole. The results in Figure 4.1 show that, as expected, docetaxel increased the rate of tubulin polymerisation compared with the untreated tubulin control. In contrast, when EL102 was present a decreased rate of polymerisation was observed when compared with the control. This suggests that EL102 can inhibit tubulin polymerisation. Combining EL102 and docetaxel resulted in the reversal of the docetaxel-induced polymerisation to similar levels of inhibition produced by EL102 alone. Also, as expected nocodazole treatment impaired tubulin polymerisation. Of note, is that this decline in polymerisation occurred to a lesser extent than our compound of interest.

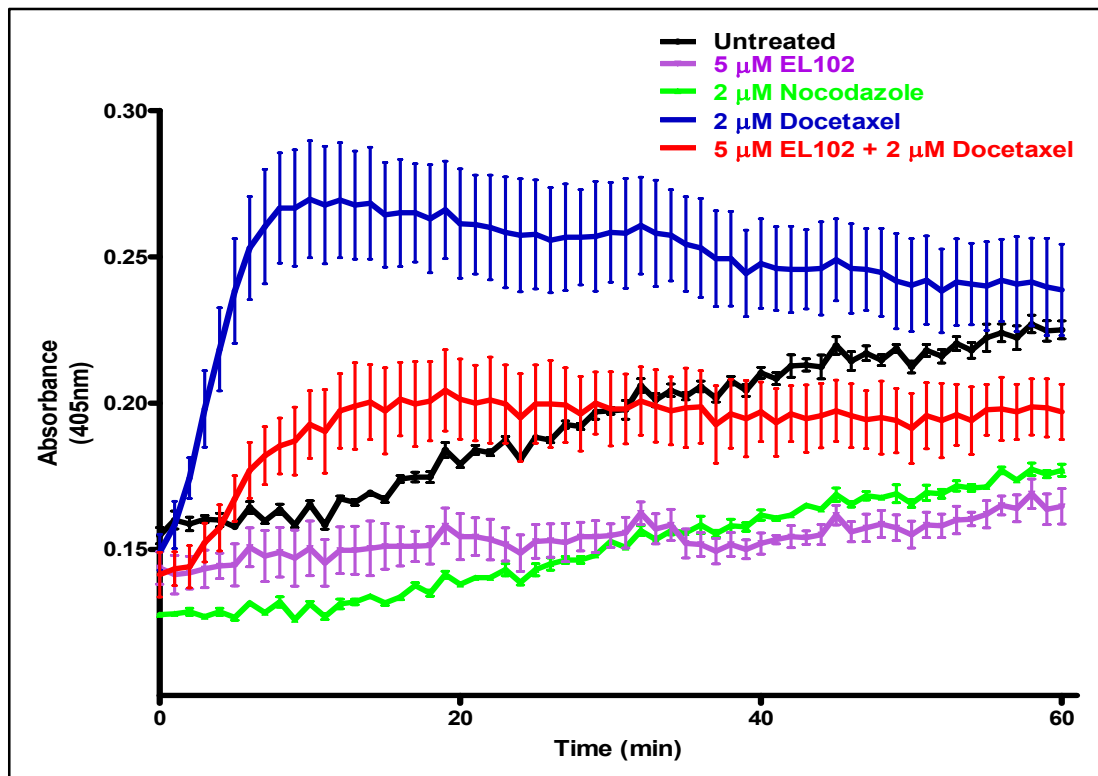


Figure 4.1 – Tubulin polymerisation assay. (Modified (Toner *et al.*, 2013)).

As EL102's effects on tubulin polymerisation had only been investigated in a cell free assay, the next step taken was to analyse this in a cellular context. The cell line DU145 was treated with concentrations of EL102, docetaxel and a combination of both. Immunofluorescent staining was carried out on these cells, as well as an untreated control culture, to detect and compare β -tubulin and acetylated tubulin expression patterns. Increased acetylation of tubulin is a marker of MT stability. DAPI was used for the staining of cellular nuclei. *Beta-* (β -) tubulin served as a marker for total cellular tubulin while acetylated tubulin was used to visualise MT stability following 24 h treatment with EL102, docetaxel and a combination of both (Figure 4.2). A 2 h exposure of cells to 320 nM nocodazole served as a positive control of MT instability. As expected, an increase in the expression of β -tubulin and acetylated tubulin was observed in response to docetaxel, while EL102 caused a reduction in acetylated tubulin. Comparison to the nocodazole control, confirmed this finding. The combination of EL102 and docetaxel caused a marked change in the distribution of acetylated tubulin.

Interestingly, perinuclear aggregation of both β - and acetylated-tubulin, as seen in Figure 4.2, after treatment with 50 and 100 nM EL102 was a widespread feature of the cultures exposed to these concentrations after 24 h.

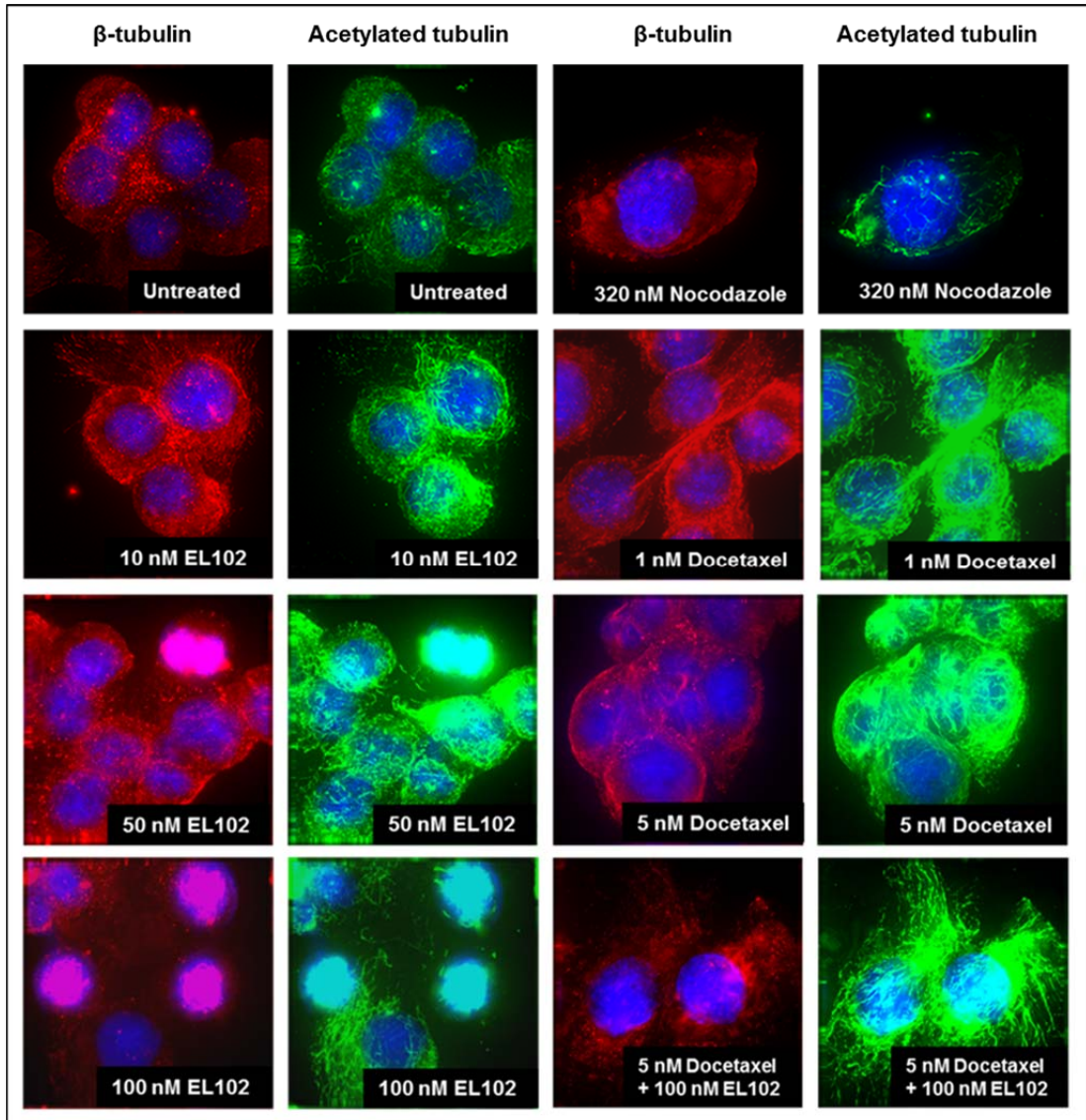


Figure 4.2 – Immunofluorescent staining of β -tubulin and acetylated tubulin in DU145 following 24 h EL102 and docetaxel treatment. (Modified (Toner *et al.*, 2013)).

4.2.2 The Impact of EL102 Treatment on Two Multi-drug Resistant Cell Models

Having determined the dose ranges of EL102, *in vitro*, in four prostate cancer models, a study was undertaken next to look at the effects of the novel compound on the viability of a panel of lung cancer cell lines with acquired cross-resistances to a variety of clinically used compounds. These cell lines, derived from poorly differentiated squamous lung carcinoma, were generously gifted by Prof. Martin Clynes, National Institute for Cellular Biotechnology at Dublin City University. Table 4.1 shows the cross-resistance profiles of parental cell line DLKP and three of its modified daughter cell lineages, DLKPA, DLKP-SQ and DLKP-SQ-Mitox. DLKPA possesses a selected resistance to doxorubicin (Adriamycin). DLKP-SQ is an anoikis-resistant subpopulation of DLKP and DLKP-SQ-Mitox is a further subset of this cell line which maintains a selected resistance to mitoxantrone. Figure 4.3 shows the comparative EL102 dose response of each of the drug-resistant variants to their respective parental cell lines.

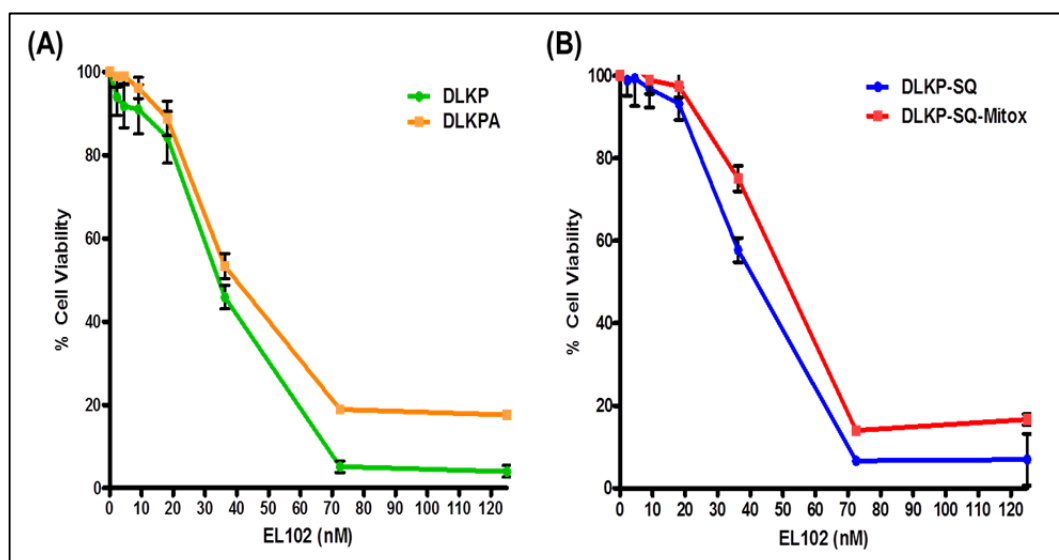


Figure 4.3 – EL102 dose-response curves of a panel of drug-resistant cell lines. (A) Cell viability assays of DLKP vs DLKPA following a 72 h treatment with EL102. (Modified (Toner *et al.*, 2013)) . **(B)** Cell viability assays of DLKP-SQ vs DLKP-SQ-Mitox following a 72 h treatment with EL102. These data ((A) and (B)) were generated in collaboration with Dr. Helena Joyce and Dr. Laura Breen, NICB, DCU.

Table 4.1 – Cross-resistance profile of DLKP, DLKPA, DLKPA-SQ and DLKP-SQ-Mitox

	DLKP IC₅₀ (nM) ± SD	DLKPA IC₅₀ (nM) ± SD	Fold Change
Adriamycin	24 ± 2	4900 ± 300	204
Docetaxel	0.2 ± 0.04	38 ± 3.0	253
Paclitaxel	1.2 ± 0.5	310 ± 25	258
Vincristine	0.9 ± 0.1	629 ± 160	691
EL102	14.4 ± 0.8	16.3 ± 1.2	1.1

	DLKP-SQ IC₅₀ (ng ml⁻¹) ± SD	DLKP-SQ-Mitox IC₅₀ (ng ml⁻¹) ± SD	Fold Change
Mitoxantrone*	0.08 ± 0.01	16.79 ± 2.27	209.87
Irinotecan*	0.08 ± 0.01	1359 ± 207	4
Epirubicin*	10.39 ± 1.5	13.93 ± 0.9	1.3
Paclitaxel*	1.65 ± 0.07	1.11 ± 2.27	0.67
Cisplatin*	731.8 ± 136.33	467.85 ± 11.80	0.63
Vinblastine*	0.63 ± 0.36	0.68 ± 0.4	1
EL102	18 ± 0.65	21 ± 1.44	1.2

*Data provided by Dr. Helena Joyce, NICB, DCU.

These cell lines were used as they have been extensively characterised for their relative acquired drug resistances (Clynes *et al.*, 1992; Heenan *et al.*, 1997; Keenan *et al.*, 2012; Law *et al.*, 1992; McBride *et al.*, 1998). Furthermore, the modes of resistance, specifically overexpression of drug efflux protein pumps, are comparable to those attained in advanced stage prostate cancer. Also of note, eight of the nine lung cancer cell lines within the NCI-60 dose response screen of EL102, showed equal sensitivity to the compound as those of the prostate (PC-3 and DU145; Chapter 1, Figure 1.8 (B)).

From the representative data shown in Figure 4.3 and summarised in Table 4.1, it is clear, each of the parental cell lines DLKP and DLKP-SQ, and their drug-resistant variants are equally sensitive to EL102 with IC_{50} fold changes between parental cell lines and their lineages < 1.3 . The DLKPA mechanism for drug resistance is due to the upregulation of drug resistance pump P-glycoprotein (P-gp or MDR1). This translational increase offers cross-resistance to an array of drugs with disparate modes of action. The acquired resistance of DLKP-SQ-Mitox is the result of an upregulation in the expression of drug resistance pump BCRP, which is another mode of resistance to drugs with varied cellular targets. Such chemotherapeutics include those capable of DNA intercalation and MT disruption. Of note, the DLKP-SQ-Mitox cell line appears to have acquired a slight increase in sensitivity to cisplatin and paclitaxel.

4.2.3 Examining the Inhibitory Effects of EL102 on a Panel of Kinases

To further explore the impact of EL102 on cellular processes and potentially determine targets of the compound in signalling pathways, a kinase inhibitor screen was commissioned by Dr. Bernd Janssen at Elara Pharmaceuticals. The competition between 1 μ M EL102 and an immobilised ligand to bind 442 DNA-labelled kinases (some of which were common mutant variants) was tested. As a control, the EL102 diluent, DMSO, was used in parallel and results for each kinase screened was noted as a percentage of this result (% control). The graph in Figure 4.4 illustrates the % control of a subset of kinases including those most significantly affected by the presence of EL102 (<65 % of control) as well as those whose receptor binding was not compromised by the presence of EL102 (mTOR and EGFR1). Of these, ankyrin repeat and kinase domain containing 1 (ANKK1; 39 %) binding was most heavily influenced by EL102 treatment. A complete list of results for this screen can be found in Appendix III.

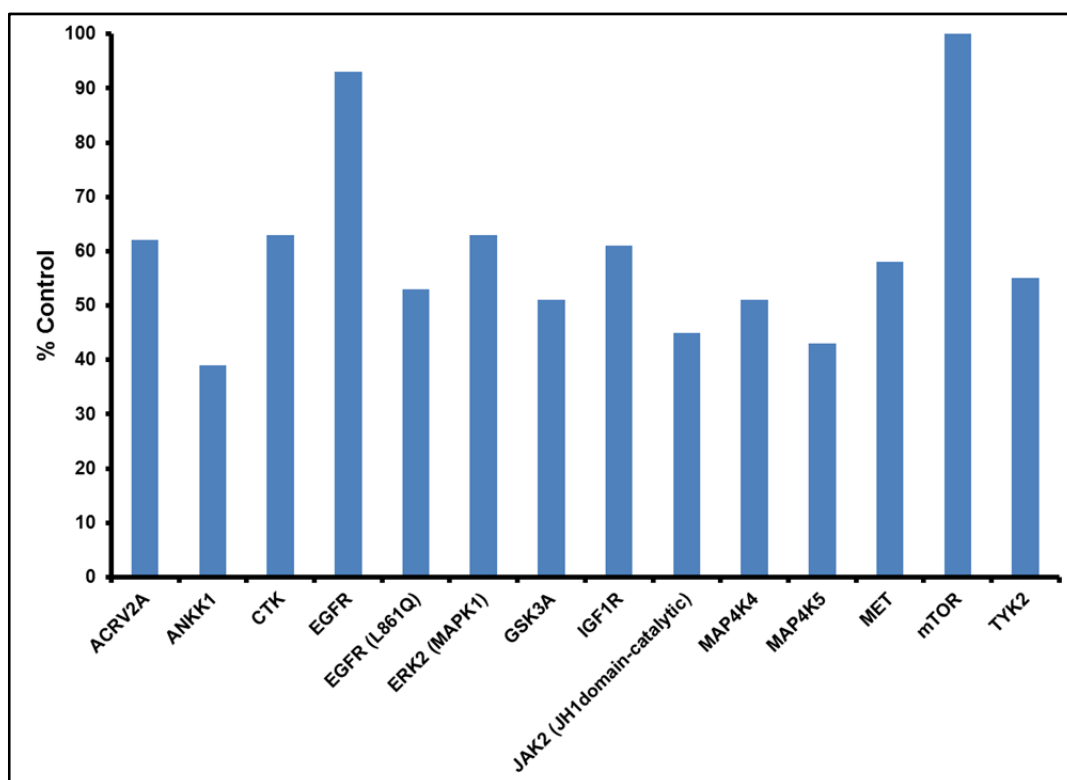


Figure 4.4 – Kinase inhibitory potential of EL102 treatment (Elara Pharmaceuticals, unpublished data).

4.2.4 EL102 Reduces Cellular HIF1 α Protein *In Vitro*

Based on the computational analysis conducted by Elara Pharmaceuticals, as mentioned previously, it was discovered that toluidine sulphonamides possessed HIF1 α -inhibitory qualities. Elsewhere, studies have found that MT disruptors can downregulate HIF1 α activities (Dachs *et al.*, 2006; Mabeesh *et al.*, 2003a). In the current study, an analysis of the HIF1 α -inhibiting quotient of EL102 was elucidated in a biological setting.

To begin with, an evaluation of EL102 as an inhibitor of HIF1 α was carried out at Elara Pharmaceuticals by Dr. Christoph Schultes and served as a pilot to the current study. Figure 4.5 (A) shows the results of HIF1 α expression in total protein isolated from HCT116 cells. HIF1 α protein levels decreased following a 4 h exposure of these cells to 100 and 500 nM EL102 in the presence of 1 % oxygen (O₂; hypoxia) while, as expected, at 21 % O₂ (normoxia), HIF1 α protein was expressed below the threshold of detectable levels in HCT116. Within the current study, to analyse the effect of hypoxia in prostate cancer cell models, PC-3 cells were treated with 100 μ M hypoxia mimetic cobalt chloride (CoCl₂), or water (Untreated) in combination with an increasing dose of EL102. Whole-cell protein was harvested, following a 24 h incubation and was analysed by Western blot for HIF1 α expression. The results in Figure 4.5 (B) show that an increasing dose of EL102 decreased both the basal and CoCl₂-induced HIF1 α protein levels. From Figure 4.5 (C), a similar decline was observed in the basal expression of HIF1 α protein in PC-3 nuclear extract, 24 h, following EL102-treatment in normoxia (21 % O₂). When hypoxia was induced within a hypoxia chamber set to 37 °C with 5 % CO₂ and 1 % O₂, the levels of HIF1 α protein expression were diminished, in the presence of EL102. It was noted, when compared to the preliminary HCT116 analysis (Figure 4.5 (A)) that, although the EL102 concentration was decreased and the exposure time lengthened, a reduction in HIF1 α expression still occurred.

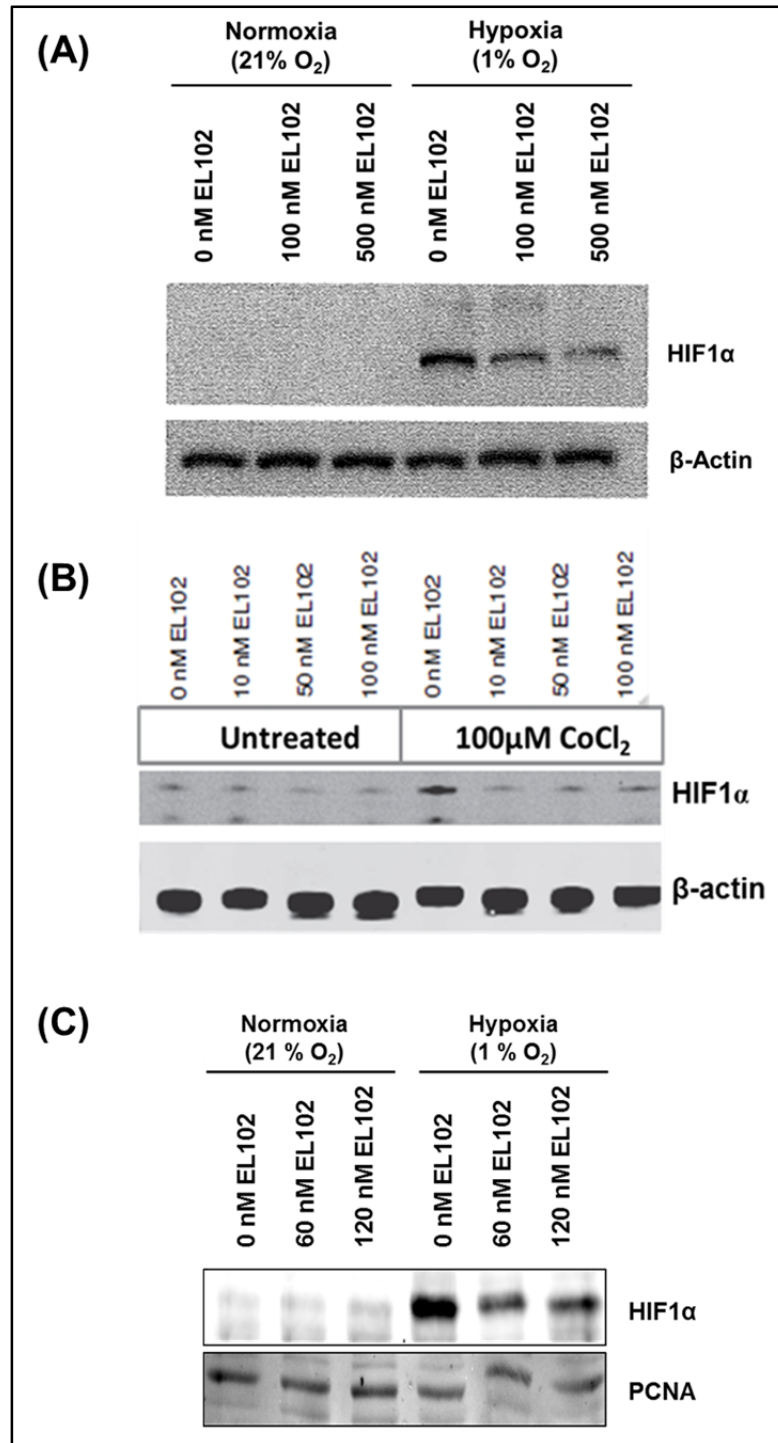
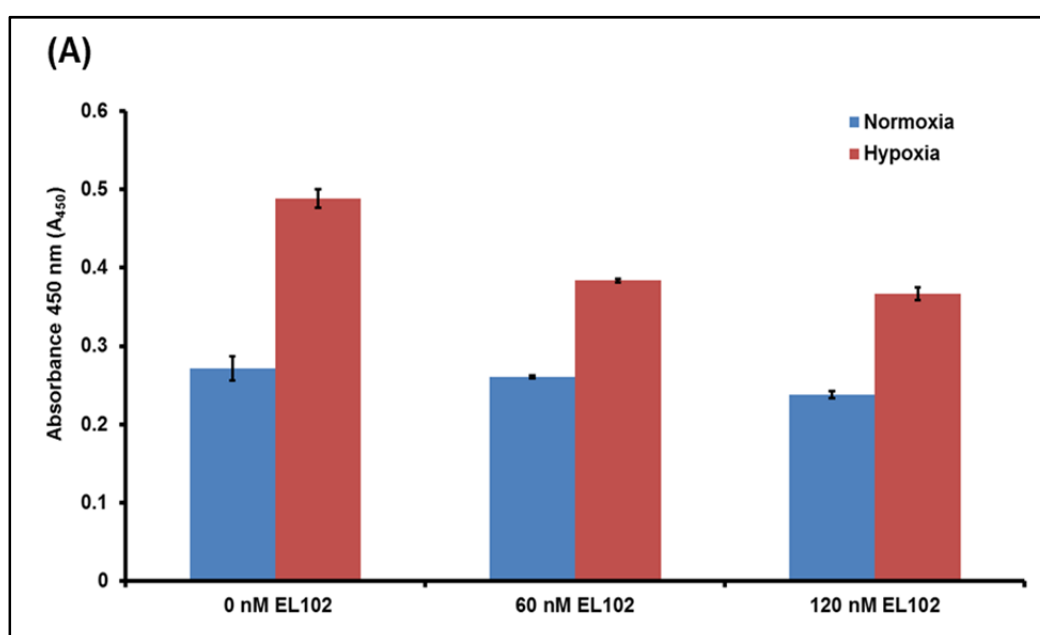


Figure 4.5 – Analysis of HIF1 α protein expression levels *in vitro* following EL102 treatment. (A) Western blot showing HIF1 α expression in total protein isolates of HCT116 following 4 h exposure to 21 % and 1 % O₂ and exposure to incremental concentrations of EL102 (Elara Pharmaceuticals, Unpublished data). **(B)** Western blot of HIF1 α expression in PC-3 whole protein extracts following EL102 treatment for 24 h in the presence of CoCl₂ (100 μ M) or water (untreated) (Toner *et al.*, 2013). **(C)** Western blot showing the levels of HIF1 α induction within nuclear protein extracts obtained from PC-3 cells treated with EL102 concentrations for 24 h in normoxia (21 % O₂) and hypoxia (1 % O₂).

4.2.5 Examining the Effects of EL102-Mediated HIF1 α Deactivation

With the EL102-associated reduction in HIF1 α protein levels observed, investigations began into how this translates to diminished intracellular activities. First, there was a need to determine if this equated to direct inhibition of HIF1 α activation. To do this, a HIF1 α TransAM ELISA was initially carried out. Following 24 h EL102 treatments, subcellular fractionation of both hypoxic and normoxic PC-3 cells was performed, as previously described (2.3.3.4). The nuclear HIF1 α moieties of cellular protein were compared to that of the untreated control (Figures 4.6 (A)). As is clearly shown, compared to the untreated controls (0 nM EL102), induction of hypoxia (1 % O₂) led to nearly double the signal of the normoxic data point indicating the expected increase in nuclear HIF1 α . Upon EL102 treatment and in hypoxia, over 24 h, a reduction in the TF's nuclear presence was observed. This countered the normoxia series which remained unchanged in spite of EL102 treatment. Furthermore, immunocytofluorescence of EL102-treated and untreated PC-3 cells was carried out to visualise the ability of EL102 to effectuate a loss of HIF1 α nuclear localisation in normoxia and hypoxia. Immunostaining of acetylated tubulin was used as a measure of the MT destabilising capacity of the compound. This effect was seen to be exacerbated in hypoxic conditions upon treatment with 60 nM EL102. The nucleus was made visible through use of counterstain DAPI.



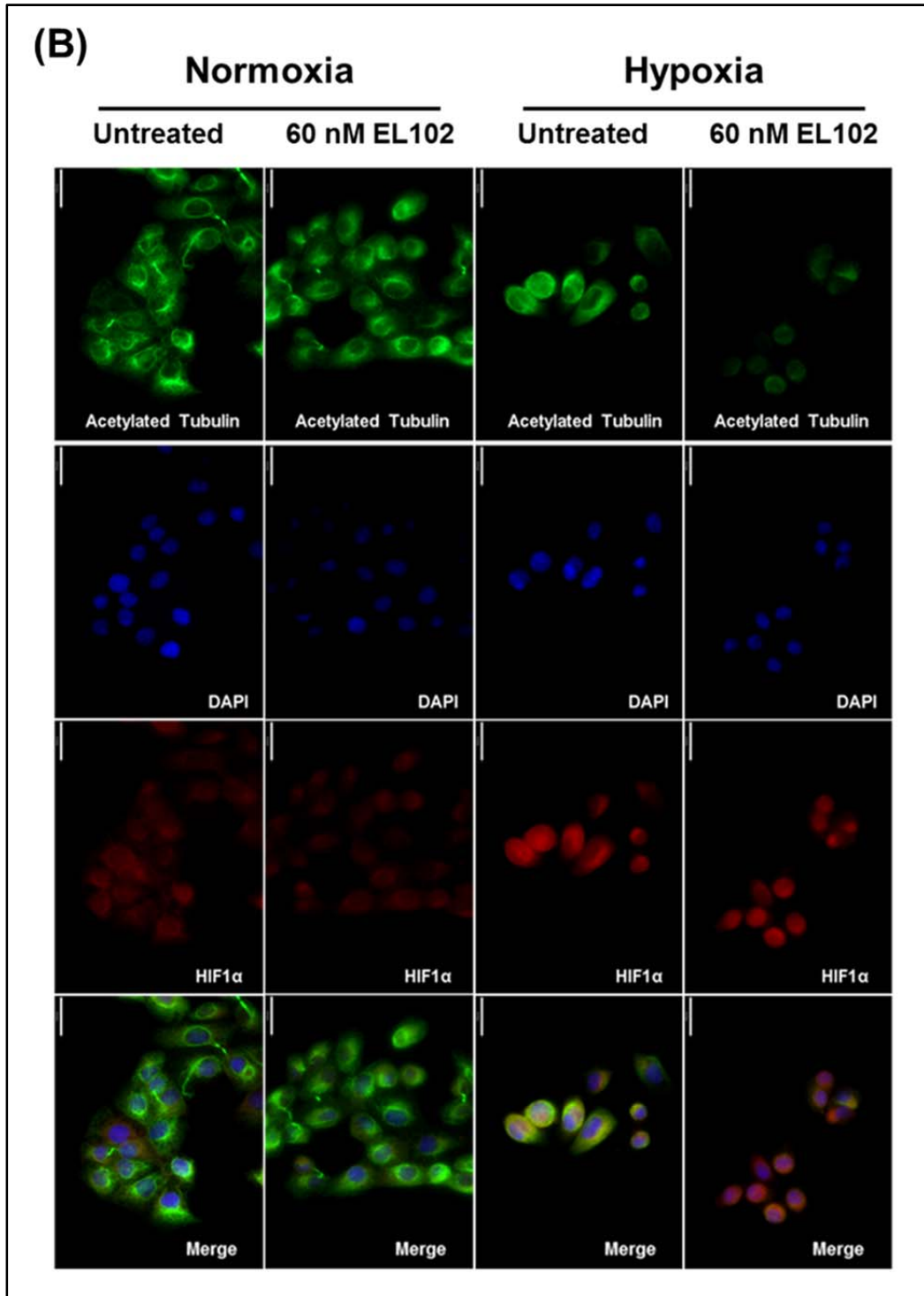


Figure 4.6 – HIF1α is deactivated through the activities of EL102 *in vitro*. (A) HIF1α TransAM ELISA graph depicts PC-3 levels of Nuclear HIF1α. (B) Immunofluorescent microscopy (40X) of HIF1α nuclear localisation and acetylated tubulin in PC-3.

Some of the target genes of HIF1 α were examined to ascertain if the EL102-directed decrease in HIF1 α protein levels had implications for a loss of its transcriptional regulation of the cellular functions metabolism and migration. Consistent with previous investigations of HIF1 α , the prostate cancer cell line PC-3 was used to quantify potential EL102-mediated fluctuations, if any, in the transcriptional activities of HIF1 α in regulating genes glucose transporter 1 (GLUT1), lactate dehydrogenase A (LDHA) and chemokine receptor, CXCR4, following 24 h treatment in normoxia (21 % O₂) and hypoxia (1 % O₂). The expression profiles of these genes were analysed by qPCR and normalised to expression of endogenous control gene, 36B4. Figure 4.7 (A) shows the normalised fold induction of GLUT1 gene expression doubled upon induction of hypoxia. The addition of EL102 did not appear to significantly affect this GLUT1 induction and, if anything, the drug slightly increased gene amplification in normoxic conditions. From Figure 4.7 (B), the gene expression of LDHA seemed relatively unaffected by either, the onset of hypoxia, or EL102 treatment, with only slight deviations in fold induction witnessed after 24 h. Figures 4.7 (C) and (D) show CXCR4 gene transcript and protein levels, respectively, following 24 h treatment with EL102 in normoxia and hypoxia. Though there was an apparent decrease in normoxic CXCR4 gene fold induction upon treatment with 120 nM EL102, this concentration had only a slight impact on the induction of the CXCR4 gene in hypoxic conditions. Expression levels of CXCR4 protein remained relatively unaffected by 24 h EL102 treatment, regardless also, of the levels of oxygen present.

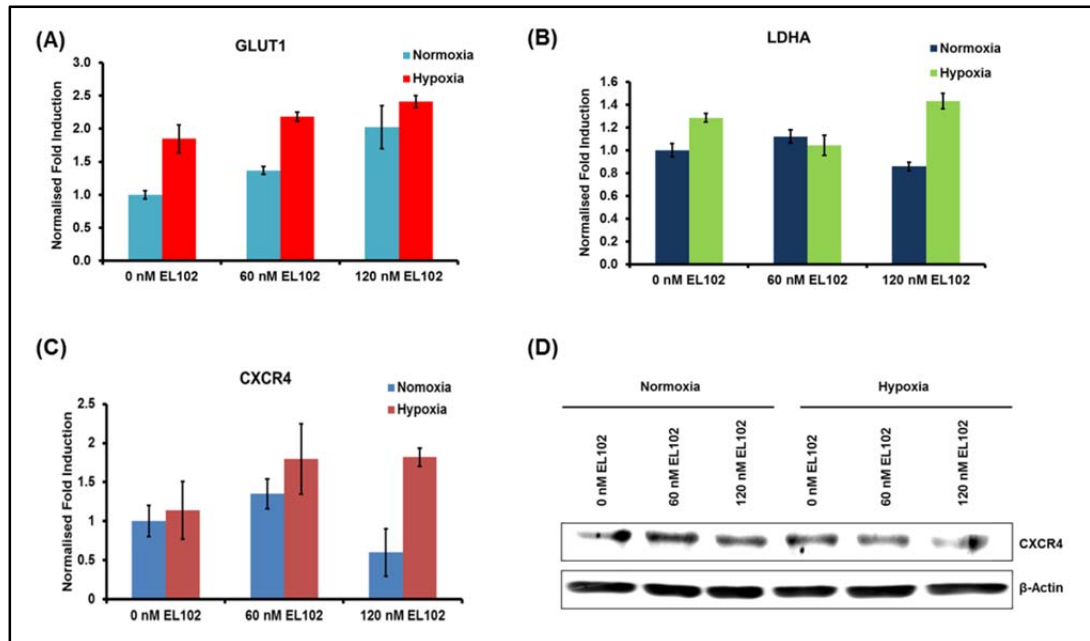


Figure 4.7 – Analysis of HIF1 α transcriptional targets in PC-3 following EL102 treatment. Normalised fold induction of the genes **(A)** GLUT1, **(B)** LDHA and **(C)** CXCR4 following 24 h EL102 treatment (0, 60, 120 nM) in hypoxia and normoxia. **(D)** Western blot analysis of CXCR4 protein expression in membranous/cytosolic protein extracted from PC-3, following 24 h EL102 treatment in normoxia and hypoxia.

4.3 Discussion

4.3.1 EL102 Destabilises Microtubule Structures *In Vitro*

In normal functioning cells and cancerous cells alike, MTs fulfil a number of roles through their continuous assembly and disassembly. Chief among these is mitosis. It is for this reason that MTs have become the target of cancer chemotherapeutics over the past few decades. Drugs with such potential are referred to as MT disruptors. The taxanes, paclitaxel and docetaxel are two such agents that bind to MTs and block their disassembly. This persistent polymerisation of the MT's tubulin filaments eventually leads to the demise of the cancerous cell. Conversely, MT disruptors such as the vinca alkaloids block the assembly of MTs reaching the same endpoint as the taxanes, namely mitotic catastrophe.

In the current study, EL102 was investigated for its potential as a disruptor of MTs. Initially, in a cell free assay, EL102 was tested for its ability to inhibit or facilitate tubulin polymerisation. Docetaxel (2 μ M) and the tubulin depolymerising agent nocodazole (2 μ M) were used as positive and negative controls of polymerisation, respectively, against EL102 (5 μ M) treatment. Also, to investigate further, the effects of combining EL102 and docetaxel (Chapter 3), tubulin was treated with both compounds simultaneously, at the above-mentioned concentrations. EL102 was shown to inhibit the polymerising effect seen in the untreated control. A reversal of the polymerising effect of docetaxel was observed in the combination treatment with EL102. Interestingly, EL102 had a greater inhibitory effect than that of nocodazole.

While the tubulin polymerisation assays provided evidence of the activities of EL102 as an inhibitor of tubulin filament construction, further intracellular investigation was necessary. An analogous *in vitro* study of EL102, employing the immunofluorescent staining of the MTs, was carried out on each of the four prostate cancer cell lines. The DU145 results shown, here, are representative of this panel. This showed that upon addition of EL102, there was a clear loss of acetylated tubulin structures which was indicative of a tubulin destabilising effect and was comparable to the effects of 2 h

exposure to 320 nM nocodazole. Of note, was the abundance of nuclear encapsulation by both acetylated-tubulin and β -tubulin, detected in cultures treated with EL102 at concentrations of 100 nM and, to a lesser extent, 50 nM. Docetaxel treatment at concentrations of 1 nM and 5 nM displayed numerous, dense acetylated tubulin filaments, as expected, while, the combination treatment of EL102 and docetaxel resulted in uneven distributions of cell-wide acetylated tubulin structures. This helped to explain the apparent antagonistic effects of these drugs when treated in combination for the initial cytotoxic assay analyses (3.2.3). These findings, coupled with the earlier cell cycle analysis data that demonstrated loss of cells from G₁ and an accumulation in G₂/M phase 24 h post-EL102 treatment, and induction of apoptosis, suggest that MT destabilisation is responsible, at least, in part for the cytotoxic effects of EL102.

As potential mechanisms of chemo-resistance employed by cancer cells, the mutation and altered isoform expression of tubulin poses as problematic for advanced prostate cancer treatment with taxanes, paclitaxel and docetaxel. Until recent years, it was widely believed upregulation of β -tubulin isoform III (β III-tubulin) conferred resistance solely to taxanes, however data has since emerged to suggest that vinca alkaloid sensitivity is also compromised by this alteration (Karki *et al.*, 2013; Mozzetti *et al.*, 2005; Ranganathan *et al.*, 1998). Novel MT destabilisers such as 2-methoxyestradiol (2ME2) do not bind to the taxane or vinca sites of tubulin, but rather the colchicine site, have been found to destabilize MTs, regardless of β III-tubulin expression levels (Stengel *et al.*, 2010). Although it is evident from the data presented, in the present study, that EL102 effectuates a loss of stable MT structure, with a loss of β -tubulin expression, it remains to be seen whether this disruption is brought about through direct binding to the colchicine, the vinca or taxane sites. Indeed its mechanism may be novel. Additionally, as is the case with certain tubulin depolymerising agents, such a mechanism may effectuate disruption of tumour angiogenesis. It has already been noted previously (3.2.2) that tumour shrinkage can be achieved by EL102 singularly or more effectively, in combination with docetaxel. Histological analysis of the tumour tissues would assist greatly in the evaluation of this.

4.3.2 EL102 Circumvents Two Classic Models of Drug Resistance *In Vitro*

Apart from the shift towards prominence of β III-tubulin, reduction in sensitivity to mitoxantrone and the taxanes paclitaxel and docetaxel may be achieved by other means. Both P-glycoprotein (MDR1) and BCRP are examples of adenosine triphosphate (ATP)-binding cassette (ABC) transport proteins, whose upregulation represents one mechanism of advanced prostate cancer drug resistance as they carry out cellular drug efflux (Gottesman *et al.*, 2002; Xie *et al.*, 2008).

In the present study, the utility of the compound of interest, EL102, for use in a chemoresistant setting, effectuated by an upregulation of MDR1 or BCRP, was determined in multi-drug resistant lung cancer cell lines DLKPA (MDR1-upregulated) and DLKP-SQ-Mitox (BCRP-upregulated). These were utilised due to the extensive analysis previously-conducted which compared each acquired resistance phenotype to that of the drug sensitive mother cell lines (Clynes *et al.*, 1992; Heenan *et al.*, 1997; Keenan *et al.*, 2012; Law *et al.*, 1992; McBride *et al.*, 1998). The effect of EL102 on these variants, in comparison to the respective progenitor cell lines of both, namely, DLKP and DLKP-SQ has shown this drug acts independently of these mechanisms. Although doxorubicin is not frequently used as a second line therapy for prostate cancer, the cross-resistance it confers in DLKPA to clinically used taxanes is significant and well-documented (Clynes *et al.*, 1992; Heenan *et al.*, 1996; Heenan *et al.*, 1997; Moran *et al.*, 2009). Combined with the capacity of EL102 to bring about cell death in each of the cell lines of prostate cancer that were assayed, an apparent circumvention of MDR1- and BCRP- mediated resistance mechanisms, here, further supports a utility of the drug in the treatment prostate cancer clinically. The taxanes paclitaxel and docetaxel as well as the DNA intercalating mitoxantrone remain the most commonly used second line therapies for advanced prostate cancer, globally. Eventually, however, there progresses a clinically more aggressive chemotherapy-refractory phase which, until the development of next generation cabazitaxel, remained untreatable. Cabazitaxel, similar to its precursor family members, acts to super-stabilise cellular MTs, resulting in

mitotic catastrophe. An upregulation in MDR1 and BCRP has been shown to have little effect on the function of cabazitaxel, though the adverse side-effect of neutropenia remains a drawback, reminiscent of its predecessors (Hussar & Daniels, 2010; Sanofi-Aventis, 2010). Like cabazitaxel, EL102 is not a substrate of either of these pumps which presents as advantageous in this terminal phase of treatment. It should, however, be noted that while BCRP and MDR1 are central mechanisms of drug resistance in prostate cancer, they are not unique. Other mechanisms of drug resistance include changes to growth factor receptor signalling such as that of IGFR, VEGFR and EGFR (Dahut *et al.*, 2013; Jones *et al.*, 2004; Lin *et al.*, 2013). Hypoxia-related resistance, tubulin mutation and altered tubulin isoform expression, combined with upregulation of other drug pumps, for instance, MRP1, MDR2 as well as NFkB activation, also give selective advantages to cancer cells throughout chemo-intervention (O'Neill *et al.*, 2011; Seruga *et al.*, 2011; Zhang *et al.*, 2012). Such multi-adaptive phenotypes force the need to enlist the combination treatment of more novel therapies with many cellular applications as is seen with EL102.

4.3.3 The Ability of EL102 to Inhibit HIF1 α and Certain Kinases May Have Significant Clinical Applications

In addition to the previously mentioned modes of EL102 operation, it was determined that the compound, in its capacity as a toluidine sulphonamide, decreased HIF1 α expression *in vitro*. This was observed in the whole protein analysis of EL102-treated PC-3 cells in normoxia and hypoxic-mimicking conditions of cobalt chloride (CoCl₂) treatment as well as in the nuclear extracts of cells cultured in 1 % O₂. It is clear from these data that this is a mechanism distinct from tubulin polymerisation which is a contributing factor to cell death observed. It should also be noted that EL102's effects on MT stability was heightened in hypoxic environs as evidenced by the loss in acetylated tubulin in the immunocytofluorescence study. This was not surprising as transmission of the survival cues normally provided by HIF1 α in response to hypoxia had been attenuated. An analysis of the inhibitory functions of EL102 (1 μ M) on a panel of 442 kinases was conducted by Elara Pharmaceuticals. It was clear from this screen that the drop in HIF1 α

activation cannot be attributed to perturbation of the mTOR pathway, with no change in the binding of mTOR to the immobilised ligand witnessed upon treatment with EL102 over the control. Interestingly, an EL102-induced binding inhibition of 47 % EGFR (L861Q) was observed when compared to the control. This mutation has been shown to confer sensitivity, of the receptor, to tyrosine kinase inhibitors (TKIs) in 2 % of non-small cell lung cancer (NSCLC) (Mitsudomi & Yatabe, 2010). By comparison, only a 7 % inhibition of wild type EGFR binding occurs in the presence of EL102. Also worth noting is that EGF is known to play a role in modulation of HIF1 α through the mTOR pathway in prostate cancer and EGFR mutations assist disease progression (Edwards *et al.*, 2006; Hudson *et al.*, 2002). It has also been hypothesised that this regulation may involve MET which, in turn, has previously been shown to be upregulated in response to EGFR mutations incurring resistance from TKIs in NSCLC (Engelman *et al.*, 2007; Turke *et al.*, 2010). 40 % inhibition of IGFR binding was the product of EL102 treatment. As mentioned previously, changes to IGFR expression can increase chemo-resistance. Although, the receptor binding, here, is muted in the presence of EL102, perhaps mutation or an increase in expression may serve to diminish the potency of EL102.

ELISA analysis of nuclear HIF1 α suggests a reduction in its activation. Additionally, though the inhibition of HIF1 α through EL102-treatment occurred, the negative effects of this, on downstream HIF α targets GLUT1, LDHA and CXCR4 were not immediately obvious following 24 h hypoxia exposure. This suggests that whilst expression of these genes is complemented by the activities of the TF, they are not solely reliant on it. Also, as there remains much more, at present, to be uncovered about the role of HIF1 α in prostate cancer progression, the true importance of toluidine sulphonamides cannot be realised in these preliminary studies (Huang *et al.*, 2014; Semenza, 2012).

Chapter 5:

Investigating the Potential Role of EL102 as a Disruptor of Androgen Receptor Signalling in Prostate Cancer

5.1 Introduction

The androgen receptor (AR) is known to play a key role in the progression of prostate cancer (Huggins & Hodges, 1941). In recent decades, there has been a growing interest in the need to curtail the activities of AR in tackling this selective advantage (Carver, 2014). The production of male testosterone is dependent on the pituitary secretion, luteinising hormone releasing hormone (LH-RH), also known as gonadotropin releasing hormone (GnRH). Drugs such as goserelin acetate, are GnRH agonists and these have been shown to, for short periods of time, inhibit the progression of prostate cancer in patients. This occurs by stimulating excessive and sustained production of testosterone which in turn, causes a negative feedback loop, thus reducing androgen production. GnRH agonists are usually administered in the late stages of prostate cancer (Blackburn & Albert, 1959). Synthesis of the more potent androgen dihydrotestosterone (DHT) from testosterone can be blocked directly through treatment with 5 α -reductase inhibitors (5-ARI) such as dutasteride and finasteride (Saartok *et al.*, 1984; Vermeulen *et al.*, 1989; Yamana *et al.*, 2010). Another method of reducing AR signalling is the use of AR antagonists. Bicalutamide (Casodex or CDX) is one example of anti-androgen which binds directly to and antagonises AR (Kolvenbag *et al.*, 1998). In spite of these pharmaceutical advancements for tackling a cellular mechanism advantageous cancer, the disease usually progresses to a point where these treatments become ineffective and chemotherapy is required.

So far, this body of work has explored the mechanisms of EL102-induced cell death, inhibition of HIF1 α and the disruption of microtubules (MTs). The effect of the drug on the interactions of ligands binding to cell receptors has remained untouched. A preliminary study commissioned at Elara Pharmaceuticals by Dr. Christoph Schultes aimed to explore these interactions. This work had suggested the ability of EL102 to disrupt the binding of nuclear receptors to their cognate ligands above all others, as shown in section 5.2.1. Elara investigated whether EL102 deterred binding of radiolabelled ligands to AR, progesterone receptor (PR), oestrogen receptor (ER), glucocorticoid receptor (GR) and peroxisome proliferator-activated receptor *gamma* (PPAR γ), amongst others (See Appendix IV). As these

preliminary assays were cell-free in nature, the current study aimed to confirm the disruption of the mechanism of AR signalling, *in vitro*, using the classic model of AR signal transduction, the LNCaP cell line.

5.2 Results

5.2.1 Ligand–Nuclear Receptor Interaction in the Presence of EL102

A broad spectrum cell-free screen of the potential of 1 μ M EL102 to affect, negatively, the binding of radiolabelled ligands to their cognate receptors was carried out. Overall, 71 receptors were assayed (for complete results see Appendix IV) and amongst these were the nuclear receptors, PPAR γ (human recombinant protein), GR (derived from IM-9 cytosolic protein), ER (derived from MCF7 cytosolic protein), PR (derived from T47D cytosolic protein) and AR (derived from LNCaP cytosolic protein). As shown in Figure 5.1 (A), non-steroidal receptor PPAR γ and steroidal receptor GR exhibited similar percentages of inhibition of control specific binding (35 % and 34 %, respectively) whereas ER binding showed signs of only mild inhibition in the presence of EL102. The most profound inhibition, in all 71 receptor bindings assayed, was that of the PR and AR, with 95 % and 89 % inhibition of control specific binding witnessed, respectively. Further to this diverse profile of the inhibitory potential of 1 μ M EL102, a dose response (0–10 μ M EL102) analysis of the receptors PR and AR, was conducted by Elara. Similar to the results of the above mentioned assay, Figure 5.1 (B) shows that EL102 elicited a more heightened inhibition of PR binding (IC_{50} 31 nM) over that of AR (IC_{50} 96 nM) with the given concentrations.

While the concentrations of EL102 required for disruption of radiolabelled ligands binding to these purified receptors, in a cell-free environment, spanned the low-mid nanomolar range, it was anticipated that, *in vitro*, cellular analysis would require much lower concentrations to elicit a biological response. Analysis of the effect on AR binding was the focus of further scrutiny due to the potential clinical implications for prostate cancer treatment.

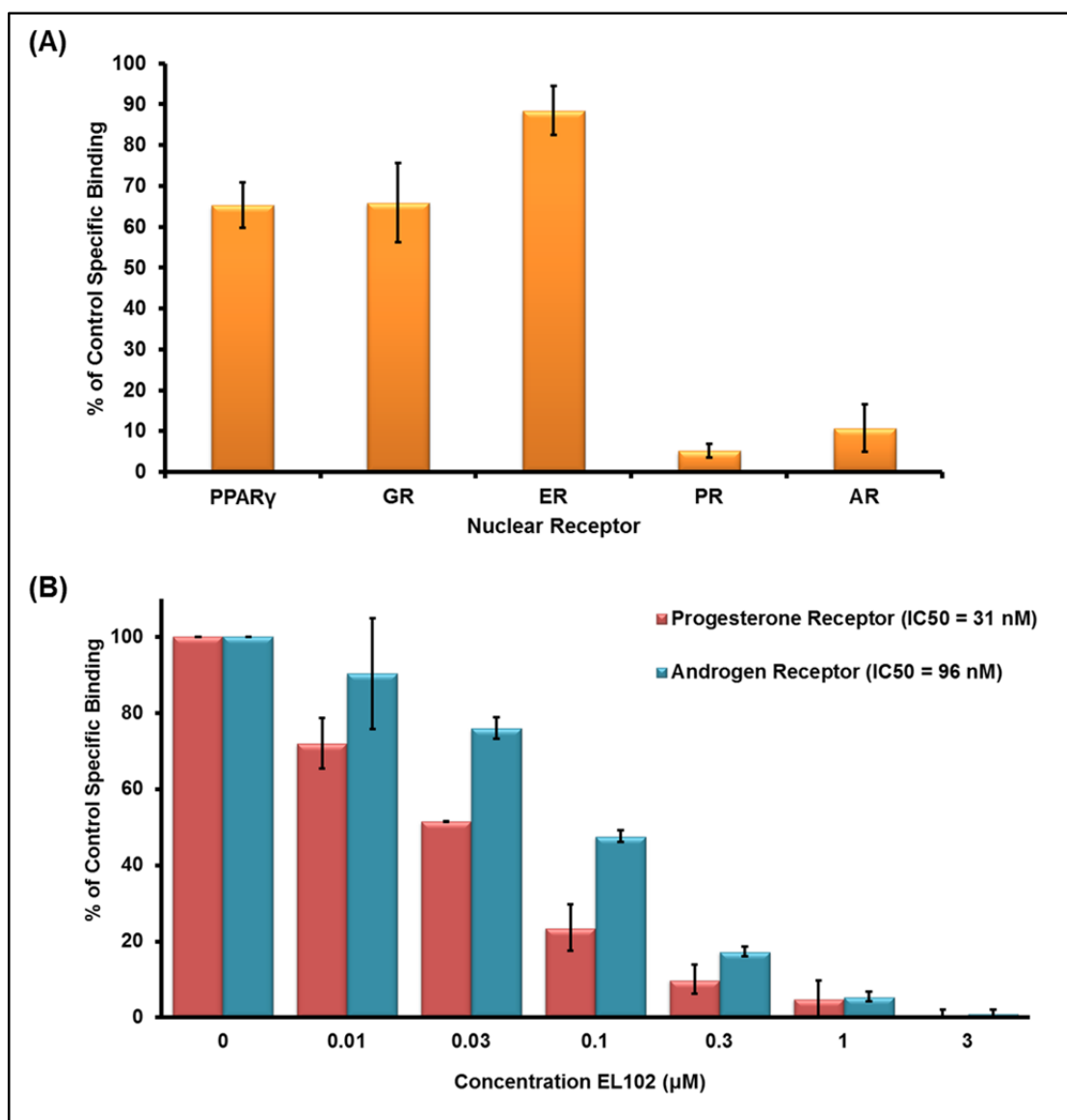


Figure 5.1 – Radiolabelled nuclear receptor ligand binding assay. (A) Competitive binding of radiolabelled ligands to their cognate receptors peroxisome proliferator-activated receptor *gamma* (PPAR γ), glucocorticoid receptor (GR), oestrogen receptor (ER), progesterone receptor (PR) and androgen receptor (AR) was assayed in the presence of 1 μ M EL102. **(B)** EL102 dose response of radiolabelled [3 H]progesterone and [3 H]methyltrienolone ([3 H]R1881) binding to PR and AR, respectively. Error \pm SD. (This unpublished data was generated by Dr. Christoph Schultes and was provided by Elara Pharmaceuticals).

5.2.2 Determination of the Cytotoxic Profile of EL102 in the AR-Positive Cell Line LNCaP

SRB assays were carried out to determine the dose range of EL102 in the AR-positive and androgen-responsive cell line LNCaP. This cell type, derived from the lymph node tumour resulting from metastasis of a prostate cancer, is the well-characterised model of AR signalling, *in vitro*. Initially, it was deemed necessary to carry out a dose-response assay of the effect of EL102 on these cells. As demonstrated in Figure 5.2, LNCaP exhibits an IC_{50} of 48.2 nM. This is higher than the values obtained from the cell viability analyses, reported in section 3.2.1, carried out on the metastatic cell lines of PC-3 and DU145, which were shown to have IC_{50} s of 37 and 40 nM (\pm SD), respectively. It is also worth noting that the AR-positive cell lines, CWR22 and 22Rv1, had exhibited IC_{50} s of 24 and 21 nM (\pm SD), respectively. This makes LNCaP the most EL102-resistant model from the subset of prostate cancer cell lines analysed, in the current study.

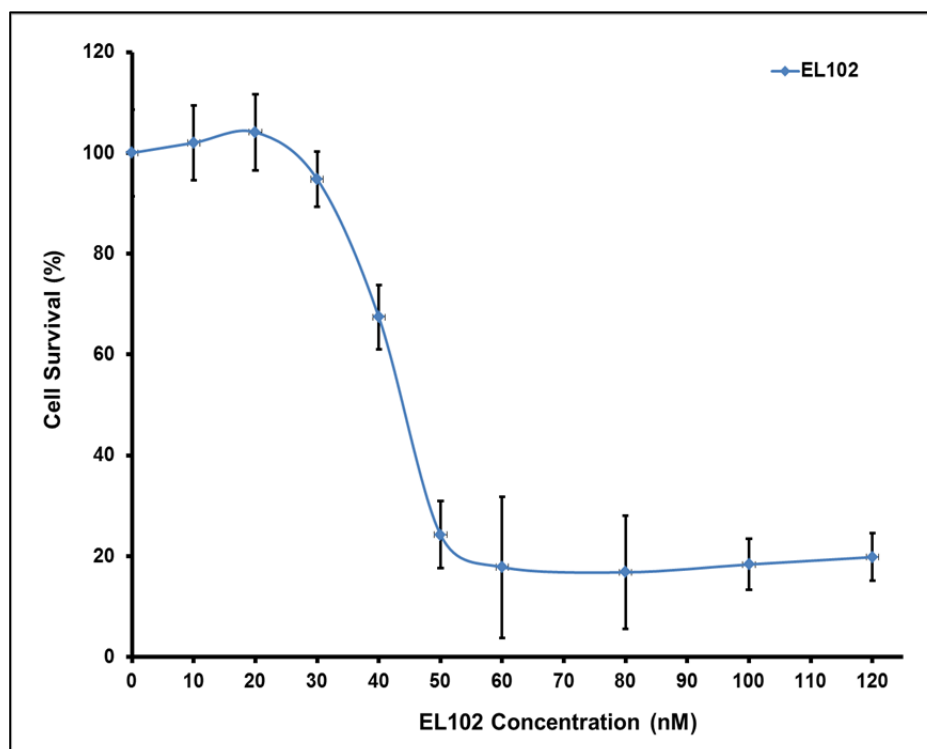


Figure 5.2 – EL102 dose response curve of LNCaP (Error, \pm SD).

5.2.3 EL102 Decreases AR Protein and AR Gene Expression *In Vitro*

As AR ligand binding inhibition by EL102 had, previously, been analysed in a cell-free setting by Elara Pharmaceuticals, it was necessary to carry out an analysis of this mechanism using cell line LNCaP. Whole protein lysates were analysed for AR expression following 24 h treatment of EL102 (0–120 nM) along with simultaneous doses of, either, vehicle, ethanol, or the synthetic androgen, R1881 (1 nM), as presented in Figure 5.3 (A). The whole protein isolates from vehicle-treated cells were seen to have a decreased expression of AR upon exposure to incremental concentrations of EL102. There was an apparent recovery of AR expression, however, in cells treated with 1 nM R1881. With or without androgen treatment, and as expected, AR expression was absent from the cell lysates of PC-3, a cell line which does not endogenously express AR (van Bokhoven *et al.*, 2003). The activation of AR was explored by analysis of the nuclear translocation of AR following 18 h treatment of LNCaP with EL102 (0, 50 and 100 nM) and known AR antagonist CDX (500 nM). Also, as determined previously, EL102 is a MT destabilising agent and for this reason the effects of vinca alkaloid, vincristine (VCR), treatment (40 nM) on nuclear translocation were examined, 18 h post-treatment. The results in Figure 5.3 (B) show that when fractionated and analysed by Western blot, protein from LNCaP revealed an apparent increase in cytosolic AR expression upon R1881 treatment, regardless of drug treatment. Ethanol (vehicle) treated LNCaP, on the other hand, showed an overall lack of cytosolic AR protein expression upon drug exposure. Though nuclear localised AR was present in the protein isolated from androgen deficient cells at largely equal concentrations, in each of the treatment conditions, nuclear AR was notably decreased in the cells treated with 100 nM EL102, 40 nM VCR and 500 nM CDX. Figure 5.3 (C) reveals that there was a decrease in transcriptional levels of AR following EL102 and CDX exposure for 18 h. In the presence of 1 nM R1881, drug treatment-free LNCaP had an 8-fold increase in the level of AR gene transcript induction as determined by quantitative polymerase chain reaction (qPCR) analysis.

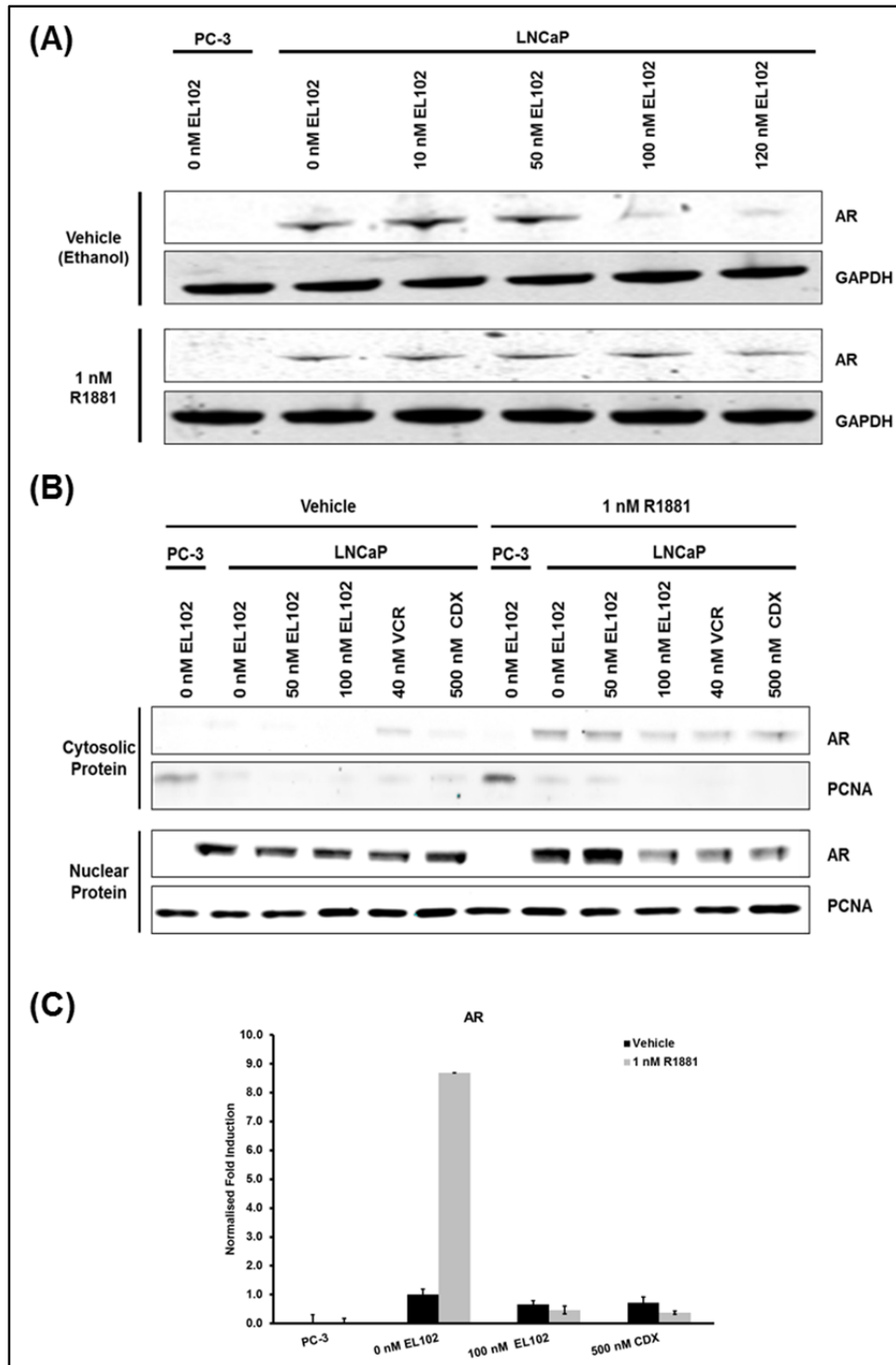


Figure 5.3 – LNCaP protein and gene expression of AR following simultaneous treatment with EL102 and 1nM R1881/vehicle. (A) Western blot analysis of AR protein expression following 24 h EL102 treatment. **(B)** Fractionation of LNCaP and PC-3 cellular protein for the detection of AR following 18 h EL102 (0, 50 and 100 nM), vincristine (VCR; 40 nM) or bicalutamide (CDX; 500 nM) treatment. **(C)** AR transcript level analysis by qPCR following 18 h EL102 (0 and 100 nM) or CDX (500 nM) treatment in the presence of vehicle (ethanol) or 1 nM R1881.

5.2.4 The Expression Patterns of AR Following EL102 Treatment May Be Partially Attributed to Its Microtubule-Destabilising Effect

As previously indicated, EL102 is a MT destabiliser and AR expression has been shown to decrease upon EL102 treatment. Previous studies have analysed MT disruptors in their capacity to dysregulate AR signalling *in vitro* (Zhu *et al.*, 2010). In the current study, the expression patterns of AR in LNCaP, following 100 nM EL102 treatment over 18 h, were compared to those of untreated cells or cells treated with 60 nM nocodazole, a known MT disruptor. Each condition was analysed in the presence of 1 nM synthetic androgen, R1881 or vehicle, ethanol. Figure 5.4 clearly shows that, in the absence of androgen (i.e. Vehicle-treated cells), those not treated with either nocodazole or EL102, displayed a well-organised and an evenly distributed network of MTs as well as diffuse AR expression. Upon 100 nM EL102 treatment, definition of the MT structures was lost and AR expression was decreased and became confined to the nuclear region. Nocodazole treatment, on the other hand, led to a loss of acetylated tubulin, yet the expression of AR remained consistent with that of the untreated i.e. diffuse and cytosolic. As expected, AR expression was upregulated and appeared more localised to the nuclear cellular region upon R1881 treatment in the drug-free cells. In cells treated with EL102, in the presence of androgen, there was a pattern of reduced structural definition of the MTs combined with nuclear confinement of acetylated tubulin (typical of EL102 activity, Figure 4.2, Chapter 4) and AR, which remains at low levels of expression. This was similar to that observed in androgen-deficient cells subject to the same drug treatment. Nocodazole-treated cells, in the presence of androgen, though lacking in acetylated tubulin, exhibited a slightly more increased expression of diffuse cytosolic AR than androgen deprived counterparts, though this was arguably less nuclear localised than drug-free R1881-treated cells.

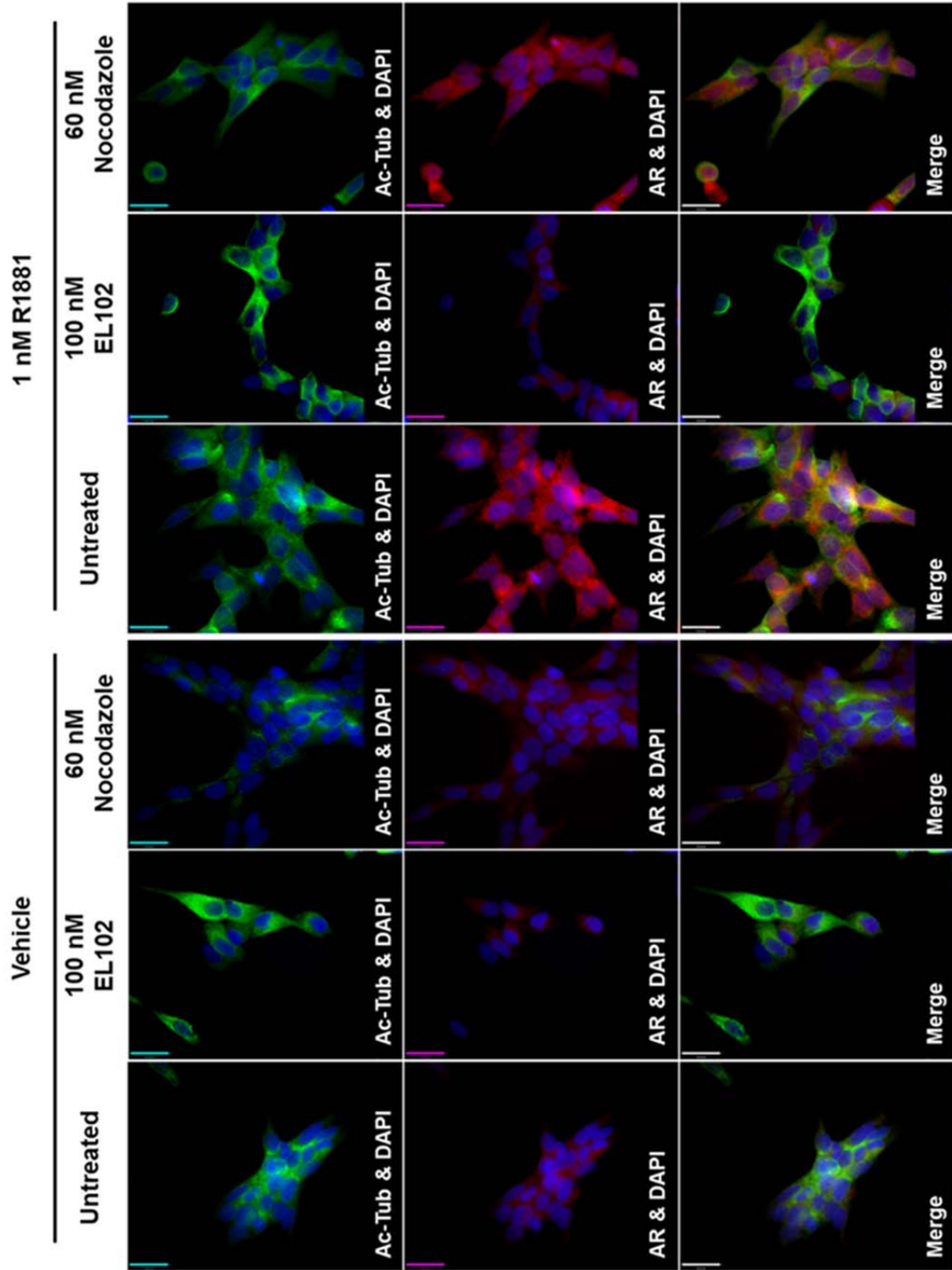


Figure 5.4 – Immunocytofluorescence of AR and acetylated tubulin (Ac-Tub) in the presence or absence of 1 nM R1881 and microtubule disruptors.

5.2.5 EL102 Disrupts the Binding of AR to Androgen Response Elements in a Dose-Dependent Manner

To test the efficacy of EL102 as an anti-androgen, reporter gene assays were set up using LNCaP and PC-3 cells. These cells were transiently transfected with either of the luciferase reporter constructs, PSA-407E-luc plasmid and MMTV-luc plasmid. Each of these luciferase constructs contain androgen response elements in their promoters, which are regulated by the binding of AR making them reporters of androgen activation. Cells were simultaneously co-transfected with β -galactosidase reporter plasmid, CMV- β -gal, as an indicator of transfection efficiency. Plasmids were cloned, purified by maxiprep and identified by agarose gel imaging of the product of restriction digest at BamHI restriction sites as shown in Figure 5.5 (A). Following transient transfection, LNCaP (Figure 5.5 (B)) and PC-3 (Figure 5.5 (C)) were treated with DMSO, 50 nM EL102, 100 nM EL102 or 500 nM of known AR antagonist bicalutamide (CDX) for 24 h, in the presence or absence of 1nM R1881. Figure 5.5 (B) shows that the AR expressing cell line, LNCaP, demonstrated minimal loss of basal AR activation (indicated by the DMSO control) in the vehicle-treated cohort. Conversely, the presence of 1 nM synthetic androgen, R1881, in DMSO-treated control demonstrated an increase in AR activities as reported by both transfection groups. There was a marked decrease in the binding of endogenous AR to the AREs of the reporter plasmids following treatment of EL102 or CDX. Also, as expected, the luciferase activities of MMTV-luc were much greater than those of PSA-407E-luc. Figure 5.5 (C) indicates that despite transient transfection of ARE-containing plasmids and the viability of cells thereafter, the lack of endogenous AR expression in PC-3 elicited no change to the activities of reporter gene signal after 24 h, in the presence or absence of androgen or upon drug treatment. Taken together, these data indicate that EL102 inhibits the binding of AR to AREs, mechanistically similar to the effects of AR antagonist CDX and in a dose-dependent manner.

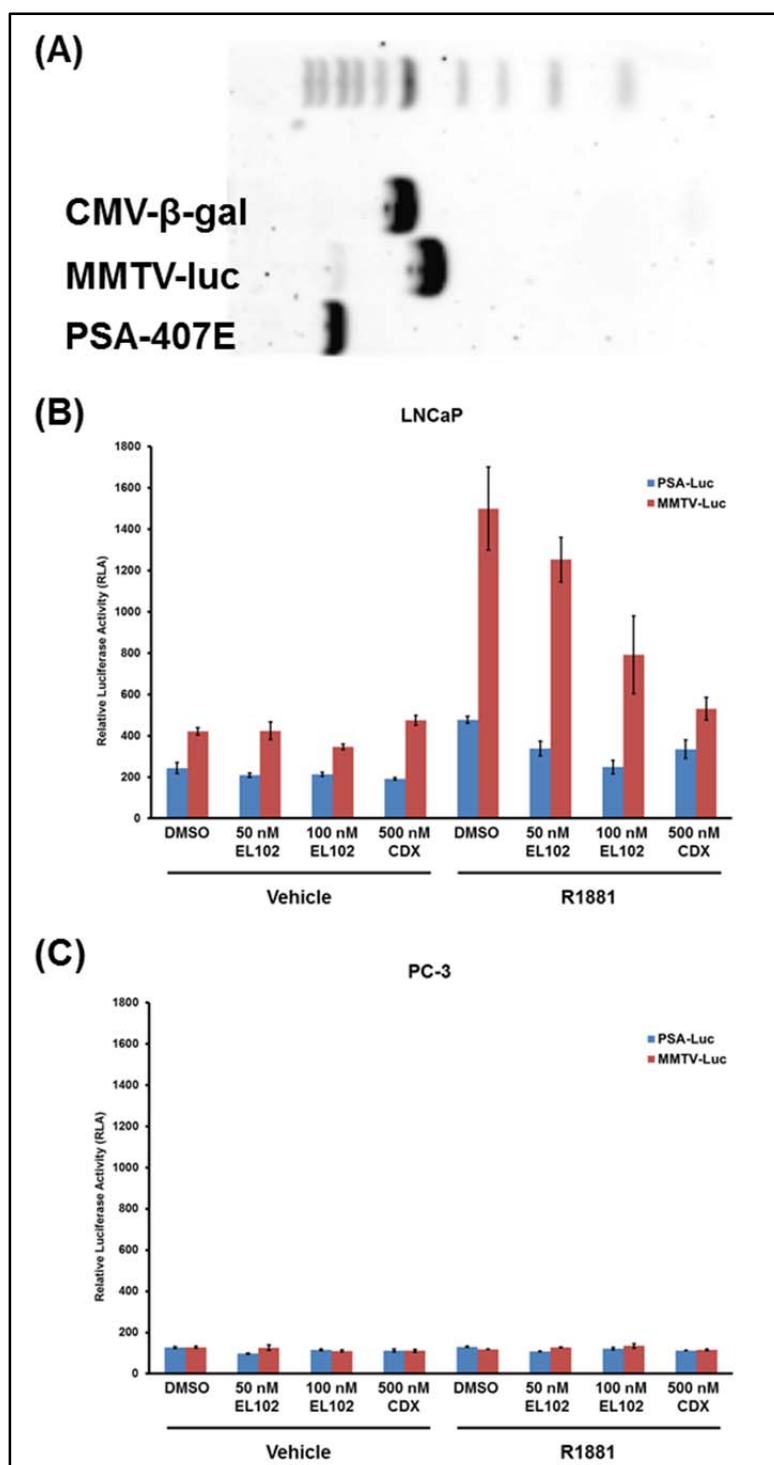


Figure 5.5 – Reporter gene assay of endogenous AR activation in response to EL102 antagonism. (A) BamHI restriction digests of maxiprep purified plasmids PSA-407E-luc, MMTV-luc and CMV- β -gal run in 1 % agarose gel (Gel Red stained) and imaged on gel imager. Luciferase activity normalised to β -gal activity of **(B)** LNCaP and **(C)** PC-3 transiently transfected with reporter constructs PSA-407E-luc or MMTV-luc and CMV- β -gal that were treated for 24 h with DMSO, EL102 or CDX, in the presence or absence of synthetic androgen, R1881 (Error, \pm SEM).

5.2.6 The *In Vitro* Effects of EL102 on AR-Induced CXCR4 Expression and CXCR4-Mediated Migration

Androgen-mediated upregulation of CXCR4 gene expression in LNCaP was observed following qPCR analysis of cells treated for 18 h with 10 nM R1881 and is shown in Figure 5.6 (A). In order to determine if, through its capacity as an AR antagonist, EL102 could affect the resulting increased CXCR4-mediated migration which had been previously reported (Frigo *et al.*, 2009), a migration assay was carried out observing the changes in migratory potential of LNCaP towards chemo-attractant CXCL12 (SDF1 α) in the presence or absence of 1 nM R1881. As shown in Figure 5.6 (B), with the exception of EL102 (100 nM) treated-cells there is little difference between the potentials of vehicle-treated LNCaP cells migrating towards FBS (10 %) and of those migrating towards SDF1 α (400 ng ml⁻¹) over a 52 h incubation. Figure 5.6 (C) indicates that in the presence of androgen, though there is a slight decline in movement of cells toward SDF upon EL102 (50 nM and 100 nM) exposure, when compared to that of the compound-free, untreated control, migration still occurs in a pattern consistent with untreated cells moving toward FBS. The greatest reduction in migration in the presence of androgen is seen in the cells treated with 500 nM CDX.

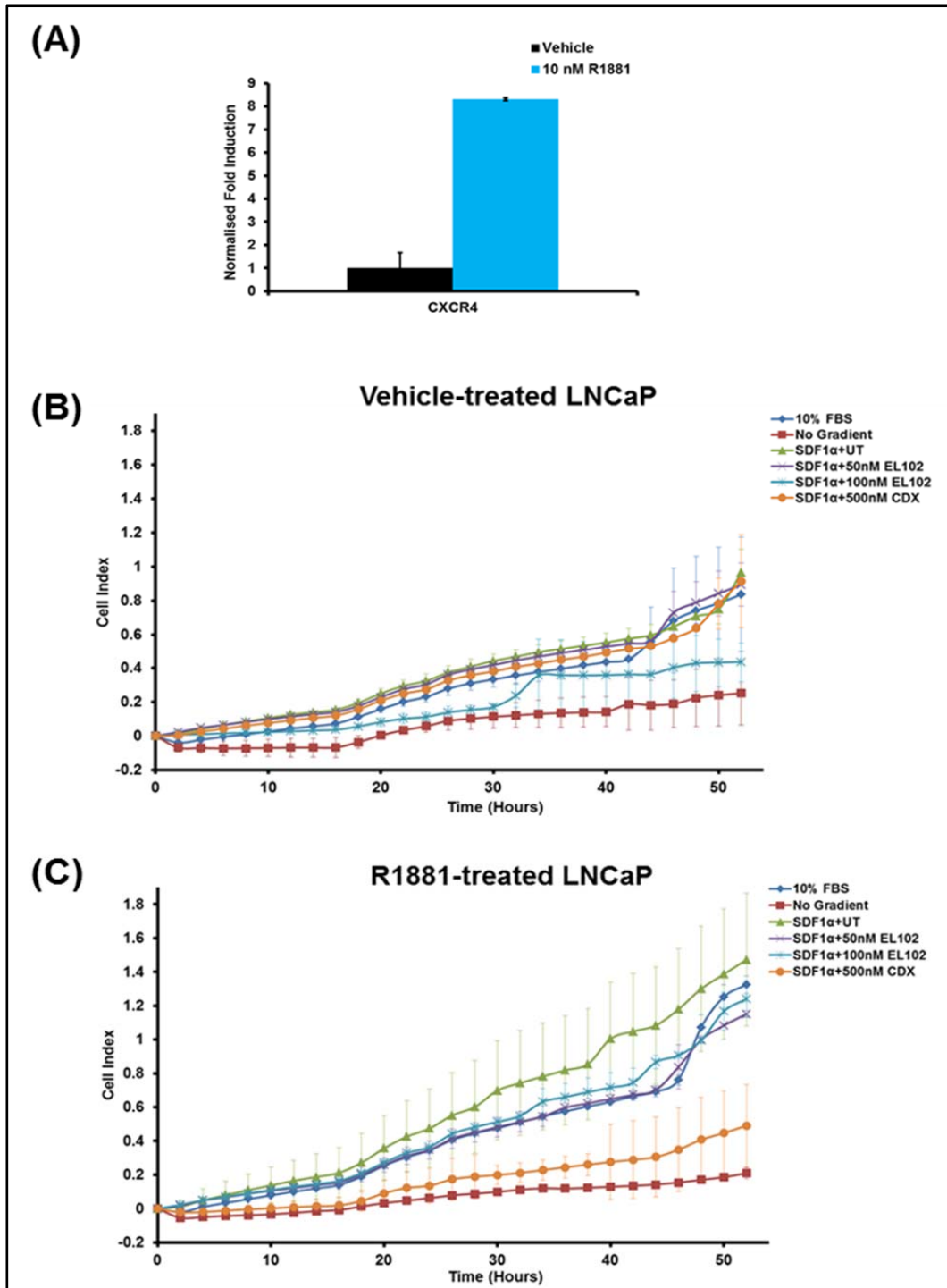


Figure 5.6 – Analysis of CXCR4 expression and function in response to EL102 treatment *in vitro*. **(A)** The levels of CXCR4 gene transcript fold induction in LNCaP cells following 18 h EL102 treatment in the presence or absence of 10 nM R1881. **(B)** Real-time analysis of LNCaP cell migration over 52 h towards CXCL12 (SDF1 α ; 400 ng ml⁻¹) in the presence of vehicle (ethanol) and EL102 or CDX treatments. **(C)** Real-time analysis of LNCaP cell migration over 52 h towards CXCL12 (SDF1 α ; 400 ng ml⁻¹) in the presence of 1 nM R1881 following EL102 or CDX treatments.

5.3 Discussion

5.3.1 EL102 Inhibits the Binding of Androgen and Progesterone to AR and PR, Respectively, in a Cell-Free Assay

As witnessed in a cell-free assay, the binding of radiolabelled ligands ($[^3\text{H}]$ methyltrienolone and $[^3\text{H}]$ progesterone) to their cognate receptors, AR and PR, is significantly diminished upon EL102 treatment. Interestingly, both receptors have similar rates of decline in their binding capacity in the presence of this toluidine sulphonamide. This observation was not surprising given the shared homology of the receptors. PR has, in fact, been the subject of much analysis in the field of prostate cancer. In one immunostaining study, it was noted that one third of tissue samples from prostate cancer patients with Gleason grade 3 and 4 exhibited PR expression whereas samples from patients with Gleason grade 5 exhibited an increase of almost 30 % on that. 60 % of the metastatic tumour tissues stained in this study exhibited moderate to strong expression of PR while 54 % of androgen insensitive tumours showed the same. The expression of PR in the normal functioning tissue of the prostate is not abnormal. PR expression is present mostly in the smooth muscle tissue and fibroblasts of the prostatic stroma. Although its precise role is not fully understood, current data seem to indicate that this expression may play a significant part in maintaining the balance of chemokine signalling and thus has a suppressive effect on the migration of prostate cancer from its organ confined state. If this emerging evidence holds true, such inhibition of the PR signalling pathway may be detrimental to the clinical development of EL102 as a therapy for prostate cancer (Yu *et al.*, 2014). On the other hand, the emergence of data that suggest PR mRNA expression is induced by ER α in advanced metastases and may provide a selective advantage to these cells (Bonkhoff *et al.*, 2001). Attenuation of this oestrogen-induced expression may be clinically beneficial.

The fact that EL102 inhibits AR ligand binding may have large implications for the treatment of prostate cancer and may serve to complement already existing anti-androgen therapy. It may also serve as a means of sensitising androgen dependant cells to treatment.

5.3.2 EL102 Inhibits Expression and Activation of AR *In Vitro*

The use of LNCaP as a model of AR signalling has been well-established, globally (Culig, 2003; Kobayashi *et al.*, 2013; Kung & Evans, 2009). The current study has determined that LNCaP is the most resistant cell line in the panel of five prostate cancer cell lines used for this analysis of the *in vitro* effects of EL102. The cell type's resistance may be attributed to the ability of endogenously expressed AR to upregulate MRP4-mediated drug resistance in the cell line as has been reported, previously (Cai *et al.*, 2007). In the current study, evidence is shown of the potential of EL102 to inhibit LNCaP AR expression at both a transcript and a protein expression level. Further evidence of this agent's anti-AR potential was displayed in its effectiveness to induce a blockade of the interaction of endogenously expressed AR with AREs, present in reporter gene constructs of PSA-407E-luc and MMTV-luc.

In our study of EL102, proteomic analysis has shown that the deactivation of AR by EL102 may not be attributed to its function as a MT inhibitor in the way that nocodazole failed to induce a similar pattern of nuclear-localised immunostaining. Interestingly, though nuclear staining of AR was witnessed in EL102-treated cells in the presence of R1881, Western blot data suggest an evenly reduced AR activation detected in the nuclear fractions of protein isolates from LNCaP cells treated with EL102, CDX and VCR. This may indicate a potential role for VCR, as an anti-androgen or, at the very least, that its mechanism of the disruption of MTs differs more from that of nocodazole than that of EL102.

Another utility offered by EL102 in its role as an AR antagonist may be seen in future studies, through reduced potential for androgen-mediated upregulation of cellular HIF1 α . HIF1 α expression has been shown, elsewhere, to upregulate in response to activated AR (Mabjeesh *et al.*, 2003b). Having already determined the HIF1 α -inhibitory role of EL102 in the current study, this AR inhibition, by the compound of interest, may strengthen this effect, adding to its anti-cancer potential.

Previous studies have shown the CXCR4-mediated migration is increased in response to androgens (Frigo *et al.*, 2009). In the current study, EL102 had not appeared to have had a significant effect on this process.

In summary, the compound EL102 demonstrates significant potential as an anti-androgen treatment, based on *in vitro* analyses. Here, it is shown that the level of nuclear-translocated AR protein was decreased by EL102 treatment as were the levels of AR transcript. This was further supported by the observed reduction in activation of endogenous AR upon EL102 treatment, in cells transiently-transfected with ARE-constructs.

Chapter 6:

Final Discussion

6.1 Overview

Drug discovery and development for clinical use can be an exhaustive and expensive process. Advances in computer modelling techniques of 2D- and 3D-QSAR, like those employed in determining the utility of the novel drug class of toluidine sulphonamides, have been instrumental in avoiding such high attrition (Wendt & Cramer, 2008; Wendt *et al.*, 2011b). These and other techniques guide the synthesis of next generation treatments and may help reduce adverse interactions and improve the efficacy of predecessor compounds. While the NCI-60 screening panel is a good biological starting point for the testing of compounds arising from such computational predictions, it is ultimately limited to the arrival at an endpoint wherein the assayed cells are found to be either alive or dead at the given concentration, without any further biological data accrued (Monks *et al.*, 1991; Shoemaker, 2006). Fortunately, EL102 demonstrated initial success in meeting these criteria, within the panel of cell lines assayed, with many of these sensitive to its cytotoxic effects. Among the most affected cancer tissue models tested were those of the prostate, lung, breast, kidney and colon (unpublished data; Figure 1.8 (B)). The aim of this project was to determine whether EL102, of the class of compounds known as toluidine sulphonamides, had potential for the treatment of prostate cancer and if so, to further uncover the mechanisms of action that assist this process through elucidation of the intracellular targets of the small molecule inhibitor. The research presented, here, demonstrates that EL102 is toxic to each of the constituent prostate cancer cell lines of a panel of five, decreasing cell viability by 50 % (IC_{50}) within a concentration dose range of ~20–50 nM. Its potential for use as a single agent was ascertained through *in vitro* and *in vivo* experimentation while also exhibiting efficacy as a companion treatment with docetaxel, in the reduction in tumour mass witnessed. Initial data from the *in vivo* study also indicate EL102 is well-tolerated. Though *in vitro* investigation shows this drug is a MT-destabilising agent, the use of EL102 extends beyond this to roles such as targeting of key survival signalling pathways. For one, drug resistance in the form of MDR1 and BCRP upregulation, a common tumour tissue feature in advanced prostate cancer, did not appear to hinder EL102

cytotoxicity in the models studied (Toner *et al.*, 2013). HIF1 α survival cues and AR signalling were diminished, in cell lines, through EL102 exposure. Combined, all of these aspects make EL102 a prime candidate for further analysis and promote its use particularly as a treatment of prostate cancer.

6.2 HIF1 α Inhibition and MT Disruption in Cancer Treatment

The use of MT depolymerising agents, that also inhibit HIF1, is not a novel concept in cancer treatment. The estradiol derivative 2-methoxyestradiol (2ME2) has been trialled clinically in recent years due, in large part, to the finding that it is well-tolerated upon oral administration (Mabjeesh *et al.*, 2003a). In the current study, pre-clinical *in vivo* investigation has shown the same to be true of EL102 however it is a big leap to suggest that this drug, in its current guise, is a suitable treatment for prostate cancer, given the limited range of knowledge presented, here, on the likely effects of the drug. A good starting point should have been histological analysis of these xenograft tumours, following dosing regimens with EL102 and docetaxel however these tissue samples were not retained upon measurement of their shrinkage. A similar compound in the class of toluidine sulphonamides, known as ELR510444, was examined in studies parallel to that of our drug of interest, at the University of Texas, San Antonio. Like EL102, ELR510444 was found to exhibit anti-MT activity as well as an ability to inhibit HIF1 α , with cell viability assays determining an IC₅₀ of ~30 nM in breast cancer cell MDA-MB-231. This drug, when tested as an individual treatment in MDA-MB-231 murine xenograft models, revealed a similar reduction in tumour volume to that which resulted from EL102 exposure, in the current CWR22-murine study. In the analysis of the MDA-MB-231 mouse model, ELR510444 matched the effects of ABT-751, an anti-mitotic sulphonamide with comparable structure and modes of action (Risinger *et al.*, 2011). Initially, ABT-751 had shown promise in early clinical trials as a combined treatment with docetaxel in patients with metastatic castrate-resistant prostate cancer (mCRPC). It should be noted that a high degree of adverse side-effects, both non-haematological and haematological, was witnessed within this clinical study which has since been terminated (Michels *et al.*, 2010). Clinical trials of ABT-751 treatment in paediatric neuroblastoma that has recurred or is

chemotherapy-unresponsive are currently ongoing (Fox *et al.*, 2014). With similarly acting drugs indicating tentative success, there is certainly a platform for the establishment of MT-destabilisers, such as EL102, for cancer therapy. ABT-751's success to date also highlights the importance of gathering information of a treatment in one disease type to benefit another.

6.3 Castration-Resistance and Chemotherapy-Resistance in Prostate Cancer

This body of work pointed to the various inhibitory roles of EL102 in prostate cancer. Amongst these was the apparent disruption to AR signal transduction. With little difference witnessed in the IC_{50} concentrations determined between cell viability assays of androgen responsive cell line CWR22 and its androgen insensitive progeny, cell line 22Rv1, expression of functional AR did not obviate a weakness to be exploited by EL102 treatment. Equally, the advent of androgen deprivation therapy (ADT) failure, as frequently occurs in prostate cancer progression did not present as an obstacle for treatment. Likewise, the most EL102-resistant of the five prostate cancer cell lines tested was LNCaP, a classic *in vitro* model of functional AR signalling. It may, therefore, be assumed that while the effects of AR signal disruption by EL102 complement its therapeutic profile through multi-vectored chemical assault on vital cancer cell processes, other factors are at work in LNCaP, reducing the potency of the drug. Similarly, if the engagement of this drug in the blockade of AR signals allows for less freely available drug then, logically, a higher concentration could be required to elicit the interaction with other potential targets of its activity. Previous studies have shown that HIF1 α and AR signal in tandem to endure certain stresses. For instance, AR has been shown to increase HIF1 α at both transcriptional and translational levels while conversely, others have demonstrated the promotion of AR transcriptional regulation through the actions of HIF1 α (Boddy *et al.*, 2005; Mabeesh *et al.*, 2003b). Furthermore, mutations within the oxygen-dependent degradation domain of HIF1 α are frequently found in CRPC tumour tissues and have been implicated in augmented treatment resistance (Anastasiadis *et al.*, 2002). EL102 in its dual

inhibitory role as a suppressor of these processes further promotes its development, clinically.

Drug resistance encountered in treatment of prostate cancer patients in the latter disease stages, remains problematic. The emergence of tumours expressing elevated levels of protein efflux pumps, MDR1 (P-gp), MRP1 and BCRP, correlates with a reduction in the therapeutic effects of mainstay treatment, docetaxel (Bhangal *et al.*, 2000; Sanchez *et al.*, 2009; van Brussel *et al.*, 1999). While our studies involved the use of drug resistant squamous lung cell phenotypes, that have been well-documented, prostate cancer equivalents would have, perhaps, strengthened the observation that upregulation of MDR1 had no impact on the mechanism of EL102 *in vitro*. The same is true of the models used to demonstrate how EL102 is not a substrate of BCRP. Incidentally, BCRP-overexpressing cells have been shown to partake in the efflux of androgens. This suggests that eradication of high expressers of BCRP by EL102 may, in fact, have a deleterious effect on the population of cells, allowing those that do not efflux androgens to thrive. One study has implicated Pim1 kinase in the phosphorylation of BCRP and subsequent docetaxel-resistance in prostate cancer (Xie *et al.*, 2008). In the kinase inhibitor screen, carried out by Elara Pharmaceuticals (Chapter 4), the kinase Pim1 was one of those assayed which did not show a decrease in activity upon EL102 exposure. Future investigations should focus on the role if any, that this kinase may play in EL102's drug resistance-circumvention in prostate cancer. It must also be stated that induction of a multi-drug resistance phenotype in the prostate cancer cell lines DU145 and PC-3 is more likely to result from increased MRP1 expression than that of MDR1 (Zalcberg *et al.*, 2000). Although, not directly associated with insensitivity to docetaxel, MRP4 is expressed at significant levels in prostatic tissue and is known to increase upon androgen exposure (Cai *et al.*, 2007; Ho *et al.*, 2008). These data again support the need for future experiments, analysing drug-resistant models specific to prostate cancer.

Also associated with this disease state is a modification of the *beta* tubulin isoform profiles of prostate cancer cells. β III-tubulin upregulation, in particular, is known to be a poor prognostic marker in prostate cancer

progression and is associated with a reduced chemotherapy response (Galletti *et al.*, 2007; Seruga *et al.*, 2011). Although our findings, here, highlight an EL102-directed reduction in the organised expression of overall β -tubulin and acetylated tubulin, it is unknown the extent to which β III-tubulin profiles are reduced. In the study of ELR510444, models of β III-overexpression demonstrated that treatment with this particular toluidine sulphonamide had the ability to circumvent such resistance (Risinger *et al.*, 2011). Perhaps, replication of these experiments with our drug of interest would be a prudent future step.

Even though much work has been done to demystify the mechanisms of drug resistance in prostate cancer, there is still a requirement for further understanding. While the development of cabazitaxel has helped prolong life in those presenting with cancers that are unaffected by docetaxel administration, there often occurs a reduction in the quality of life. Neutropenia is one adverse side-effect of cabazitaxel regimens (de Bono *et al.*, 2010; Sanofi-Aventis, 2010). Perhaps treatments such as EL102 might delay such onset and when used in combination may potentiate the anti-cancer activities of this and other therapeutic agents, facilitating re-evaluation of the dose concentrations.

EL102, as a tubulin inhibitor, may participate in the disruption of AR signal transduction in a manner consistent with others tested. In a study that supports the combined approach of using MT-disruptors during ADT, investigators found that treatment with tubulin destabilisers and polymerisers served to curb AR signalling. Specifically, ligand independent, EGF-mediated activation of AR was perturbed by these MT-targeting agents which sequestered the receptor to the cytosol (Zhu *et al.*, 2010).

6.4 Experimental Critique

While this thesis puts forward the first documented evidence of the therapeutic use of EL102, there is much to be discussed in the way of experimental procedure. Certainly there existed limitations in the current study which were hard to overcome. Firstly, until relatively recently, much of the preliminary data carried out by Elara Pharmaceuticals was not made

available due to its confidential status. Also, the work carried out here was conducted in parallel to the group that worked on the drug ELR510444 without any communication between research teams. While common conclusions about the two toluidine sulphonamides were reached independently, lending credence to the properties outlined, a collaborative effort could have avoided delay of reaching end-points throughout the experimental process.

On a more technical note, with the kinase inhibitor screen of EL102, no replicates were used for each condition ($n=1$). In my opinion, 'hits' from this screen should have been followed through, for further testing. This would have greatly improved the statistical significance of the result, although, it does line up the possibility for further cell-based exploration. Also worth mentioning is that ANKK1, a kinase which has been the focus of many cognitive and behavioural disorders, was observed to have the greatest decrease in activity within the parameters of this assay (Lee *et al.*, 2013; Pan *et al.*, 2015; Yao *et al.*, 2015). This may indicate a potential use for EL102, or future derivatives of EL102, in medical conditions distinct from cancer, although, equally, this may be problematic if found to effect adverse reactions *in vivo*.

The data provided from the screen of radio-labelled ligand binding was central to the establishment of AR investigations. This data also showed a role for EL102 as a disruptor of PR signalling which was not the focus of this study, but may lay the foundations for future experiments.

One unexpected result encountered in the early analysis of EL102 showed that caspase3 activation was not as pronounced as was anticipated, especially in cells treated with docetaxel. Though these data were obtained from several repeats ($n \geq 3$), the fluorogenic substrate used for each replicate was sourced from the same batch which, it has transpired, may not have been stored in a consistently functional freezer. In order to discount this variable, caspase3 assays should be repeated using fresh reagents so as to definitively score the involvement of the enzyme in the apoptosis induction incurred by EL102.

Interestingly, EL102-induced inhibition of HIF1 α , in PC-3, did not appear to produce the expected reduction in the expression levels of its transcriptional targets as is observed in alternate cancer cell lines (Serganova *et al.*, 2011; Zhang *et al.*, 1999). GLUT1 and LDHA gene transcript levels remained relatively low, regardless of hypoxia induction. The same was true for CXCR4 gene expression. As alluded to previously, the part of HIF1 α signalling in prostate development has yet to be clearly described.

Microarray studies of AR-positive prostate cancer *in vitro* models, have determined that androgens positively upregulate the CXCR4 gene, while other studies have demonstrated that this contributes to improved CXCR4-mediated migration (Frigo *et al.*, 2009; Kazmin *et al.*, 2006). When the AR-inhibitory function of EL102 was assessed, in the current study, treatment with the compound did not impinge on this augmented movement of LNCaP cells towards the CXCL12-rich chamber nor were levels of CXCR4 transcript increased. In reviewing the experimental conditions, I have found that an overnight pre-treatment of cells with EL102, in the presence or absence of androgens before their seeding to wells of the migration assay plate, could have been a more worthwhile scientific endeavour. Following this extended pre-treatment, the differences in the cells migratory potentials could have been more obvious than those observed.

6.5 Conclusions

In conclusion, I have reaffirmed that toluidine sulphonamides and in particular, EL102, show early promise for use in the treatment of prostate cancer. In this series of preclinical experiments I have established that EL102 institutes cell death and its mode of action complements a reduction in tumour volume in a CWR22 xenograft mouse model. Furthermore, EL102 appears to enact its effects through the inhibition of HIF1 α and disruption of microtubule stability. EL102 is also capable of circumventing MDR1 and BCRP-mediated drug resistance and can interrupt androgen receptor signal transduction.

Future studies will endeavour uncover the precise molecular targets of these processes by way of *in vitro* and *in vivo* analyses as outlined above.

Chapter 7:

Bibliography

Adashi EY (1994) The climacteric ovary as a functional gonadotropin-driven androgen-producing gland. *Fertility and sterility* **62**: 20-27

Alonso J, Lopez AE, Muelbaier M, Ammenn J, Wendt B, Lewis J, Schultes C, Janssen B. (2012) TOLUIDINE SULFONAMIDES AND THEIR USE. Elara Pharmaceuticals GmbH (Heidelberg, DE), United States.

Anastasiadis AG, Ghafar MA, Salomon L, Vacherot F, Benedit P, Chen MW, Shabsigh A, Burchardt M, Chopin DK, Shabsigh R, Buttyan R (2002) Human hormone-refractory prostate cancers can harbor mutations in the O(2)-dependent degradation domain of hypoxia inducible factor-1alpha (HIF-1alpha). *J Cancer Res Clin Oncol* **128**: 358-362

Antonarakis ES, Eisenberger MA (2013) Phase III trials with docetaxel-based combinations for metastatic castration-resistant prostate cancer: time to learn from past experiences. *Journal of clinical oncology : official journal of the American Society of Clinical Oncology* **31**: 1709-1712

Apostoli AJ, Nicol CJ (2012) PPAR Medicines and Human Disease: The ABCs of It All. *PPAR research* **2012**: 504918

Aragon-Ching JB (2014) Further analysis of PREVAIL: enzalutamide use in chemotherapy-naive men with metastatic castration-resistant prostate cancer. *Asian journal of andrology* **16**: 803-804

Artal-Sanz M, Samara C, Syntichaki P, Tavernarakis N (2006) Lysosomal biogenesis and function is critical for necrotic cell death in *Caenorhabditis elegans*. *The Journal of cell biology* **173**: 231-239

Ash D, Flynn A, Battermann J, de Reijke T, Lavagnini P, Blank L (2000) ESTRO/EAU/EORTC recommendations on permanent seed implantation for localized prostate cancer. *Radiother Oncol* **57**: 315-321

Aumüller G (1979) *Prostate Gland and Seminal Vesicles*, Berlin: Springer-Verlag.

Aus G, Abbou CC, Bolla M, Heidenreich A, Schmid HP, van Poppel H, Wolff J, Zattoni F (2005) EAU guidelines on prostate cancer. *European urology* **48**: 546-551

Bailar JC, 3rd, Mellinger GT, Gleason DF (1966) Survival rates of patients with prostatic cancer, tumor stage, and differentiation--preliminary report. *Cancer chemotherapy reports Part 1* **50**: 129-136

Batson OV (1940) The Function of the Vertebral Veins and Their Role in the Spread of Metastases. *Annals of surgery* **112**: 138-149

Bautista OM, Kusek JW, Nyberg LM, McConnell JD, Bain RP, Miller G, Crawford ED, Kaplan SA, Sihelnik SA, Brawer MK, Lepor H (2003) Study design of the Medical Therapy of Prostatic Symptoms (MTOPS) trial. *Controlled clinical trials* **24**: 224-243

Bellamy WT (1996) P-glycoproteins and multidrug resistance. *Annu Rev Pharmacol Toxicol* **36**: 161-183

Benderra Z, Faussat AM, Sayada L, Perrot JY, Chaoui D, Marie JP, Legrand O (2004) Breast cancer resistance protein and P-glycoprotein in 149 adult acute myeloid leukemias. *Clinical cancer research : an official journal of the American Association for Cancer Research* **10**: 7896-7902

Berthold DR, Pond GR, Soban F, de Wit R, Eisenberger M, Tannock IF (2008) Docetaxel plus prednisone or mitoxantrone plus prednisone for advanced prostate cancer: updated survival in the TAX 327 study. *Journal of clinical oncology : official journal of the American Society of Clinical Oncology* **26**: 242-245

Bhangal G, Halford S, Wang J, Roylance R, Shah R, Waxman J (2000) Expression of the multidrug resistance gene in human prostate cancer. *Urol Oncol* **5**: 118-121

Biedler JL, Riehm H (1970) Cellular resistance to actinomycin D in Chinese hamster cells in vitro: cross-resistance, radioautographic, and cytogenetic studies. *Cancer research* **30**: 1174-1184

Bill-Axelson A, Holmberg L, Ruutu M, Häggman M, Andersson S, Bratell S, Spångberg A, Busch C, Nordling S, Garmo H, Palmgren J, Adami H, Norlén BJ, Johansson J (2005) Radical prostatectomy versus watchful waiting in early prostate cancer. *N Engl J Med* **352**: 1977-1984

Bissery MC, Guenard D, Gueritte-Voegelein F, Lavelle F (1991) Experimental antitumor activity of taxotere (RP 56976, NSC 628503), a taxol analogue. *Cancer research* **51**: 4845-4852

Bissinger R, Modicano P, Frauenfeld L, Lang E, Jacobi J, Faggio C, Lang F (2013) Estramustine-induced suicidal erythrocyte death. *Cell Physiol Biochem* **32**: 1426-1436

Bjurlin MA, Carter HB, Schellhammer P, Cookson MS, Gomella LG, Troyer D, Wheeler TM, Schlossberg S, Penson DF, Taneja SS (2013) Optimization of initial prostate biopsy in clinical practice: sampling, labeling and specimen processing. *The Journal of urology* **189**: 2039-2046

Blackburn CM, Albert A (1959) Effects of 2-methyl-dihydrotestosterone and of testosterone on human pituitary gonadotropin. *The Journal of clinical endocrinology and metabolism* **19**: 603-607

Boddy JL, Fox SB, Han C, Campo L, Turley H, Kanga S, Malone PR, Harris AL (2005) The androgen receptor is significantly associated with vascular endothelial growth factor and hypoxia sensing via hypoxia-inducible factors HIF-1a, HIF-2a, and the prolyl hydroxylases in human prostate cancer. *Clinical cancer research : an official journal of the American Association for Cancer Research* **11**: 7658-7663

Bonkhoff H, Fixemer T, Hunsicker I, Remberger K (2001) Progesterone receptor expression in human prostate cancer: correlation with tumor progression. *Prostate* **48**: 285-291

Bookout AL, Jeong Y, Downes M, Yu R, Evans RM, Mangelsdorf DJ. (2006) Tissue-specific expression patterns of nuclear receptors.

Bostwick DG, Cooner WH, Denis L, Jones GW, Scardino PT, Murphy GP (1992) The association of benign prostatic hyperplasia and cancer of the prostate. *Cancer* **70**: 291-301

Breier A, Gibalova L, Seres M, Barancik M, Sulova Z (2013) New insight into p-glycoprotein as a drug target. *Anti-cancer agents in medicinal chemistry* **13**: 159-170

Broker LE, Kruyt FA, Giaccone G (2005) Cell death independent of caspases: a review. *Clinical cancer research : an official journal of the American Association for Cancer Research* **11**: 3155-3162

Bruland OS, Nilsson S, Fisher DR, Larsen RH (2006) High-linear energy transfer irradiation targeted to skeletal metastases by the alpha-emitter ²²³Ra: adjuvant or alternative to conventional modalities? *Clinical cancer research : an official journal of the American Association for Cancer Research* **12**: 6250s-6257s

Burriss H, Irvin R, Kuhn J, Kalter S, Smith L, Shaffer D, Fields S, Weiss G, Eckardt J, Rodriguez G, *et al.* (1993) Phase I clinical trial of taxotere administered as either a 2-hour or 6-hour intravenous infusion. *Journal of clinical oncology : official journal of the American Society of Clinical Oncology* **11**: 950-958

Buyyounouski MK, Price RA, Jr., Harris EE, Miller R, Tome W, Schefter T, Parsai EI, Konski AA, Wallner PE (2010) Stereotactic body radiotherapy for primary management of early-stage, low- to intermediate-risk prostate cancer: report of the American Society for Therapeutic Radiology and Oncology Emerging Technology Committee. *Int J Radiat Oncol Biol Phys* **76**: 1297-1304

Cai C, Omwancha J, Hsieh CL, Shemshedini L (2007) Androgen induces expression of the multidrug resistance protein gene MRP4 in prostate cancer cells. *Prostate cancer and prostatic diseases* **10**: 39-45

Cande C, Vahsen N, Garrido C, Kroemer G (2004) Apoptosis-inducing factor (AIF): caspase-independent after all. *Cell Death Differ* **11**: 591-595

Cao Y, Eble JM, Moon E, Yuan H, Weitzel DH, Landon CD, Nien CY, Hanna G, Rich JN, Provenzale JM, Dewhirst MW (2013) Tumor cells upregulate normoxic HIF-1alpha in response to doxorubicin. *Cancer research* **73**: 6230-6242

Carew JS, Esquivel JA, 2nd, Espitia CM, Schultes CM, Mulbaier M, Lewis JD, Janssen B, Giles FJ, Nawrocki ST (2012) ELR510444 inhibits tumor growth and angiogenesis by abrogating HIF activity and disrupting microtubules in renal cell carcinoma. *PLoS one* **7**: e31120

Carver BS (2014) Strategies for targeting the androgen receptor axis in prostate cancer. *Drug Discov Today* **19**: 1493-1497

Castro E, Goh CL, Eeles RA (2013) Prostate cancer screening in BRCA and Lynch syndrome mutation carriers. *American Society of Clinical Oncology educational book / ASCO American Society of Clinical Oncology Meeting*

Catalona WJ, Richie JP, Ahmann FR, Hudson MA, Scardino PT, Flanigan RC, deKernion JB, Ratliff TL, Kavoussi LR, Dalkin BL, *et al.* (1994) Comparison of digital rectal examination and serum prostate specific antigen in the early detection of prostate cancer: results of a multicenter clinical trial of 6,630 men. *The Journal of urology* **151**: 1283-1290

Chang CQ, Yesupriya A, Rowell JL, Pimentel CB, Clyne M, Gwinn M, Khoury MJ, Wulf A, Schully SD (2014) A systematic review of cancer GWAS and candidate gene meta-analyses reveals limited overlap but similar effect sizes. *European journal of human genetics : EJHG* **22**: 402-408

Chang KH, Li R, Papari-Zareei M, Watumull L, Zhao YD, Auchus RJ, Sharifi N (2011) Dihydrotestosterone synthesis bypasses testosterone to drive castration-resistant prostate cancer. *Proceedings of the National Academy of Sciences of the United States of America* **108**: 13728-13733

Chang SS (2007) Treatment options for hormone-refractory prostate cancer. *Reviews in urology* **9 Suppl 2**: S13-18

Chen L, Li Y, Yu H, Zhang L, Hou T (2012) Computational models for predicting substrates or inhibitors of P-glycoprotein. *Drug Discov Today* **17**: 343-351

Chodak GW, Krupski TL, Aral IA, Hassan Aziz H, Giasullo M, Gomella LG. (2015) Prostate Cancer. In Kim ED (ed.). Medscape Urology, Vol. 2015, p. Prostate Cancer. Prostate cancer is the most common noncutaneous cancer in men in the United States.

Claessens F, Alen P, Devos A, Peeters B, Verhoeven G, Rombauts W (1996) The androgen-specific probasin response element 2 interacts differentially with androgen and glucocorticoid receptors. *The Journal of biological chemistry* **271**: 19013-19016

Claessens F, Denayer S, Van Tilborgh N, Kerkhofs S, Helsen C, Haelens A (2008) Diverse roles of androgen receptor (AR) domains in AR-mediated signaling. *NRS* **6**

Clegg NJ, Wongvipat J, Joseph JD, Tran C, Ouk S, Dilhas A, Chen Y, Grillot K, Bischoff ED, Cai L, Aparicio A, Dorow S, Arora V, Shao G, Qian J, Zhao H, Yang G, Cao C, Sensintaffar J, Wasielewska T, Herbert MR, Bonnefous C, Darimont B, Scher HI, Smith-Jones P, Klang M, Smith ND, De Stanchina E, Wu N, Ouerfelli O, Rix PJ, Heyman RA, Jung ME, Sawyers CL, Hager JH (2012) ARN-509: a novel antiandrogen for prostate cancer treatment. *Cancer research* **72**: 1494-1503

Clynes M, Redmond A, Moran E, Gilvarry U (1992) Multiple drug-resistance in variant of a human non-small cell lung carcinoma cell line, DLKP-A. *Cytotechnology* **10**: 75-89

Coffey DS, Pienta KJ (1987) New concepts in studying the control of normal and cancer growth of the prostate. *Progress in clinical and biological research* **239**: 1-73

Collin M, Geunard D, Geuritte-Voegelein F, Poitier P. (1989a) Process for the preparation of taxol and 10-deacetyltaxol. In Sante R-P (ed.), US.

Collin M, Geunard D, Geuritte-Voegelein F, Poitier P. (1989b) Taxol derivatives, their preparation and pharmaceutical compositions containing them. In Sante R-P (ed.), US.

Consortium (1999) A unified nomenclature system for the nuclear receptor superfamily. *Cell* **97**: 161-163

Cooperberg MR, Freedland SJ, Pasta DJ, Elkin EP, Presti JC, Jr., Amling CL, Terris MK, Aronson WJ, Kane CJ, Carroll PR (2006) Multiinstitutional validation of the UCSF cancer of the prostate risk assessment for prediction of recurrence after radical prostatectomy. *Cancer* **107**: 2384-2391

Cooperberg MR, Pasta DJ, Elkin EP, Litwin MS, Latini DM, Du Chane J, Carroll PR (2005) The University of California, San Francisco Cancer of the Prostate Risk Assessment score: a straightforward and reliable preoperative predictor of disease recurrence after radical prostatectomy. *The Journal of urology* **173**: 1938-1942

Culig Z (2003) Role of the androgen receptor axis in prostate cancer. *Urology* **62**: 21-26

Culine S, Kattan J, Zanetta S, Theodore C, Fizazi K, Droz JP (1998) Evaluation of estramustine phosphate combined with weekly doxorubicin in patients with androgen-independent prostate cancer. *American journal of clinical oncology* **21**: 470-474

D'Amico AV, Whittington R, Malkowicz SB, Schultz D, Blank K, Broderick GA, Tomaszewski JE, Renshaw AA, Kaplan I, Beard CJ, Wein A (1998) Biochemical outcome after radical prostatectomy, external beam radiation therapy, or interstitial radiation therapy for clinically localized prostate cancer. *JAMA : the journal of the American Medical Association* **280**: 969-974

Dachs GU, Steele AJ, Coralli C, Kanthou C, Brooks AC, Gunningham SP, Currie MJ, Watson AI, Robinson BA, Tozer GM (2006) Anti-vascular agent Combretastatin A-4-P modulates hypoxia inducible factor-1 and gene expression. *BMC Cancer* **6**: 280

Dahut WL, Madan RA, Karakunnel JJ, Adelberg D, Gulley JL, Turkbey IB, Chau CH, Spencer SD, Mulquin M, Wright J, Parnes HL, Steinberg SM, Choyke PL, Figg WD (2013) Phase II clinical trial of cediranib in patients with metastatic castration-resistant prostate cancer. *BJU international* **111**: 1269-1280

Darshan MS, Loftus MS, Thadani-Mulero M, Levy BP, Escuin D, Zhou XK, Gjyrezi A, Chanel-Vos C, Shen R, Tagawa ST, Bander NH, Nanus DM, Giannakakou P (2011) Taxane-induced blockade to nuclear accumulation of the androgen receptor predicts clinical responses in metastatic prostate cancer. *Cancer research* **71**: 6019-6029

Datta K, Muders M, Zhang H, Tindall DJ (2010) Mechanism of lymph node metastasis in prostate cancer. *Future Oncol* **6**: 823-836

Davison SL, Bell R (2006) Androgen physiology. *Seminars in reproductive medicine* **24**: 71-77

de Bono JS, Logothetis CJ, Molina A, Fizazi K, North S, Chu L, Chi KN, Jones RJ, Goodman OB, Jr., Saad F, Staffurth JN, Mainwaring P, Harland S, Flaig TW, Hutson TE, Cheng T, Patterson H, Hainsworth JD, Ryan CJ, Sternberg CN, Ellard SL, Flechon A, Saleh M, Scholz M, Efstathiou E, Zivi A, Bianchini D, Loriot Y, Chieffo N, Kheoh T, Haqq CM, Scher HI (2011) Abiraterone and increased survival in metastatic prostate cancer. *The New England journal of medicine* **364**: 1995-2005

de Bono JS, Oudard S, Ozguroglu M, Hansen S, Machiels JP, Kocak I, Gravis G, Bodrogi I, Mackenzie MJ, Shen L, Roessner M, Gupta S, Sartor AO (2010) Prednisone plus cabazitaxel or mitoxantrone for metastatic castration-resistant prostate cancer progressing after docetaxel treatment: a randomised open-label trial. *Lancet* **376**: 1147-1154

De Marzo AM, Platz EA, Sutcliffe S, Xu J, Gronberg H, Drake CG, Nakai Y, Isaacs WB, Nelson WG (2007) Inflammation in prostate carcinogenesis. *Nature reviews Cancer* **7**: 256-269

de Ruiter PE, Teuwen R, Trapman J, Dijkema R, Brinkmann AO (1995) Synergism between androgens and protein kinase-C on androgen-regulated gene expression. *Mol Cell Endocrinol* **110**: R1-6

deKernion JB, Lindner A (1984) Chemotherapy of hormonally unresponsive prostatic carcinoma. *The Urologic clinics of North America* **11**: 319-326

DeMuelenaere GF, Sandison AG (1976) Treatment of locally advanced prostatic carcinoma. *The British journal of radiology* **49**: 944-947

Doehn C, Sommerauer M, Jocham D (2006) Drug evaluation: Degarelix--a potential new therapy for prostate cancer. *Idrugs* **9**: 565-572

Domingo-Domenech J, Oliva C, Rovira A, Codony-Servat J, Bosch M, Filella X, Montagut C, Tapia M, Campas C, Dang L, Rolfe M, Ross JS, Gascon P, Albanell J, Mellado B (2006) Interleukin 6, a nuclear factor-kappaB target, predicts resistance to docetaxel in hormone-independent prostate cancer and nuclear factor-kappaB inhibition by PS-1145 enhances docetaxel antitumor activity. *Clinical cancer research : an official journal of the American Association for Cancer Research* **12**: 5578-5586

Douros J, Suffness M (1981) New natural products under development at the National Cancer Institute. *Recent results in cancer research Fortschritte der Krebsforschung Progres dans les recherches sur le cancer* **76**: 153-175

Doyle LA, Yang W, Abruzzo LV, Krogmann T, Gao Y, Rishi AK, Ross DD (1998) A multidrug resistance transporter from human MCF-7 breast cancer cells. *Proceedings of the National Academy of Sciences of the United States of America* **95**: 15665-15670

Duellman SJ, Calaoagan JM, Sato BG, Fine R, Klebansky B, Chao WR, Hobbs P, Collins N, Sambucetti L, Laderoute KR (2010) A novel steroidal inhibitor of estrogen-related receptor alpha (ERR alpha). *Biochemical pharmacology* **80**: 819-826

Dunzendorfer U, Feller H (1981) The effect of alpha-difluoromethylornithine and tartaric acid on sperm count, seminal gamma GT, FSH, LH, testosterone and steroid excretion in patients with chronic prostatitis. *Andrologia* **13**: 100-107

Durk MR, Chan GN, Campos CR, Peart JC, Chow EC, Lee E, Cannon RE, Bendayan R, Miller DS, Pang KS (2012) 1alpha,25-Dihydroxyvitamin D3-liganded vitamin D receptor increases expression and transport activity of P-glycoprotein in isolated rat brain capillaries and human and rat brain microvessel endothelial cells. *Journal of neurochemistry* **123**: 944-953

Edwards J, Traynor P, Munro AF, Pirret CF, Dunne B, Bartlett JM (2006) The role of HER1-HER4 and EGFRvIII in hormone-refractory prostate cancer. *Clinical cancer research : an official journal of the American Association for Cancer Research* **12**: 123-130

Eisermann K, Wang D, Jing Y, Pascal LE, Wang Z (2013) Androgen receptor gene mutation, rearrangement, polymorphism. *Translational andrology and urology* **2**: 137-147

Engel JB, Schally AV (2007) Drug Insight: clinical use of agonists and antagonists of luteinizing-hormone-releasing hormone. *Nature clinical practice Endocrinology & metabolism* **3**: 157-167

Engelman JA, Zejnullahu K, Mitsudomi T, Song Y, Hyland C, Park JO, Lindeman N, Gale CM, Zhao X, Christensen J, Kosaka T, Holmes AJ, Rogers AM, Cappuzzo F, Mok T, Lee C, Johnson BE, Cantley LC, Janne PA (2007) MET amplification leads to gefitinib resistance in lung cancer by activating ERBB3 signaling. *Science* **316**: 1039-1043

Epstein JI, Allsbrook WC, Jr., Amin MB, Egevad LL (2005) The 2005 International Society of Urological Pathology (ISUP) Consensus Conference on Gleason Grading of Prostatic Carcinoma. *The American journal of surgical pathology* **29**: 1228-1242

Extra JM, Rousseau F, Bruno R, Clavel M, Le Bail N, Marty M (1993) Phase I and pharmacokinetic study of Taxotere (RP 56976; NSC 628503) given as a short intravenous infusion. *Cancer research* **53**: 1037-1042

Fabbri F, Amadori D, Carloni S, Brigliadori G, Tesei A, Ulivi P, Rosetti M, Vannini I, Arienti C, Zoli W, Silvestrini R (2008) Mitotic catastrophe and apoptosis induced by docetaxel in hormone-refractory prostate cancer cells. *J Cell Physiol* **217**: 494-501

Fellows GJ, Clark PB, Beynon LL, Boreham J, Keen C, Parkinson MC, Peto R, Webb JN (1992) Treatment of advanced localised prostatic cancer by orchiectomy, radiotherapy, or combined treatment. A Medical Research Council Study. Urological Cancer Working Party--Subgroup on Prostatic Cancer. *British journal of urology* **70**: 304-309

Ferrero JM, Chamorey E, Oudard S, Dides S, Lesbats G, Cavaglione G, Nouyrigat P, Foa C, Kaphan R (2006) Phase II trial evaluating a docetaxel-capecitabine combination as treatment for hormone-refractory prostate cancer. *Cancer* **107**: 738-745

Folkman J (2007) Angiogenesis: an organizing principle for drug discovery? *Nature reviews Drug discovery* **6**: 273-286

Fox E, Mosse YP, Meany HM, Gurney JG, Khanna G, Jackson HA, Gordon G, Shusterman S, Park JR, Cohn SL, Adamson PC, London WB, Maris JM, Balis FM (2014) Time to disease progression in children with relapsed or refractory neuroblastoma treated with ABT-751: a

report from the Children's Oncology Group (ANBL0621). *Pediatric blood & cancer* **61**: 990-996

Frame FM, Maitland NJ (2011) Cancer stem cells, models of study and implications of therapy resistance mechanisms. *Advances in experimental medicine and biology* **720**: 105-118

Frigo DE, Sherk AB, Wittmann BM, Norris JD, Wang Q, Joseph JD, Toner AP, Brown M, McDonnell DP (2009) Induction of Kruppel-like factor 5 expression by androgens results in increased CXCR4-dependent migration of prostate cancer cells in vitro. *Mol Endocrinol* **23**: 1385-1396

Galletti E, Magnani M, Renzulli ML, Botta M (2007) Paclitaxel and docetaxel resistance: molecular mechanisms and development of new generation taxanes. *ChemMedChem* **2**: 920-942

Garcia JA, Hutson TE, Shepard D, Elson P, Dreicer R (2011) Gemcitabine and docetaxel in metastatic, castrate-resistant prostate cancer: results from a phase 2 trial. *Cancer* **117**: 752-757

Gewirtz DA (1999) A critical evaluation of the mechanisms of action proposed for the antitumor effects of the anthracycline antibiotics adriamycin and daunorubicin. *Biochemical pharmacology* **57**: 727-741

Gleason DF (1977) *Urologic Pathology: The Prostate*, Philadelphia: Lea and Febiger.

Goldstein AS, Lawson DA, Cheng D, Sun W, Garraway IP, Witte ON (2008) Trop2 identifies a subpopulation of murine and human prostate basal cells with stem cell characteristics. *Proceedings of the National Academy of Sciences of the United States of America* **105**: 20882-20887

Goodman J, Walsh V (2001) *The story of taxol : nature and politics in the pursuit of an anti-cancer drug*, Cambridge ; New York: Cambridge University Press.

Gottesman MM, Fojo T, Bates SE (2002) Multidrug resistance in cancer: role of ATP-dependent transporters. *Nat Rev Cancer* **2**: 48-58

Grabstald H, Elliott JL (1953) Transrectal biopsy of the prostate. *J Am Med Assoc* **153**: 563-565

Graff JN, Chamberlain ED (2015) Sipuleucel-T in the treatment of prostate cancer: an evidence-based review of its place in therapy. *Core evidence* **10**: 1-10

Greenberger LM, Horak ID, Filpula D, Sapra P, Westergaard M, Frydenlund HF, Albaek C, Schroder H, Orum H (2008) A RNA antagonist of hypoxia-inducible factor-1alpha, EZN-2968, inhibits tumor cell growth. *Mol Cancer Ther* **7**: 3598-3608

Greenlee RT, Hill-Harmon MB, Murray T, Thun M (2001) Cancer statistics, 2001. *CA Cancer J Clin* **51**: 15-36

Gronemeyer H (1992) Control of transcription activation by steroid hormone receptors. *FASEB J* **6**: 2524-2529

Grugni M, Cassin M, Colella G, De MS, Pardi G, Pavesi P. (2006) Indole derivatives with antitumor activity. Google Patents.

Guillonneau B, Vallancien G (2000) Laproscopic Radical Prostatectomy: The Montsouris Technique. *The Journal of urology* **163**: 1643-1649

Haiman CA, Han Y, Feng Y, Xia L, Hsu C, Sheng X, Pooler LC, Patel Y, Kolonel LN, Carter E, Park K, Le Marchand L, Van Den Berg D, Henderson BE, Stram DO (2013) Genome-wide testing of putative functional exonic variants in relationship with breast and prostate cancer risk in a multiethnic population. *PLoS Genet* **9**: e1003419

Heenan M, Kavanagh K, Redmond A, Maher M, Dolan E, O'Neill P, Moriarty M, Clynes M (1996) Absence of correlation between chemo- and radioresistance in a range of human tumour cell lines. *Cytotechnology* **19**: 237-242

Heenan M, O'Driscoll L, Cleary I, Connolly L, Clynes M (1997) Isolation from a human MDR lung cell line of multiple clonal subpopulations which exhibit significantly different drug resistance. *Int J Cancer* **71**: 907-915

Heidegger I, Massoner P, Eder IE, Pircher A, Pichler R, Aigner F, Bektic J, Horninger W, Klocker H (2013) Novel therapeutic approaches for the treatment of castration-resistant prostate cancer. *J Steroid Biochem Mol Biol* **138C**: 248-256

Henriksen G, Breistol K, Bruland OS, Fodstad O, Larsen RH (2002) Significant antitumor effect from bone-seeking, alpha-particle-emitting (223)Ra demonstrated in an experimental skeletal metastases model. *Cancer research* **62**: 3120-3125

Hernes EH, Fossa SD, Vaage S, Ogreid P, Heilo A, Paus E (1997) Epirubicin combined with estramustine phosphate in hormone-resistant prostate cancer: a phase II study. *Br J Cancer* **76**: 93-99

Hewitson KS, McNeill LA, Riordan MV, Tian YM, Bullock AN, Welford RW, Elkins JM, Oldham NJ, Bhattacharya S, Gleadle JM, Ratcliffe PJ, Pugh CW, Schofield CJ (2002) Hypoxia-inducible

factor (HIF) asparagine hydroxylase is identical to factor inhibiting HIF (FIH) and is related to the cupin structural family. *The Journal of biological chemistry* **277**: 26351-26355

Ho LL, Kench JG, Handelsman DJ, Scheffer GL, Stricker PD, Grygiel JG, Sutherland RL, Henshall SM, Allen JD, Horvath LG (2008) Androgen regulation of multidrug resistance-associated protein 4 (MRP4/ABCC4) in prostate cancer. *Prostate* **68**: 1421-1429

Holmes FA, Walters RS, Theriault RL, Forman AD, Newton LK, Raber MN, Buzdar AU, Frye DK, Hortobagyi GN (1991) Phase II trial of taxol, an active drug in the treatment of metastatic breast cancer. *Journal of the National Cancer Institute* **83**: 1797-1805

Horoszewicz JS, Leong SS, Chu TM, Wajsman ZL, Friedman M, Papsidero L, Kim U, Chai LS, Kakati S, Arya SK, Sandberg AA (1980) The LNCaP cell line--a new model for studies on human prostatic carcinoma. *Progress in clinical and biological research* **37**: 115-132

Hua VN, Schaeffer AJ (2004) Acute and chronic prostatitis. *The Medical clinics of North America* **88**: 483-494

Huang X, Zhou J, Liu J, Tang B, Zhao F, Qu Y (2014) Biological characteristics of prostate cancer cells are regulated by hypoxia-inducible factor 1alpha. *Oncology letters* **8**: 1217-1221

Hudson CC, Liu M, Chiang GG, Otterness DM, Loomis DC, Kaper F, Giaccia AJ, Abraham RT (2002) Regulation of hypoxia-inducible factor 1alpha expression and function by the mammalian target of rapamycin. *Molecular and cellular biology* **22**: 7004-7014

Huggins C, Hodges CV (1941) Studies on Prostatic Cancer: I. The Effect of Castration, of Estrogen and of Androgen Injection on Serum Phosphatases in Metastatic Carcinoma of the Prostate. *Cancer research* **167**: 293-297

Huggins CB (1947) Diagnosis and treatment of cancer of the prostate. *Marquette medical review* **12**: 213-215

Hussar DA, Daniels WL (2010) New drugs: Sipuleucel-T, cabazitaxel, and collagenase clostridium histolyticum. *Journal of the American Pharmacists Association : JAPhA* **50**: 772-775

Ivan M, Kondo K, Yang H, Kim W, Valiando J, Ohh M, Salic A, Asara JM, Lane WS, Kaelin WG, Jr. (2001) HIF1alpha targeted for VHL-mediated destruction by proline hydroxylation: implications for O2 sensing. *Science* **292**: 464-468

Iwai K, Yamanaka K, Kamura T, Minato N, Conaway RC, Conaway JW, Klausner RD, Pause A (1999) Identification of the von Hippel-lindau tumor-suppressor protein as part of an active

E3 ubiquitin ligase complex. *Proceedings of the National Academy of Sciences of the United States of America* **96**: 12436-12441

Jaakkola P, Mole DR, Tian YM, Wilson MI, Gielbert J, Gaskell SJ, von Kriegsheim A, Hebestreit HF, Mukherji M, Schofield CJ, Maxwell PH, Pugh CW, Ratcliffe PJ (2001) Targeting of HIF- α to the von Hippel-Lindau ubiquitylation complex by O₂-regulated prolyl hydroxylation. *Science* **292**: 468-472

Jackson JR, Patrick DR, Dar MM, Huang PS (2007) Targeted anti-mitotic therapies: can we improve on tubulin agents? *Nature reviews Cancer* **7**: 107-117

Jaffray DA, Yan D, Wong JW (1999) Managing geometric uncertainty in conformal intensity-modulated radiation therapy. *Semin Radiat Oncol* **9**: 4-19

Janvilisri T, Venter H, Shahi S, Reuter G, Balakrishnan L, van Veen HW (2003) Sterol transport by the human breast cancer resistance protein (ABCG2) expressed in *Lactococcus lactis*. *The Journal of biological chemistry* **278**: 20645-20651

Jarman M, Barrie SE, Llera JM (1998) The 16,17-double bond is needed for irreversible inhibition of human cytochrome p45017 α by abiraterone (17-(3-pyridyl)androsta-5, 16-dien-3 β -ol) and related steroidal inhibitors. *Journal of medicinal chemistry* **41**: 5375-5381

Jemal A, Bray F, Center MM, Ferlay J, Ward E, Forman D (2011) Global cancer statistics. *CA Cancer J Clin* **61**: 69-90

Jian-Xin D, Mark M, Photon R. (2006) Lonidamine analogs. Google Patents.

Jiang BH, Jiang G, Zheng JZ, Lu Z, Hunter T, Vogt PK (2001) Phosphatidylinositol 3-kinase signaling controls levels of hypoxia-inducible factor 1. *Cell Growth Differ* **12**: 363-369

Jones HE, Goddard L, Gee JM, Hiscox S, Rubini M, Barrow D, Knowlden JM, Williams S, Wakeling AE, Nicholson RI (2004) Insulin-like growth factor-I receptor signalling and acquired resistance to gefitinib (ZD1839; Iressa) in human breast and prostate cancer cells. *Endocr Relat Cancer* **11**: 793-814

Kahl P, Gullotti L, Heukamp LC, Wolf S, Friedrichs N, Vorreuther R, Solleder G, Bastian PJ, Ellinger J, Metzger E, Schule R, Buettner R (2006) Androgen receptor coactivators lysine-specific histone demethylase 1 and four and a half LIM domain protein 2 predict risk of prostate cancer recurrence. *Cancer research* **66**: 11341-11347

Kaighn ME, Lechner JF, Narayan KS, Jones LW (1978) Prostate carcinoma: tissue culture cell lines. *National Cancer Institute monograph*: 17-21

Kallio PJ, Wilson WJ, O'Brien S, Makino Y, Poellinger L (1999) Regulation of the hypoxia-inducible transcription factor 1 α by the ubiquitin-proteasome pathway. *The Journal of biological chemistry* **274**: 6519-6525

Kantoff PW, Higano CS, Shore ND, Berger ER, Small EJ, Penson DF, Redfern CH, Ferrari AC, Dreicer R, Sims RB, Xu Y, Frohlich MW, Schellhammer PF (2010) Sipuleucel-T immunotherapy for castration-resistant prostate cancer. *The New England journal of medicine* **363**: 411-422

Kaplan SA, McConnell JD, Rohrborn CG, Meehan AG, Lee MW, Noble WR, Kusek JW, Nyberg LM, Jr. (2006) Combination therapy with doxazosin and finasteride for benign prostatic hyperplasia in patients with lower urinary tract symptoms and a baseline total prostate volume of 25 ml or greater. *The Journal of urology* **175**: 217-220; discussion 220-211

Karki R, Mariani M, Andreoli M, He S, Scambia G, Shahabi S, Ferlini C (2013) β III-Tubulin: biomarker of taxane resistance or drug target? *Expert Opinion on Therapeutic Targets* **17**: 461-472

Kattan MW, Eastham JA, Stapleton AM, Wheeler TM, Scardino PT (1998) A preoperative nomogram for disease recurrence following radical prostatectomy for prostate cancer. *Journal of the National Cancer Institute* **90**: 766-771

Kattan MW, Potters L, Blasko JC, Beyer DC, Fearn P, Cavanagh W, Leibel S, Scardino PT (2001) Pretreatment nomogram for predicting freedom from recurrence after permanent prostate brachytherapy in prostate cancer. *Urology* **58**: 393-399

Kattan MW, Zelefsky MJ, Kupelian PA, Scardino PT, Fuks Z, Leibel SA (2000) Pretreatment nomogram for predicting the outcome of three-dimensional conformal radiotherapy in prostate cancer. *Journal of clinical oncology : official journal of the American Society of Clinical Oncology* **18**: 3352-3359

Kazmin D, Prytkova T, Cook CE, Wolfinger R, Chu TM, Beratan D, Norris JD, Chang CY, McDonnell DP (2006) Linking ligand-induced alterations in androgen receptor structure to differential gene expression: a first step in the rational design of selective androgen receptor modulators. *Mol Endocrinol* **20**: 1201-1217

Keenan J, Joyce H, Aherne S, O'Dea S, Doolan P, Lynch V, Clynes M (2012) Olfactomedin III expression contributes to anoikis-resistance in clonal variants of a human lung squamous carcinoma cell line. *Exp Cell Res* **318**: 593-602

Kikuno N, Urakami S, Nakamura S, Hiraoka T, Hyuga T, Arichi N, Wake K, Sumura M, Yoneda T, Kishi H, Shigeno K, Shiina H, Igawa M (2007) Phase-II study of docetaxel, estramustine

phosphate, and carboplatin in patients with hormone-refractory prostate cancer. *European urology* **51**: 1252-1258

Kim Y, Kislinger T (2013) Novel approaches for the identification of biomarkers of aggressive prostate cancer. *Genome medicine* **5**: 56

Kobayashi T, Inoue T, Kamba T, Ogawa O (2013) Experimental evidence of persistent androgen-receptor-dependency in castration-resistant prostate cancer. *Int J Mol Sci* **14**: 15615-15635

Koivisto P, Kononen J, Palmberg C, Tammela T, Hyytinen E, Isola J, Trapman J, Cleutjens K, Noordzij A, Visakorpi T, Kallioniemi OP (1997) Androgen receptor gene amplification: a possible molecular mechanism for androgen deprivation therapy failure in prostate cancer. *Cancer research* **57**: 314-319

Kolvenbag GJ, Furr BJ, Blackledge GR (1998) Receptor affinity and potency of non-steroidal antiandrogens: translation of preclinical findings into clinical activity. *Prostate cancer and prostatic diseases* **1**: 307-314

Kramer G, Schwarz S, Hagg M, Havelka AM, Linder S (2006) Docetaxel induces apoptosis in hormone refractory prostate carcinomas during multiple treatment cycles. *Br J Cancer* **94**: 1592-1598

Krishnamurthy P, Ross DD, Nakanishi T, Bailey-Dell K, Zhou S, Mercer KE, Sarkadi B, Sorrentino BP, Schuetz JD (2004) The stem cell marker Bcrp/ABCG2 enhances hypoxic cell survival through interactions with heme. *The Journal of biological chemistry* **279**: 24218-24225

Kumar S, Joshi KS, Deore V, Bhonde MR, Yewalkar NN, Padgaonkar AA, Rathos MJ, Kulkarni-Almeida AA, Parikh S, Dagia NM. (2009) Pyridyl derivatives, their preparation and use. Google Patents.

Kumar VL, Majumder PK (1995) Prostate gland: structure, functions and regulation. *International urology and nephrology* **27**: 231-243

Kung AL, Zabludoff SD, France DS, Freedman SJ, Tanner EA, Vieira A, Cornell-Kennon S, Lee J, Wang B, Wang J, Memmert K, Naegeli HU, Petersen F, Eck MJ, Bair KW, Wood AW, Livingston DM (2004) Small molecule blockade of transcriptional coactivation of the hypoxia-inducible factor pathway. *Cancer Cell* **6**: 33-43

Kung HJ, Evans CP (2009) Oncogenic activation of androgen receptor. *Urol Oncol* **27**: 48-52

Laderoute KR, Calaoagan JM, Chao WR, Peters RH, Hobbs PD, Tanabe M, Amin K. (2006) Method and composition for inhibiting cell proliferation and angiogenesis. Google Patents.

Laudet V, Gronemeyer H (2002) General organization of nuclear receptors. . In *The Nuclear Receptor FactsBook*. Academic Press

Law E, Gilvarry U, Lynch V, Gregory B, Grant G, Clynes M (1992) Cytogenetic comparison of two poorly differentiated human lung squamous cell carcinoma lines. *Cancer Genet Cytogenet* **59**: 111-118

Lawton C, Won M, Pilepich M, Asbell S, Shipley W, Hanks G, Cox J, Perez C, Sause W, Doggett S, al e (1991) Long-term treatment sequelae following external beam irradiation for adenocarcinoma of the prostate: analysis of RTOG studies 7506 and 7706. *Int J Radiat Oncol Biol Phys* **21**: 935-939

Lee K, Belinsky MG, Bell DW, Testa JR, Kruh GD (1998) Isolation of MOAT-B, a widely expressed multidrug resistance-associated protein/canalicular multispecific organic anion transporter-related transporter. *Cancer research* **58**: 2741-2747

Lee SH, Lee BH, Lee JS, Chai YG, Choi MR, Han DM, Ji H, Jang GH, Shin HE, Choi IG (2013) The association of DRD2 -141C and ANKK1 TaqIA polymorphisms with alcohol dependence in Korean population classified by the Lesch typology. *Alcohol Alcohol* **48**: 426-432

Leong KG, Wang BE, Johnson L, Gao WQ (2008) Generation of a prostate from a single adult stem cell. *Nature* **456**: 804-808

Lepor H (1999) The pathophysiology of lower urinary tract symptoms in the aging male population. Prostatic Diseases. In *Prostatic Diseases*, H L (ed), 1 edn, 1, pp 163-196. Philadelphia, PA: WB Saunders/Elsevier

Lin J, Wu H, Shi H, Pan W, Yu H, Zhu J (2013) Combined inhibition of epidermal growth factor receptor and cyclooxygenase-2 leads to greater anti-tumor activity of docetaxel in advanced prostate cancer. *PloS one* **8**: e76169

Linn DE, Yang X, Sun F, Xie Y, Chen H, Jiang R, Chumsri S, Burger AM, Qiu Y (2010) A Role for OCT4 in Tumor Initiation of Drug-Resistant Prostate Cancer Cells. *Genes Cancer* **1**: 908-916

Lockie AC (1981) Symptomatic cure of prostatitis with metronidazole. *Lancet* **2**: 475

Lowsley OS (1912) The development of the human prostate gland with reference to the development of other structures at the neck of the urinary bladder. *American Journal of Anatomy* **13**

Mabjeesh NJ, Escuin D, LaVallee TM, Pribluda VS, Swartz GM, Johnson MS, Willard MT, Zhong H, Simons JW, Giannakakou P (2003a) 2ME2 inhibits tumor growth and angiogenesis by disrupting microtubules and dysregulating HIF. *Cancer Cell* **3**: 363-375

Mabjeesh NJ, Post DE, Willard MT, Kaur B, Van Meir EG, Simons JW, Zhong H (2002) Geldanamycin induces degradation of hypoxia-inducible factor 1 α protein via the proteasome pathway in prostate cancer cells. *Cancer research* **62**: 2478-2482

Mabjeesh NJ, Willard MT, Frederickson CE, Zhong H, Simons JW (2003b) Androgens stimulate hypoxia-inducible factor 1 activation via autocrine loop of tyrosine kinase receptor/phosphatidylinositol 3'-kinase/protein kinase B in prostate cancer cells. *Clinical cancer research : an official journal of the American Association for Cancer Research* **9**: 2416-2425

MacDonald R, Wilt TJ (2005) Alfuzosin for treatment of lower urinary tract symptoms compatible with benign prostatic hyperplasia: a systematic review of efficacy and adverse effects. *Urology* **66**: 780-788

Majumder PK, Febbo PG, Bikoff R, Berger R, Xue Q, McMahon LM, Manola J, Brugarolas J, McDonnell TJ, Golub TR, Loda M, Lane HA, Sellers WR (2004) mTOR inhibition reverses Akt-dependent prostate intraepithelial neoplasia through regulation of apoptotic and HIF-1-dependent pathways. *Nat Med* **10**: 594-601

Malaeb BS, Yu X, McBean AM, Elliott SP (2012) National trends in surgical therapy for benign prostatic hyperplasia in the United States (2000-2008). *Urology* **79**: 1111-1116

Manfredi JJ, Horwitz SB (1984) Taxol: an antimitotic agent with a new mechanism of action. *Pharmacology & therapeutics* **25**: 83-125

Mani SA, Guo W, Liao MJ, Eaton EN, Ayyanan A, Zhou AY, Brooks M, Reinhard F, Zhang CC, Shipitsin M, Campbell LL, Polyak K, Brisken C, Yang J, Weinberg RA (2008) The epithelial-mesenchymal transition generates cells with properties of stem cells. *Cell* **133**: 704-715

Marcinkiewicz K, Scotland KB, Boorjian SA, Nilsson EM, Persson JL, Abrahamsson PA, Allegrucci C, Hughes IA, Gudas LJ, Mongan NP (2012) The androgen receptor and stem cell pathways in prostate and bladder cancers (review). *International journal of oncology* **40**: 5-12

Maxwell PH, Wiesener MS, Chang GW, Clifford SC, Vaux EC, Cockman ME, Wykoff CC, Pugh CW, Maher ER, Ratcliffe PJ (1999) The tumour suppressor protein VHL targets hypoxia-inducible factors for oxygen-dependent proteolysis. *Nature* **399**: 271-275

McBride S, Meleady P, Baird A, Dinsdale D, Clynes M (1998) Human lung carcinoma cell line DLKP contains 3 distinct subpopulations with different growth and attachment properties. *Tumour Biol* **19**: 88-103

McGuire WP, Rowinsky EK, Rosenshein NB, Grumbine FC, Ettinger DS, Armstrong DK, Donehower RC (1989) Taxol: a unique antineoplastic agent with significant activity in advanced ovarian epithelial neoplasms. *Annals of internal medicine* **111**: 273-279

McNeal JE (1969) Origin and development of carcinoma in the prostate. *Cancer* **23**: 24-34

McNeal JE (1978) Origin and evolution of benign prostatic enlargement. *Investigative urology* **15**: 340-345

McNeal JE (1980) The anatomic heterogeneity of the prostate. *Progress in clinical and biological research* **37**: 149-160

Mediavilla-Varela M, Pacheco FJ, Almaguel F, Perez J, Sahakian E, Daniels TR, Leoh LS, Padilla A, Wall NR, Lilly MB, De Leon M, Casiano CA (2009) Docetaxel-induced prostate cancer cell death involves concomitant activation of caspase and lysosomal pathways and is attenuated by LEDGF/p75. *Mol Cancer* **8**: 68

Mettlin CJ, Murphy G (1994) The National Cancer Data Base report on prostate cancer. *Cancer* **74**: 1640-1648

Mettlin CJ, Murphy GP, McGinnis LS, Menck HR (1995) The National Cancer Data Base report on prostate cancer. American College of Surgeons Commission on Cancer and the American Cancer Society. *Cancer* **76**: 1104-1112

Metzger E, Wissmann M, Yin N, Muller JM, Schneider R, Peters AH, Gunther T, Buettner R, Schule R (2005) LSD1 demethylates repressive histone marks to promote androgen-receptor-dependent transcription. *Nature* **437**: 436-439

Michels J, Ellard SL, Le L, Kollmannsberger C, Murray N, Tomlinson Guns ES, Carr R, Chi KN (2010) A phase IB study of ABT-751 in combination with docetaxel in patients with advanced castration-resistant prostate cancer. *Annals of oncology : official journal of the European Society for Medical Oncology / ESMO* **21**: 305-311

Milecki P, Martenka P, Antczak A, Kwias Z (2010) Radiotherapy combined with hormonal therapy in prostate cancer: the state of the art. *Cancer management and research* **2**: 243-253

Mimeault M, Johansson SL, Vankatraman G, Moore E, Henichart JP, Depreux P, Lin MF, Batra SK (2007) Combined targeting of epidermal growth factor receptor and hedgehog

signaling by gefitinib and cyclopamine cooperatively improves the cytotoxic effects of docetaxel on metastatic prostate cancer cells. *Mol Cancer Ther* **6**: 967-978

Miners JO, Birkett DJ (1998) Cytochrome P4502C9: an enzyme of major importance in human drug metabolism. *British journal of clinical pharmacology* **45**: 525-538

Minotti G, Menna P, Salvatorelli E, Cairo G, Gianni L (2004) Anthracyclines: molecular advances and pharmacologic developments in antitumor activity and cardiotoxicity. *Pharmacological reviews* **56**: 185-229

Mitsudomi T, Yatabe Y (2010) Epidermal growth factor receptor in relation to tumor development: EGFR gene and cancer. *The FEBS journal* **277**: 301-308

Monks A, Scudiero D, Skehan P, Shoemaker R, Paull K, Vistica D, Hose C, Langley J, Cronise P, Vaigro-Wolff A, *et al.* (1991) Feasibility of a high-flux anticancer drug screen using a diverse panel of cultured human tumor cell lines. *Journal of the National Cancer Institute* **83**: 757-766

Montgomery RB, Mostaghel EA, Vessella R, Hess DL, Kalhorn TF, Higano CS, True LD, Nelson PS (2008) Maintenance of intratumoral androgens in metastatic prostate cancer: a mechanism for castration-resistant tumor growth. *Cancer research* **68**: 4447-4454

Moore KL, Dalley AF (2006) *Clinically Oriented Anatomy*, 5th edn.: Lippincott Williams & Wilkins.

Moore MJ, Osoba D, Murphy K, Tannock IF, Armitage A, Findlay B, Coppin C, Neville A, Venner P, Wilson J (1994) Use of palliative end points to evaluate the effects of mitoxantrone and low-dose prednisone in patients with hormonally resistant prostate cancer. *Journal of clinical oncology : official journal of the American Society of Clinical Oncology* **12**: 689-694

Moran BW, Anderson FP, Devery A, Cloonan S, Butler WE, Varughese S, Draper SM, Kenny PT (2009) Synthesis, structural characterisation and biological evaluation of fluorinated analogues of resveratrol. *Bioorganic & medicinal chemistry* **17**: 4510-4522

Moslemi MK, Abedin Zadeh M (2010) A modified technique of simple suprapubic prostatectomy: no bladder drainage and no bladder neck or hemostatic sutures. *Urology journal* **7**: 51-55

Mozzetti S, Ferlini C, Concolino P, Filippetti F, Raspaglio G, Prislei S, Gallo D, Martinelli E, Ranelletti FO, Ferrandina G, Scambia G (2005) Class III beta-tubulin overexpression is a prominent mechanism of paclitaxel resistance in ovarian cancer patients. *Clinical cancer research : an official journal of the American Association for Cancer Research* **11**: 298-305

Munoz M, Henderson M, Haber M, Norris M (2007) Role of the MRP1/ABCC1 multidrug transporter protein in cancer. *IUBMB life* **59**: 752-757

Murphy L, Clynes M, Keenan J (2007) Proteomic analysis to dissect mitoxantrone resistance-associated proteins in a squamous lung carcinoma. *Anticancer Res* **27**: 1277-1284

Murphy RA, Watson AY, Rhodes JA (1984) Biological sources of nerve growth factor. *Applied neurophysiology* **47**: 33-42

Murphy WK, Fossella FV, Winn RJ, Shin DM, Hynes HE, Gross HM, Davilla E, Leimert J, Dhingra H, Raber MN, *et al.* (1993) Phase II study of taxol in patients with untreated advanced non-small-cell lung cancer. *Journal of the National Cancer Institute* **85**: 384-388

N.C.I. US. (1991) Clinical Brochure:Taxol (NSC 125973). In Bathesda MDoCT (ed.).

Narita S, Tsuchiya N, Kumazawa T, Maita S, Numakura K, Obara T, Tsuruta H, Saito M, Inoue T, Horikawa Y, Satoh S, Nanjyo H, Habuchi T (2012) Short-term clinicopathological outcome of neoadjuvant chemohormonal therapy comprising complete androgen blockade, followed by treatment with docetaxel and estramustine phosphate before radical prostatectomy in Japanese patients with high-risk localized prostate cancer. *World J Surg Oncol* **10**: 1

NCRI. (2011) All Ireland Cancer Atlas 1995-2007.

NCRI. (2014) Cancer in Ireland 1994 - 2011 : Annual report of the National Cancer Registry 2014. National Cancer Registry Ireland.

Nelson WG, De Marzo AM, Isaacs WB (2003) Prostate cancer. *The New England journal of medicine* **349**: 366-381

Nicholson RI, Walker KJ, Maynard PV (1980) Anti-tumour potential of a new luteinizing hormone releasing hormone analogue, ICI 118630. *Eur J Cancer Suppl* **1**: 295-299

Nickerson T, Chang F, Lorimer D, Smeekens SP, Sawyers CL, Pollak M (2001) In vivo progression of LAPC-9 and LNCaP prostate cancer models to androgen independence is associated with increased expression of insulin-like growth factor I (IGF-I) and IGF-I receptor (IGF-IR). *Cancer research* **61**: 6276-6280

Nilsson S, Larsen RH, Fossa SD, Balteskard L, Borch KW, Westlin JE, Salberg G, Bruland OS (2005) First clinical experience with alpha-emitting radium-223 in the treatment of skeletal

metastases. *Clinical cancer research : an official journal of the American Association for Cancer Research* **11**: 4451-4459

Nishio N, Katsura T, Ashida K, Okuda M, Inui K (2005) Modulation of P-glycoprotein expression in hyperthyroid rat tissues. *Drug metabolism and disposition: the biological fate of chemicals* **33**: 1584-1587

Noguchi T, Fujimoto H, Sano H, Miyajima A, Miyachi H, Hashimoto Y (2005) Angiogenesis inhibitors derived from thalidomide. *Bioorg Med Chem Lett* **15**: 5509-5513

Nussey S, Whitehead S (2001) *Endocrinology: An Integrated Approach*: BIOS Scientific Publishers Ltd.

O'Neill AJ, Prencipe M, Dowling C, Fan Y, Mulrane L, Gallagher WM, O'Connor D, O'Connor R, Devery A, Corcoran C, Rani S, O'Driscoll L, Fitzpatrick JM, Watson RW (2011) Characterisation and manipulation of docetaxel resistant prostate cancer cell lines. *Mol Cancer* **10**: 126

Oh WK, Halabi S, Kelly WK, Werner C, Godley PA, Vogelzang NJ, Small EJ (2003) A phase II study of estramustine, docetaxel, and carboplatin with granulocyte-colony-stimulating factor support in patients with hormone-refractory prostate carcinoma: Cancer and Leukemia Group B 99813. *Cancer* **98**: 2592-2598

Oldridge EE, Pellacani D, Collins AT, Maitland NJ (2012) Prostate cancer stem cells: are they androgen-responsive? *Mol Cell Endocrinol* **360**: 14-24

Orsted DD, Bojesen SE (2013) The link between benign prostatic hyperplasia and prostate cancer. *Nat Rev Urol* **10**: 49-54

Palayoor ST, Tofilon PJ, Coleman CN (2003) Ibuprofen-mediated reduction of hypoxia-inducible factors HIF-1alpha and HIF-2alpha in prostate cancer cells. *Clinical cancer research : an official journal of the American Association for Cancer Research* **9**: 3150-3157

Pan YQ, Qiao L, Xue XD, Fu JH (2015) Association between ANKK1 (rs1800497) polymorphism of DRD2 gene and attention deficit hyperactivity disorder: A meta-analysis. *Neurosci Lett* **590**: 101-105

Papandreou I, Cairns RA, Fontana L, Lim AL, Denko NC (2006) HIF-1 mediates adaptation to hypoxia by actively downregulating mitochondrial oxygen consumption. *Cell metabolism* **3**: 187-197

Pazdur R, Newman RA, Newman BM, Fuentes A, Benvenuto J, Bready B, Moore D, Jr., Jaiyesimi I, Vreeland F, Bayssas MM, *et al.* (1992) Phase I trial of Taxotere: five-day schedule. *Journal of the National Cancer Institute* **84**: 1781-1788

Peinemann F, Grouven U, Hemkens LG, Bartel C, Borchers H, Pinkawa M, Heidenreich A, Sauerland S (2011) Low-dose rate brachytherapy for men with localized prostate cancer. *The Cochrane database of systematic reviews*: CD008871

Persson BE, Ronquist G (1996) Non-bacterial prostatitis. *Lancet* **348**: 761

Petrylak DP, Tangen CM, Hussain MH, Lara PN, Jr., Jones JA, Taplin ME, Burch PA, Berry D, Moinpour C, Kohli M, Benson MC, Small EJ, Raghavan D, Crawford ED (2004) Docetaxel and estramustine compared with mitoxantrone and prednisone for advanced refractory prostate cancer. *The New England journal of medicine* **351**: 1513-1520

Pinto A, Cruz P (2012) Radium-223 chloride: a new treatment option for metastatic castration-resistant prostate carcinoma. *Drugs in R&D* **12**: 227-233

Pollak M (2001) Insulin-like growth factors and prostate cancer. *Epidemiologic reviews* **23**: 59-66

Pollak M, Beamer W, Zhang JC (1998) Insulin-like growth factors and prostate cancer. *Cancer Metastasis Rev* **17**: 383-390

Pouyssegur J, Dayan F, Mazure NM (2006) Hypoxia signalling in cancer and approaches to enforce tumour regression. *Nature* **441**: 437-443

Pretlow TG, Wolman SR, Micale MA, Pelley RJ, Kursh ED, Resnick MI, Bodner DR, Jacobberger JW, Delmoro CM, Giaconia JM, *et al.* (1993) Xenografts of primary human prostatic carcinoma. *Journal of the National Cancer Institute* **85**: 394-398

Price D (1963) Comparative Aspects of Development and Structure in the Prostate. *National Cancer Institute monograph* **12**: 1-27

Purushottamachar P, Godbole AM, Gediya LK, Martin MS, Vasaitis TS, Kwegyir-Afful AK, Ramalingam S, Ates-Alagoz Z, Njar VC (2013) Systematic structure modifications of multitarget prostate cancer drug candidate galeterone to produce novel androgen receptor down-regulating agents as an approach to treatment of advanced prostate cancer. *Journal of medicinal chemistry* **56**: 4880-4898

Ranganathan S, Benetatos CA, Colarusso PJ, Dexter DW, Hudes GR (1998) Altered beta-tubulin isotype expression in paclitaxel-resistant human prostate carcinoma cells. *Br J Cancer* **77**: 562-566

Rettie AE, Jones JP (2005) Clinical and toxicological relevance of CYP2C9: drug-drug interactions and pharmacogenetics. *Annu Rev Pharmacol Toxicol* **45**: 477-494

Rezvani HR, Ali N, Nissen LJ, Harfouche G, de Verneuil H, Taieb A, Mazurier F (2011) HIF-1alpha in epidermis: oxygen sensing, cutaneous angiogenesis, cancer, and non-cancer disorders. *The Journal of investigative dermatology* **131**: 1793-1805

Richardson GD, Robson CN, Lang SH, Neal DE, Maitland NJ, Collins AT (2004) CD133, a novel marker for human prostatic epithelial stem cells. *Journal of cell science* **117**: 3539-3545

Rinaldo F, Li J, Wang E, Muders M, Datta K (2007) RalA regulates vascular endothelial growth factor-C (VEGF-C) synthesis in prostate cancer cells during androgen ablation. *Oncogene* **26**: 1731-1738

Risinger AL, Westbrook CD, Encinas A, Mulbaier M, Schultes CM, Wawro S, Lewis JD, Janssen B, Giles FJ, Mooberry SL (2011) ELR510444, a novel microtubule disruptor with multiple mechanisms of action. *The Journal of pharmacology and experimental therapeutics* **336**: 652-660

Ritz E (1983) Diagnosing prostatitis. *Lancet* **1**: 821

Rivero VE, Motrich RD, Maccioni M, Riera CM (2007) Autoimmune etiology in chronic prostatitis syndrome: an advance in the understanding of this pathology. *Critical reviews in immunology* **27**: 33-46

Robinson-Rechavi M, Garcia HE, Laudet V (2003) The Nuclear Receptor Superfamily. *Journal of cell science* **116**: 585-586

Roehrborn CG (2008) Pathology of benign prostatic hyperplasia. *International journal of impotence research* **20 Suppl 3**: S11-18

Roninson IB, Broude EV, Chang BD (2001) If not apoptosis, then what? Treatment-induced senescence and mitotic catastrophe in tumor cells. *Drug resistance updates : reviews and commentaries in antimicrobial and anticancer chemotherapy* **4**: 303-313

Ross RW, Galsky MD, Febbo P, Barry M, Richie JP, Xie W, Fennessy FM, Bhatt RS, Hayes J, Choueiri TK, Tempany CM, Kantoff PW, Taplin ME, Oh WK (2012) Phase 2 study of neoadjuvant docetaxel plus bevacizumab in patients with high-risk localized prostate cancer : A Prostate Cancer Clinical Trials Consortium trial. *Cancer*

Rowinsky EK, Cazenave LA, Donehower RC (1990) Taxol: a novel investigational antimicrotubule agent. *Journal of the National Cancer Institute* **82**: 1247-1259

Roy AK, Tyagi RK, Song CS, Lavrovsky Y, Ahn SC, Oh TS, Chatterjee B (2001) Androgen receptor: structural domains and functional dynamics after ligand-receptor interaction. *Annals of the New York Academy of Sciences* **949**: 44-57

Roy D, Sin SH, Lucas A, Venkataramanan R, Wang L, Eason A, Chavakula V, Hilton IB, Tamburro KM, Damania B, Dittmer DP (2013) mTOR inhibitors block Kaposi sarcoma growth by inhibiting essential autocrine growth factors and tumor angiogenesis. *Cancer research* **73**: 2235-2246

Saad F, Fizazi K, Jinga V, Efstathiou E, Fong PC, Hart LL, Jones R, McDermott R, Wirth M, Suzuki K, MacLean DB, Wang L, Akaza H, Nelson J, Scher HI, Dreicer R, Webb IJ, de Wit R (2015) Orteronel plus prednisone in patients with chemotherapy-naive metastatic castration-resistant prostate cancer (ELM-PC 4): a double-blind, multicentre, phase 3, randomised, placebo-controlled trial. *Lancet Oncol*

Saartok T, Dahlberg E, Gustafsson J (1984) Relative binding affinity of anabolic-androgenic steroids: comparison of the binding to the androgen receptors in skeletal muscle and in prostate, as well as to sex hormone-binding globulin. *Endocrinology* **114**: 2100-2106

Saeki M, Kurose K, Hasegawa R, Tohkin M (2011) Functional analysis of genetic variations in the 5'-flanking region of the human MDR1 gene. *Molecular genetics and metabolism* **102**: 91-98

Saelens X, Festjens N, Parthoens E, Vanoverberghe I, Kalai M, van Kuppeveld F, Vandenabeele P (2005) Protein synthesis persists during necrotic cell death. *The Journal of cell biology* **168**: 545-551

Salembier C, Lavagnini P, Nickers P, Mangili P, Rijnders A, Polo A, Venselaar J, Hoskin P (2007) Tumour and target volumes in permanent prostate brachytherapy: a supplement to the ESTRO/EAU/EORTC recommendations on prostate brachytherapy. *Radiother Oncol* **83**: 3-10

Sanchez C, Mendoza P, Contreras HR, Vergara J, McCubrey JA, Huidobro C, Castellon EA (2009) Expression of multidrug resistance proteins in prostate cancer is related with cell sensitivity to chemotherapeutic drugs. *Prostate* **69**: 1448-1459

Sanofi-Aventis (2010) Cabazitaxel [Package Insert]. Bridgewater, New Jersey, USA. *Sanofi-Aventis*

Sartor O, Coleman R, Nilsson S, Heinrich D, Helle SI, O'Sullivan JM, Fossa SD, Chodacki A, Wiechno P, Logue J, Widmark A, Johannessen DC, Hoskin P, James ND, Solberg A, Syndikus I, Vogelzang NJ, O'Bryan-Tear CG, Shan M, Bruland OS, Parker C (2014) Effect of radium-223 dichloride on symptomatic skeletal events in patients with castration-resistant prostate

cancer and bone metastases: results from a phase 3, double-blind, randomised trial. *Lancet Oncol* **15**: 738-746

Schellhammer PF, Chodak G, Whitmore JB, Sims R, Frohlich MW, Kantoff PW (2013) Lower baseline prostate-specific antigen is associated with a greater overall survival benefit from sipuleucel-T in the Immunotherapy for Prostate Adenocarcinoma Treatment (IMPACT) trial. *Urology* **81**: 1297-1302

Schiff PB, Fant J, Horwitz SB (1979) Promotion of microtubule assembly in vitro by taxol. *Nature* **277**: 665-667

Schioppa T, Uranchimeg B, Sacconi A, Biswas SK, Doni A, Rapisarda A, Bernasconi S, Sacconi S, Nebuloni M, Vago L, Mantovani A, Melillo G, Sica A (2003) Regulation of the chemokine receptor CXCR4 by hypoxia. *The Journal of experimental medicine* **198**: 1391-1402

Schultes C, Lewis JD. (2009) NCI-60 Data Analysis. Elara Pharmaceuticals GMBH.

Semenza GL (2003) Targeting HIF-1 for cancer therapy. *Nature reviews Cancer* **3**: 721-732

Semenza GL (2012) Hypoxia-inducible factors: mediators of cancer progression and targets for cancer therapy. *Trends Pharmacol Sci* **33**: 207-214

Semenza GL, Wang GL (1992) A nuclear factor induced by hypoxia via de novo protein synthesis binds to the human erythropoietin gene enhancer at a site required for transcriptional activation. *Molecular and cellular biology* **12**: 5447-5454

Serganova I, Rizwan A, Ni X, Thakur SB, Vider J, Russell J, Blasberg R, Koutcher JA (2011) Metabolic imaging: a link between lactate dehydrogenase A, lactate, and tumor phenotype. *Clinical cancer research : an official journal of the American Association for Cancer Research* **17**: 6250-6261

Seruga B, Ocana A, Tannock IF (2011) Drug resistance in metastatic castration-resistant prostate cancer. *Nat Rev Clin Oncol* **8**: 12-23

Sfakianos JP, Thorner DA, Dovirak O, Weiss JP, Karanikolas NT (2011) Optimizing prostate cancer detection during biopsy by standardizing the amount of tissue examined per core. *BJU international* **108**: 1578-1581

Sfanos K, Hempel H, De Marzo A (2014) The Role of Inflammation in Prostate Cancer. In *Inflammation and Cancer*, Aggarwal BB, Sung B, Gupta SC (eds), Vol. 816, 7, pp 153-181. Springer Basel

Shepard DR, Dreicer R, Garcia J, Elson P, Magi-Galluzzi C, Raghavan D, Stephenson AJ, Klein EA (2009) Phase II trial of neoadjuvant nab-paclitaxel in high risk patients with prostate cancer undergoing radical prostatectomy. *The Journal of urology* **181**: 1672-1677; discussion 1677

Shoemaker RH (2006) The NCI60 human tumour cell line anticancer drug screen. *Nature reviews Cancer* **6**: 813-823

Shweiki D, Itin A, Soffer D, Keshet E (1992) Vascular endothelial growth factor induced by hypoxia may mediate hypoxia-initiated angiogenesis. *Nature* **359**: 843-845

Small EJ, Srinivas S, Egan B, McMillan A, Rearden TP (1996) Doxorubicin and dose-escalated cyclophosphamide with granulocyte colony-stimulating factor for the treatment of hormone-resistant prostate cancer. *Journal of clinical oncology : official journal of the American Society of Clinical Oncology* **14**: 1617-1625

Sramkoski RM, Pretlow TG, 2nd, Giaconia JM, Pretlow TP, Schwartz S, Sy MS, Marengo SR, Rhim JS, Zhang D, Jacobberger JW (1999) A new human prostate carcinoma cell line, 22Rv1. *In Vitro Cell Dev Biol Anim* **35**: 403-409

Steive H (1930) "Männliche Genitalorgane". *Handbuch der mikroskopischen Anatomie des Menschen* **VII**: 1-399

Stengel C, Newman SP, Leese MP, Potter BV, Reed MJ, Purohit A (2010) Class III beta-tubulin expression and in vitro resistance to microtubule targeting agents. *Br J Cancer* **102**: 316-324

Stierle A, Strobel G, Stierle D (1993) Taxol and taxane production by *Taxomyces andreanae*, an endophytic fungus of Pacific yew. *Science* **260**: 214-216

Stone KR, Mickey DD, Wunderli H, Mickey GH, Paulson DF (1978) Isolation of a human prostate carcinoma cell line (DU 145). *Int J Cancer* **21**: 274-281

Sullivan GF, Amenta PS, Villanueva JD, Alvarez CJ, Yang JM, Hait WN (1998) The expression of drug resistance gene products during the progression of human prostate cancer. *Clinical cancer research : an official journal of the American Association for Cancer Research* **4**: 1393-1403

Sweeney CJ, Chamberlain D (2015) Insights into E3805: the CHAARTED trial. *Future Oncol* **11**: 897-899

Tannock IF, de Wit R, Berry WR, Horti J, Pluzanska A, Chi KN, Oudard S, Theodore C, James ND, Turesson I, Rosenthal MA, Eisenberger MA (2004) Docetaxel plus prednisone or

mitoxantrone plus prednisone for advanced prostate cancer. *The New England journal of medicine* **351**: 1502-1512

Tannock IF, Osoba D, Stockler MR, Ernst DS, Neville AJ, Moore MJ, Armitage GR, Wilson JJ, Venner PM, Coppin CM, Murphy KC (1996) Chemotherapy with mitoxantrone plus prednisone or prednisone alone for symptomatic hormone-resistant prostate cancer: a Canadian randomized trial with palliative end points. *Journal of clinical oncology : official journal of the American Society of Clinical Oncology* **14**: 1756-1764

Tester W, Ackler J, Tijani L, Leighton J (2006) Phase I/II study of weekly docetaxel and vinblastine in the treatment of metastatic hormone-refractory prostate carcinoma. *Cancer J* **12**: 299-304

Tew KD (1983) The mechanism of action of estramustine. *Seminars in oncology* **10**: 21-26

Tew KD, Erickson LC, White G, Wang AL, Schein PS, Hartley-Asp B (1983) Cytotoxicity of estramustine, a steroid-nitrogen mustard derivative, through non-DNA targets. *Mol Pharmacol* **24**: 324-328

Toner AP (2008) KLF5: A Potential Therapeutic Target in Androgen Receptor Positive Prostate Cancer. M.Sc. Thesis, Biochemistry, National University of Ireland, Galway, Kennys Bookbindery Galway

Toner AP, McLaughlin F, Giles FJ, Sullivan FJ, O'Connell E, Carleton LA, Breen L, Dunne G, Gorman AM, Lewis JD, Glynn SA (2013) The novel toluidine sulphonamide EL102 shows pre-clinical in vitro and in vivo activity against prostate cancer and circumvents MDR1 resistance. *Br J Cancer* **109**: 2131-2141

Tran C, Ouk S, Clegg NJ, Chen Y, Watson PA, Arora V, Wongvipat J, Smith-Jones PM, Yoo D, Kwon A, Wasielewska T, Welsbie D, Chen CD, Higano CS, Beer TM, Hung DT, Scher HI, Jung ME, Sawyers CL (2009) Development of a second-generation antiandrogen for treatment of advanced prostate cancer. *Science* **324**: 787-790

Tryggvadottir L, Vidarsdottir L, Thorgeirsson T, Jonasson JG, Olafsdottir EJ, Olafsdottir GH, Rafnar T, Thorlacius S, Jonsson E, Eyfjord JE, Tulinius H (2007) Prostate cancer progression and survival in BRCA2 mutation carriers. *Journal of the National Cancer Institute* **99**: 929-935

Turke AB, Zejnullahu K, Wu YL, Song Y, Dias-Santagata D, Lifshits E, Toschi L, Rogers A, Mok T, Sequist L, Lindeman NI, Murphy C, Akhavanfard S, Yeap BY, Xiao Y, Capelletti M, Iafrate AJ, Lee C, Christensen JG, Engelman JA, Janne PA (2010) Preexistence and clonal selection of MET amplification in EGFR mutant NSCLC. *Cancer Cell* **17**: 77-88

Umesono K, Evans RM (1989) Determinants of target gene specificity for steroid/thyroid hormone receptors. *Cell* **57**: 1139-1146

van Bokhoven A, Varella-Garcia M, Korch C, Johannes WU, Smith EE, Miller HL, Nordeen SK, Miller GJ, Lucia MS (2003) Molecular characterization of human prostate carcinoma cell lines. *Prostate* **57**: 205-225

van Brussel JP, van Steenbrugge GJ, Romijn JC, Schroder FH, Mickisch GH (1999) Chemosensitivity of prostate cancer cell lines and expression of multidrug resistance-related proteins. *Eur J Cancer* **35**: 664-671

Veenema RJ (1953) A simplified prostatic perineal biopsy punch. *The Journal of urology* **69**: 320-322

Verhamme KM, Dieleman JP, Bleumink GS, van der Lei J, Sturkenboom MC, Artibani W, Begaud B, Berges R, Borkowski A, Chappel CR, Costello A, Dobronski P, Farmer RD, Jimenez Cruz F, Jonas U, MacRae K, Pientka L, Rutten FF, van Schayck CP, Speakman MJ, Tiellac P, Tubaro A, Vallencien G, Vela Navarrete R (2002) Incidence and prevalence of lower urinary tract symptoms suggestive of benign prostatic hyperplasia in primary care--the Triumph project. *European urology* **42**: 323-328

Vermeulen A, Giagulli VA, De Schepper P, Buntinx A, Stoner E (1989) Hormonal effects of an orally active 4-azasteroid inhibitor of 5 alpha-reductase in humans. *Prostate* **14**: 45-53

Vichai V, Kirtikara K (2006) Sulforhodamine B colorimetric assay for cytotoxicity screening. *Nature protocols* **1**: 1112-1116

Walsh PC (1988) Radical retropubic prostatectomy with reduced morbidity: an anatomic approach. *NCI monographs : a publication of the National Cancer Institute*: 133-137

Walsh PC, Lepor H, Eggleston JC (1983) Radical prostatectomy with preservation of sexual function: anatomical and pathological considerations. *Prostate* **4**: 473-485

Wang GL, Jiang BH, Rue EA, Semenza GL (1995) Hypoxia-inducible factor 1 is a basic-helix-loop-helix-PAS heterodimer regulated by cellular O₂ tension. *Proceedings of the National Academy of Sciences of the United States of America* **92**: 5510-5514

Wang X, Sykes DB, Miller DS (2010) Constitutive androstane receptor-mediated up-regulation of ATP-driven xenobiotic efflux transporters at the blood-brain barrier. *Mol Pharmacol* **78**: 376-383

Wang Z, Chen Y, Liang H, Bender A, Glen RC, Yan A (2011) P-glycoprotein substrate models using support vector machines based on a comprehensive data set. *Journal of chemical information and modeling* **51**: 1447-1456

Wani MC, Taylor HL, Wall ME, Coggon P, McPhail AT (1971) Plant antitumor agents. VI. The isolation and structure of taxol, a novel antileukemic and antitumor agent from *Taxus brevifolia*. *Journal of the American Chemical Society* **93**: 2325-2327

Weiss RB, Donehower RC, Wiernik PH, Ohnuma T, Gralla RJ, Trump DL, Baker JR, Jr., Van Echo DA, Von Hoff DD, Leyland-Jones B (1990) Hypersensitivity reactions from taxol. *Journal of clinical oncology : official journal of the American Society of Clinical Oncology* **8**: 1263-1268

Wendt B, Cramer RD (2008) Quantitative Series Enrichment Analysis (QSEA): a novel procedure for 3D-QSAR analysis. *Journal of computer-aided molecular design* **22**: 541-551

Wendt B, Mulbaier M, Wawro S, Schultes C, Alonso J, Janssen B, Lewis J (2011a) Toluidinesulfonamide hypoxia-induced factor 1 inhibitors: alleviating drug-drug interactions through use of PubChem data and comparative molecular field analysis guided synthesis. *Journal of medicinal chemistry* **54**: 3982-3986

Wendt B, Uhrig U, Bos F (2011b) Capturing structure-activity relationships from chemogenomic spaces. *Journal of chemical information and modeling* **51**: 843-851

Wenger RH (2002) Cellular adaptation to hypoxia: O₂-sensing protein hydroxylases, hypoxia-inducible transcription factors, and O₂-regulated gene expression. *FASEB J* **16**: 1151-1162

WHO (2014) *World Cancer Report 2014*, Vol. Chapter 5.

Williams PA, Cosme J, Ward A, Angove HC, Matak Vinkovic D, Jhoti H (2003) Crystal structure of human cytochrome P450 2C9 with bound warfarin. *Nature* **424**: 464-468

Wilson CM, McPhaul MJ (1994) A and B forms of the androgen receptor are present in human genital skin fibroblasts. *Proceedings of the National Academy of Sciences of the United States of America* **91**: 1234-1238

Wilson TE, Paulsen RE, Padgett KA, Milbrandt J (1992) Participation of non-zinc finger residues in DNA binding by two nuclear orphan receptors. *Science* **256**: 107-110

Wojcieszek P, Bialas B (2012) Prostate cancer brachytherapy: guidelines overview. *Journal of contemporary brachytherapy* **4**: 116-120

Womble PR, VanVeldhuizen PJ, Nisbet AA, Reed GA, Thrasher JB, Holzbeierlein JM (2011) A phase II clinical trial of neoadjuvant ketoconazole and docetaxel chemotherapy before radical prostatectomy in high risk patients. *The Journal of urology* **186**: 882-887

Xie Y, Xu K, Linn DE, Yang X, Guo Z, Shimelis H, Nakanishi T, Ross DD, Chen H, Fazli L, Gleave ME, Qiu Y (2008) The 44-kDa Pim-1 kinase phosphorylates BCRP/ABCG2 and thereby promotes its multimerization and drug-resistant activity in human prostate cancer cells. *The Journal of biological chemistry* **283**: 3349-3356

Yamana K, Labrie F, Luu-The V. (2010) Hormone molecular biology and clinical investigation. De Gruyter, Berlin.

Yao J, Pan YQ, Ding M, Pang H, Wang BJ (2015) Association between DRD2 (rs1799732 and rs1801028) and ANKK1 (rs1800497) polymorphisms and schizophrenia: a meta-analysis. *American journal of medical genetics Part B, Neuropsychiatric genetics : the official publication of the International Society of Psychiatric Genetics* **168B**: 1-13

Yewalkar N, Deore V, Padgaonkar A, Manohar S, Sahu B, Kumar P, Jalota-Badhwar A, Joshi KS, Sharma S, Kumar S (2010) Development of novel inhibitors targeting HIF-1alpha towards anticancer drug discovery. *Bioorg Med Chem Lett* **20**: 6426-6429

Yu F, White SB, Zhao Q, Lee FS (2001) HIF-1alpha binding to VHL is regulated by stimulus-sensitive proline hydroxylation. *Proceedings of the National Academy of Sciences of the United States of America* **98**: 9630-9635

Yu Y, Lee JS, Xie N, Li E, Hurtado-Coll A, Fazli L, Cox M, Plymate S, Gleave M, Dong X (2014) Prostate stromal cells express the progesterone receptor to control cancer cell mobility. *PLoS one* **9**: e92714

Zalcberg J, Hu XF, Slater A, Parisot J, El-Osta S, Kantharidis P, Chou ST, Parkin JD (2000) MRP1 not MDR1 gene expression is the predominant mechanism of acquired multidrug resistance in two prostate carcinoma cell lines. *Prostate cancer and prostatic diseases* **3**: 66-75

Zhang B, Suer S, Livak F, Adediran S, Vemula A, Khan MA, Ning Y, Hussain A (2012) Telomere and Microtubule Targeting in Treatment-sensitive and Treatment-resistant Human Prostate Cancer Cells. *Mol Pharmacol*

Zhang JZ, Behrooz A, Ismail-Beigi F (1999) Regulation of glucose transport by hypoxia. *American journal of kidney diseases : the official journal of the National Kidney Foundation* **34**: 189-202

Zhang S, Murtha PE, Young CY (1997) Defining a functional androgen responsive element in the 5' far upstream flanking region of the prostate-specific antigen gene. *Biochemical and biophysical research communications* **231**: 784-788

Zhong H, De Marzo AM, Laughner E, Lim M, Hilton DA, Zagzag D, Buechler P, Isaacs WB, Semenza GL, Simons JW (1999) Overexpression of hypoxia-inducible factor 1alpha in common human cancers and their metastases. *Cancer research* **59**: 5830-5835

Zhu B, Kyprianou N (2005) Transforming growth factor beta and prostate cancer. *Cancer Treat Res* **126**: 157-173

Zhu ML, Horbinski CM, Garzotto M, Qian DZ, Beer TM, Kyprianou N (2010) Tubulin-targeting chemotherapy impairs androgen receptor activity in prostate cancer. *Cancer research* **70**: 7992-8002

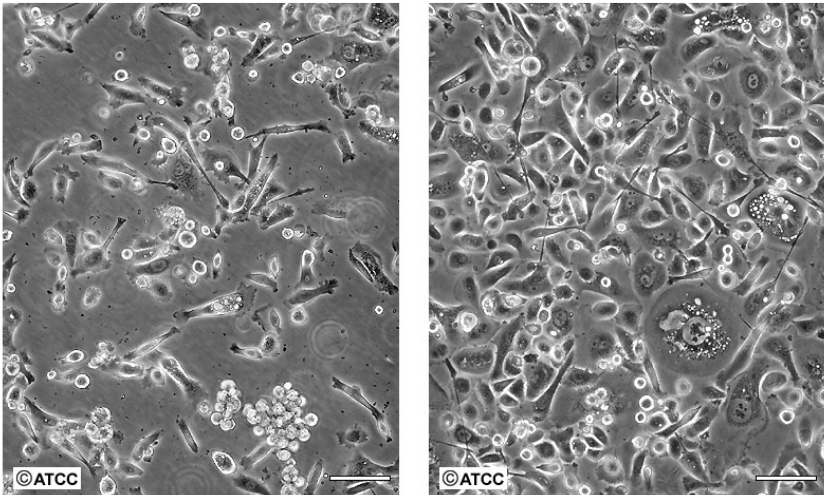
Zietman AL, DeSilvio ML, Slater JD, Rossi CJ, Jr., Miller DW, Adams JA, Shipley WU (2005) Comparison of conventional-dose vs high-dose conformal radiation therapy in clinically localized adenocarcinoma of the prostate: a randomized controlled trial. *JAMA : the journal of the American Medical Association* **294**: 1233-1239

Appendix I

Cell Line Specifications

**Spec sheets obtained from the ATCC website Accessed
March 28th 2015.**

	PC-3 (ATCC[®] CRL-1435[™])
Organism	<i>Homo sapiens</i> , human
Tissue	prostate; derived from metastatic site: bone
Product Format	frozen
Morphology	epithelial
Culture Properties	adherent (The cells form clusters in soft agar and can be adapted to suspension growth)
Biosafety Level	1
Disease	grade IV, adenocarcinoma
Age	62 years adult
Gender	male
Ethnicity	Caucasian
Applications	This cell line is a suitable transfection host.
Storage Conditions	liquid nitrogen vapor phase
Karyotype	The line is near-triploid with a modal number of 62 chromosomes. There are nearly 20 marker chromosomes commonly found in each cell; and normal N2, N3, N4, N5, N12, and N15 are not found. No normal Y chromosomes could be detected by Q-band analysis.

	<p>ATCC Number: CRL-1435 Designation: PC-3</p>  <p>Low Density Scale Bar = 100µm High Density Scale Bar = 100µm</p>
Derivation	The PC-3 was initiated from a bone metastasis of a grade IV prostatic adenocarcinoma from a 62-year-old male Caucasian.
Clinical Data	62 years adult Caucasian male The PC-3 was initiated from a bone metastasis of a grade IV prostatic adenocarcinoma from a 62-year-old male Caucasian.
Antigen Expression	HLA A1, A9
Genes Expressed	HLA A1, A9
Tumorigenic	Yes
Effects	Yes, in semi-solid medium Yes, tumors developed within 21 days at 100 % frequency (5/5) in nude mice inoculated subcutaneously with 10(7) cells.
Comments	The cells exhibit low acid phosphatase and testosterone-5- <i>alpha</i> reductase activities.
Complete Growth Medium	The base medium for this cell line is ATCC-formulated F-12K Medium, Catalog No. 30-2004. To make the complete growth medium, add the following components to the base medium: fetal bovine serum to a final concentration of 10 %.
Subculturing	<p>Volumes are given for a 75 cm² flask. Increase or decrease the amount of dissociation medium needed proportionally for culture vessels of other sizes. Corning® T-75 flasks (catalog #430641) are recommended for subculturing this product.</p> <ol style="list-style-type: none"> 1. Remove and discard culture medium. 2. Briefly rinse the cell layer with 0.25 % (w/v) Trypsin-0.53 mM EDTA solution to remove all traces of serum that contains trypsin inhibitor.

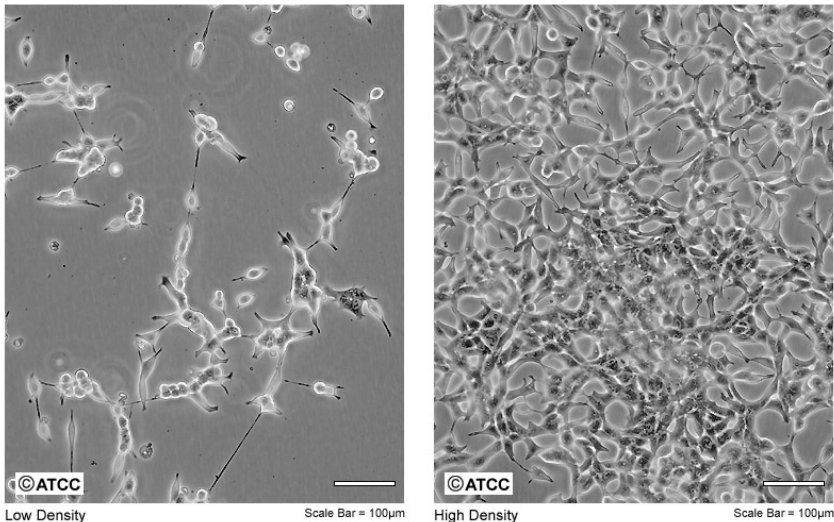
	<p>3. Add 2.0 to 3.0 mL of Trypsin-EDTA solution to flask and observe cells under an inverted microscope until cell layer is dispersed (usually within 5 to 15 minutes). Note: To avoid clumping do not agitate the cells by hitting or shaking the flask while waiting for the cells to detach. Cells that are difficult to detach may be placed at 37 °C to facilitate dispersal.</p> <p>4. Add 6.0 to 8.0 mL of complete growth medium and aspirate cells by gently pipetting.</p> <p>5. Add appropriate aliquots of the cell suspension to new culture vessels.</p> <p>6. Incubate cultures at 37 °C.</p> <p>Subcultivation Ratio: A subcultivation ratio of 1:3 to 1:6 is recommended Medium Renewal: 2 to 3 times per week</p>
Cryopreservation	<p>Freeze medium: Complete growth medium supplemented with 5 % (v/v) DMSO Storage temperature: liquid nitrogen vapor phase</p>
Culture Conditions	<p>Atmosphere: air, 95 %; carbon dioxide (CO₂), 5 % Temperature: 37 °C</p>

	DU 145 (ATCC® HTB-81™)
Organism	<i>Homo sapiens</i> , human
Tissue	prostate; derived from metastatic site: brain
Product Format	frozen
Morphology	epithelial
Culture Properties	adherent
Biosafety Level	1
Disease	carcinoma
Age	69 years
Gender	male
Ethnicity	Caucasian
Applications	This cell line is a suitable transfection host.
Storage Conditions	liquid nitrogen vapor temperature
Karyotype	This is a hypotriploid human cell line. Both 61 and 62 chromosome numbers had the highest rate of occurrence in 30 metaphase counts. The rate of higher ploidies was 3 %. The t(11q12q), del(11)(q23), 16q+, del(9)(p11), del(1)(p32) and 6 other marker chromosomes were found in most cells. The N13 was usually absent. The Y chromosome is abnormal through translocation to an unidentified chromosomal segment. The X chromosome was present in single copy.
Clinical Data	69 years Caucasian male
Antigen Expression	Antigen expression: Blood Type O; Rh+
Tumorigenic	Yes
Effects	Yes, in nude mice; forms adenocarcinoma (grade II) consistent with prostatic primary
Comments	The line is not detectably hormone sensitive, is only weakly positive for acid phosphatase and isolated cells form colonies in soft agar. The cells do not express prostate antigen. Ultrastructural analyses of both the cell line and original tumor revealed microvilli, tonofilaments, desmosomes, any mitochondria, well-developed Golgi and heterogenous lysosomes.
Complete Growth Medium	The base medium for this cell line is ATCC-formulated Eagle's Minimum Essential Medium, Catalog No. 30-2003. To make the complete growth medium, add the following components to the base medium: fetal bovine serum to a final concentration of 10 %.

Subculturing	<ol style="list-style-type: none"> 1. Remove and discard culture medium. 2. Briefly rinse the cell layer with 0.25 % (w/v) Trypsin - 0.53 mM EDTA solution to remove all traces of serum which contains trypsin inhibitor. 3. Add 2.0 to 3.0 mL of Trypsin-EDTA solution to flask and observe cells under an inverted microscope until cell layer is dispersed (usually within 5 to 15 minutes). Note: To avoid clumping do not agitate the cells by hitting or shaking the flask while waiting for the cells to detach. Cells that are difficult to detach may be placed at 37 °C to facilitate dispersal. 4. Add 6.0 to 8.0 mL of complete growth medium and aspirate cells by gently pipetting. 5. Add appropriate aliquots of the cell suspension to new culture vessels. Corning® T-75 flasks (catalog #430641) are recommended for subculturing this product. 6. Incubate cultures at 37 °C. <p>Subcultivation Ratio: A subcultivation ratio of 1:4 to 1:6 is recommended</p> <p>Medium Renewal: 2 to 3 times per week</p>
Cryopreservation	<p>Freeze medium: Complete growth medium, 95 %; DMSO, 5 %</p> <p>Storage temperature: liquid nitrogen vapor temperature</p>
Culture Conditions	<p>Atmosphere: air, 95 %; carbon dioxide (CO₂), 5 %</p> <p>Temperature: 37 °C</p>

	22Rv1 (ATCC® CRL-2505™)
Organism	<i>Homo sapiens</i> , human
Tissue	prostate
Cell Type	Epithelial
Product Format	frozen
Morphology	epithelial
Culture Properties	adherent
Biosafety Level	2
Disease	carcinoma
Storage Conditions	liquid nitrogen vapor phase
Karyotype	49,XY,del(1)(p10),+i(1)(q10),der(2)t(2;4)(p13;q31)del(2)(q13q33),der(4)t(2;4)(p13;q31),t(6;14)(q15;q32),+7,+12[5]/50,ide m,+3[1]
Derivation	22Rv1 is a human prostate carcinoma epithelial cell line derived from a xenograft that was serially propagated in mice after castration-induced regression and relapse of the parental, androgen-dependent CWR22 xenograft.
Antigen Expression	prostate specific antigen (PSA)
Receptor Expression	androgen receptor
Tumorigenic	Yes
Effects	Yes, forms tumors in nude mice
Comments	The cell line expresses prostate specific antigen (PSA). Growth is weakly stimulated by dihydroxytestosterone and lysates are immunoreactive with androgen receptor antibody by Western blot analysis. Growth is stimulated by epidermal growth factor (EGF) but is not inhibited by transforming growth factor <i>beta</i> -1 (TGF <i>beta</i> -1). Recently , it has been shown that 22Rv1 prostate carcinoma cells produce high-titer of the human retrovirus XMRV (xenotropic murine leukemia virus-related virus).
Complete Growth Medium	The base medium for this cell line is ATCC-formulated RPMI-1640 Medium, Catalog No. 30-2001. To make the complete growth medium, add the following components to the base medium: fetal bovine serum to a final concentration of 10 %.
Subculturing	Volumes used in this protocol are for 75 cm ² flask; proportionally reduce or increase amount of dissociation medium for culture vessels of other sizes.

	<ol style="list-style-type: none"> 1. Remove and discard culture medium. 2. Briefly rinse the cell layer with 0.25 % (w/v) Trypsin-0.53mM EDTA solution to remove all traces of serum that contains trypsin inhibitor. 3. Add 2.0 to 3.0 mL of Trypsin-EDTA solution to flask and observe cells under an inverted microscope until cell layer is dispersed (usually within 5 to 15 minutes). <p>Note: To avoid clumping do not agitate the cells by hitting or shaking the flask while waiting for the cells to detach. Cells that are difficult to detach may be placed at 37 °C to facilitate dispersal.</p> <ol style="list-style-type: none"> 4. Add 6.0 to 8.0 mL of complete growth medium and aspirate cells by gently pipetting. 5. Add appropriate aliquots of the cell suspension to new culture vessels. 6. Incubate cultures at 37 °C <p>Subculture Ratio: 1:3 to 1:6 Medium Renewal: Every 2 to 3 days. Note: For more information on enzymatic dissociation and subculturing of cell lines consult Chapter 10 in Culture of Animal Cells, a manual of Basic Technique by R. Ian Freshney, 3rd edition, published by Alan R. Liss, N.Y., 1994.</p>
Cryopreservation	Freeze medium: Complete growth medium supplemented with 5 % (v/v) DMSO Storage temperature: liquid nitrogen vapor phase
Culture Conditions	Temperature: 37 °C
Population Doubling Time	40 hours

	LNCaP clone FGC (ATCC® CRL-1740™)
Organism	<i>Homo sapiens</i> , human
Tissue	prostate; derived from metastatic site: left supraclavicular lymph node
Product Format	frozen
Morphology	epithelial
Culture Properties	adherent, single cells and loosely attached clusters
Biosafety Level	1
Disease	carcinoma
Age	50 years adult
Gender	male
Ethnicity	Caucasian
Applications	This cell line is suitable as a transfection host.
Storage Conditions	liquid nitrogen vapor phase
Karyotype	This is a hypotetraploid human cell line. The modal chromosome number was 84, occurring in 22 % of cells. However, cells with chromosome counts of 86 (20 %) and 87 (18 %) also occurred at high frequencies. The rate of cells with higher ploidies was 6.0 %.
Images	<p>ATCC Number: CRL-1740 Designation: LNCaP clone FGC</p>  <p>©ATCC Low Density Scale Bar = 100µm ©ATCC High Density Scale Bar = 100µm</p>
Derivation	LNCaP clone FGC was isolated in 1977 by J.S. Horoszewicz, <i>et al.</i> , from a needle aspiration biopsy of the left supraclavicular lymph node of a 50-year-old Caucasian male (blood type B+) with confirmed diagnosis of metastatic prostate carcinoma.
Clinical Data	50 years adult

	<p>from a needle aspiration biopsy of the left supraclavicular lymph node of a 50-year-old Caucasian male (blood type B+) with confirmed diagnosis of metastatic prostate carcinoma.</p> <p>Caucasian Male</p>
Receptor Expression	androgen receptor, positive; estrogen receptor, positive Ref
Genes Expressed	human prostatic acid phosphatase; prostate specific antigen
Cellular Products	human prostatic acid phosphatase; prostate specific antigen
Tumorigenic	Yes
Effects	Yes, in soft agar Yes, the cells are tumorigenic in nude mice
Comments	<p>These cells are responsive to 5-<i>alpha</i>-dihydrotestosterone (growth modulation and acid phosphatase production). The cells do not produce a uniform monolayer, but grow in clusters which should be broken apart by repeated pipetting when subcultures are prepared. They attach only lightly to the substrate, do not become confluent and rapidly acidify the medium. Growth is very slow. The cells should be allowed to incubate undisturbed for the first 48 hours after subculture. When flask cultures are shipped, the majority of the cells become detached from the flask and float in the medium. Upon receipt, incubate the flask (in the usual position for monolayer cultures) for 24 to 48 hours to allow the cells to re-attach. The medium can then be removed and replaced with fresh medium. If desired, the contents of the flask can be collected, centrifuged at 300 X g for 15 minutes, resuspended in 10 mL of medium and dispensed into a single flask.</p>
Complete Growth Medium	The base medium for this cell line is ATCC-formulated RPMI-1640 Medium, Catalog No. 30-2001. To make the complete growth medium, add the following components to the base medium: fetal bovine serum to a final concentration of 10 %.
Subculturing	<p>Volumes are given for a 75 cm² flask. Increase or decrease the amount of dissociation medium needed proportionally for culture vessels of other sizes. Corning® T-75 flasks (catalog #430641) are recommended for subculturing this product</p> <ol style="list-style-type: none"> 1. Remove and discard culture medium. 2. Briefly rinse the cell layer with 0.25 % (w/v) Trypsin-0.53 mM EDTA solution to remove all traces of serum that contains trypsin inhibitor. 3. Add 2.0 to 3.0 mL of Trypsin-EDTA solution to flask

	<p>and observe cells under an inverted microscope until cell layer is dispersed (usually within 5 to 15 minutes). Note: To avoid clumping do not agitate the cells by hitting or shaking the flask while waiting for the cells to detach. Cells that are difficult to detach may be placed at 37 °C to facilitate dispersal.</p> <ol style="list-style-type: none"> 4. Add 6.0 to 8.0 mL of complete growth medium and aspirate cells by gently pipetting. 5. Add appropriate aliquots of the cell suspension to new culture vessels. Maintain cultures at a cell concentration between 1×10^4 and 2×10^5 cells/cm². 6. Incubate cultures at 37 °C. <p>Subcultivation Ratio: A subcultivation ratio of 1:3 to 1:6 is recommended Medium Renewal: Twice per week</p>
Cryopreservation	<p>Freeze medium: Complete growth medium supplemented with 5 % (v/v) DMSO Storage temperature: liquid nitrogen vapor phase</p>
Culture Conditions	<p>Atmosphere: air, 95 %; carbon dioxide (CO₂), 5 % Temperature: 37 °C</p>
Population Doubling Time	<p>about 34 hours</p>

Appendix II

**Toner *et al.* Br J Cancer
(2013)**

Keywords: prostate cancer; chemotherapeutic; toluidine sulphonamide; taxane; MDR1 drug resistance; Hif1

The novel toluidine sulphonamide EL102 shows pre-clinical *in vitro* and *in vivo* activity against prostate cancer and circumvents MDR1 resistance

A P Toner¹, F McLaughlin², F J Giles^{1,3}, F J Sullivan^{1,3,4}, E O'Connell⁵, L A Carleton⁶, L Breen⁷, G Dunne⁷, A M Gorman⁶, J D Lewis² and S A Glynn^{*,1}

¹Prostate Cancer Institute, National University of Ireland Galway, Galway, Ireland; ²Elara Pharmaceuticals GmbH, Heidelberg, Germany; ³HRB Clinical Research Facilities Galway & Dublin, National University of Ireland Galway and Trinity College, Dublin, Ireland; ⁴Department of Radiation Oncology, Galway University Hospital, Galway, Ireland; ⁵National Centre for Biomedical Engineering Science, National University of Ireland Galway, Galway, Ireland; ⁶Apoptosis Research Centre, School of Natural Sciences, National University of Ireland Galway, Galway, Ireland and ⁷National Institute for Cellular Biotechnology, Dublin City University, Dublin, Ireland

Background: Taxanes are routinely used for the treatment of prostate cancer, however the majority of patients eventually develop resistance. We investigated the potential efficacy of EL102, a novel toluidine sulphonamide, in pre-clinical models of prostate cancer.

Methods: The effect of EL102 and/or docetaxel on PC-3, DU145, 22Rv1 and CWR22 prostate cancer cells was assessed using cell viability, cell cycle analysis and PARP cleavage assays. Tubulin polymerisation and immunofluorescence assays were used to assess tubulin dynamics. CWR22 xenograft murine model was used to assess effects on tumour proliferation. Multidrug-resistant lung cancer DLKPA was used to assess EL102 in a MDR1-mediated drug resistance background.

Results: EL102 has *in vitro* activity against prostate cancer, characterised by accumulation in G2/M, induction of apoptosis, inhibition of Hif1 α , and inhibition of tubulin polymerisation and decreased microtubule stability. *In vivo*, a combination of EL102 and docetaxel exhibits superior tumour inhibition. The DLKP cell line and multidrug-resistant DLKPA variant (which exhibits 205 to 691-fold greater resistance to docetaxel, paclitaxel, vincristine and doxorubicin) are equally sensitive to EL102.

Conclusion: EL102 shows potential as both a single agent and within combination regimens for the treatment of prostate cancer, particularly in the chemoresistance setting.

Prostate cancer is the second most common cancer diagnosed in men globally, accounting for 13.6% of all cancer cases in men worldwide (<http://globocan.iarc.fr>) in 2008. In the United States, the National Cancer Institute (NCI) estimates that 241 740 men will have been diagnosed with and 28 170 men will have died of cancer of the prostate during 2012 (<http://seer.cancer.gov>). Several

choices exist for the treatment of early prostate cancer, including radical prostatectomy, external beam radiation and prostate brachytherapy, with similar outcomes (Peinemann *et al*, 2011). Despite advances in primary treatment of prostate cancer, in a subset of patients the disease progresses and distant metastases develop. While these patients can initially be treated with androgen

*Correspondence: Dr S Glynn; E-mail: sharon.glynn@nuigalway.ie

Received 17 May 2013; revised 13 August 2013; accepted 14 August 2013

© 2013 Cancer Research UK. All rights reserved 0007–0920/13



ablation therapies, eventually their cancer will become refractory and they will succumb to their illness. In the mid-2000s, introduction of taxane-based therapies improved the outcomes of patients with metastatic castrate-resistant prostate cancer, extending survival by several months. The taxane family, which includes paclitaxel, docetaxel and the newly approved cabazitaxel are natural or semi-synthetic plant derivatives that are widely used in the treatment of metastatic castrate-resistant prostate cancer (mCRPC). Their mechanisms of action have been widely reported (Rowinsky *et al*, 1990; Jackson *et al*, 2007) and have been shown to act as mitotic arresting agents (Wani *et al*, 1971; Douros and Suffness, 1981). The dynamic ability of a cell to assemble and disassemble the architecture of the microtubules from and to tubulin components, respectively, is curtailed greatly by the introduction of taxanes (Manfredi and Horwitz, 1984). Phase III trials demonstrated that docetaxel–estradiol combinations conferred median survival advantage of ~3 months compared with the standard mitoxantrone–prednisone combination (Petrylak *et al*, 2004; Berthold *et al*, 2008). Since 2010, an additional six drugs have been approved for use in patients with metastatic castrate-resistant prostate cancer. These include drugs targeting androgen receptor activity (abiraterone acetate and enzalutamide), drugs targeting bone metastasis and the micro-environment (denosumab and alpharadin), immunotherapeutics (Sipuleucel-T) and new taxanes (cabazitaxel) (Heidegger *et al*, 2013).

It is postulated that combination treatments of docetaxel with alternative cytotoxics could prevent this late-stage resistance, with such other compounds acting in an additive or synergistic fashion. While phase II trials with various combinations of new drugs have suggested promise for emerging docetaxel combination therapies (Oh *et al*, 2003; Ferrero *et al*, 2006; Tester *et al*, 2006; Kikuno *et al*, 2007; Garcia *et al*, 2011), of note is the fact that no drug has yet been shown to provide survival benefit when combined with docetaxel in phase III trials (Antonarakis and Eisenberger, 2013). This suggests that there is a need to identify novel compounds for efficacy as single agents or for use in combination with taxane-based therapies.

Here, we present preliminary data on the efficacy of a novel toluidine sulphonamide, EL102, *in vitro* against prostate cancer cell lines and in an *in vivo* prostate cancer xenograft mouse model, demonstrating EL102's ability to work in combination with docetaxel, and circumvent multiple drug resistance mediated by P-glycoprotein (Pgp). EL102 was identified by Elara Pharmaceuticals as a potential chemotherapeutic agent during a screen of novel small molecule inhibitors using the NCI-60 cell line panel assessing for growth inhibition potential. EL102 is a later generation derivative of the family of toluidine sulphonamide hypoxia-induced factor 1 (Hif1 α) inhibitors described by (Wendt *et al*, 2011). This is the first report on the biological actions of EL102 on cancer cells, focusing on its use as an anti-prostate cancer chemotherapeutic.

MATERIALS AND METHODS

Ethics statement. Tumour xenograft models were performed at EPO Experimental Pharmacology and Oncology Berlin-Buch GmbH, Germany. These studies were performed under the approval A0452/08 (Landesamt für Gesundheit und Soziales, Berlin). The study was performed according to the German Animal Protection Law and the UICC (2010).

Chemicals. The compound EL102 was developed and supplied by Elara Pharmaceuticals GmbH (Heidelberg, Germany). Docetaxel was purchased from Sigma-Aldrich (Dublin, Ireland; #01885-

5MG-F). Unless otherwise stated, all chemicals were obtained from Sigma-Aldrich.

Cell lines. DU145, PC-3, 22Rv1 and CWR22 were sourced from the American Type Culture Collection (ATCC) (Manassas, VA, USA) and cultured according to recommendations. In brief, CWR22 and 22Rv1 were cultured in RPMI 1640 medium with L-glutamine (Sigma, #R8758), and supplemented with 10% fetal bovine serum (FBS) (Sigma, #F7524). DU145 was cultured in Minimum Essential Medium (1 \times) with Earles (Gibco, Bio-Sciences, Dun Laoghaire, Ireland; #22561-021) supplemented with 10% FBS. PC-3 was cultured in F12 Nutrient Mixture (HAM) medium, with L-glutamine (Gibco #21765-029) supplemented with 10% FBS. Non-small cell lung carcinoma, DLKP and its doxorubicin-selected variant DLKPA (Pgp-mediated resistance) was developed by the National Institute for Cellular Biotechnology (Dublin City University, Dublin, Ireland) and maintained in DMEM/Hams F12 (1 : 1) supplemented with 5% FBS and 1% L-glutamine. With the exception of RPMI 1640 and FBS (Sigma), all media and supplements were Gibco (Life Technologies), purchased from Bio-Sciences. All media contained 1% of (100 \times) antibiotic-antimycotic (Life Technologies) with the exception of DLKP and DLKPA.

Prostate cancer cell line toxicity assays. Sulforhodamine B (SRB)-based assays were used to assess the effects of docetaxel and EL102 administration on cell viability as previously described (Vichai and Kirtikara, 2006). In brief, the relevant amounts of docetaxel or EL102, or combinations of both were preloaded into a 96-well plate (Sarstedt, Ireland) using the Perkin Elmer Janus Automated Workstation. Cells were trypsinised, counted and dispensed by the robotics into a 96-well cell culture plate, at a cell density of 1.9×10^4 cells per well. The drugs were then transferred by the robotics from the drug plate to the 96-well cell culture plate. This was left in culture for 72 h at 37 °C in a 5% CO₂ incubator. Separately, three rows of a non-drug-treated 96-well plate were seeded with the same cell density. After 2–4 h incubation at 37 °C, 5% CO₂, to allow for attachment of cells, 100 μ l of fixative (cold 10% trichloroacetic acid (TCA) (Sigma, #T0699)) was added to the wells and left to incubate at 4 °C for 30 min. Wells were then submerged in distilled water and tapped dry four times, to ensure complete removal of TCA. The plate was left to air dry. This plate served as day 0 plate. The 72-h incubated drug-treated plates were fixed in the same way. All plates were subsequently stained with 0.057% SRB solution in 1% acetic acid for 30 min and washed four times with 1% acetic acid, to remove excess stain. These were allowed to air dry. Stain was eluted by addition of 10 mM Tris base solution to the wells followed by 30 min incubation. Plates were read at 531 nm using a Victor X5 Multilabel plate reader. Mean optical density values of Day 0 plates were subtracted from those of sample plates. A percentage viability curve was calculated based on these values and the IC₅₀ was determined. Error was presented at \pm the percentage coefficient variant (%CV). All cytotoxicity assays were conducted in triplicate.

Multidrug-resistant cell line toxicity assays. Cells were trypsinised and resuspended in fresh media at 2×10^4 cells per ml. A volume of 100 μ l of cell suspension was seeded into each well of a 96-well plate and cultured overnight in 5% CO₂ at 37 °C. Varying concentrations of EL102 or docetaxel were added in replicate ($n=8$) and incubated at 37 °C for a further 72 h. After this incubation, media were removed from each well, which was then washed twice with 100 μ l Dulbecco's phosphate buffered saline (dPBS). Having aspirated the last of the dPBS, 100 μ l of freshly prepared phosphatase substrate (10 mM *p*-nitrophenol phosphate in 0.1 M sodium acetate (Sigma, #N7653-100ML), 0.1% Triton X-100 (Merck, Darmstadt, Germany; pH 5.5) was added to each well (Martin and Clynes, 1991). Plates were incubated in the dark at 37 °C for 2 h. The enzymatic reaction was stopped by the

addition of 50 μ l of 1 M NaOH to each well. The plates were read on a dual beam plate reader at 405 nm with a reference wavelength of 620 nm. A percentage viability curve was calculated based on these values and the IC₅₀ was determined. Error was presented at \pm the percentage coefficient variant (%CV). All cytotoxicity assays were conducted in triplicate.

Sub-G1 and cell cycle analysis by flow cytometry. Cells were seeded at a density of 1.3×10^5 cells per well in a final volume of 2 ml/well in a six-well plate and left to attach overnight at 37 °C in a 5% CO₂ incubator. Cells were treated with 1 ml of medium spiked with appropriate concentrations of EL102, docetaxel or both. Following treatments, plates were returned to the incubator for 24, 48 and 72 h. The medium from each well liquid fraction was transferred to labelled 15 ml tubes. Remaining attached cells were gently washed with 300 μ l Hanks' balanced salt solution (Sigma, #H6648) at room temperature. These washings were retained and added to the medium in the appropriate labelled 15-ml tubes. Cells were trypsinised with 750 μ l trypsin-EDTA for 5 min at 37 °C. Trypsinisation was stopped by re-addition of 1 ml of medium from the appropriate well of origin. Cell suspensions were combined with the medium in the appropriate 15-ml tubes, and cell pellets were collected by centrifugation at $1000 \times g$ at 4 °C for 5 min using soft acceleration. The supernatant was removed and the cell pellets were placed on ice. Pellets were resuspended in 500 μ l ice-cold dPBS (Sigma, #D8537) and transferred to labelled 1.5-ml tubes. Cell pellets were again recovered following centrifugation at 4 °C for 5 min at $1000 \times g$ and supernatant was discarded. Cells were resuspended in 150 μ l dPBS. A volume of 350 μ l ice-cold 100% ethanol was added dropwise to the cell suspension while vortexing, to avoid clumping. Cells were incubated on ice for 30 min. Following overnight storage at -20 °C, cells were then centrifuged at $1000 \times g$ for 5 min using soft acceleration. Each pellet was washed in 500 μ l dPBS and suspension was centrifuged at $1000 \times g$ for 5 min using soft acceleration, after which supernatant was removed. Each cell pellet was resuspended in propidium iodide, PI/RNase staining buffer (BD Pharmingen, BD Biosciences, Oxford, England; #550825). Sample suspensions were incubated in the dark for 15–20 min and measured by flow cytometry on BD FACSCanto II (BD Biosciences), channel PE. Logarithmic and linear regression was performed as needed for SubG₁ and cell cycle analyses. Flow cytometric analyses were conducted using Cyflogic software (CyFlo Ltd, Turku, Finland).

Tubulin polymerisation assay. The HST-tubulin polymerization assay kit (Cytoskeleton, Tebu-Bio, Peterborough, UK; #BK004P) was used as per the manufacturer's instructions. In brief, the assay was performed using a 96-well plate. To each well, with the exception of the blank control, 4 mg/ml of tubulin was added. Each well contained a concentration of the drug of interest and G-PEM buffer (80 mM PIPES, pH 6.9; 2 mM MgCl₂; 0.5 mM EGTA; 1 mM GTP). Drug concentrations used included 5 μ M EL102, 2 μ M docetaxel and 5 μ M EL102 and 2 μ M docetaxel combined. A concentration of 2 μ M of nocodazole was used as an inhibitor of tubulin polymerisation control. The 96-well plate was read on a 96-well plate reading spectrophotometer in kinetic mode (61 cycles: 1 s read per well per min) at wavelength 405 nm. Readings were zeroed by the blank control and mean sample values were calculated with error bars \pm s.e.m.

Tumour xenograft models. CWR22 tumours were taken from an *in vivo* passage, cut into small fragments and transplanted subcutaneously (s.c.) into the flank of 48 nude mice. At day 13, when the tumours were palpable, mice were randomised into 10 groups with 8 mice each and treatment initiated. The groups included: (A) vehicle (10% DMSO, 10% Cremophor, aqua per os (p.o.)), (B) docetaxel 12 mg kg⁻¹ intravenously (i.v.), (C) EL102 12 mg kg⁻¹ via p.o. (0700 hours and 1700 hours daily),

(D) EL102 15 mg kg⁻¹ via p.o. (E) docetaxel 12 mg kg⁻¹ via i.v. and EL102 12 mg kg⁻¹ via p.o. and (F) docetaxel 12 mg kg⁻¹ via i.v. and EL102 15 mg kg⁻¹ via p.o. The injection volume was 5 ml kg⁻¹. The different tumour groups were sacrificed on separate days for ethical reasons (large tumours). Tumour diameter of the s.c. tumour and mouse body weight were measured twice a week with a caliper. Tumour volumes were calculated according to $V = (\text{length} \times (\text{width})^2) / 2$. Tumour xenograft models were performed at EPO Experimental Pharmacology and Oncology Berlin-Buch GMBH, Germany. These studies were performed under the approval A0452/08 (Landesamt für Gesundheit und Soziales, Berlin). The study was performed according to the German Animal Protection Law and the UICCR, 2010.

Western blot analysis. Cells were seeded in 10-cm³ dishes at a cell density of 1×10^6 per dish, and treated with the relevant doses of EL102 and docetaxel for the required time period. After treatment, cells were rinsed twice with cold PBS and lysed directly on the dish with cold RIPA buffer (Pierce, Fisher Scientific, Dublin, Ireland; #89900) supplemented with protease inhibitors (Pierce, #78410), scraped, and spun at 14 000 g for 15 min at 4 °C. Supernatant was collected and stored at -20 °C for western blot analysis of protein expression. Extracted protein was quantified using a BCA kit (Fisher Scientific, Dublin, Ireland). Both PARP and Hif1 α levels were detected through use of primary anti-PARP rabbit polyclonal antibody (Cell Signaling Technology Inc., Danvers, Massachusetts, USA; #9542) and anti-Hif1 α rabbit polyclonal antibody (Millipore, Temecula, California, USA; #07-628), respectively. The anti-PARP antibody was diluted 1:1000 and anti-Hif1 α antibody was diluted 1:1500 in 5% skimmed milk reconstituted in 1 \times Tris-buffered saline (TBS) (pH 8) 0.1% Tween. These dilutions were added to the transfer membrane, and shaken overnight at 4 °C, following a 1 h RT blocking in 5% skimmed milk in TBS. Mouse monoclonal anti- β -actin antibody (Thermo-Scientific Pierce, Fisher Scientific, Dublin, Ireland; #10624754) was used to confirm even protein loading. Secondary antibodies used were IRDye 800CW goat anti-rabbit IgG (LI-COR Biosciences, Cambridge, UK; #926-32211) and IRDye 680LT goat anti-mouse IgG (LI-COR Biosciences; #926-68020) and detection was imaged on the LI-COR ODYSSEY CLx imaging system.

Immunocytofluorescence. Coverslips, pre-sterilised in 100% ethanol, were inserted to the base of each well of a six-well plate. Cells were seeded at a density of 1×10^6 per well and allowed overnight attachment at 37 °C, in a 5% CO₂ incubator. Cell treatment and fixation was carried out at the relevant time points. Cells were fixed for 10 min in ice-cold methanol. For immunocytofluorescence, primary antibodies against β -tubulin (Abcam, Cambridge, UK #AB6046), diluted 1:200, and acetylated tubulin (Sigma, #T6793), diluted 1:200, were used with secondary fluorescent conjugates Rhodamine Red-X-AffiniPure Fab Fragment goat anti-mouse IgG (H + L) (Jackson ImmunoResearch Europe Ltd., Suffolk, UK #JAC-115297003), diluted 1:50, and Alexa Fluor 647 donkey anti-rabbit IgG (Invitrogen, Bio Sciences, Dun Laoghaire, Ireland; #A31573), diluted 1:50, respectively. These cells were counterstained with mounting medium SlowFade Gold antifade reagent (Invitrogen; #S36936) supplemented with 4',6-diamidino-2-phenylindole dihydrochloride (DAPI) (Sigma; #D8417) diluted 1:100 and coverslips were fixed to slides using nail varnish. Staining was imaged using Delta Vision Core Imaging System C0607 (Applied Precision, Issaquah, WA, USA). Image analysis was conducted using SoftWoRx software (Applied Precision) and FIJI software (GPL v2).

Statistics. Data analysis was performed using GraphPad Prism Version 5. All statistical tests were 2-sided, and an association was considered statistically significant with *P*-values < 0.05. The Student's *t*-test was used to analyse differences between treatment

groups in cell culture experiments. IC_{50} values were calculated using log (inhibitor) vs normalised response curve ($Y = 100 / (1 + 10^{(X - \log IC_{50})})$). For the xenograft model, a one-way ANOVA with Tukey's multiple comparisons test was used to determine whether there were significant differences in the tumour volumes or body weights between the treatment groups. Additionally, linear regression was used to fit a slope to the tumour growth curve to determine whether the rate of growth differed between the treatment groups.

RESULTS

EL102 inhibits prostate cancer cell line viability *in vitro*. EL102, whose chemical structure is shown in Figure 1A, is a novel toluidine sulphonamide. To determine whether EL102 could have utility as a chemotherapeutic agent in prostate cancer, we determined the effects of increasing doses of EL102 on prostate cancer cell line viability in comparison to the clinically used docetaxel. A panel of four prostate cancer cell lines were used in this study, including CWR22 (androgen receptor (AR)-positive, androgen dependent, non-metastatic), its daughter cell line 22Rv1 (AR-positive, androgen independent, non-metastatic), PC-3 (AR-negative, derived from metastatic bone lesion) and DU145 (AR-negative, derived from metastatic brain lesion). Figures 1B and C demonstrate the effects of increasing doses of EL102 and docetaxel as single agents, respectively, on prostate cancer cell line viability over a 3-day drug exposure. This demonstrates that while docetaxel is more potent than EL102, both EL102 and docetaxel decrease prostate cancer cell viability in a dose-dependent manner. Table 1 shows that CWR22 and 22Rv1 are equally sensitive to docetaxel (IC_{50} 0.4–0.6 nM), while bone metastatic cell line, PC-3, is 2.5–10 fold more resistant to docetaxel than the other cell lines (IC_{50} 3.8 nM). EL102 inhibited cell proliferation with an IC_{50} of ~21–40 nM. By comparison, bone metastatic PC-3 cells were twofold more resistant than CWR22

and 22Rv1 to EL102, and were equally as sensitive as brain metastatic cell line DU145.

Cell lines with MDR1-mediated drug resistance are sensitive to EL102. A classic method of chemotherapeutic drug resistance involves the overexpression of drug resistance pump Pgp. We tested EL102 in a poorly differentiated squamous lung carcinoma cell line pair: DLKP and its doxorubicin-selected variant DLKPA (Clynes *et al*, 1992). Table 2 shows that DLKPA is cross-resistant to the taxanes, docetaxel (253-fold) and paclitaxel (258-fold). Its

Table 1. Prostate cancer cell line inhibition by docetaxel and EL102

Cell line	Docetaxel (nM) $IC_{50} \pm$ s.d.	EL102 (nM) $IC_{50} \pm$ s.d.
CWR22	0.4 ± 0.01	24.0 ± 1.41
22Rv1	0.6 ± 0.15	21.7 ± 2.31
DU145	1.5 ± 0.18	40.3 ± 7.71
PC-3	3.8 ± 0.76	37.0 ± 2.00

Abbreviation: s.d. = standard deviation.

Table 2. Cross-resistance profile of DLKP and DLKPA

	DLKP $IC_{50} \pm$ s.d.	DLKPA $IC_{50} \pm$ s.d.	Fold change
Adriamycin (nM)	24 ± 2	4900 ± 300	204
Docetaxel (nM)	0.15 ± 0.04	38 ± 3.0	253
Paclitaxel (nM)	1.2 ± 0.5	310 ± 25	258
EL102 (nM)	14.4 ± 0.8	16.3 ± 1.2	1.1
Vincristine (nM)	0.91 ± 0.1	629 ± 160	691

Abbreviation: s.d. = standard deviation.

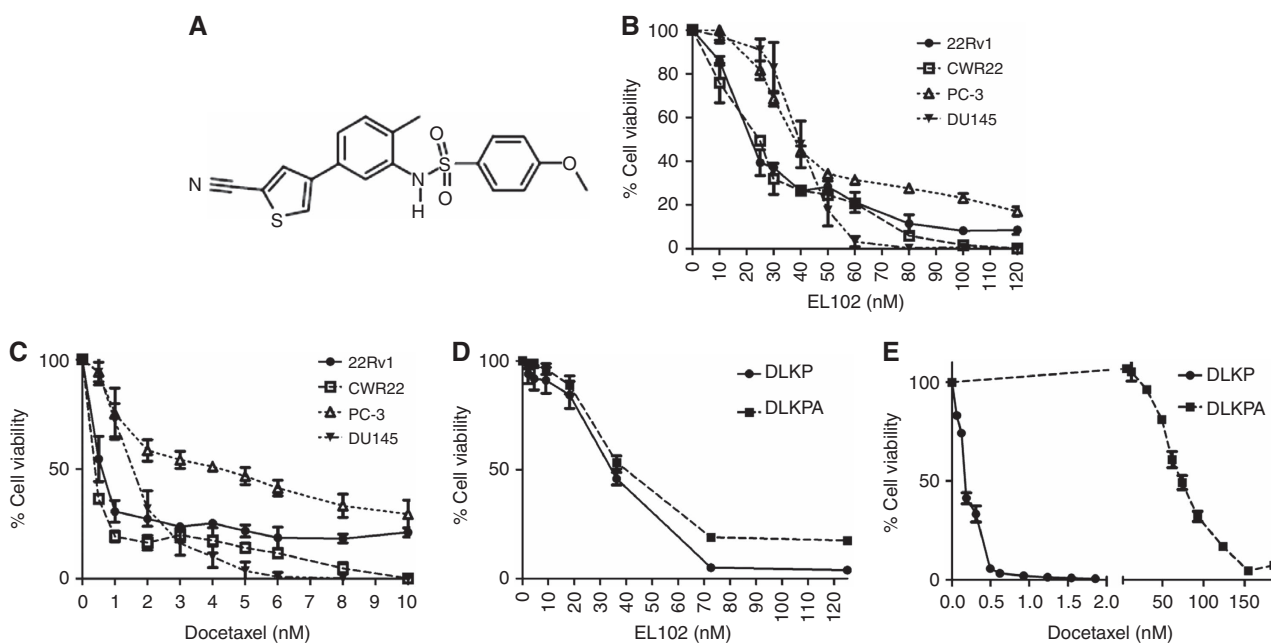


Figure 1. Impact of EL102 and docetaxel on prostate cancer cell line viability *in vitro*. (A) Chemical structure of EL102. (B) Dose response effects of EL102 on prostate cancer cell line viability over 72-h exposure. (C) Dose response effects of docetaxel on prostate cancer cell line viability over 72-h exposure. (D) Effect of EL102 on doxorubicin and docetaxel-resistant DLKPA lung cancer cell line viability vs DLKP parental lung cancer cell line. (E) Comparison of docetaxel sensitivity in the doxorubicin and docetaxel-resistant DLKPA lung cancer cell line viability vs DLKP parental lung cancer cell line.

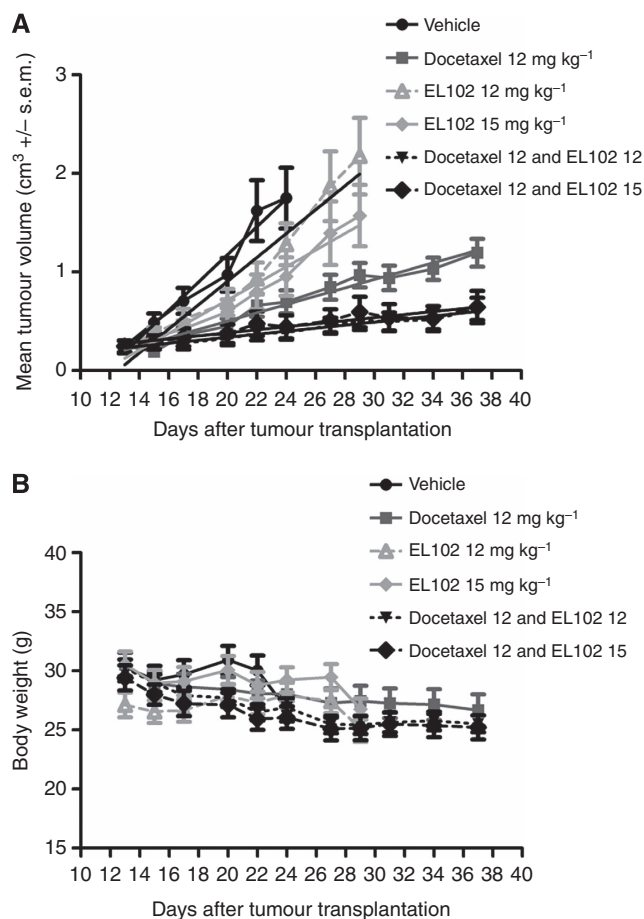


Figure 2. Impact of EL102 and docetaxel alone and in combination on CWR22 xenograft tumour volume. (A) Effect of vehicle vs 12 mg kg⁻¹ docetaxel, vs 12 mg kg⁻¹ EL102, vs 15 mg kg⁻¹ EL102, vs 12 mg kg⁻¹ docetaxel plus 12 mg kg⁻¹ EL102, vs 12 mg kg⁻¹ docetaxel plus 15 mg kg⁻¹ EL102, on CWR22 tumour volume using a 5-day on/2-day off schedule (tumour volume (cm³) ± s.e.m.). (See Supplementary Table 1 for one-way ANOVA comparing tumour volume at each time point). (B) Effect of vehicle vs 12 mg kg⁻¹ docetaxel, vs 12 mg kg⁻¹ EL102, vs 15 mg kg⁻¹ EL102, vs 12 mg kg⁻¹ docetaxel plus 12 mg kg⁻¹ EL102, vs 12 mg kg⁻¹ docetaxel plus 15 mg kg⁻¹ EL102, on mouse body weight (Note: vehicle group killed on day 24 due to tumour size). (See Supplementary Table 2 for one-way ANOVA comparing body weight at each time point.)

mechanism of resistance is primarily through overexpression of Pgp as previously described (Keenan *et al*, 2009; Collins *et al*, 2010; Dunne *et al*, 2011). While DLKPA overexpresses Pgp, it does not express the MRP1 or BCRP drug resistance pumps (Collins *et al*, 2010). Figure 1D and Table 2 shows that while the DLKPA variant is resistant to docetaxel, both parent cell line DLKP and its drug-resistant variant DLKPA are equally sensitive to EL102 (Figure 1E).

EL102 potentiates the effects of docetaxel *in vivo*. To determine whether EL102 could be used in combination with docetaxel *in vivo*, we examined the ability of the combination of docetaxel with EL102 to inhibit tumour growth in a CWR22 xenograft mouse model (Figure 2A). While administration of 12 mg kg⁻¹ EL102 using a 5-day on/2-day off regimen did not significantly inhibit rate of tumour growth compared with vehicle (slope (R^2): vehicle 0.1414 ± 0.01438 (0.9603) vs EL102 12 mg kg⁻¹, 0.1210 ± 0.01179 (0.9462), F -test: $P=0.3385$), increasing the dosage to 15 mg kg⁻¹ EL102 did inhibit the rate of tumour growth compared with vehicle (slope (R^2): vehicle 0.1414 ± 0.01438 (0.9603) vs EL102 15 mg kg⁻¹, 0.08451 ± 0.006934 (0.9612), F -test: $P=0.003$).

Administration of 12 mg kg⁻¹ docetaxel decreased the rate of tumour growth more efficiently than EL102 (slope (R^2): vehicle 0.1414 ± 0.01438 (0.9603) vs docetaxel 12 mg kg⁻¹ 0.04230 ± 0.002531 (0.9688), F -test: $P<0.0001$), while the combination of both drugs had the largest effect on inhibition of tumour growth, suggesting that these drugs work well together in combination *in vivo* (slope (R^2): vehicle 0.1414 ± 0.01438 (0.9603) vs docetaxel 12 mg kg⁻¹ and EL 102 12 mg kg⁻¹ 0.01533 ± 0.0008838 (0.9709), F -test: $P<0.0001$ or vehicle, 0.1414 ± 0.01438 (0.9603) vs docetaxel 12 mg kg⁻¹ and EL 102 15 mg kg⁻¹, 0.01537 ± 0.001704 (0.9003), F -test: $P<0.0001$). Comparison of the docetaxel arm vs the combination arms showed a significant difference in the rate of tumour growth indicating that the addition of EL102 to docetaxel improves anti-tumour activity (F -test, $P<0.0001$). Supplementary Table 1 describes the results of a one-way ANOVA test on this model, using a Tukey's *post-hoc* test to assess statistical difference in tumour volume between the treatment arms at different time points. Additionally to determine if combining EL102 and docetaxel was well tolerated by the mice with minimal adverse effects, we compared changes in mean body weight between the treatment arms and found no significant differences between the groups compared with vehicle or between different treatment arms (Figure 2B). Supplementary Table 2 describes the results of a one-way ANOVA test on this model, using a Tukey's *post-hoc* test to assess statistical difference in body weights between the treatment arms at different time points.

EL102 is cytotoxic to prostate cancer cell lines and induces cellular apoptosis.

As demonstrated in Figure 1B and Table 1, EL102 is a potent inhibitor of prostate cancer cell viability, and when combined with docetaxel *in vivo* inhibits tumour growth to a greater extent than either alone (Figure 2A). In an attempt to further address the mechanisms driving the combination of the two agents we performed an *in vitro* combination assay looking at the impact of the combining EL102 and docetaxel on cell viability (Figure 3). Results show that *in vitro*, combining EL102 and docetaxel does not have an additive effect on inhibition of cell viability. To determine whether these effects were cytostatic or cytotoxic, we quantified the number of cells in subG₁ phase indicating loss of cellular DNA and entry into late apoptosis using logarithmic scale propidium iodide flow cytometry (Figure 4). Cells were exposed to increasing doses of EL102 and docetaxel. EL102 was an equally strong inducer of apoptosis at 100 nM in all four prostate cancer cell lines, while it failed to induce apoptosis at 10 nM of EL102 (Figure 4A–D), despite inhibiting cell viability by approximately 25–30% at 10 nM (Figures 3A–D). Apoptosis was detectable at 24 h and steadily increased over the next 48 h (72 h total), indicating that EL102-dependent inhibition of cell viability is partially due to cytotoxic effects, namely induction of apoptosis. Similarly, docetaxel induced apoptosis in all 4 cell lines in a dose-dependent and temporal manner. When EL102 and docetaxel were administered in combination *in vitro*, no additive effects were seen on the levels of apoptosis in these cell lines (Figure 4), similar to the cell viability assays (Figure 3). Of note though is that while 10 nM of EL102 failed to induce increased apoptosis (Figure 4), it did lead to significantly decreased % cell viability compared to control (Figure 3) in each cell line, indicating non-apoptosis effects at low concentrations. Figures 5A–D shows representative histograms from these experiments in the DU145 prostate cancer cell line. In addition to demonstrating an increase in subG₁ accumulation, the histograms indicated that combining the agents altered the cell cycle dynamics. These effects in DU145 are quantified at 24 (Figure 5E), 48 (Figure 5F) and 72 (Figure 5G) h, and demonstrate that combining EL102 and docetaxel causes greater loss of cells from G₁ and accumulation in G₂/M than either alone by 24 h at low doses. Also of interest in the combination assays cell profile images is a peak beyond the G₂/M peak which

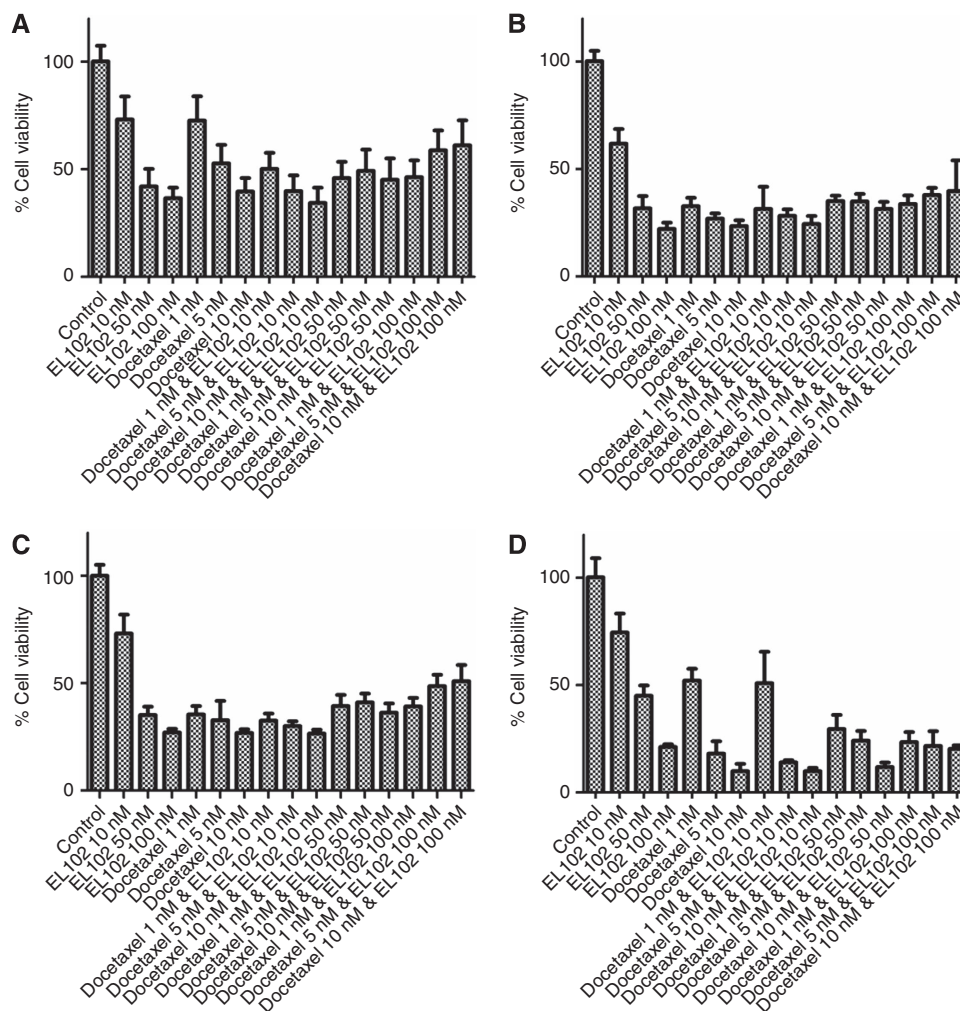


Figure 3. Impact of EL102 and docetaxel combination treatment on prostate cancer cell line viability *in vitro*. Effect of EL102 and docetaxel in combination of *in vitro* cell viability after 72 h in (A) CWR22, (B) 22Rv1, (C) PC-3 and (D) DU145 prostate cancer cell. (See Supplementary Table 3 for results of one-way ANOVA comparing cell viability between each treatment.)

represents a subset of cells with increased DNA content (8X). Apoptosis induction upon *in vitro* EL102 and docetaxel administration was further evidenced by detection of PARP cleavage in protein extracted from DU145 cell lysate, 24 and 48 h post-treatment. PARP cleavage increases in a dose-dependent manner and over time with the strongest detection seen in lysates of cells cultured with dual treatments at 48 h (Figure 4E).

EL102 has both cytostatic and cytotoxic effects. Figure 5 indicated that EL102 may cause accumulation of cells in G_2/M . To further quantify the accumulation of cells in the various phases of the cell cycle after exposure to EL102 we performed linear scale propidium iodide flow cytometry. Figure 5 shows that EL102 causes loss of cells in G_1 , and accumulation of cells in G_2/M within 24 h. This is accompanied by an increase in the number of cells in sub G_1 indicating that EL102 has both cytostatic and cytotoxic effects. By 72 h, the majority of cells have entered apoptosis as indicated by accumulation in sub G_1 , and the decrease in the number of cells in G_2/M . Additionally we again observed a peak beyond G_2/M which represent a subset of cells with increased DNA content (8X), which may represent a subset of cells which advanced through the cell cycle with incomplete cell division.

EL102 inhibits tubulin polymerisation and microtubule formation. The cytotoxic activity of taxanes is exerted by promoting and stabilizing microtubule assembly, while preventing physiological microtubule depolymerisation. To determine the effects of EL102

on taxane induced microtubule assembly, we examined the effects of docetaxel and EL102 on the rate of tubulin polymerisation (Figure 6). As expected docetaxel increased the rate of tubulin polymerisation compared with control untreated tubulin. In contrast, EL102 exhibited a decreased rate of polymerisation compared with control, indicating that EL102 may be an inhibitor of tubulin polymerisation. We also examined the effect of combining EL102 with docetaxel on tubulin polymerisation rates, which resulted in inhibition of docetaxel induced tubulin polymerisation to levels of inhibition similar to EL102 alone, suggests that these drugs may antagonise each other with respect to their effects on tubulin polymerisation. To connect tubulin polymerisation in a cell-free system to effects on mitosis, we have performed immunofluorescence assays of β -tubulin and acetylated tubulin in DU145 to visualise the microtubules and examine the effects of EL102, docetaxel and combination of both (Figure 7). The data shows an increase in the expression of β -tubulin and acetylated tubulin in response to docetaxel, while EL102 causes a reduction in acetylated tubulin. The combination of EL102 and docetaxel caused a marked change in the distribution of acetylated tubulin becoming increasingly disorganised consistent with a destabilising effect. This coupled with the cell cycle analysis showing loss of cells from G_1 and accumulation in G_2/M at 24 h post treatment (Figure 8) and induction of apoptosis does suggest that microtubule destabilisation is responsible in part for the cytotoxic effects of EL102.

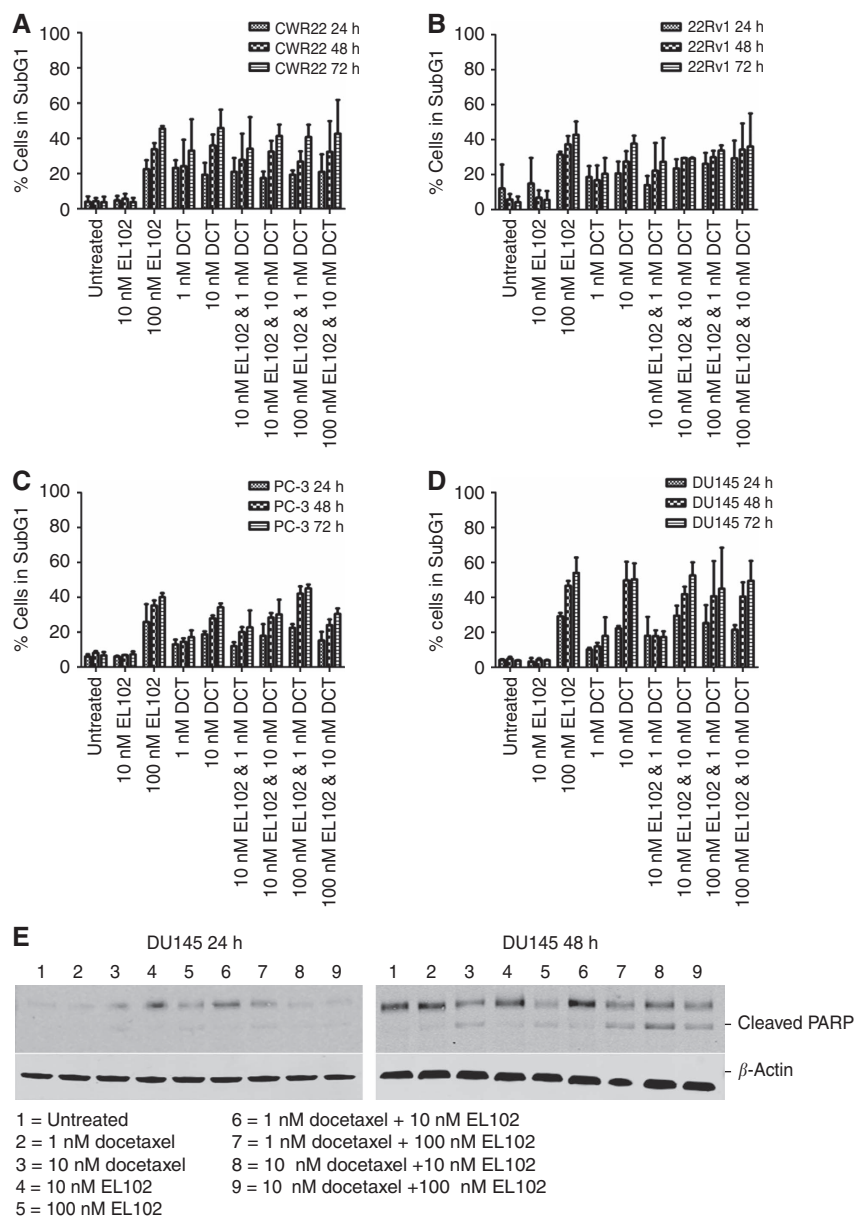


Figure 4. Induction of cellular apoptosis by EL102 and docetaxel. Apoptosis in (A) CWR22, (B) 22Rv1, (C) PC-3 and (D) DU145 prostate cancer cell lines as measured by the percentage of cells accumulated in subG₁. (See Supplementary Table 4 for results of one-way ANOVA comparing cells in subG₁/apoptosis between each treatment). (E) PARP cleavage in DU145 protein lysates 24 and 48 h post treatment with EL102 and docetaxel by western blot. Abbreviation: DCT = docetaxel.

EL102 inhibits Hif1 α protein expression. EL102 is a later generation derivative of the family of toluidine sulphonamide designed to inhibit Hif1 α described by (Wendt *et al*, 2011). We therefore examined the ability of EL102 to inhibit Hif1 α in prostate cancer cells (Figure 9). In normoxia, EL102 modestly inhibited Hif1 α expression at 50 and 100 nM, but had no effect at 10 nM. We then used cobalt chloride to artificially induce hypoxia-increasing Hif1 α expression, and found that EL102 decreased Hif1 α at as little as 10 nM.

DISCUSSION

We have established the potential of a novel toluidine sulphonamide EL102 as a potential broad spectrum anti-prostate cancer therapeutic agent. We found that prostate cancer cell lines were

sensitive to EL102 at an IC₅₀ range of 20–40 nM. Our metastatic prostate cancer cell lines PC-3 and DU145, which are both AR negative and represent castrate-resistant metastatic disease are equally responsive to EL102. The AR-positive cell lines CWR22 and 22Rv1 are twofold more sensitive to EL102 than the metastatic DU145 and PC-3 cell lines.

EL102 is a next-generation derivative of the prototype toluidine sulphonamide compound 1 Hif1 inhibitor (Wendt *et al*, 2011). EL102 was identified as a potential chemotherapeutic agent during a screen of compound 1-derived novel small molecule inhibitors using the NCI-60 cell line panel assessing for growth inhibition potential (not shown). Therefore, we assessed its efficacy for use in the treatment of prostate cancer as a single agent and in combination with the clinically available docetaxel. Docetaxel is a member of the taxane family and is approved for use in prostate cancer patients with castrate-resistant metastatic disease, having been found to provide a modest increase in median survival time

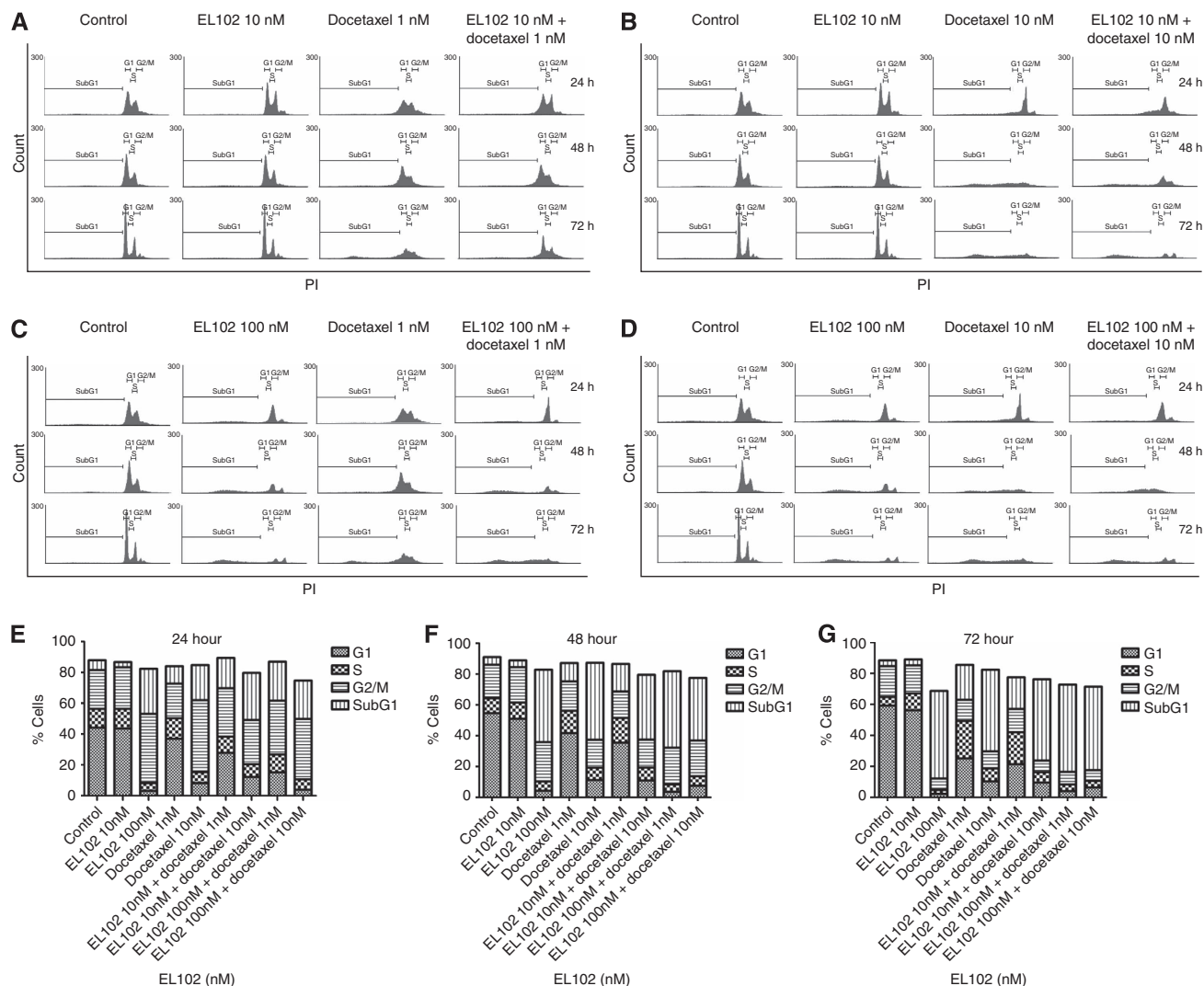


Figure 5. Cell cycle analysis of DU145 cell accumulation in G1, S, G2/M and subG₁ after EL102, docetaxel or combination treatment. Cell cycle profiles of DU145 cells, with markers indicating the G1, S, G2/M and subG₁ cells, after exposure to (A) 10 nM EL102 or 1 nM docetaxel, or 10 nM EL102 and 1 nM docetaxel, (B) 10 nM EL102 or 10 nM docetaxel, or 10 nM EL102 and 10 nM docetaxel, (C) 100 nM EL102 or 1 nM docetaxel, or 100 nM EL102 and 1 nM docetaxel, (D) 100 nM EL102 or 10 nM docetaxel, or 100 nM EL102 and 10 nM docetaxel for 24, 48 and 72 h. Graphs of cell cycle analysis of accumulation of DU145 in the G1, S, G2/M and sub-G₁ phase in response to 0, 10 and 100 nM EL102, 1 and 10 nM docetaxel and combinations of each at (E) 24, (F) 48, (G) 72 h as measured by propidium iodide flow cytometry.

when used in combination with prednisone, compared with mitoxantrone and prednisone (19.2 months *vs* 16.3 months median survival) in the TAX327 trial (Berthold *et al*, 2008), and when in combination with extramustine compared with mitoxantrone and prednisone (17.5 months *vs* 15.6 months median survival) in the SWOG9912 trial (Petrylak *et al*, 2004). Until the approval of six new agents in the last 3 years, docetaxel had been the standard of care in the castrate-resistant metastatic setting. Attempts to combine docetaxel with other agents have been largely unsuccessful in terms of efficacy and side-effects (Antonarakis and Eisenberger, 2013).

We observed that EL102 is a cytotoxic agent and also displays cytostatic properties, through flow cytometric analysis of PI-stained cells cultured for 24, 48 and 72 h, following treatment. This was evidenced by the increased number of cells seen in subG₁ and G₂/M phase of cell cycle, demonstrating that EL102 induces apoptosis and causes G₂/M arrest, preventing the cell from entering into mitosis. Further investigation showed that EL102 inhibited tubulin polymerisation and caused destabilisation of the microtubules in DU145 prostate cancer cells. Induction of

apoptosis, following 24 and 48 h EL102 treatment was confirmed through western blot analysis of PARP cleavage. Additionally, we found that EL102 decreased Hif1 α expression in normoxia and hypoxia *in vitro*, indicating an additional mechanism of action to microtubule destabilisation. Future studies will explore in depth the ability of EL102 to inhibit cell migration and invasion *in vitro* and inhibit a PC-3 xenograft model of bone metastasis, given the role of microtubules in cell polarisation and cell invasion. We will also explore the impact of Hif1 α inhibition by EL102 in PC-3 xenograft mouse models and its subsequent effects on the expression of hypoxia-inducible genes, which regulate several key biological processes, including cell proliferation, angiogenesis, metabolism, apoptosis, immortalisation and migration, essential for tumour progression (Harris, 2002).

Several clinical trials have been conducted recently exploring the potential of neoadjuvant chemotherapy in patients with high-risk localised prostate cancer (Womble *et al*, 2011; Narita *et al*, 2012; Ross *et al*, 2012). The results of these trials suggest a benefit to patients in terms of reductions in tumour volume and PSA levels (Womble *et al*, 2011; Ross *et al*, 2012). Given the equal sensitivity

of AR-positive CWR22 and 22Rv1 to EL102 despite their different sensitivity to androgen, this suggests that EL102 could potentially be used in a castrate sensitive setting before the development of hormone resistance. To further investigate this, we postulated that CWR22 cells would respond to EL102 as single agent. This was confirmed in the CWR22 prostate xenograft model.

As mentioned previously attempts to combine docetaxel with other agents have been largely unsuccessful (Antonarakis and

Eisenberger, 2013). In this study, our *in vivo* investigations found that the combination of EL102 and docetaxel decreased tumour proliferation of CWR22 xenograft to a great extent than either drug alone. The combination of docetaxel and EL102 significantly decreased tumour growth to a greater extent than either alone in a xenograft model of CWR22. While combining the drugs *in vitro* doesn't have an additive effect on induction of apoptosis, it appears to increase the loss of cells from G₁ and accumulation in G₂/M than either drug alone suggesting the combination may increase cytostatic effects. Additionally combining EL102 and docetaxel, one essentially a tubulin polymerisation destabiliser and the other a tubulin polymerisation stabiliser had an antagonistic effect resulting initially in a slower rate of initial polymerisation followed by inhibition of further polymerisation. Future studies will examine whether EL102's ability to inhibit Hif1 α in hypoxic tumours contributes to the observed effects of the combination. Possible downstream effects of Hif1 α inhibition include inhibition of angiogenesis and metastasis.

There is no current cure for castrate-resistant metastatic prostate cancer. Novel adjuvant chemotherapies are continually being developed to address this, with the approval of six new agents since 2010. Recently, clinical trials involving next-generation taxane, cabazitaxel in combination with abiraterone acetate, have begun recruiting patients with preliminary findings expected in 2015. Cabazitaxel is a microtubule-stabilising agent, and is effective in treating patients that have become resistant to docetaxel treatment through overexpression of Pgp (O'Neill *et al*, 2011; Zhang *et al*, 2012), as cabazitaxel is not a substrate for Pgp (Mita *et al*, 2009). Abiraterone functions through disruption of critical steps of androgen formation by direct inhibition of CYP17 activity. This results in reduced levels of circulating androgen and slower progression of prostate cancer in castrate-resistant patients (O'Donnell *et al*, 2004; Agarwal *et al*, 2010). Thus, combining

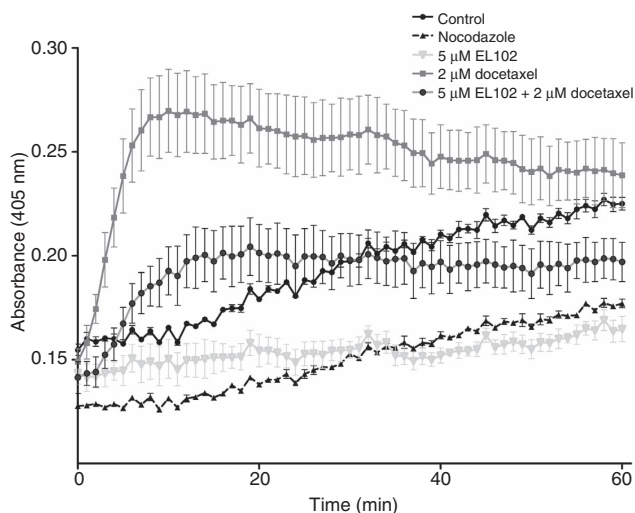


Figure 6. Impact of EL102 and docetaxel alone and in combination on tubulin polymerisation activity. The change in OD \pm s.e.m over time (mins) was measured following tubulin's treatment with 5 μ M EL102, 2 μ M docetaxel and a combination of both vs untreated and 2 μ M nocodazole.

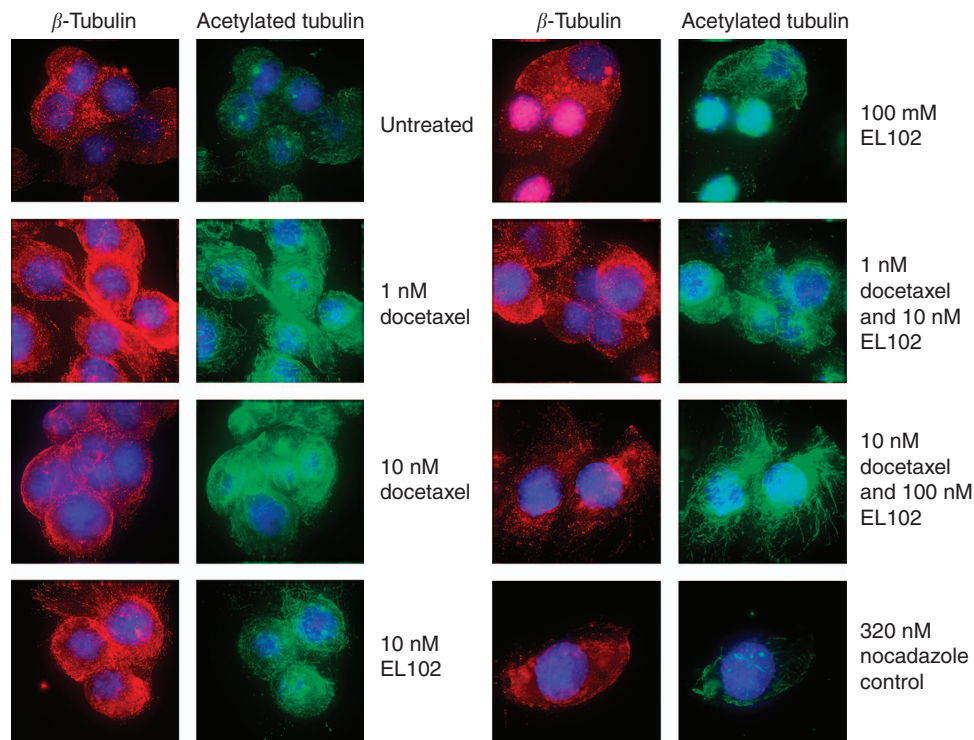


Figure 7. Effect of EL102 on microtubule destabilisation. The effects of EL102 treatments (0, 10, 100 nM), docetaxel treatments (0, 1 and 10 nM) and a combination of both, on microtubule stability in DU145 prostate cancer cells were determined. Following 24 h post-treatment incubation at optimum conditions, cells were fixed with ice-cold methanol and simultaneously stained with Rabbit anti- β -tubulin and anti-acetylated tubulin antibodies. Microtubules were visualised using Alexa Fluor 647 donkey anti-rabbit IgG secondary and Rhodamine Red-X-AffiniPure Fab Fragment goat anti-mouse IgG. Nuclei were counterstained using DAPI.

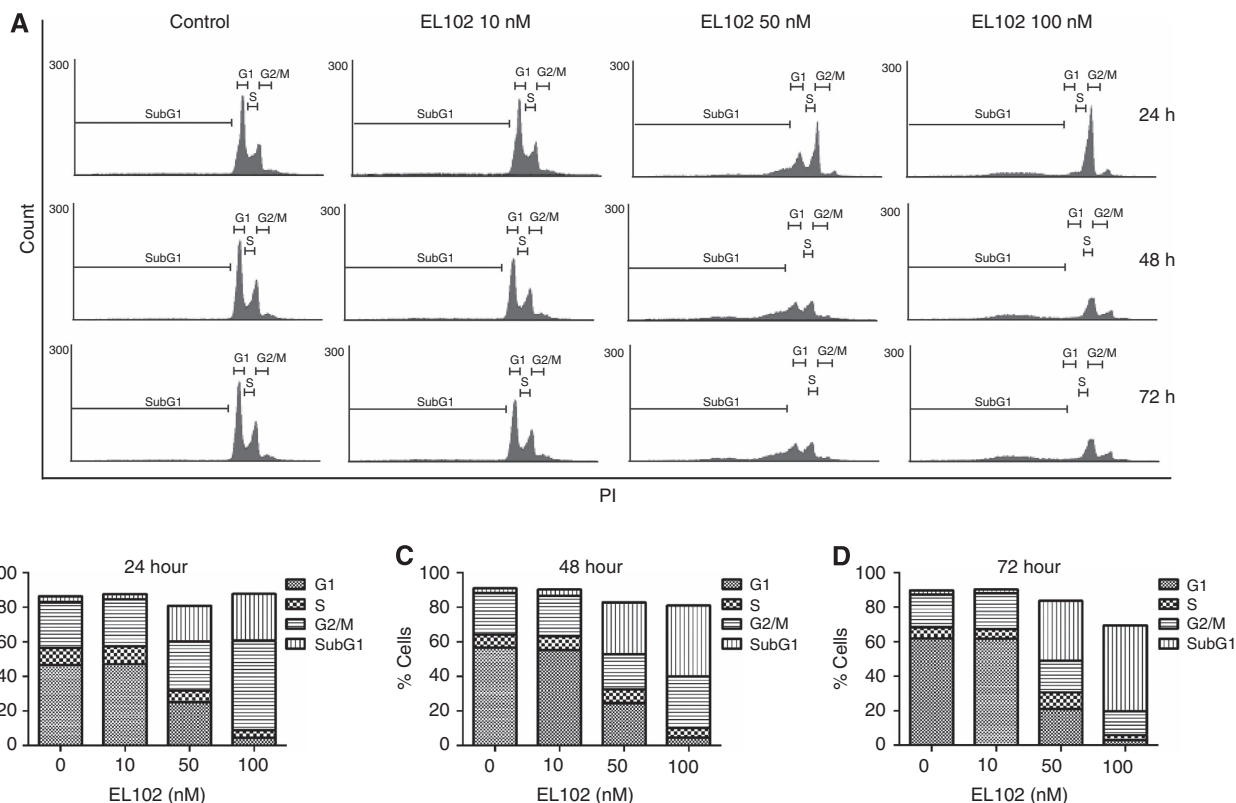


Figure 8. Representative cell cycle analysis of dose response effects of EL102-treated DU145. (A) Histograms of cell cycle analysis of accumulation of DU145 in the G₁, S, G₂/M and sub-G₁ phase in response to 0, 10, 50 and 100 nM EL102 at (B) 24, (C) 48, (D) 72 h as measured by linear propidium iodide flow cytometry.

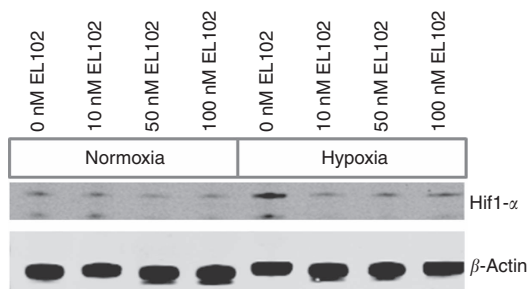


Figure 9. EL102 inhibits Hif1 α in normoxia and hypoxia. EL102 inhibited Hif1 α in normoxia at 50 and nM. When cells were treated with 100 μ m cobalt chloride to induce hypoxia and Hif1 α , EL102 was able to inhibit Hif1a stabilisation at 10 nM.

cabazitaxel and abiraterone acetate, allows us to target multiple pathways in mCRPC, while also eliminating Pgp mediated drug resistance. This lends further credence to the argument for introducing novel compounds, such as EL102 which has mechanisms distinct from the mainstay therapies that may work synergistically.

Interestingly, we also found that EL102 overcame Pgp-mediated resistance in the Pgp overexpressing lung cancer cell lines DLKPA, which is cross-resistant to doxorubicin, paclitaxel, docetaxel and vincristine (Clynes *et al*, 1992). While Pgp is an important mechanism of drug resistance in prostate cancer, it is not the only one. Other mechanisms of resistance include altered growth factor receptor pathway activation (e.g., IGFR, VEGFR, EGFR), hypoxia-related resistance, tubulin mutation and altered tubulin isoform expression, and upregulation of other drug pumps in addition to MDR1 (e.g. BCRP, MRP1, MDR2) and

NF κ B activation (O'Neill *et al*, 2011; Seruga *et al*, 2011; Zhang *et al*, 2012).

In summary, we present data on the efficacy of EL102 as a novel chemotherapeutic agent with potential for the treatment of prostate cancer. We show that EL102 is active in both castration-sensitive and castration-resistant prostate cancer cell lines. EL102 enhances the potency of docetaxel in a xenograft model of the CWR22 prostate cancer. Finally, EL102 is not a substrate for Pgp-mediated drug resistance, indicating that it may be of use in a chemotherapy refractory setting.

ACKNOWLEDGEMENTS

We would like to thank Professor Martin Clynes and Ms Helena Joyce, Dublin City University and Dr Howard Fearnhead and Dr Aideen Ryan, National University of Ireland, Galway, for their advice on this study. We also wish to thank Professor Kevin Sullivan, Emma Harte and Aisling O'Connor for their assistance and expertise in imaging. This work was supported by the Galway University Foundation (RNR1008 to AT, FJS and SAG), the Health Research Board of Ireland Clinical Research Facility, Galway (RSU004 to FJG) and work carried out by EOC in the NCBES High Throughput Screening core facility supported by the PRTL15 Advancing Medicine through Discovery programme.

REFERENCES

Agarwal N, Hutson TE, Vogelzang NJ, Sonpavde G (2010) Abiraterone acetate: a promising drug for the treatment of castration-resistant prostate cancer. *Future Oncol* 6(5): 665–679.

- Antonarakis ES, Eisenberger MA (2013) Phase III trials with docetaxel-based combinations for metastatic castration-resistant prostate cancer: time to learn from past experiences. *J Clin Oncol* **31**(14): 1709–1712.
- Berthold DR, Pond GR, Soban F, de Wit R, Eisenberger M, Tannock IF (2008) Docetaxel plus prednisone or mitoxantrone plus prednisone for advanced prostate cancer: updated survival in the TAX 327 study. *J Clin Oncol* **26**(2): 242–245.
- Clynes M, Redmond A, Moran E, Gilvarry U (1992) Multiple drug-resistance in variant of a human non-small cell lung carcinoma cell line, DLKP-A. *Cytotechnology* **10**(1): 75–89.
- Collins DM, Crown J, O'Donovan N, Devery A, O'Sullivan F, O'Driscoll L, Clynes M, O'Connor R (2010) Tyrosine kinase inhibitors potentiate the cytotoxicity of MDR-substrate anticancer agents independent of growth factor receptor status in lung cancer cell lines. *Invest New Drugs* **28**(4): 433–444.
- Douros J, Suffness M (1981) New natural products under development at the National Cancer Institute. *Recent Results Cancer Res* **76**: 153–175.
- Dunne G, Breen L, Collins DM, Roche S, Clynes M, O'Connor R (2011) Modulation of P-gp expression by lapatinib. *Invest New Drugs* **29**(6): 1284–1293.
- Ferrero JM, Chamorey E, Oudard S, Dides S, Lesbats G, Cavaglione G, Nouyrigat P, Foa C, Kaphan R (2006) Phase II trial evaluating a docetaxel-capecitabine combination as treatment for hormone-refractory prostate cancer. *Cancer* **107**(4): 738–745.
- Garcia JA, Hutson TE, Shepard D, Elson P, Dreicer R (2011) Gemcitabine and docetaxel in metastatic, castrate-resistant prostate cancer: results from a phase 2 trial. *Cancer* **117**(4): 752–757.
- German Animal Protection Law and the UICCR (2010) 'Guidelines for the welfare and use of animals in cancer research'. *Brit J Cancer* **102**: 1555–1577.
- Harris AL (2002) Hypoxia—a key regulatory factor in tumour growth. *Nat Rev Cancer* **2**(1): 38–47.
- Heidegger I, Massoner P, Eder IE, Pircher A, Pichler R, Aigner F, Bektic J, Horninger W, Klocker H (2013) Novel therapeutic approaches for the treatment of castration-resistant prostate cancer. *J Steroid Biochem Mol Biol* **138C**: 248–256.
- Jackson JR, Patrick DR, Dar MM, Huang PS (2007) Targeted anti-mitotic therapies: can we improve on tubulin agents? *Nat Rev Cancer* **7**(2): 107–117.
- Keenan J, Murphy L, Henry M, Meleady P, Clynes M (2009) Proteomic analysis of multidrug-resistance mechanisms in adriamycin-resistant variants of DLKP, a squamous lung cancer cell line. *Proteomics* **9**(6): 1556–1566.
- Kikuno N, Urakami S, Nakamura S, Hiraoka T, Hyuga T, Arichi N, Wake K, Sumura M, Yoneda T, Kishi H, Shigeno K, Shiina H, Igawa M (2007) Phase-II study of docetaxel, estramustine phosphate, and carboplatin in patients with hormone-refractory prostate cancer. *Eur Urol* **51**(5): 1252–1258.
- Manfredi JJ, Horwitz SB (1984) Taxol: an antimetabolic agent with a new mechanism of action. *Pharmacol Therap* **25**(1): 83–125.
- Martin A, Clynes M (1991) Acid phosphatase: endpoint for in vitro toxicity tests. *In Vitro Cell Dev Biol* **27A**(3 Pt 1): 183–184.
- Mita AC, Denis LJ, Rowinsky EK, Debono JS, Goetz AD, Ochoa L, Forouzes B, Beeram M, Patnaik A, Molpus K, Semiond D, Besenval M, Tolcher AW (2009) Phase I and pharmacokinetic study of XRP6258 (RPR 116258A), a novel taxane, administered as a 1-hour infusion every 3 weeks in patients with advanced solid tumors. *Clin Cancer Res* **15**(2): 723–730.
- Narita S, Tsuchiya N, Kumazawa T, Maita S, Numakura K, Obara T, Tsuruta H, Saito M, Inoue T, Horikawa Y, Satoh S, Nanjyo H, Habuchi T (2012) Short-term clinicopathological outcome of neoadjuvant chemohormonal therapy comprising complete androgen blockade, followed by treatment with docetaxel and estramustine phosphate before radical prostatectomy in Japanese patients with high-risk localized prostate cancer. *World J Surg Oncol* **10**: 1.
- O'Donnell A, Judson I, Dowsett M, Raynaud F, Dearnaley D, Mason M, Harland S, Robbins A, Halbert G, Nutley B, Jarman M (2004) Hormonal impact of the 17 α -hydroxylase/C(17,20)-lyase inhibitor abiraterone acetate (CB7630) in patients with prostate cancer. *Br J Cancer* **90**(12): 2317–2325.
- O'Neill AJ, Prencepe M, Dowling C, Fan Y, Mulrane L, Gallagher WM, O'Connor D, O'Connor R, Devery A, Corcoran C, Rani S, O'Driscoll L, Fitzpatrick JM, Watson RW (2011) Characterisation and manipulation of docetaxel resistant prostate cancer cell lines. *Mol Cancer* **10**: 126.
- Oh WK, Halabi S, Kelly WK, Werner C, Godley PA, Vogelzang NJ, Small EJ (2003) A phase II study of estramustine, docetaxel, and carboplatin with granulocyte-colony-stimulating factor support in patients with hormone-refractory prostate carcinoma: Cancer and Leukemia Group B 99813. *Cancer* **98**(12): 2592–2598.
- Peinemann F, Grouven U, Hemkens LG, Bartel C, Borchers H, Pinkawa M, Heidenreich A, Sauerland S (2011) Low-dose rate brachytherapy for men with localized prostate cancer. *Cochrane Database Syst Rev* (7): CD008871.
- Petrylak DP, Tangen CM, Hussain MH, Lara Jr. PN, Jones JA, Taplin ME, Burch PA, Berry D, Moynour C, Kohli M, Benson MC, Small EJ, Raghavan A, Crawford ED (2004) Docetaxel and estramustine compared with mitoxantrone and prednisone for advanced refractory prostate cancer. *N Engl J Med* **351**(15): 1513–1520.
- Ross RW, Galsky MD, Febbo P, Barry M, Richie JP, Xie W, Fennessy FM, Bhatt RS, Hayes J, Choueiri TK, Tempny CM, Kantoff PW, Taplin ME, Oh WK (2012) Phase 2 study of neoadjuvant docetaxel plus bevacizumab in patients with high-risk localized prostate cancer: a Prostate Cancer Clinical Trials Consortium trial. *Cancer* **118**(19): 4777–4784.
- Rowinsky EK, Cazenave LA, Donehower RC (1990) Taxol: a novel investigational antimicrotubule agent. *J Natl Cancer Inst* **82**(15): 1247–1259.
- Seruga B, Ocana A, Tannock IF (2011) Drug resistance in metastatic castration-resistant prostate cancer. *Nat Rev Clin Oncol* **8**(1): 12–23.
- Tester W, Ackler J, Tijani L, Leighton J (2006) Phase I/II study of weekly docetaxel and vinblastine in the treatment of metastatic hormone-refractory prostate carcinoma. *Cancer J* **12**(4): 299–304.
- Vichai V, Kirtikara K (2006) Sulforhodamine B colorimetric assay for cytotoxicity screening. *Nat Protoc* **1**(3): 1112–1116.
- Wani MC, Taylor HL, Wall ME, Coggon P, McPhail AT (1971) Plant antitumor agents. VI. The isolation and structure of taxol, a novel antileukemic and antitumor agent from *Taxus brevifolia*. *J Am Chem Soc* **93**(9): 2325–2327.
- Wendt B, Mulbaier M, Wawro S, Schultes C, Alonso J, Janssen B, Lewis J (2011) Toluidinesulfonamide hypoxia-induced factor 1 inhibitors: alleviating drug-drug interactions through use of PubChem data and comparative molecular field analysis guided synthesis. *J Med Chem* **54**(11): 3982–3986.
- Womble PR, VanVeldhuizen PJ, Nisbet AA, Reed GA, Thrasher JB, Holzbeierlein JM (2011) A phase II clinical trial of neoadjuvant ketoconazole and docetaxel chemotherapy before radical prostatectomy in high risk patients. *J Urol* **186**(3): 882–887.
- Zhang B, Suer S, Livak F, Adediran S, Vemula A, Khan MA, Ning Y, Hussain A (2012) Telomere and microtubule targeting in treatment-sensitive and treatment-resistant human prostate cancer cells. *Mol Pharmacol* **82**(2): 310–321.



This work is licensed under the Creative Commons Attribution-NonCommercial-Share Alike 3.0 Unported License. To view a copy of this license, visit <http://creativecommons.org/licenses/by-nc-sa/3.0/>

Supplementary Information accompanies this paper on British Journal of Cancer website (<http://www.nature.com/bjc>)

Appendix III

Ambit KinomeScan

Compound Name	Screening Conc (nM)
ELR510547-3	1000
ELR510552-3	1000



Primary Screen Report

Requester: Bernd Janssen

Company: ELARA Pharmaceuticals

Study Date: 9/14/2009

Report Date: 9/14/2009

Quote ID: MAXXP01245A

Order ID: ELR001-01-p-00001

Product: scanMAX

Number of Kinases Tested: 442

Compounds Screened: 2

A handwritten signature in blue ink, appearing to read "Paul Gallant", written over a horizontal line.

Paul Gallant

Senior Director

Screening & Commercial Operations

KINOMEScan™

paul@kinomescan.com

(858) 531-6713 cell

(858) 334-2195 phone

(858) 334-2192 fax

www.kinomescan.com

4215 Sorrento Valley Blvd.

San Diego, CA 92121

Kinase Target	ELR510547-3	ELR510552-3
Ambit Gene Symbol	%Ctrl @ 1000nM	%Ctrl @ 1000nM
AAK1	81	76
ABL1(E255K)-phosphorylated	96	100
ABL1(F317I)-nonphosphorylated	88	91
ABL1(F317I)-phosphorylated	100	100
ABL1(F317L)-nonphosphorylated	100	99
ABL1(F317L)-phosphorylated	100	100
ABL1(H396P)-nonphosphorylated	100	100
ABL1(H396P)-phosphorylated	100	100
ABL1(M351T)-phosphorylated	100	100
ABL1(Q252H)-nonphosphorylated	88	98
ABL1(Q252H)-phosphorylated	86	87
ABL1(T315I)-nonphosphorylated	58	72
ABL1(T315I)-phosphorylated	100	95
ABL1(Y253F)-phosphorylated	100	100
ABL1-nonphosphorylated	100	100
ABL1-phosphorylated	100	100
ABL2	100	100
ACVR1	100	100
ACVR1B	52	100
ACVR2A	77	62
ACVR2B	100	80
ACVRL1	100	100
ADCK3	100	100
ADCK4	97	100
AKT1	100	100
AKT2	93	89
AKT3	82	75
ALK	76	100
AMPK-alpha1	100	89
AMPK-alpha2	97	79
ANKK1	35	39
ARK5	72	74
ASK1	100	92
ASK2	95	91
AURKA	100	100
AURKB	77	91
AURKC	75	86
AXL	77	80
BIKE	44	73
BLK	100	100
BMPR1A	100	100
BMPR1B	94	100
BMPR2	85	87
BMX	99	98
BRAF	93	100
BRAF(V600E)	100	100
BRK	100	100
BRSK1	100	100

Kinase Target	ELR510547-3	ELR510552-3
Ambit Gene Symbol	%Ctrl @ 1000nM	%Ctrl @ 1000nM
BRSK2	100	100
BTK	93	86
CAMK1	100	100
CAMK1D	100	100
CAMK1G	100	77
CAMK2A	97	100
CAMK2B	100	97
CAMK2D	100	81
CAMK2G	100	76
CAMK4	100	100
CAMKK1	100	84
CAMKK2	100	74
CASK	92	86
CDC2L1	100	97
CDC2L2	95	100
CDC2L5	100	100
CDK11	100	100
CDK2	92	94
CDK3	100	100
CDK4-cyclinD1	100	100
CDK4-cyclinD3	100	100
CDK5	97	98
CDK7	83	76
CDK8	100	100
CDK9	86	84
CDKL1	100	100
CDKL2	100	100
CDKL3	100	100
CDKL5	100	100
CHEK1	36	97
CHEK2	92	100
CIT	97	95
CLK1	100	99
CLK2	100	95
CLK3	100	95
CLK4	85	81
CSF1R	100	100
CSK	100	95
CSNK1A1	100	100
CSNK1A1L	100	99
CSNK1D	98	93
CSNK1E	100	99
CSNK1G1	100	100
CSNK1G2	92	92
CSNK1G3	100	96
CSNK2A1	86	79
CSNK2A2	87	84
CTK	56	63
DAPK1	100	86

Kinase Target	ELR510547-3	ELR510552-3
Ambit Gene Symbol	%Ctl @ 1000nM	%Ctl @ 1000nM
DAPK2	100	100
DAPK3	100	100
DCAMKL1	100	100
DCAMKL2	86	89
DCAMKL3	100	94
DDR1	100	100
DDR2	78	89
DLK	81	82
DMPK	99	79
DMPK2	100	100
DRAK1	100	98
DRAK2	100	100
DYRK1A	100	100
DYRK1B	100	98
DYRK2	66	69
EGFR	100	93
EGFR(E746-A750del)	82	100
EGFR(G719C)	97	100
EGFR(G719S)	100	92
EGFR(L747-E749del, A750P)	85	91
EGFR(L747-S752del, P753S)	78	91
EGFR(L747-T751del,Sins)	71	77
EGFR(L858R)	86	89
EGFR(L858R,T790M)	100	100
EGFR(L861Q)	44	53
EGFR(S752-I759del)	90	79
EGFR(T790M)	94	100
EIF2AK1	89	96
EPHA1	100	100
EPHA2	100	97
EPHA3	99	98
EPHA4	100	100
EPHA5	84	79
EPHA6	100	97
EPHA7	100	100
EPHA8	100	90
EPHB1	100	100
EPHB2	87	78
EPHB3	100	92
EPHB4	100	100
EPHB6	92	97
ERBB2	100	100
ERBB3	59	68
ERBB4	100	100
ERK1	76	96
ERK2	37	63
ERK3	100	100
ERK4	61	100
ERK5	100	96

Kinase Target	ELR510547-3	ELR510552-3
Ambit Gene Symbol	%Ctl @ 1000nM	%Ctl @ 1000nM
ERK8	81	100
ERN1	100	100
FAK	91	93
FER	63	73
FES	100	94
FGFR1	100	100
FGFR2	100	88
FGFR3	87	100
FGFR3(G697C)	100	95
FGFR4	100	91
FGR	95	100
FLT1	100	100
FLT3	100	100
FLT3(D835H)	93	93
FLT3(D835Y)	100	100
FLT3(ITD)	100	100
FLT3(K663Q)	100	100
FLT3(N841I)	85	100
FLT3(R834Q)	80	97
FLT4	100	100
FRK	100	100
FYN	89	86
GAK	99	98
GCN2(Kin.Dom.2,S808G)	85	81
GRK1	100	100
GRK4	100	100
GRK7	68	86
GSK3A	49	51
GSK3B	95	100
HCK	86	75
HIPK1	93	83
HIPK2	100	100
HIPK3	100	100
HIPK4	86	90
HPK1	88	100
HUNK	100	93
ICK	100	97
IGF1R	35	61
IKK-alpha	73	88
IKK-beta	84	100
IKK-epsilon	100	100
INSR	87	74
INSRR	98	100
IRAK1	22	100
IRAK3	100	99
IRAK4	100	100
ITK	100	100
JAK1(JH1 domain-catalytic)	100	100
JAK1(JH2 domain-pseudokinase)	100	100

Kinase Target	ELRS10547-3	ELRS10552-3
Ambit Gene Symbol	%Ctl @ 1000nM	%Ctl @ 1000nM
JAK2(JH1domain-catalytic)	45	45
JAK3(JH1domain-catalytic)	100	100
JNK1	100	98
JNK2	100	98
JNK3	100	100
KIT	100	100
KIT(A829P)	81	93
KIT(D816H)	84	88
KIT(D816V)	100	97
KIT(L576P)	94	84
KIT(V559D)	89	86
KIT(V559D,T670I)	89	93
KIT(V559D,V654A)	100	100
LATS1	79	80
LATS2	100	100
LCK	92	96
LIMK1	100	100
LIMK2	100	100
LKB1	88	100
LOK	100	99
LRRK2	100	100
LRRK2(G2019S)	100	100
LTK	83	87
LYN	79	92
LZK	100	100
MAK	98	100
MAP3K1	100	100
MAP3K15	100	90
MAP3K2	100	100
MAP3K3	100	93
MAP3K4	98	98
MAP4K2	92	100
MAP4K3	100	100
MAP4K4	55	51
MAP4K5	75	43
MAPKAPK2	100	92
MAPKAPK5	100	99
MARK1	100	100
MARK2	100	100
MARK3	100	100
MARK4	100	77
MAST1	90	88
MEK1	100	100
MEK2	88	90
MEK3	82	81
MEK4	84	79
MEK5	75	78
MEK6	100	98
MELK	93	100

Kinase Target	ELRS10547-3	ELRS10552-3
Ambit Gene Symbol	%Ctl @ 1000nM	%Ctl @ 1000nM
MERTK	100	100
MET	82	58
MET(M1250T)	84	93
MET(Y1235D)	91	94
MINK	100	100
MKK7	100	100
MKNK1	79	85
MKNK2	100	100
MLCK	100	98
MLK1	86	74
MLK2	100	91
MLK3	88	100
MRCKA	95	95
MRCKB	93	88
MST1	58	83
MST1R	92	100
MST2	88	100
MST3	100	98
MST4	95	100
MTOR	100	100
MUSK	100	100
MYLK	87	85
MYLK2	77	87
MYLK4	93	100
MYO3A	100	100
MYO3B	36	92
NDR1	91	100
NDR2	100	100
NEK1	100	100
NEK11	85	100
NEK2	86	95
NEK3	100	100
NEK4	100	100
NEK5	96	85
NEK6	100	100
NEK7	100	100
NEK9	100	91
NIM1	100	100
NLK	81	92
OSR1	99	95
p38-alpha	88	100
p38-beta	65	100
p38-delta	96	100
p38-gamma	83	100
PAK1	100	92
PAK2	98	99
PAK3	83	91
PAK4	100	95
PAK5	100	100

Kinase Target	ELR510547-3	ELR510552-3
Ambit Gene Symbol	%Ch @ 1000nM	%Ch @ 1000nM
PAK7	100	100
PCTK1	100	100
PCTK2	98	96
PCTK3	58	77
PDGFRA	70	81
PDGFRB	78	85
PDPK1	100	100
PFCDPK1(P.falciparum)	100	100
PFPK5(P.falciparum)	100	100
PFTAIRE2	97	100
PFTK1	100	100
PHKG1	98	100
PHKG2	100	100
PIK3C2B	94	82
PIK3C2G	100	100
PIK3CA	100	100
PIK3CA(C420R)	100	89
PIK3CA(E542K)	88	89
PIK3CA(E545A)	100	100
PIK3CA(E545K)	100	100
PIK3CA(H1047L)	100	83
PIK3CA(H1047Y)	69	77
PIK3CA(I800L)	100	99
PIK3CA(M1043I)	100	98
PIK3CA(Q546K)	100	97
PIK3CB	100	100
PIK3CD	68	73
PIK3CG	100	99
PIK4CB	100	67
PIM1	100	100
PIM2	100	87
PIM3	77	86
PIPSK1A	92	92
PIPSK1C	100	100
PIPSK2B	74	76
PIPSK2C	82	100
PKAC-alpha	100	97
PKAC-beta	94	94
PKMYT1	86	88
PKN1	100	100
PKN2	84	100
PKNB(M.tuberculosis)	99	100
PLK1	100	100
PLK2	91	100
PLK3	100	100
PLK4	91	88
PRKCD	100	100
PRKCE	50	89
PRKCH	100	91

Kinase Target	ELR510547-3	ELR510552-3
Ambit Gene Symbol	%Ch @ 1000nM	%Ch @ 1000nM
PRKC1	100	100
PRKCQ	100	100
PRKD1	86	85
PRKD2	100	100
PRKD3	100	100
PRKG1	100	100
PRKG2	84	83
PRKR	100	100
PRKX	100	99
PRP4	100	100
PYK2	100	100
QSK	98	100
RAF1	94	97
RET	100	100
RET(M918T)	100	100
RET(V804L)	100	100
RET(V804M)	100	100
RIOK1	100	100
RIOK2	91	100
RIOK3	100	100
RIPK1	100	98
RIPK2	87	100
RIPK4	100	100
RIPK5	97	93
ROCK1	100	100
ROCK2	83	95
ROS1	100	100
RPS6KA4(Kin.Dom.1-N-terminal)	100	100
RPS6KA4(Kin.Dom.2-C-terminal)	100	100
RPS6KA5(Kin.Dom.1-N-terminal)	97	93
RPS6KA5(Kin.Dom.2-C-terminal)	100	100
RSK1(Kin.Dom.1-N-terminal)	100	100
RSK1(Kin.Dom.2-C-terminal)	96	96
RSK2(Kin.Dom.1-N-terminal)	100	100
RSK3(Kin.Dom.1-N-terminal)	92	100
RSK3(Kin.Dom.2-C-terminal)	94	98
RSK4(Kin.Dom.1-N-terminal)	100	100
RSK4(Kin.Dom.2-C-terminal)	100	100
S6K1	100	100
SBK1	100	100
SgK110	82	100
SGK3	100	100
SIK	100	100
SIK2	92	90
SLK	97	90
SNARK	99	100
SNRK	100	100
SRC	100	100
SRMS	95	79

Kinase Target	ELR510547-3	ELR510552-3
Ambit Gene Symbol	%Ctrl @ 1000nM	%Ctrl @ 1000nM
SRPK1	100	97
SRPK2	100	100
SRPK3	100	100
STK15	100	100
STK33	100	100
STK35	93	95
STK36	100	100
STK39	64	100
SYK	98	91
TAK1	80	86
TAOK1	93	84
TAOK2	100	96
TAOK3	100	100
TBK1	98	99
TEC	89	95
TESK1	83	100
TGFBR1	100	91
TGFBR2	100	91
TIE1	92	72
TIE2	76	86
TLK1	94	100
TLK2	100	96
TNK	94	87
TNK1	93	100
TNK2	100	92
TNN3K	100	97
TRKA	100	95
TRKB	94	100
TRKC	92	89
TRPM6	93	98
TSSK1B	100	100
TTK	98	91
TXK	93	88
TYK2(JH1domain-catalytic)	61	74
TYK2(JH2domain-pseudokinase)	49	55
TYRO3	100	100
ULK1	100	100
ULK2	100	100
ULK3	100	100
VEGFR2	100	88
VRK2	96	93
WEE1	97	81
WEE2	100	96
YANK1	100	100
YANK2	100	100
YANK3	84	86
YES	97	97
YSK1	78	86
YSK4	100	100

Kinase Target	ELR510547-3	ELR510552-3
Ambit Gene Symbol	%Ctrl @ 1000nM	%Ctrl @ 1000nM
ZAK	100	100
ZAP70	99	90

%Ctrl Legend

0%<1	1%<10	10%<35	≥35
------	-------	--------	-----

Appendix IV

Cerep Diversity Profile

From: ELARA PHARMACEUTICALS GmbH

Client Compound ID	ELR-510547	Cerep ID	17121-1				
Reference Number	Batch Number	Submitted FW	Submitted MW	Purity	Received Form	Stock Solution	Flag
-	-	385.50	-	-	Powder	1.E-02 M DMSO*	-

Client Compound ID	ELR-510552	Cerep ID	17121-2				
Reference Number	Batch Number	Submitted FW	Submitted MW	Purity	Received Form	Stock Solution	Flag
-	-	384.50	-	-	Powder	1.E-02 M DMSO*	-

FW: Formula Weight - MW: Molecular Weight

*: Depending on the assay volume and solvent tolerance, the stock solutions were diluted to [100x], [333x] or [1000x] in 100% solvent, then either added directly or further diluted to [10x] or [5x] in H2O or HBSS before addition to the assay well (final solvent concentration kept constant).

Assay Cerep Compound I.D.	Client Compound I.D.	Test Concentration (M)	% Inhibition of Control Specific Binding
A₁ (h) (antagonist radioligand)			
17121-1	ELR-510547	1.0E-06	36
17121-2	ELR-510552	1.0E-06	46
A_{2A} (h) (agonist radioligand)			
17121-1	ELR-510547	1.0E-06	10
17121-2	ELR-510552	1.0E-06	39
A₂ (h) (agonist radioligand)			
17121-1	ELR-510547	1.0E-06	73
17121-2	ELR-510552	1.0E-06	84
α₁ (non-selective) (antagonist radioligand)			
17121-1	ELR-510547	1.0E-06	-4
17121-2	ELR-510552	1.0E-06	-3
α₂ (non-selective) (antagonist radioligand)			
17121-1	ELR-510547	1.0E-06	9
17121-2	ELR-510552	1.0E-06	1
β₁ (h) (agonist radioligand)			
17121-1	ELR-510547	1.0E-06	6
17121-2	ELR-510552	1.0E-06	14
β₂ (h) (agonist radioligand)			
17121-1	ELR-510547	1.0E-06	8
17121-2	ELR-510552	1.0E-06	12
AT₁ (h) (antagonist radioligand)			
17121-1	ELR-510547	1.0E-06	3
17121-2	ELR-510552	1.0E-06	5
AT₂ (h) (agonist radioligand)			
17121-1	ELR-510547	1.0E-06	5
17121-2	ELR-510552	1.0E-06	0
BZD (oentral) (agonist radioligand)			
17121-1	ELR-510547	1.0E-06	-4
17121-2	ELR-510552	1.0E-06	-3
B₁ (h) (agonist radioligand)			
17121-1	ELR-510547	1.0E-06	6
17121-2	ELR-510552	1.0E-06	6
B₂ (h) (agonist radioligand)			
17121-1	ELR-510547	1.0E-06	-7
17121-2	ELR-510552	1.0E-06	2
CB₁ (h) (agonist radioligand)			
17121-1	ELR-510547	1.0E-06	18
17121-2	ELR-510552	1.0E-06	16
CB₂ (h) (agonist radioligand)			
17121-1	ELR-510547	1.0E-06	-2
17121-2	ELR-510552	1.0E-06	12
CCK₁ (CCK_α) (h) (agonist radioligand)			
17121-1	ELR-510547	1.0E-06	-3
17121-2	ELR-510552	1.0E-06	7
CCK₂ (CCK_β) (h) (agonist radioligand)			
17121-1	ELR-510547	1.0E-06	-15
17121-2	ELR-510552	1.0E-06	-4
CRF₁ (h) (agonist radioligand)			
17121-1	ELR-510547	1.0E-06	-10
17121-2	ELR-510552	1.0E-06	-5
D₁ (h) (antagonist radioligand)			
17121-1	ELR-510547	1.0E-06	16
17121-2	ELR-510552	1.0E-06	10

Assay Cerep Compound I.D.	Client Compound I.D.	Test Concentration (M)	% of Control Specific Binding		
			1 st	2 nd	Mean
D₃ (h) (antagonist radioligand)					
17121-1	ELR-510547	1.0E-06	79.2	83.0	81.1
17121-2	ELR-510552	1.0E-06	50.1	37.3	43.7
D_{4L} (h) (antagonist radioligand)					
17121-1	ELR-510547	1.0E-06	88.2	88.8	88.6
17121-2	ELR-510552	1.0E-06	88.8	90.9	89.9
ET_A (h) (agonist radioligand)					
17121-1	ELR-510547	1.0E-06	97.8	91.4	94.6
17121-2	ELR-510552	1.0E-06	99.6	92.9	96.2
ET_B (h) (agonist radioligand)					
17121-1	ELR-510547	1.0E-06	93.9	91.5	92.7
17121-2	ELR-510552	1.0E-06	78.2	103.5	90.8
GABA (non-selective) (agonist radioligand)					
17121-1	ELR-510547	1.0E-06	104.1	93.6	88.9
17121-2	ELR-510552	1.0E-06	98.1	96.4	97.2
AMPA (agonist radioligand)					
17121-1	ELR-510547	1.0E-06	111.2	111.2	111.2
17121-2	ELR-510552	1.0E-06	115.9	118.3	117.1
kalnate (agonist radioligand)					
17121-1	ELR-510547	1.0E-06	75.5	75.0	76.2
17121-2	ELR-510552	1.0E-06	125.6	113.7	119.8
NMDA (antagonist radioligand)					
17121-1	ELR-510547	1.0E-06	100.6	88.6	94.8
17121-2	ELR-510552	1.0E-06	101.4	116.8	109.1
H₁ (h) (antagonist radioligand)					
17121-1	ELR-510547	1.0E-06	99.8	94.3	97.1
17121-2	ELR-510552	1.0E-06	99.2	92.8	96.0
H₂ (h) (antagonist radioligand)					
17121-1	ELR-510547	1.0E-06	137.7	122.8	130.2
17121-2	ELR-510552	1.0E-06	137.1	100.2	118.7
H₃ (h) (agonist radioligand)					
17121-1	ELR-510547	1.0E-06	82.9	83.2	83.1
17121-2	ELR-510552	1.0E-06	97.0	90.5	93.8
i₁ (agonist radioligand)					
17121-1	ELR-510547	1.0E-06	112.4	90.5	101.6
17121-2	ELR-510552	1.0E-06	99.8	97.6	98.7
i₂ (antagonist radioligand)					
17121-1	ELR-510547	1.0E-06	105.4	89.4	97.4
17121-2	ELR-510552	1.0E-06	106.6	102.9	104.7
BLT₁ (LTB₄) (h) (agonist radioligand)					
17121-1	ELR-510547	1.0E-06	89.3	85.3	87.3
17121-2	ELR-510552	1.0E-06	85.4	87.3	86.4
CysLT₁ (LTD₄) (h) (agonist radioligand)					
17121-1	ELR-510547	1.0E-06	122.9	124.3	123.8
17121-2	ELR-510552	1.0E-06	108.9	113.8	111.4
MC₄ (h) (agonist radioligand)					
17121-1	ELR-510547	1.0E-06	121.3	111.9	116.8
17121-2	ELR-510552	1.0E-06	106.1	103.5	104.8
M (non-selective) (antagonist radioligand)					
17121-1	ELR-510547	1.0E-06	124.4	100.5	112.4
17121-2	ELR-510552	1.0E-06	123.5	119.2	121.3
NK₁ (h) (agonist radioligand)					
17121-1	ELR-510547	1.0E-06	130.2	121.0	125.8
17121-2	ELR-510552	1.0E-06	84.7	85.2	84.8
NK₂ (h) (agonist radioligand)					
17121-1	ELR-510547	1.0E-06	97.0	99.2	98.1
17121-2	ELR-510552	1.0E-06	95.4	98.4	96.9
NK₃ (h) (antagonist radioligand)					
17121-1	ELR-510547	1.0E-06	116.2	118.0	117.1
17121-2	ELR-510552	1.0E-06	113.7	115.7	114.7

Assay Cerep Compound I.D.	Client Compound I.D.	Test Concentration (M)	% of Control Specific Binding		Mean
			1 st	2 nd	
Y (non-selective) (agonist radioligand)					
17121-1	ELR-510547	1.0E-06	100.3	105.1	102.7
17121-2	ELR-510552	1.0E-06	102.2	114.6	108.6
N neuronal α-BGTX-insensitive (α4β2) (agonist radioligand)					
17121-1	ELR-510547	1.0E-06	98.2	95.5	97.0
17121-2	ELR-510552	1.0E-06	96.0	101.5	98.8
opioid (non-selective) (antagonist radioligand)					
17121-1	ELR-510547	1.0E-06	102.0	95.0	98.6
17121-2	ELR-510552	1.0E-06	103.5	94.6	99.1
NOP (ORL1) (h) (agonist radioligand)					
17121-1	ELR-510547	1.0E-06	80.5	102.6	91.8
17121-2	ELR-510552	1.0E-06	103.2	98.2	100.7
PPARY (h) (agonist radioligand)					
17121-1	ELR-510547	1.0E-06	79.0	68.3	73.8
17121-2	ELR-510552	1.0E-06	69.2	61.4	66.3
PCP (antagonist radioligand)					
17121-1	ELR-510547	1.0E-06	91.5	80.6	88.1
17121-2	ELR-510552	1.0E-06	88.7	88.0	88.4
EP₃ (h) (agonist radioligand)					
17121-1	ELR-510547	1.0E-06	95.1	98.1	96.8
17121-2	ELR-510552	1.0E-06	97.4	88.1	92.7
IP (PGI₂) (h) (agonist radioligand)					
17121-1	ELR-510547	1.0E-06	107.3	109.5	108.8
17121-2	ELR-510552	1.0E-06	94.3	95.0	94.7
P2X (agonist radioligand)					
17121-1	ELR-510547	1.0E-06	109.7	119.7	114.7
17121-2	ELR-510552	1.0E-06	109.3	94.1	101.7
P2Y (agonist radioligand)					
17121-1	ELR-510547	1.0E-06	103.0	101.3	102.1
17121-2	ELR-510552	1.0E-06	102.6	98.6	100.7
5-HT (non-selective) (agonist radioligand)					
17121-1	ELR-510547	1.0E-06	92.3	89.6	91.0
17121-2	ELR-510552	1.0E-06	94.3	81.6	87.9
σ (non-selective) (agonist radioligand)					
17121-1	ELR-510547	1.0E-06	110.3	98.5	104.4
17121-2	ELR-510552	1.0E-06	95.6	71.6	83.7
OR (h) (agonist radioligand)					
17121-1	ELR-510547	1.0E-06	94.3	71.0	82.8
17121-2	ELR-510552	1.0E-06	59.1	72.6	68.0
ER (non-selective) (h) (agonist radioligand)					
17121-1	ELR-510547	1.0E-06	97.3	86.6	92.0
17121-2	ELR-510552	1.0E-06	92.6	84.3	88.6
PR (h) (agonist radioligand)					
17121-1	ELR-510547	1.0E-06	5.3	2.8	4.1
17121-2	ELR-510552	1.0E-06	6.4	4.0	6.2
AR (h) (agonist radioligand)					
17121-1	ELR-510547	1.0E-06	26.5	48.7	37.8
17121-2	ELR-510552	1.0E-06	6.7	14.5	10.8
TRH₁ (h) (agonist radioligand)					
17121-1	ELR-510547	1.0E-06	95.6	95.7	96.7
17121-2	ELR-510552	1.0E-06	99.3	104.2	101.7
V_{1a} (h) (agonist radioligand)					
17121-1	ELR-510547	1.0E-06	89.4	90.6	90.1
17121-2	ELR-510552	1.0E-06	102.6	91.2	97.0
V₂ (h) (agonist radioligand)					
17121-1	ELR-510547	1.0E-06	97.7	92.1	94.9
17121-2	ELR-510552	1.0E-06	111.0	94.0	102.6
Ca²⁺ channel (L, dihydropyridine site) (antagonist radioligand)					
17121-1	ELR-510547	1.0E-06	89.1	104.6	98.9
17121-2	ELR-510552	1.0E-06	77.5	79.6	78.8

Assay Cerep Compound I.D.	Client Compound I.D.	Test Concentration (M)	% of Control Specific Binding		Mean
			1 st	2 nd	
Ca²⁺ channel (L, diltiazem site) (benzothiazepines) (antagonist radioligand)					
17121-1	ELR-510547	1.0E-06	90.6	74.4	82.8
17121-2	ELR-510552	1.0E-06	74.7	84.2	79.6
Ca²⁺ channel (L, verapamil site) (phenylalkylamine) (antagonist radioligand)					
17121-1	ELR-510547	1.0E-06	104.2	96.0	100.1
17121-2	ELR-510552	1.0E-06	104.2	94.7	89.6
K_{ATP} channel (antagonist radioligand)					
17121-1	ELR-510547	1.0E-06	90.1	105.1	87.8
17121-2	ELR-510552	1.0E-06	100.5	85.8	83.1
K_v channel (antagonist radioligand)					
17121-1	ELR-510547	1.0E-06	106.3	102.8	104.6
17121-2	ELR-510552	1.0E-06	99.2	104.0	101.8
8K_{Ca} channel (antagonist radioligand)					
17121-1	ELR-510547	1.0E-06	86.8	95.6	81.2
17121-2	ELR-510552	1.0E-06	86.6	96.8	81.7
Na⁺ channel (site 2) (antagonist radioligand)					
17121-1	ELR-510547	1.0E-06	96.3	87.5	81.9
17121-2	ELR-510552	1.0E-06	97.8	82.0	89.9
Cl⁻ channel (GABA-gated) (antagonist radioligand)					
17121-1	ELR-510547	1.0E-06	75.5	76.0	76.7
17121-2	ELR-510552	1.0E-06	56.5	53.1	64.8
norepinephrine transporter (h) (antagonist radioligand)					
17121-1	ELR-510547	1.0E-06	89.4	80.8	85.1
17121-2	ELR-510552	1.0E-06	85.3	79.0	82.2
dopamine transporter (h) (antagonist radioligand)					
17121-1	ELR-510547	1.0E-06	98.1	89.4	83.8
17121-2	ELR-510552	1.0E-06	65.8	88.3	77.0
GABA transporter (antagonist radioligand)					
17121-1	ELR-510547	1.0E-06	122.6	104.2	113.4
17121-2	ELR-510552	1.0E-06	116.0	102.9	109.4
choline transporter (CHT1) (h) (antagonist radioligand)					
17121-1	ELR-510547	1.0E-06	102.3	103.8	103.0
17121-2	ELR-510552	1.0E-06	118.1	122.3	120.2
5-HT transporter (h) (antagonist radioligand)					
17121-1	ELR-510547	1.0E-06	96.3	91.2	83.7
17121-2	ELR-510552	1.0E-06	84.2	89.1	86.8

Follow-Up Dose Response

Assay Cerep Compound I.D.	Client Compound I.D.	Test Concentration (M)	% of Control Specific Binding		Mean
			1 st	2 nd	
Ca²⁺ channel (L, diltiazem site) (benzothiazepines) (antagonist radioligand)					
17121-1	ELR-510547	1.0E-06	90.6	74.4	82.8
17121-2	ELR-510552	1.0E-06	74.7	84.2	79.6
Ca²⁺ channel (L, verapamil site) (phenylalkylamine) (antagonist radioligand)					
17121-1	ELR-510547	1.0E-06	104.2	96.0	100.1
17121-2	ELR-510552	1.0E-06	104.2	94.7	89.6
K_{ATP} channel (antagonist radioligand)					
17121-1	ELR-510547	1.0E-06	90.1	105.1	87.8
17121-2	ELR-510552	1.0E-06	100.5	85.8	83.1
K_v channel (antagonist radioligand)					
17121-1	ELR-510547	1.0E-06	106.3	102.8	104.6
17121-2	ELR-510552	1.0E-06	99.2	104.0	101.8
8K_{Ca} channel (antagonist radioligand)					
17121-1	ELR-510547	1.0E-06	86.8	95.6	81.2
17121-2	ELR-510552	1.0E-06	86.6	96.8	81.7
Na⁺ channel (site 2) (antagonist radioligand)					
17121-1	ELR-510547	1.0E-06	96.3	87.5	81.9
17121-2	ELR-510552	1.0E-06	97.8	82.0	89.9
Cl⁻ channel (GABA-gated) (antagonist radioligand)					
17121-1	ELR-510547	1.0E-06	75.5	76.0	76.7
17121-2	ELR-510552	1.0E-06	56.5	53.1	64.8
norepinephrine transporter (h) (antagonist radioligand)					
17121-1	ELR-510547	1.0E-06	89.4	80.8	85.1
17121-2	ELR-510552	1.0E-06	85.3	79.0	82.2
dopamine transporter (h) (antagonist radioligand)					
17121-1	ELR-510547	1.0E-06	98.1	89.4	83.8
17121-2	ELR-510552	1.0E-06	65.8	88.3	77.0
GABA transporter (antagonist radioligand)					
17121-1	ELR-510547	1.0E-06	122.6	104.2	113.4
17121-2	ELR-510552	1.0E-06	116.0	102.9	109.4
choline transporter (CHT1) (h) (antagonist radioligand)					
17121-1	ELR-510547	1.0E-06	102.3	103.8	103.0
17121-2	ELR-510552	1.0E-06	118.1	122.3	120.2
5-HT transporter (h) (antagonist radioligand)					
17121-1	ELR-510547	1.0E-06	96.3	91.2	83.7
17121-2	ELR-510552	1.0E-06	84.2	89.1	86.8